Expression and function of human macrophage heparan sulfate proteoglycans

Laura Elisabeth Collins

Kennedy Institute of Rheumatology
Lincoln College
University of Oxford

A thesis submitted for the degree Doctor of Philosophy
in Molecular and Cellular Medicine

Abstract

Among the hundreds of ligands for heparan sulfate (HS) are chemokines, cytokines, and growth factors, giving this proteoglycan a potentially central role in the regulation of immune responses. The biosynthesis of HS is regulated during inflammation with consequent changes to ligand binding and activity in multiple cell types including myeloid cells. In this thesis, I aimed to comprehensively describe the changes in expression of HS core proteins and biosynthetic enzymes in human primary monocytes and polarised monocyte-derived macrophages, and to investigate the contribution of HS proteoglycans to macrophage functions. Using a custom-designed microfluidic array card, I performed transcriptome analysis of HS-associated gene expression and discovered significant changes at all stages of macrophage maturation and polarisation, revealing that maturation is associated with increased capacity for HS biosynthesis and that pro- and anti-inflammatory macrophages have substantially different HS composition. Of particular interest was the reciprocal regulation observed between the 6-O-sulfotransferase (*HS6ST1*) and its functional partner the sulfatase (*SULF2*), which add and remove the 6-O-sulfate group to HS chains, respectively. Using siRNA knockdown of *HS6ST1* in monocyte-derived macrophages to ablate 6-O-sulfation of HS, I determined that this modification does not contribute to phagocytosis or migration. Moreover, its absence did not affect macrophage polarisation, whereas total sulfate ablation using sodium chlorate did, suggesting that sulfate modifications at other positions are more important. *HS6ST1* knockdown altered post-translational regulation of monocyte chemoattractant protein 1 (MCP-1), indicating the 6-O-sulfate group of HS modulates retention of this and potentially other mediators on the cell surface.

Acknowledgements

Grateful thanks to my primary supervisor, Dr Linda Troeberg, for her endless support, wisdom, and patience. Thanks to my second supervisor, Professor Claudia Monaco, and the whole Monaco group, for taking me in when Linda moved from the University of Oxford to the University of East Anglia. Thanks also to Lynn for her generosity with reagents and her time, and to Kristin for teaching me many of the techniques included in this thesis. I gratefully acknowledge the support of the Kennedy Trust for providing my studentship and the laboratory resources to complete this project. I must also thank my parents for their unfailing support over the years, and particularly my Mum for her meticulous proofreading of this thesis.

Table of contents

Table of Figures

Table of Tables

List of abbreviations

18S	18S ribosomal RNA
AGRN	agrin
ANOVA	analysis of variance
APC	allophycocyanin
APRIL	a proliferation inducing ligand
APS	ammonium persulfate
AT	anti-thrombin
BCR	B-cell receptor
BMP	Bone morphogenetic protein
BSA	Bovine serum albumin
CCL	chemokine ligand
CD	cluster of differentiation
cDNA	complementary DNA
CHO	Chinese hamster ovary
COPD	chronic obstructive pulmonary disease
COVID-19	Coronavirus disease caused by SARS-CoV-2
CS	chondroitin sulfate
Ct	cycle threshold
CXCL	chemokine (C-X-C motif) ligand
DAMP	damage-associated molecular pattern
DAPI	4',6-diamidino-2-phenylindole
DC	dendritic cell

DC-SIGN	dendritic cell-specific intercellular adhesion molecule-2-grabbing non-integrin (CD209)
DNA	deoxyribonucleic acid
DS	dermatan sulfate
E. coli	*Escherichia coli*
ECM	extracellular matrix
EDTA	ethylenediaminetetraacetic acid
ELISA	enzyme-linked immunosorbent assay
ERK	extracellular signal-related kinase
EXT	exostosin
EXTL	exostosin-like
FBS	fetal bovine serum
Fc	fragment crystallizible
FcR	receptor for the Fc region of antibodies
FGF	fibroblast growth factor
FGFR	fibroblast growth factor receptor
FITC	fluorescein isothiocyanate
GAG	glycosaminoglycan
GAPDH	glyceraldehyde 3-phosphate dehydrogenase
GDNF	glial cell-derived neurotrophic factor
GlcA	glucuronic acid
GLCE	C5 epimerase
GlcNAc	N-acetylglucosamine
GM-CSF	granulocyte-macrophage colony-stimulating factor

GPC	glypican
GPI	glycophosphatidylinositol
HBSS	Hank's buffered saline solution
HCl	hydrochloric acid
HGF	hepatocyte growth factor
HME	hereditary multiple exostoses
HPLC	high-performance liquid chromatography
HPSE	heparanase
HRP	horseradish peroxidase
HS	heparan sulfate
HS2ST	heparan sulfate 2-O-sulfotransferase
HS3ST	heparan sulfate 3-O-sulfotransferase
HS6ST	heparan sulfate 6-O-sulfotransferase
HSCs	hematopoietic stem cells
HSPG	heparan sulfate proteoglycan
HSPG2	heparan sulfate proteoglycan 2 (perlecan)
HSV-1	herpes simplex virus 1
HUVEC	human umbilical vascular endothelial cells
i.v.	intravenous
IBD	inflammatory bowel disease
ICAM1	intercellular adhesion molecule 1
IFN	interferon
Ig	Immunoglobulin
IL	interleukin

iNOS	inducible nitric oxide synthase
IRF5	interferon regulatory factor 5
KD	knockdown
LDL	low density lipoprotein
LPS	lipopolysaccharide
M-CSF	macrophage colony stimulating factor
MAPK	mitogen-activated protein kinase
MARCO	macrophage receptor with collagenous structure
MCP-1	monocyte chemotactic protein 1
MFI	median fluorescence intensity
MHC	major histocompatability complex
MIP-1	macrophage inflammatory protein 1
MOI	multiplicity of infection
MRC1	mannose receptor C-type 1
mRNA	messenger RNA
MTS	3-(4,5-dimethylthiazol-2-yl)-5-(3-carboxymethoxyphenyl)-2-(4-sulfophenyl)-2H-tetrazolium
NDST	N-deacetylase/N-sulfotransferase
NHS	National Health Service
NLR	NOD-like receptor
NO	nitric oxide
NOS2	nitric oxide synthase 2
PAMP	pathogen-associated molecular patterns
PAPS	3'-phosphoadenosine-5'-phosphosulfate

PBMC	peripheral blood mononuclear cell
PBS	phosphate buffered saline
PE	phycoerythrin
Pen-Strep	penicillin-streptomycin
PerCP	peridinin-chlorophyll-protein complex
PFA	paraformaldehyde
PMA	phorbol 12-myristate 13-acetate
PMN	polymorphonuclear neutrophils
PRR	pattern recognition receptor
PSGL1	P-selectin glycoprotein ligand-1
PVDF	polyvinylidene difluoride
qPCR	quantitative polymerase chain reaction
RA	rheumatoid arthritis
RANTES	regulated upon activation, normal T cell expressed and presumably secreted
RNA	ribonucleic acid
ROS	reactive oxygen species
RPLP0	ribosomal protein lateral stalk subunit P0
RPMI	Roswell Park Memorial Institute
SD	standard deviation
SDC	syndecan
SDS	sodium dodecyl sulfate
SDS-PAGE	sodium dodecyl sulfate polyacrylamide gel electrophoresis
Shh	sonic hedgehog

siRNA	small interfering RNA
SNP	single nucleotide polymorphism
SPR	surface plasmon resonance
STAT	signal transducer and activator of transcription
SULF	sulfatase
TAM	tumour-associated macrophage
TCA	trichloroacetic acid
TGF	transforming growth factor
TGFBR3	TGF-beta receptor 3
Th1	T helper lymphocytes type 1
Th2	T helper lymphocytes type 2
TLR	toll-like receptor
TMB	3,3'5,5'-tetramethylbenzidine
TNF	tumour necrosis factor
Tris	tris(hydroxymethyl)aminomethane
VCAM1	vascular cell adhesion molecule 1
VEGF	vascular endothelial growth factor

Chapter 1: Introduction

1.1 Inflammation

Inflammation is the body's defence mechanism against potentially harmful stimuli such as tissue damage and pathogens, and serves to accelerate removal of the stimulus and coordinate tissue repair. A network of soluble ligands and their signalling pathways coordinates the inflammatory response, resulting in increased vascular permeability, recruitment of immune cells, and ultimately repair of the tissue (Libby, 2007). The combined action of myriad effector molecules in the affected tissue leads to the signs we associate with inflammation: redness, swelling, and pain (Hannoodee and Nasuruddin, 2021).

To initiate an inflammatory response, pathogen-associated molecular patterns (PAMPs) and damage-associated molecular patterns (DAMPs) are recognised by pattern-recognition receptors (PRRs) such as the Toll-like receptors (TLRs), NOD-like receptors (NLRs) and C-type lectins (Kumar et al., 2011). PAMPs are conserved molecular patterns expressed by pathogens but not self cells, including bacterial lipopolysaccharide, mucins, and viral nucleic acids (Zindel and Kubes, 2020). DAMPs are cell components not accessible to receptors under homeostatic conditions and are released by stressed or damaged cells due to loss of membrane integrity and release of intracellular components, or are cryptic epitopes formed by degradation of self components such as ECM molecules (Frevert et al., 2018).

PRRs are found on the cell surface and in the cytoplasm of non-immune cells such as endothelial cells, and specialised immune cells resident in the tissue such as mast

cells and dendritic cells (Janeway and Medzhitov, 2002). Signalling through these receptors activates downstream pathways leading to upregulation of inflammatory mediators such as cytokines and chemokines that promote leukocyte recruitment (Takeuchi and Akira, 2010). Other bioactive mediators are released including histamine and serotonin that regulate vasodilation and increase vascular permeability, facilitating movement of fluid from the blood into the tissue (Medzhitov, 2008). Activated endothelium becomes permissible to leukocyte extravasation (Figure 1.1), a hallmark of inflammation directed by concentration gradients of chemokines and beginning with a well-defined series of steps known as the leukocyte adhesion cascade (Ley et al., 2007).

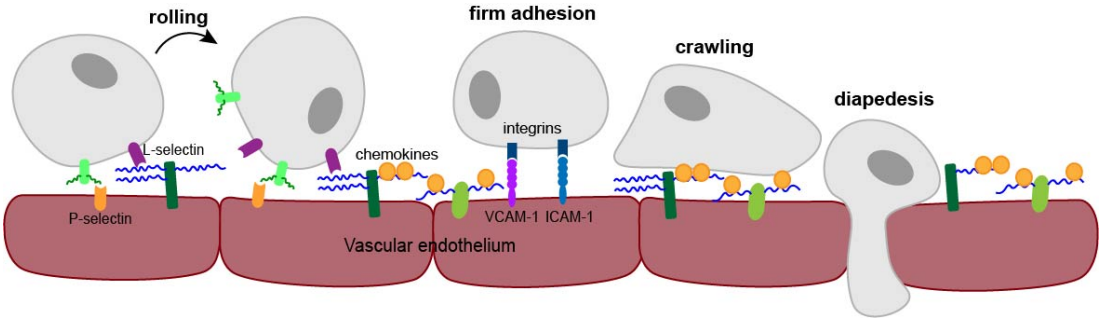

Figure 1.1 Leukocyte recruitment and trafficking across the vessel wall.
Circulating leukocytes interact with the activated endothelial cells of post-capillary venules near the site of inflammation via selectins and their carbohydrate ligands. This loose tethering facilitates leukocyte rolling directed by concentration gradients of immobilised chemokines, which also activate leukocyte integrins leading to arrest and firm adhesion. Leukocytes crawl towards the site of inflammation along the luminal surface of the vascular endothelium then exit the vessel into the inflamed tissue.

Leukocytes in the circulation are captured by endothelial cells via interactions between selectins and various glycosylated ligands such as P-selectin glycoprotein ligand-1 (PSGL1) (Moore et al., 1995) and heparan sulfate (Koenig et al., 1998). E-selectin and P-selectin are upregulated by activated endothelial cells (Smith, 1993), and L-selectin is constitutively expressed by leukocytes (Ivetic et al., 2019). This

tethering of leukocytes by selectins facilitates rolling along the lumenal surface of the endothelium where they encounter gradients of chemokines that activate leukocytes and trigger inside-out signalling resulting in integrin activation. Leukocyte integrins include LFA-1 (CD11a), expressed by neutrophils, monocytes, and lymphocytes, and Mac-1 (CD11b) found mainly on neutrophils and monocytes (Mitroulis et al., 2015). The binding of activated integrins to immunoglobulin superfamily members such as ICAM1 and VCAM1 on endothelial cells leads to leukocyte arrest, firm adhesion, and crawling directed by the chemokine gradient (Johnston and Butcher, 2002). Diapedesis from the vessel into the tissue requires that the leukocyte breaches the endothelium, either between adjacent endothelial cells (paracellular route) or through an endothelial cell (transcellular route), and then crosses the basement membrane and pericyte sheath (Filippi, 2019).

Once recruited, leukocytes have various mechanisms to destroy invading pathogens, including phagocytosis and digestion of unicellular organisms such as bacteria. Effector molecules produced by innate immune cells include reactive oxygen species (ROS), reactive nitrogen species, proteinase 3, cathepsin G, and elastase (Fang, 2004; Korkmaz et al., 2010). Since these effectors do not discriminate between microbial and host targets, collateral damage to the host is unavoidable but can be limited by timely resolution of the inflammatory response (Feehan and Gilroy, 2019; Nathan, 2002). A return to homeostasis may not always occur, however, and failure to resolve acute inflammation can lead to chronic inflammation, which underlies many diseases (Nathan and Ding, 2010). Persistent immune activation occurs when the injurious agent cannot be removed, such as with crystal arthritis (gout) or

asbestosis (Franklin et al., 2016), or off-targeted responses directed against self-antigens result in autoimmunity, such as in rheumatoid arthritis (Firestein and McInnes, 2017).

1.2 Macrophages: essential coordinators of immune responses

Elie Metchnikoff first described a defensive role for cells that engulf foreign particles and other cells, and named them 'macrophage', which in Greek means 'big-eater' (Gordon, 2016). Macrophages have important roles in coordinating the activities of other immune cells by presenting antigen and secreting activating cytokines, and also are essential for phagocytic clearance of pathogens and dead cells (Fujiwara and Kobayashi, 2005). All tissues of the body contain resident macrophage populations that act as sentinels and regulators of homeostasis, such as Kupffer cells in the liver, Langerhans cells in the skin, and microglial cells in the brain (Epelman et al., 2014). These tissue-resident macrophages are largely seeded before birth by embryonic precursors deriving from the yolk sack or the foetal liver, and self-renew independently of bone marrow hematopoietic stem cells (HSCs) (Guilliams et al., 2013; Hashimoto et al., 2013). These cells are among the first line of defence against potential invaders, detecting non-self molecules via PRRs and alerting other cells of the immune system to the danger by secretion of cytokines.

Additionally, in the post-natal mammal there is a dynamic population of monocyte-derived macrophages deriving from HSC progenitors in the bone marrow, which circulate in the blood for a few days and constitute 4-10% of nucleated cells in the blood (Coillard and Segura, 2019; Shi and Pamer, 2011). Under homeostatic

conditions, monocytes can circulate and patrol tissues, fulfilling a sentinel role by collecting antigen and carrying it to draining lymph nodes (Jakubzick et al., 2013). During acute inflammation or infection, emergency myelopoiesis produces more monocytes that are recruited locally via the leukocyte adhesion cascade and then differentiate into macrophages to supplement the local tissue-resident population (Murray and Wynn, 2011).

1.2.2 Polarisation of macrophages *in vivo* and *in vitro*

During recruitment to a site of inflammation, monocytes mature into macrophages and acquire a phenotype appropriate to the nature of the immunological challenge on the basis of signals in the microenvironment (Mosser and Edwards, 2008). Such signals may include cytokines, PAMPs, DAMPs, and trigger the expression of relevant effector molecules by macrophages (Atri et al., 2018). The acquisition of specific protein and gene signatures in response to microenvironmental stimuli is termed 'polarisation', and confers different functions including phagocytosis, bactericidal activity, indirect activation of other immune cells via cytokine secretion, and direct activation of adaptive immune cells by antigen presentation and co-stimulation (Martinez et al., 2008).

Polarised macrophages have historically been classified into two groups, M1 and M2, in parallel with the Th1/Th2 division in T cells (Mills et al., 2000). 'Classically activated' M1 macrophages were observed to develop in response to pro-inflammatory cytokines such as IFN-γ secreted by Th1 cells during infection by intracellular pathogens (Shapouri-Moghaddam et al., 2018). These cells have high

antigen-presenting capacity, making them potent inducers of an adaptive immune response, and secrete pro-inflammatory cytokines and anti-microbial products (Mills and Ley, 2014). An 'alternatively activated' form of macrophage was later described in response to the Th2 cytokines IL-4 and IL-13 produced in helminth infection and named M2 (Loke et al., 2002). More recent classification systems recognise a broader range of potential macrophage-polarising stimuli and multiple types of 'M2' or alternatively activated macrophage (Martinez and Gordon, 2014). According to this newer classification system, IL-4 and IL-13, produced by Th2 cells, basophils, eosinophils, and mast cells, produce a macrophage phenotype called M2a. A different sort of non-classically-activated macrophage was classified as M2b: these cells are polarised by exposure to immune complexes and LPS, produce high amounts of IL-10 but low amounts of IL-12, and promote Th2 differentiation and humoral response. The third category, M2c, develops in response to glucocorticoids or IL-10, resulting in an immunoregulatory, pro-fibrotic phenotype **(**Figure 1.2A**)** (Juhas et al., 2015). GM-CSF and M-CSF have also been added to the list of M1 and M2 stimuli, respectively, as they produce macrophages *in vitro* with some aspects of the M1 and M2 phenotypes (Jaguin et al., 2013). Each category of polarised macrophage is associated with particular surface markers, transcriptomic signatures, and cytokine secretion that are often used to identify them *in vitro* or *in vivo* (Martinez et al., 2006).

In addition to expression of receptors and secretion of effector molecules such as cytokines and chemokines (Mantovani et al., 2004), polarising stimuli cause a measurable shift in the metabolic profiles of macrophages (Zhu et al., 2015). M1

stimuli such as LPS induce a shift from oxidative metabolism to anaerobic glycolysis, which diverts intermediates such as citrate into biosynthesis of anti-microbial products such as reactive oxygen species (ROS), whereas M2 stimuli such as IL-4 have little effect (Haschemi et al., 2012).

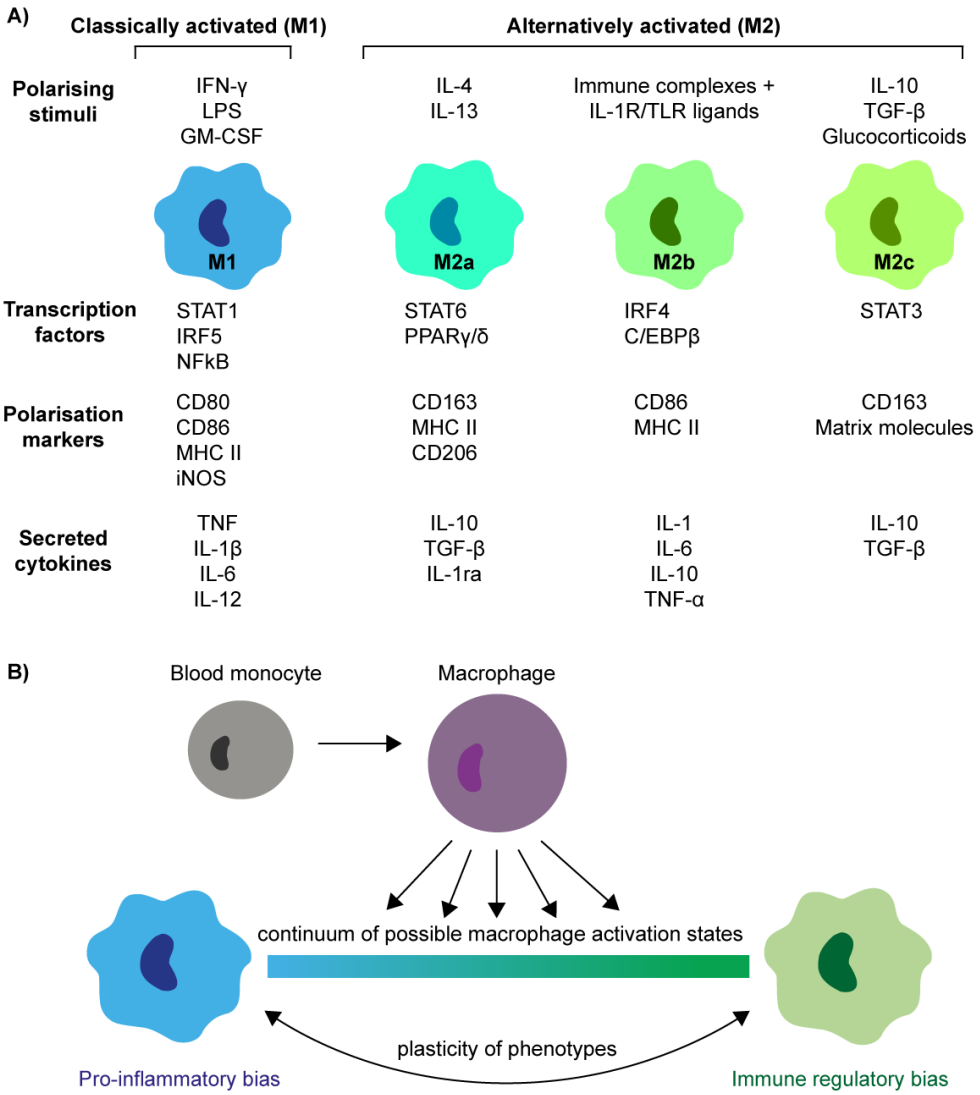

Figure 1.2 Cartoon representing a simplified model of human macrophage ontogeny and diverse phenotypes.
A) Monocyte-derived macrophages arise when blood monocytes are recruited from the circulation into the tissue and respond to the combination of inflammatory signals in the microenvironment to acquire an activation state appropriate to the nature of the immunological challenge. B) The myriad possible activation states may be simplified by thinking of it as a two-dimensional continuum with more inflammatory macrophages, previously defined as M1, at one end, and less inflammatory more reparative macrophages, previously known as M2, at the other.

Metabolism of the amino acid L- arginine is also regulated in polarised macrophages, with murine M1 macrophages showing upregulation of the inducible nitric oxide synthase (iNOS) that metabolises L-arginine to NO, which is required for macrophage cytotoxic activity (MacMicking et al., 1997), and L-citrulline. In contrast, M2 macrophages are characterized by upregulation of arginase-1 that converts L-arginine to ornithine and urea. Ornithine is required for synthesis of polyamines, which regulate cell growth, and is a precursor of proline required for collagen synthesis, and thus may be involved in tissue repair or remodelling processes (Rath et al., 2014). Arginase also depletes arginine and thus suppresses T cell activation (Munder et al., 2006) and reduces substrate available for iNOS.

It is unclear to what extent M1 and M2 classification systems represent real populations of macrophages *in vivo*, where cells are exposed to a plethora of immune stimuli and their complex phenotypes do not fall into discrete populations. Indeed, each combination of stimuli *in vitro* is associated with a unique transcriptomic signature, forming a spectrum of possible macrophage activation states (Xue et al., 2014), suggesting that macrophages *in vivo* adopt a unique activation state in response to the particular combination of immune stimuli in their microenvironment **(**Figure 1.2B**).** However, the M1/M2 paradigm retains some usefulness as representing different extremes on the spectrum of possible macrophage activation states, particularly *in vitro* where reductionist systems are used testing the effect of only a few polarising stimuli.

1.2.3 Macrophages in pathology

Regardless of the classification system used, there is no doubt that macrophages are highly diverse cells with a multitude of effector phenotypes that develop in response to the unique combination of immune stimuli they encounter (Zhou et al., 2014). In addition to their functional diversity, there is strong evidence for plasticity in macrophages suggesting they are not terminally differentiated cells as once thought but are able to adapt their phenotype in response to changes in their microenvironment (Locati et al., 2020). Failure to polarise appropriately at the onset of an immune response can lead to inability to clear pathogens, while failure to adapt phenotype to changes in microenvironment can result in impaired resolution of the immune response and thus chronic inflammation (Murray and Wynn, 2011).

Typically the first monocyte-derived macrophages recruited to a site of infection would adopt a 'M1' pro-inflammatory phenotype in response to bacterial (Kim et al., 2011; Rydstrom and Wick, 2007), viral, or protozoal (Sponaas et al., 2009) pathogens, and failure to recruit these cells leads to uncontrolled infection and failure to clear the pathogen (Dunay et al., 2008; Robben et al., 2005). M1 macrophages are specialised for eradication of intracellular pathogens through a high level of phagocytosis and antigen presentation to activate adaptive immune cells, and the respiratory burst that produces reactive oxygen species (ROS) and nitric oxide (NO). Mounting a more M2-like macrophage response enables pathogens to establish chronic infection and intracellular replication (Holscher et al., 2006; Iniesta et al., 2005) and can sometimes be engineered by the pathogen itself as a form of immune

escape, as has been demonstrated for protozoal parasites of the Leishmania genus (Kumar et al., 2018a; Kumar et al., 2018b).

However, M2 macrophage polarisation is essential in some contexts, for which the prototypic example is helminth infection (Horsnell and Brombacher, 2010). Helminth-derived glycans induce a strong Th2 response and thus IL-4/IL-13 production and alternative activation of recruited macrophages (Mohrs et al., 2001; Reece et al., 2006), promoting expulsion of the worm (Zhao et al., 2008) and repair of tissue damage (Urban et al., 1998). M2 polarisation is associated with the upregulation of a different repertoire of phagocytic receptors to classically activated macrophages, including MRC1, Dectin-1, and DC-SIGN as well as increased pinocytosis to acquire foreign antigen from large extracellular pathogens whose size impede their phagocytic uptake (Montaner et al., 1999).

M2-like reparative macrophages are also required for resolution of inflammation after infection or tissue injury to protect against the damage that would be caused by unchecked ‘M1’ macrophage activity such as production of ROS (Griffiths et al., 2017). Growth factors secreted by M2 macrophages promote myofibroblast differentiation and angiogenesis, while arginase metabolism promotes collagen deposition. Many infections are characterized by an initial pro-inflammatory phase where the macrophages express M1 markers, followed by a resolving phase in which macrophages adopt a more M2-like phenotype (Pearce and MacDonald, 2002). Spatial as well as temporal regulation of macrophage polarisation is also a feature of some pathologies such as tuberculosis granulomas, where M1 macrophages are

found in the inner region of granulomas close to the mycobacteria, whereas M2 macrophages are located on the fibrotic margins (Mattila et al., 2013). In many immune responses however, the traditional dichotomy is likely to be an oversimplification of the diverse macrophage activation states present: simultaneous detection of M1 and M2 markers has been reported (Bystrom et al., 2008), and the inherent plasticity of macrophages is evident in their transition from pro-inflammatory to pro-resolving over time (Arnold et al., 2007; Huang et al., 2015). Persistence of pro-inflammatory macrophages inhibits inflammation resolution, with higher levels of M1-associated cytokines detectable in chronic wounds than acutely resolving ones (Sindrilaru et al., 2011). However, excessive M2 activation can also be detrimental, with macrophage-driven ECM deposition leading to pathological fibrosis (Murray et al., 2011; Vidal et al., 2008).

Dysregulation of macrophage polarisation and functions is also thought to underlie many chronic non-infectious diseases (Bashir et al., 2016). Single nucleotide polymorphisms (SNPs) that lead to over-activation of IRF5, a transcription factor driving M1 polarisation (Krausgruber et al., 2011), have been associated with numerous autoimmune and inflammatory diseases including IBD (Dideberg et al., 2007) and RA (Dieguez-Gonzalez et al., 2008), suggesting that excessive pro-inflammatory activity of macrophages makes individuals more susceptible to developing these conditions.

Macrophages are important drivers of atherosclerosis where they accumulate in the vessel wall and take up lipids, becoming foam cells (Chistiakov et al., 2017).

Macrophages expressing M1 markers are mainly detectable in the lesion shoulder, which is unstable and prone to rupture, while a mixture of M1 and M2 markers are seen in the necrotic core. Symptomatic patients have more M1 macrophages during an acute ischaemic attack, whereas asymptomatic plaques have more M2 macrophages (Stoger et al., 2012).

In addition to their microbicidal activities, pro-inflammatory macrophages are also effective against transformed self cells and are protective in tumourigenesis where they amplify Th1 responses. However, macrophages isolated from advanced tumours often have a more M2-like, immunosuppressive phenotype that promotes growth and angiogenesis of the tumour whilst inhibiting anti-tumour immune responses (Gallina et al., 2006). It is now believed that tumours actively recruit monocytes (Qian et al., 2011) and that tumour-derived factors polarise these tumour-associated macrophages (TAMs) in order to support their own growth and metastasis (Zhang et al., 2011), with increased M2-like polarisation correlating with poor survival in cancer patients (Buscher et al., 2017).

Obesity is also associated with chronic inflammation, with adipose tissue macrophages switching from an M2 phenotype in lean adipose tissue to a pro-inflammatory population in obese adipose (Lumeng et al., 2007). Secretion of pro-inflammatory cytokines by these M1-like macrophages leads to insulin resistance.

1.3 Heparan sulfate proteoglycans (HSPGs)

The inflammatory response, including recruitment and polarisation of monocyte-derived macrophages, relies on a large number of soluble signalling molecules including chemokines, cytokines, and growth factors (Martinez and Gordon, 2014). In addition to changes in expression level, the activity of these inflammatory mediators is regulated by their interactions with extracellular molecules such as heparan sulfate proteoglycans (HSPGs) (Collins and Troeberg, 2019).

Heparan sulfate proteoglycans are ubiquitously expressed on cell surfaces, in extracellular matrices and basement membranes (Li and Kusche-Gullberg, 2016). They consist of long, linear heparan sulfate (HS) polysaccharide chains, covalently attached to one of several types of core protein, including: the four transmembrane syndecan family members, the seven GPI-anchored glypicans, and secreted extracellular matrix proteins such as agrin, perlecan, and type XVIII collagen (Annaval et al., 2020). There are some core proteins that are only decorated with HS chains in certain tissues or under certain conditions (e.g. TGFBR3, CD44) and are thus considered part-time HSPGs (Jackson et al., 1995; Segarini and Seyedin, 1988).

1.3.1 Synthesis of HSPGs

Biosynthesis of HS occurs in the cis/medial stacks of the Golgi by the concerted action of several enzymes (Figure 1.3) (Kreuger and Kjellen, 2012). It is initiated by formation of a xylose-galactose-galactose-glucuronic acid tetrasaccharide linkage region on specific serine residues on the core protein. This linkage region is common to both HS and the related sulfated polysaccharides chondroitin sulfate (CS) and

dermatan sulfate (DS). For HS biosynthesis, the exostosin-like (EXTL1-3) enzymes transfer an N-acetylglucosamine (GlcNAc) residue as the fourth residue of the tetrasaccharide (Kitagawa et al., 1999).

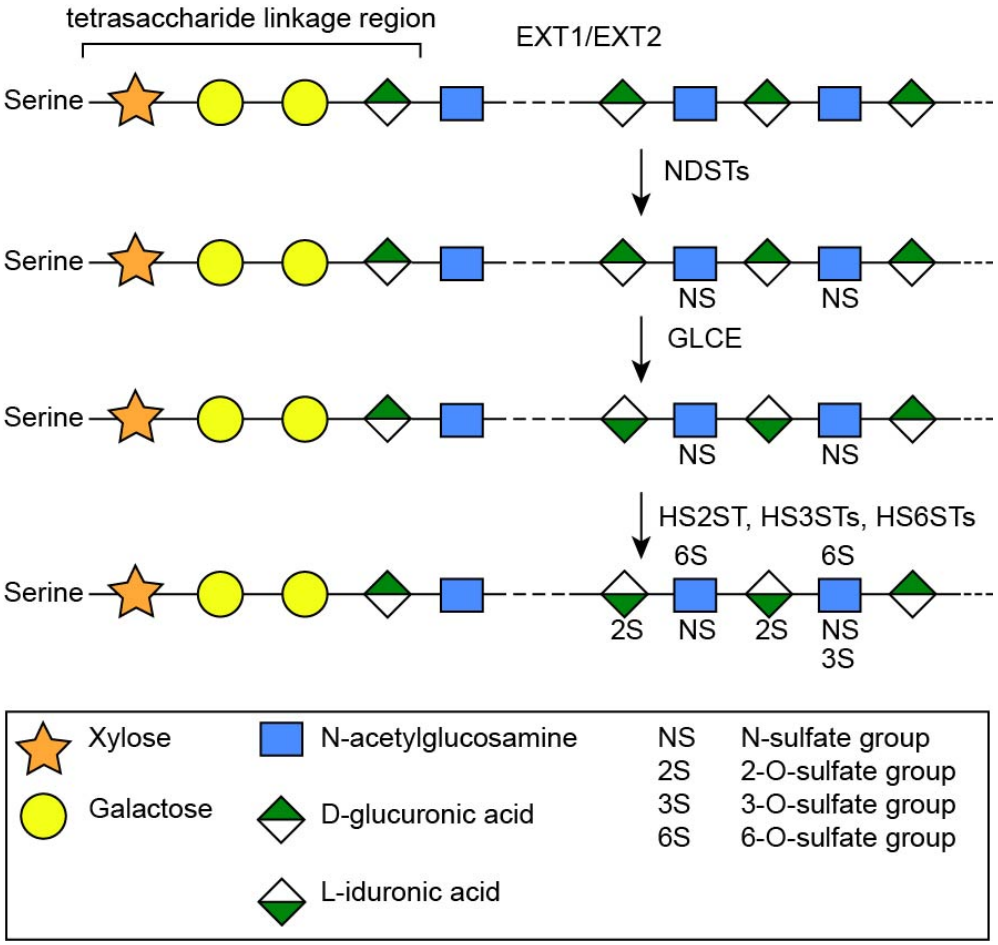

Figure 1.3 Schematic representation of heparan sulfate biosynthesis.
The linker tetrasaccharide sequence attaches to serine residues on the core protein and the HS backbone is elongated by the two polymerases EXT1 and EXT2 that alternately add N-acetylglucosamine and glucuronic acid. These disaccharide residues are subjected to a range of possible modifications by N-deacetylase/N-sulfotransferases (NDSTs), epimerase (GLCE) and 2-, 3- and 6-O-sulfotransferases, resulting in regions of high or low modification and many different HS epitopes.

After commitment to HS rather than CS biosynthesis by EXTLs, the HS polysaccharide backbone is elongated by alternate addition of glucuronic acid (GlcA) and N-acetyl-glucosamine (GlcNAc) by EXT1 and EXT2. These enzymes form a heterodimeric complex although both enzymes are capable of transferring both

sugars (Lind et al., 1998). The two protein isoforms appear to be non-redundant as mutations in either one lead to hereditary multiple exostoses (HME) (Zak et al., 2002). HS can be 50-250 disaccharide units long (20-100 kDa) (Xu and Esko, 2014), and there is evidence to suggest that some of the biosynthetic enzymes are also involved in regulating chain length. For example, siRNA knockdown of EXLT3 led to increased chain length, suggesting that one role of this isoform is chain termination (Busse et al., 2007).

Coincident with elongation of the backbone, HS undergoes sequential enzymatic modifications beginning with N-deacetylation N-sulfation of GlcNAc residues by the four NDST protein isoforms. For all sulfation reactions of HS, the sulfate donor is 3'-phosphoadenosine-5'-phosphosulfate (PAPS). Processive activity of NDSTs along an HS chain results in formation of extended N-sulfated domains (Carlsson et al., 2008). The observation that subsequent modifications occur in these N-sulfated regions suggests this reaction is a pre-requisite for the activity of other HS-modifying enzymes (Maccarana et al., 1996). However, some 6-O-sulfation occurs even when NDST1 and NDST2 have been deleted, so N-sulfation may promote further modification without being strictly necessary for enzyme activity (Holmborn et al., 2004). NDST1 and 2 are thought to have different activities as selective knockouts of these isoforms resulted in different sulfation patterns (Ledin et al., 2006).

The epimerase enzyme (GLCE) converts D-glucuronic acid to L-iduronic acid, which is a better substrate for 2-O-sulfation by the 2-O-sulfotransferase (HS2ST). GLCE and HS2ST co-localize in the Golgi and may interact physically and

functionally (Pinhal et al., 2001). Epimerization is reversible but precluded by 2-O-sulfation of iduronic acid or 6-O-sulfation of a neighbouring glucosamine. There are three 6-O-sulfotransferases (HS6STs) and seven 3-O-sulfotransferases (HS3STs) that are thought to have subtly different specificities. All three HS6ST protein isoforms preferentially act on N-sulfated glucosamine residues with an adjacent 2-O-sulfated IdoA residue (Jemth et al., 2003; Smeds et al., 2003). HS3ST protein isoforms show distinct expression levels in various human tissues but 3-O-sulfation remains the least studied HS modification, due largely to the lack of suitable standards for disaccharide analysis (Thacker et al., 2014). The most established role for 3-O-sulfotransferases is forming the anti-thrombin III binding site on heparin (Hao et al., 2019).

Mammalian HS biosynthetic enzymes are transmembrane proteins inside the Golgi. Multiple interactions between different enzymes of the HS biosynthetic pathway have been reported, such as the heterodimerization of EXT1 and EXT2 and colocalization of GLCE and HS2ST. Additionally, NDST1 and EXT2 were found to co-immunoprecipitate, and overexpression of EXT2 led to increased NDST1 expression and thus elevated N-sulfation (Presto et al., 2008). These observations led to the hypothesis of a ‘GAGosome’ (Esko and Selleck, 2002): a macromolecular complex consisting of multiple enzymes acting in concert to most efficiently synthesize HS. However, such a complex has not been isolated and its existence remains speculative.

Modification of HS occurs in a non-template-dependent manner and enzymatic reactions do not run to completion, resulting in highly heterogenous chains with regions of dense sulfation separated by relatively unmodified sequences and zones of intermediate sulfation at the junctions (Murphy et al., 2004). These highly sulfated regions are akin to heparin, which shares the same backbone as HS but with much more extensive sulfation and is attached to the core protein serglycin, predominantly in mast cells. The number of possible combinations of modification of HS disaccharides and the ordering of these into different motifs leads to enormous potential diversity, and thus HS is possibly the most information-dense structure in nature (Turnbull and Field, 2007).

1.3.2 HS structure is further regulated after synthesis

Uniquely among the modifications of HS, the 6-O-sulfate group can be removed post-synthetically after the GAG has been transported to the cell surface via its core protein (Hossain et al., 2010). Two isoforms of the endo-6-O-sulfatase exist in mammals and birds: SULF1 and SULF2, and they act to post-synthetically modify the fine structure of HS (Morimoto-Tomita et al., 2002) (Figure 1.4). They have been found both in the membrane fraction, indicating association with the cell membrane, and in conditioned medium, indicating diffusion away from the cell of origin (Lamanna et al., 2008), which suggests that SULFs may be able to modify both cell-associated and ECM HS chains. SULF activity could theoretically affect the activity of any ligand requiring 6-O-sulfated motifs for binding, and removal of 6-O-sulfate groups has been shown to regulate the signalling of morphogens such as Wnt

(Fellgett et al., 2015; Tran et al., 2012) and BMPs (Meyers et al., 2013) during development.

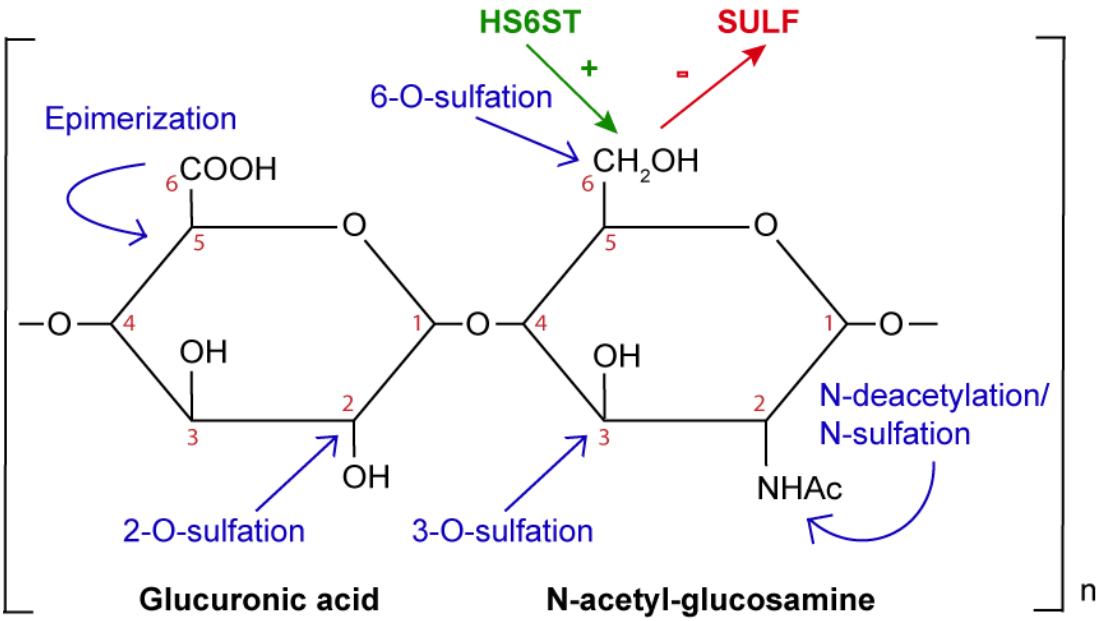

Figure 1.4 Schematic demonstrating the opposing roles of HS6ST and SULF enzymes in modulating the sulfation state of heparan sulfate.
In the Golgi apparatus, HS6ST1-3 transfer a sulfate group to the 6-O position of GlcNAc residues of newly synthesised HS chains. Once on the cell surface, the HS may have the 6-O-sulfate group removed through the activity of the extracellular sulfatase enzymes SULF1,2.

In addition, the HS chains can be cleaved by mammalian heparanase (HPSE), an endoglycosidase that cleaves HS within the chain at highly sulfated sites to form HS fragments of 10-20 sugar residues (Vreys and David, 2007). A second isoform has been identified but it is not catalytically active and antagonises the HS-degrading activities of HPSE (Levy-Adam et al., 2010). Cleavage of HS by heparanase releases growth factors sequestered in the ECM (Bashkin et al., 1989; Elkin et al., 2001) and the HS fragments retain biological activity in promoting growth factor signalling (Kato et al., 1998). As heparanase digestion also helps break down the physical barriers formed by HS, its expression is associated with processes involving cell

invasion such as leukodiapedesis (Bartlett et al., 1995; Vlodavsky et al., 1992), angiogenesis (Vlodavsky et al., 2000), and cancer metastasis (Jayatilleke and Hulett, 2020).

1.3.3 Functions of HSPGs

Besides being anchors for the biosynthesis and localization of HS chains, some core proteins have biological functions in their own right. The syndecan family play roles in cell adhesion and assembly of the ECM, as their HS chains can bind ECM components such as collagen, laminin, and fibronectin (Xian et al., 2010) and their cytoplasmic domains interact with the cytoskeleton and recruit signalling molecules (Lambaerts et al., 2009). Agrin is secreted by pre-synaptic motor neurones and regulates formation of the neuromuscular junction by promoting clustering of acetylcholine receptors (Li et al., 2018). Agrin expression has also been reported in T cells where this protein may play a role in the formation of immunological synapses between the T cell and the antigen-presenting cell, leading to T cell activation (Jury and Kabouridis, 2010). Agrin and perlecan are among the core structural components of basement membranes where they have mechanosensory properties and form reservoirs for growth factors (Melrose, 2020).

However, the vast majority of the potential biological activity of HSPGs comes from their ability to bind and regulate the activity of numerous soluble molecules through their HS chains. More than 400 protein ligands (Ori et al., 2011) are predicted to bind to the sulfated, heparin-like regions of HS, and collectively these HS-binding proteins are described as the heparan sulfate interactome. HS-binding proteins appear

to have arisen by convergent evolution as there is no one conserved HS-binding domain, sequence, or fold (Esko and Linhardt, 2009). Due to the highly anionic nature of HS, electrostatic interactions contribute substantially to protein binding but hydrogen bonding and van der Waal forces also play a role (Kjellen and Lindahl, 2018).

Particular sulfated motifs of HS facilitate binding of different ligands, so tissue-specific differences in HS structure would be expected to lead to preferential binding of particular HS ligands over others. It is thought that the fine structure of HS is regulated, at least in part, by the relative expression levels of the biosynthetic and modifying enzymes. Thus the changes in HS enzyme expression that have been reported in response to stimuli suggest that cells may dynamically regulate their HS structure in order to selectively bind ligands required for a particular response. This is supported by studies using antibodies against different HS motifs, which have shown different HS structures in different tissues (David et al., 1992; Dennissen et al., 2002), and changes in HS sulfation pattern during embryogenesis (Jenniskens et al., 2002). Moreover, changes to HS sulfation patterns have been reported during aging (Feyzi et al., 1998) and in the progression of various diseases (Chanalaris et al., 2019; Raman and Kuberan, 2010), suggesting that dysregulated HS biosynthesis or turnover may disrupt ligand interactions.

1.4 Mechanisms by which HSPGs regulate activity of their ligands

Consequences of ligand binding to HS include retention in the ECM to form a reservoir or gradient which is essential for growth factors during embryonic patterning (Yan and Lin, 2009) and for chemokines during leukocyte recruitment (Monneau et al., 2016). Binding to HS can result in juxtaposition of two proteins into close proximity with one another thus facilitating their interaction, as has been shown for thrombin and anti-thrombin III (Dementiev et al., 2004; Li et al., 2004). In some cases, binding to HS may promote binding to the cognate receptor, directly through binding both ligand and receptor, as is the case for FGF-2-FGFR (Chapter 1.4.2), or indirectly by localizing the ligand close to its receptor at the cell surface, as has been reported for IL-10 (Salek-Ardakani et al., 2000). However, if the HS-binding site and the receptor-binding site overlap then interaction with HS may inhibit signalling, as is predicted for IFN-γ (Chapter 1.4.1), giving HS the potential for both positive and negative regulatory roles depending on context. Other consequences of binding to HS include oligomerization, as has been shown for chemokines, and protection from proteolytic inactivation (Figure 1.5).

Heparan sulfate can regulate the activity of ligands *in trans*, where the HSPG is on a presenting cell and the ligand's cognate receptor is on another cell, such as the presentation of chemokines to migrating leukocytes. Alternatively, the binding of ligands to cell-surface HSPGs may affect the activity of the same cell through regulation *in cis*, as occurs for some cytokines and growth factors. Given that a large proportion of the known HS-binding proteins are immunologically-relevant molecules such as cytokines, chemokines, and growth factors, this proteoglycan is

expected to have a central role in the regulation of inflammation and immune responses. Despite the more than 400 known binding partners of HS, the sulfation requirements for binding to HS and consequences of binding for ligand activity have been studied for relatively few. Some of the better studied examples are described in the following sections.

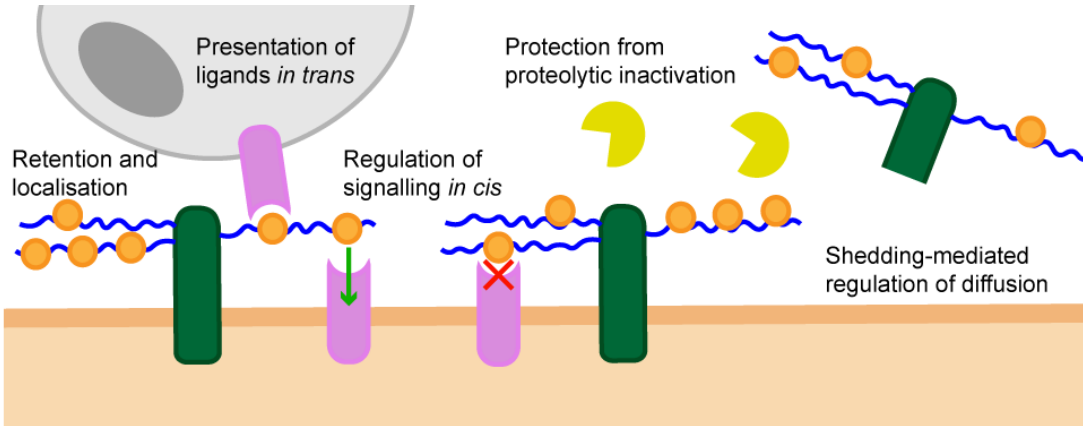

Figure 1.5 Heparan sulfate binding regulates ligand activity in multiple ways.
Binding to HS may restrict diffusion of ligands away from their site of production and form a local reservoir of bound ligand that can be liberated from the ECM when required. HS can regulate signalling *in trans* by presenting ligand to its target receptor on another cell, and *in cis* by promoting or inhibiting ligand interaction with receptors on the same cell as the HSPG. Interacting with HS can protect ligands from proteolytic inactivation. Shedding of the whole HSPG by cleavage of the core protein may result in HS-bound ligand diffusing away from the cell surface to a new site of action.

1.4.1 IFN-γ

IFN-γ has been shown to bind a basement membrane extract (matrigel) in a manner inhibitable by heparin or heparinase digestion, suggesting that HS is the ECM component responsible for binding (Lortat-Jacob et al., 1991). This retention of IFN-γ by HS may have a physiological role in protecting the cytokine from proteolytic inactivation, as free IFN-γ in the circulation is truncated and loses its antiviral activity, which is prevented by association with ECM HS or heparin (Lortat-Jacob et al., 1996). The HS-binding site of IFN-γ is located in the C-terminal portion of the

molecule, demonstrated by both monoclonal antibody blocking (Lortat-Jacob and Grimaud, 1991) and affinity analysis of IFN-γ mutants by NMR (Saesen et al., 2013). The domain of HS that supports IFN-γ binding, named the interferon-protected domain (IPD) due to its resistance to degradation when IFN-γ is bound, is highly sensitive to nitrous acid cleavage, indicating a high level of contiguous N-sulfated disaccharides (Lortat-Jacob et al., 1995). NMR studies of the IPD additionally revealed an abundance of 2-O- and 6-O-sulfate groups (Vanhaverbeke et al., 2004).

However, because the HS-binding site in the C-terminal domain of IFN-γ is also one of the polypeptide segments involved in receptor binding (Walter et al., 1995), it may be the case that HS competes with the IFN-receptor for IFN-γ binding. Indeed, surface plasmon resonance (SPR) analysis showed that pre-incubation of IFN-γ with heparin reduces its interaction with the IFN-γ receptor (Sadir et al., 1998), demonstrating the requirement for the HBD in receptor recognition. It remains unresolved whether HS acts as an inhibitor of IFN-γ signalling and whether this interaction is of biological relevance in cellular systems.

1.4.2 FGF-2

FGF-2 binds to heparin and HS with an absolute requirement for 2-O-sulfation, as only 2-O-sulfated heparin-derived oligosaccharides were able to bind FGF-2 on an affinity column (Ashikari-Hada et al., 2004), and disaccharide composition analysis of HS fragments from human skin fibroblasts segregated by affinity for FGF-2 showed that those fragments with the highest affinity for FGF-2 contained the

highest proportion of 2-O-sulfate groups (Turnbull et al., 1992). Moreover, selectively 2-O-desulfated heparins are significantly less potent than unmodified heparin or 6-O-desulfated heparin at displacing bound heparin from FGF-2 (Maccarana et al., 1993). HS also interacts with the FGF receptor and this interaction is necessary for the formation of a receptor-ligand complex as a soluble FGF-R construct fails to pull down FGF-2 unless heparin is also added (Ornitz et al., 1992). This dependence on heparin or HS is also true for cellular systems, as the FGF-receptor-ligand complex cannot be isolated from mutant CHO cells lacking the ability to synthesize HS (Yayon et al., 1991). This interaction is functionally important too for subsequent signal transduction as treatment of cells with heparinase or sodium chlorate to abolish HS sulfation significantly reduced FGF-2-dependent cell proliferation (Rapraeger et al., 1991). Unlike the sulfation requirements for FGF-2, binding of HS to the FGF receptor specifically requires 6-O-sulfation, as selectively 6-O-desulfated heparins cannot potentiate the binding of FGF-2 to its receptor (Rusnati et al., 1994) or induce proliferation (Pye et al., 1998). Exogenous heparin or HS can rescue FGF-2 signalling provided it contains 6-O- and 2-O-sulfates (Ferreras et al., 2012; Guimond et al., 1993). The crystal structure of FGF-2, FGF-receptor, and heparin suggests that in addition to promoting the interaction between growth factor and receptor, HS also facilitates dimerization of two receptor-ligand complexes (Pellegrini et al., 2000; Schlessinger et al., 2000), thus potentiating signalling and growth factor activity.

1.4.3 FGF-10

FGF-10 appears to require the presence of 2-O- and 6-O-sulfated HS for its activity during branching morphogenesis of several structures in development, with selective deletion of Hs6st1/2 and Hs2st reducing Erk activation and leading to stunted lacrimal glands (Qu et al., 2011). Exogenously added heparin can rescue FGF-10-dependent proliferation in HS-deficient cells with the requirement for 6-O-sulfate as well as 2-O- and N-sulfate groups (Patel et al., 2008). In contrast to the role of HS in facilitating receptor-ligand complex formation in FGF-2 signalling, the role of HS in FGF-10 activity appears to be in controlling its localization. Hs6st1 is predominantly expressed at the branching tips of lung buds, and although heparin rescues FGF-10 signalling after heparinase digestion it was found to result in generalised growth leading to cyst structures rather than directional budding (Izvolsky et al., 2003). Similarly, in the developing submandibular gland, 6-O-sulfated heparin promoted FGF10-dependent duct elongation, whereas 2-O- and N-sulfated heparin promoted end bud expansion (Patel et al., 2008). These results suggest that spatial and temporal changes to HS sulfation may regulate local growth factor signalling.

1.4.4 The TGF-β superfamily

Many proteins in the TGF-β superfamily bind HS, including TGF-β1 and TGF-β2, GDNF, and a number of the BMPs, with varied effects on their activity (Rider and Mulloy, 2017). Binding to HS may promote downstream signalling by retaining the growth factor close to its cell-surface receptor, which is supported by the observation that BMP-7 signalling requires cell-surface HS and this cannot be rescued in HS-deficient cells by soluble heparin (Irie et al., 2003). However, while binding to HS

may retain the growth factor in close proximity with its receptor, it may also increase its internalisation and thus inhibit signalling (Jiao et al., 2007). Interaction with HS may also inhibit signalling by competing with the receptor for growth factor binding, supported by the observation that non-HS-binding mutants of BMP-2 have increased activity (Ruppert et al., 1996). A number of physiological antagonists of this superfamily of growth factors also bind HS, such as the BMP inhibitor Noggin, which establishes morphogenetic gradients by spatially restricting BMP-4 activity (Paine-Saunders et al., 2002). Therefore HS may potentially regulate the TGF-β superfamily members through regulating their localisation and bioavailability as well as the localisation of their antagonist proteins, and the role of HS is likely to vary with tissue type, growth factor, and the combination of sulfate modifications present.

1.4.5 VEGF

There are multiple isoforms of VEGF-A that differ in the presence or absence of a heparin-binding domain, which is thought to result in different distribution in the microenvironment, with the HS-binding isoform VEGF-164 being retained by ECM HSPGs (Park et al., 1993). This spatial restriction is essential to create the concentration gradients that regulate blood vessel branching as mice expressing only the short non-HS-binding form of VEGF show impaired myocardial angiogenesis (Carmeliet et al., 1999), and displacing VEGF with heparin fragments inhibits microvessel sprouting (Norrby, 2000). In addition to restricting diffusion, binding to HS appears to be required for receptor interaction (Gitay-Goren et al., 1992). Chlorate-treated HUVECs show an impaired mitogenic response to VEGF but this can be rescued by heparin, suggesting that endogenous HS serves to promote

receptor-ligand interaction (Ono et al., 1999). The same study found that de-N-sulfated or de-6-O-sulfated heparin were ineffective at rescuing mitogenic responses, implicating these HS modifications in VEGF binding. HS may also be able to regulate the activity of VEGF in trans by presenting it to its receptor on another cell, supported by the finding that Ndst1-deficient cells did not respond to VEGFA-165 but that chimeric embryoid bodies enable wild-type cells to present signalling-competent growth factor to mutant cells (Jakobsson et al., 2006).

1.4.6 Anthithrombin-III

Anthithrombin-III (AT) is a serine protease inhibitor that circulates in the blood where it acts as an important regulator of the coagulation cascade by inhibiting thrombin, factor IXa and factor Xa. Binding to heparin or HS results in a conformational change that increases the binding of AT to target serine proteases (Huntington et al., 1996), and explains the clinical efficacy of i.v. heparin as an anti-coagulant. Inhibition of serine proteases is also accelerated by simultaneous binding of AT and its target proteases to heparin or HS, with the GAG acting as a template to approximate the two proteins and promote their interaction (Olson et al., 1992). The GAG structure with highest affinity for AT has been identified as a pentasaccharide sequence containing a critical 3-O-sulfate group and a 6-O-sulfated N-acetylglucosamine (Lindahl et al., 1983). This sequence is found in heparin and also in the heavily sulfated domains of cell-surface HS (Chen and Liu, 2005) in several tissues including vascular endothelium (de Agostini et al., 1990). Mutations disrupting the heparin-binding site of AT have been identified in patients with inherited thrombotic disorders (Lane et al., 1996).

1.5 Roles of HS in the immune system

Given that HS binds numerous chemokines, cytokines, and growth factors (Ori et al., 2011), it is expected that the fine structure of HS affects their binding, localisation and signalling, and thus regulates immune cell activity (Collins and Troeberg, 2019).

1.5.1 HS regulation of leukocyte recruitment

An important role of heparan sulfate proteoglycans in the immune response is facilitating migration of leukocytes to sites of infection or injury which they do directly by acting as ligands for leukocyte selectins and indirectly through regulating chemokine activity (Figure 1.6).

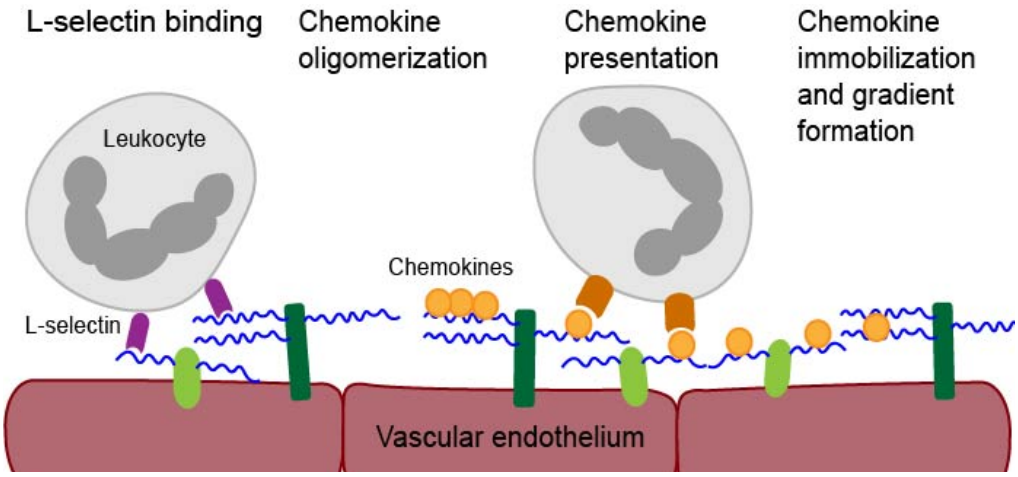

Figure 1.6 Heparan sulfate is involved in multiple steps of leukocyte recruitment.
L-selectin on leukocytes is capable of binding endothelial HS to facilitate leukocyte rolling and adhesion. Chemokines interact with HS chains on the lumenal surface which prevents them being washed away by the blood flow and enables formation of a gradient to guide leukocyte migration. HS binding also promotes chemokine oligomerisation and may be involved in presenting chemokine to its receptor.

1.5.1.1 HS as a selectin ligand

Selectins are expressed by both endothelial cells and the leukocytes that migrate across them, with leukocytes constitutively expressing L-selectin and endothelial cells upregulating P-selectin when activated. *In vitro* studies have shown that endothelial HS promotes leukocyte adhesion and rolling, as both were reduced by digestion with heparinase III (Rops et al., 2007) or genetic inactivation of genes in the HS biosynthetic pathway such as *EXT1* (Stoler-Barak et al., 2014). The observation that Ndst1-null and heparinase digested endothelium supports less binding of L-selectin suggests this leukocyte adhesion molecule may be a physiological ligand for HS (Celie et al., 2005; Rops et al., 2014). Supporting the hypothesis that L-selectin binding to HS is involved in leukocyte trafficking, pre-treating monocytes with an L-selectin-blocking antibody inhibited their adhesion to endothelial monolayers (Giuffre et al., 1997), and L-selectin-deficient mice show decreased neutrophil recruitment *in vivo* (Wang et al., 2002). Conditional deletion of *Ndst1* from endothelial cells and leukocytes in mice resulted in reduced thioglycollate-induced leukocyte homing but this was not seen in chimeras where wild-type mice received knockout bone marrow (Wang et al., 2005), providing further evidence that it is HS on the endothelium and not on the leukocyte that is critical for selectin-mediated transmigration.

1.5.1.2 HS regulation of chemokine activity

HS in the endothelial glycocalyx binds chemokines (chemotactic cytokines) and this ability to interact with GAGs is crucial for the function of certain cytokines *in vivo*. For example, mutants of MCP-1 (CCL2), RANTES (CCL5), and MIP-1β (CCL4)

that cannot bind GAGs are active in transwell migration assays *in vitro*, indicating they still interact functionally with their receptor, but do not induce cell recruitment when injected intraperitoneally into mice (Proudfoot et al., 2003). This indicates that retention by GAGs in the ECM is important for their ability to recruit leukocytes *in vivo*, and one reason for this is thought to be that interaction with GAGs prevents the chemokines being washed away by the blood flow. A transgenic mouse expressing non-HS-binding CXCL12 shows increased serum concentrations of this chemokine and reduced infiltration of leukocytes in response to acute ischaemic injury and thus reduced neovascularization (Rueda et al., 2012), supporting the importance of chemokine immobilization for localizing their activity. Additionally, the presence of HS on the vascular endothelium and ECM surrounding the blood vessels may enable the formation of a chemokine gradient to induce directional migration of leukocytes. HS from aortic and venous endothelial cells are structurally different (Lowe-Krentz and Joyce, 1991), with the HS modifications required for chemokine binding only present in post-capillary venules and small veins where leukocyte emigration occurs (Hub and Rot, 1998; Rot, 1992). Studies in which chemokines were injected demonstrated their accumulation on the luminal surface of ECs and in the ECM around smaller blood vessels which could be abolished by heparinase III treatment (Middleton et al., 1997), and fluorescent chemokine showed a gradient of staining with strongest staining closest to the vasculature which was not true for mutant chemokine lacking GAG-binding ability (Sarris et al., 2012). Swamping the directional signal provided by the chemokine gradient by addition of exogenous chemokine led to scattered DCs remote from the lymphatic vessel rather than directional migration (Weber et al., 2013).

Different chemokines have different affinities for heparin/HS (Dyer et al., 2016) and an intriguing possibility is that selective expression of different HS sulfate motifs in different tissues leads to varying abilities to retain different chemokines and thus provides a way of localizing particular chemokines in a system that might otherwise appear to have substantial redundancy (Dyer, 2020). Support for this hypothesis comes from studies showing that HS-binding mutants of chemokines, such as IL-8 (CXCL8), are less active than wild-type in a peritoneal recruitment assay, but more active in a lung recruitment assay, indicating the presence of different HS structures in these tissues with different affinities for this chemokine (Gangavarapu et al., 2012).

Moreover, CCL19 and CCL21, both ligands of the CCR7 receptor, have different affinities for HS which regulates their activity: CCL21 has the higher affinity interaction with HS so is immobilized on the endothelial surface, whereas the lower affinity of CCL19 for HS means this chemokine acts primarily in a soluble form (Schumann et al., 2010). CCL21 formed a chemokine gradient to guide DC migration but a cleaved form of CCL21 lacking the HS-binding region behaved like the soluble CCL19.

Another example of GAG affinity conferring functional differences is the observation that chemokines associated with monocyte recruitment, including CCL2, CCL3, CCL5, CCL7, and CXCL4 display a wide range of affinities for heparin (Dyer et al., 2016). These differences in binding affinities may help regulate chemokines that are produced locally at the site of inflammation but act in different

locations. For example, the low affinity of CCL7 for HS may mean it diffuses further from its site of production, consistent with its role in promoting monocyte egress from the bone marrow (Tsou et al., 2007).

Many chemokines form oligomers and this is thought to be essential to their function, as oligomerization-deficient mutants are ineffective at recruiting leukocytes *in vivo* (Proudfoot et al., 2003). Heparin has been shown to promote oligomerization of some chemokines in solution (Hoogewerf et al., 1997), which is dependent on their ability to bind GAGs as mutants of CCL2 (MCP-1) do not oligomerize on heparin. This ability to oligomerise may also increase the binding affinity for HS by increasing the number of HS-binding regions, as has been shown for CCL2 (Salanga et al., 2014). Oligomerization-deficient mutants of CCL5 and CXCL4 showed reduced affinity for heparin and HS by SPR and reduced binding to the surface of HUVECs (Dyer et al., 2016).

An unresolved question is whether chemokines are capable of simultaneously binding their receptor and HS, and whether HS is required for formation of the receptor-ligand complex as has been shown for FGF-2 (1.3.2), or rather localizes the chemokine near to its receptor but does not directly participate in binding. Some chemokines cannot simultaneously bind HS and their receptor because the two binding sites overlap, as has been shown for RANTES (CCL5), MIP-1α (CCL3) and MIP-1β (CCL4) (Graham et al., 1996; Laurence et al., 2001; Proudfoot et al., 2001). However, for chemokines such as CCL2, CXCL8 and CXCL12 the binding sites are spatially distinct so simultaneous binding is theoretically possible (Amara et al.,

1999; Chakravarty et al., 1998; Kuschert et al., 1998). It has been demonstrated for CXCL12 that simultaneous binding to HS and signalling via CXCR4 can occur, and that the presence of HS actually enhances signalling (Connell et al., 2016). However, for most chemokines, even those for which the binding sites do not overlap, steric hindrance is thought to prevent simultaneous interaction of the oligomers with HS and the receptor.

To explain the requirement for HS binding *in vivo* but not *in vitro*, and even for chemokines that cannot simultaneously bind HS and their receptor, a model known as the 'bridge model' was proposed in which oligomerization of chemokines on HS enables some subunits of the oligomer to interact with their cognate receptor (Figure 1.7). However, while CXC chemokine oligomers can bind their receptors (Veldkamp et al., 2008) CC chemokine dimers cannot because the receptor-binding site becomes inaccessible in the dimer interface (Qin et al., 2015). Moreover, effective therapeutic antibodies targeting chemokines such as CXCL10 recognise the soluble, non-GAG-bound form of the chemokine, while antibodies capable of recognising GAG-bound chemokine were ineffective at blocking migration (Bonvin et al., 2017). These observations, and the conceptual problem of how chemokines bound to HS in the thick glycocalyx layer reach their cognate receptors on leukocytes, led to the development of the 'cloud model' (Majumdar et al., 2014). In this model, endothelial HS retains chemokines locally in the tissue of origin and prevents them being washed away by the blood flow whilst also providing a sink of bound chemokine that is in equilibrium with the soluble form. Chemokine subunits that dissociate from the GAG-bound oligomers may either re-bind GAGs or bind their receptor (Graham et

al., 2019). Because of the varied sulfation requirements for binding of different chemokines and the effect of GAG chain density on chemokine affinity (Dyer et al., 2016), it may be the case that inflammatory changes to endothelial HS affect which chemokines can be retained or alter the equilibrium point between bound and unbound chemokine such that more becomes accessible to leukocyte receptors.

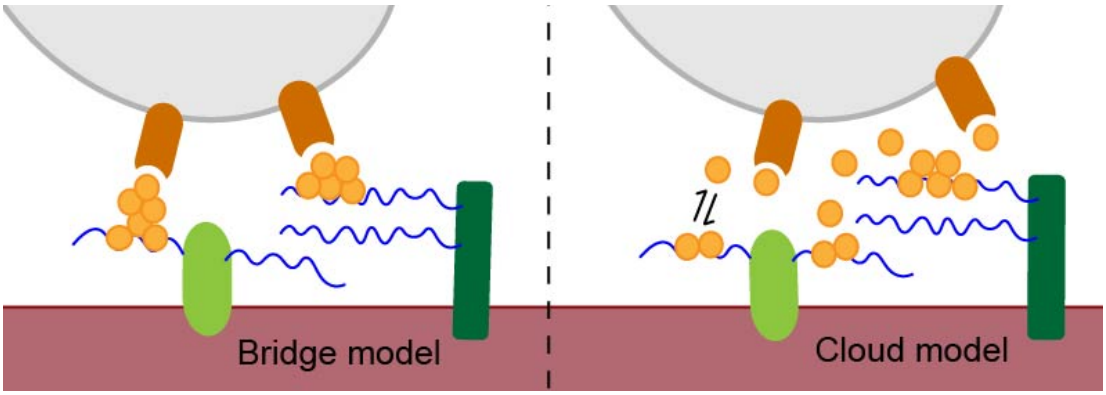

Figure 1.7 The bridge model and cloud model of chemokine-GAG interactions.
In the bridge model, chemokine oligomerization on HS chains enables some subunits to bind to the chemokine receptor on passing leukocytes, but steric hindrance makes it unlikely that chemokines can simultaneously bind their receptor and other chemokine monomers. In the cloud model, HS-binding retains chemokines near the site of production through successive rounds of disengaging and rebinding to GAGs, and provides a source of free chemokine that can activate chemokine receptors.

1.5.2 Leukocyte HS

Although most intensively studied in the context of stromal cells, HSPGs are expressed on the surface of leukocytes where they have the potential to regulate their various immune and inflammatory functions.

1.5.2.1 Roles of HS in phagocytosis

There is some evidence that cell-surface HSPGs participate in the internalisation of particles (Christianson and Belting, 2014) so may play a role in phagocytosis of

pathogens by both stromal cells and immune cells. Epithelial cells will bind and internalise beads coated with anti-HS antibodies and this is inhibited by heparinase III treatment, suggesting that interacting with HS is sufficient to trigger endocytosis of pathogens (Dehio et al., 1998). Human skin fibroblasts show binding and uptake of latex beads by a mechanism inhibitable by heparin or heparinase III, and CHO mutant cells with defective HS biosynthesis show reduced ability to internalise beads than HS-competent controls (Fukasawa et al., 1997). However, these studies were carried out in stromal cells and cell lines rather than leukocytes, so do not represent true phagocytosis where an array of specific receptors selectively recognise and internalise ligands (Stuart and Ezekowitz, 2005). Human PMNs were found to bind and internalise a HS-binding strain of *Helicobacter pylori* more efficiently than a non-HS-binding strain, and this uptake was inhibited by heparin (Chmiela et al., 1995), suggesting an HS-dependent mechanism of internalisation might be relevant to immune cells. However, the relative contribution of HS to uptake in the presence of canonical phagocytic receptors is unknown.

1.5.2.2 Regulation of cytokine signalling by leukocyte HS

Perhaps the best-studied example of HS as a co-receptor is that of HS binding to both FGF-2 and its receptor, promoting formation of the receptor-ligand complex (Chapter 1.4.2). The HS and FGF-R need not be on the same cell, however, and macrophages have been shown to present FGF-2 to target cells in a signalling-competent manner: HS-deficient BaF32 cells showed increased proliferation in response to suboptimal concentrations of FGF-2 when co-cultured with activated

macrophages, but not macrophages pre-treated with heparinase III (Clasper et al., 1999).

Binding of a ligand to leukocyte HS has the potential to promote or inhibit subsequent interaction with its cognate receptor on the same cell, depending on the ligand and whether its receptor and HS-binding sites overlap. For example, the B cell-stimulating cytokine, IL-7, binds to heparin and HS, and IL-7-induced B cell proliferation is inhibited by heparin (Clarke et al., 1995), indicating that binding of IL-7 to HS promotes simultaneous interaction with its receptor. In support of this, heparinase III treatment of primary B cells reduced both cell-surface binding of IL-7 and proliferation (Borghesi et al., 1999). Another B cell activating factor, APRIL, showed impaired ability to induce B cell signalling and proliferation in the presence of heparin or if its HS-binding domain was mutated (Kimberley et al., 2009), or if the B cells had been pre-treated with heparinase III (Sakurai et al., 2007). Moreover, B cells from Glce-/- mice, which lack iduronic acid residues of HS and are thus deficient in downstream O-sulfate modifications (Townley and Bulow, 2011), do not show cell-surface binding of APRIL or enhanced cell survival (Reijmers et al., 2011).

Similarly in monocytes, IL-10-induced upregulation of CD64 and CD16 are inhibited by addition of soluble fragments of HS or by chlorate treatment of the cells to prevent sulfation of GAGs (Salek-Ardakani et al., 2000). These data suggest that the interaction of IL-10 with cell-surface HSPGs serves to promote interaction with the IL-10-receptor, which is theoretically possible as the crystal structure of IL-10

with its receptor shows no overlap with the GAG-binding site of IL-10 (Josephson et al., 2001). However, it remains to be determined whether binding to HS directly promotes formation of the receptor-ligand complex, or whether HS facilitates IL-10 signalling indirectly by preventing diffusion of the cytokine away from the cell surface.

However, HS does not always promote ligand-receptor interactions, and some HS sulfated motifs may be inhibitory for the activity of certain cytokines. Selective deletion of *Ndst1* in murine macrophages resulted in hyperresponsiveness to IFN-β stimulation and increased production of pro-inflammatory cytokines (Gordts et al., 2014), suggesting that in normal macrophages N-sulfated HS serves to maintain a more quiescent state by sequestering this cytokine away from its receptor. It seems likely that those ligands whose HS- and receptor-binding sites overlap would experience an inhibitory effect of cell surface HS, whereas those cytokines able to bind both simultaneously might be positively regulated by HS. Further work is required to determine whether this is the case and to define the sulfated motifs required by each ligand for binding to HS.

1.5.2.3 Regulation of leukocyte HS structure in inflammation

For HS to be considered a true regulator of leukocyte functions its expression and structure must be altered during the course of an immune response and there is evidence that HS is differentially regulated according to the maturation state of the immune cell and in response to applied stimuli. For example, ligation of the pre-BCR induced upregulation of HS biosynthetic genes including Hs3st1 (Schebesta et al.,

2002), and plasma cells showed greater expression of HS biosynthetic enzymes than memory B cells (Bret et al., 2009). B cells stimulated with cytokines *in vitro* or isolated from virus-infected mice showed increased surface HS and augmented response to APRIL (Jarousse et al., 2011). Furthermore, ligation of the B cell receptor and CD40 results in a switch to the higher molecular weight form of CD44 decorated with HS chains (van der Voort et al., 2000) that is associated with promoting hepatocyte growth factor (HGF) signalling (van der Voort et al., 1999). Similarly, upregulation of this isoform of CD44 with HS attachment sites was observed upon maturation of monocytes to macrophages, which conferred the ability to present FGF-2 to BaF32 cells (Jones et al., 2000). T cells show a switch in agrin glycosylation, with resting T cells having highly glycosylated agrin and activation resulting in a switch to a weakly glycosylated form of agrin (Khan et al., 2001).

A handful of studies have shown that HSPG expression is also regulated during macrophage maturation and polarisation. Differential expression of HSPG biosynthetic machinery was observed in monocyte-derived macrophages polarised to M1 or M2 phenotypes, with M2 macrophages showing higher expression of sulfotransferases (HS2ST1, HS3ST1, HS3ST2) and more 2-O-sulfated disaccharides (Martinez et al., 2015). This regulation was shown to have functional consequences: M2 macrophages bound more FGF-2 and were more efficient at augmenting the FGF-2-dependent proliferation of a target cell line (Clasper et al., 1999), which is consistent with the role of HS in promoting FGF-2 signalling *in trans*. HSPG expression in monocytes and macrophages was also reported to be altered by activation by stimuli including LPS and TNF, which were found to upregulate

HS3ST3B (Sikora et al., 2016). Hypoxia reduced expression of several HS biosynthetic enzymes and the amount of HS (Asplund et al., 2009). HSPG expression in macrophages has, however, not been comprehensively profiled and functional consequences are poorly understood.

1.6 Project aims

The work described in this thesis was motivated by the paucity of data on regulation and function of macrophage heparan sulfate proteoglycans. Given that HSPGs are known to regulate many immune mediators, I hypothesised that their expression would be regulated during macrophage polarisation and activation, and that this would have functional consequences. My main aims were to:

1. Profile and compare the expression of HS-associated genes in monocyte-derived macrophages and macrophages polarised to represent different activation states that might occur *in vivo*
2. Test the role of macrophage HS in immunological functions, with a specific focus on 6-O-sulfate modifications driven by HS6ST1.

Chapter 2: Materials and methods

2.1 Reagents

RPMI 1640 and foetal bovine serum (FBS, qualified heat-inactivated, 10500-064) were from Gibco. Phosphate-buffered saline (PBS, 17-516F) and penicillin-streptomycin (Pen-Strep, DE17-6O2E) were from Lonza BioWhittaker. Bovine serum albumin (BSA, A7906) and ethylenediaminetetraacetic acid (EDTA) were from Sigma-Aldrich. Tween-20 (663684B) was from BDH. Ethanol (E/0665DF/17) and methanol (M/4056/17) were from Fisher Chemical. 96-well flat-bottomed plates (353072) and 150 mm cell culture plates (353025) were from Falcon.6-well plates (3516) and 12-well plates (3513) were from Corning Costar. Plasticware was from Fisherbrand and Sarstedt.

All graphs were generated in GraphPad Prism Version 7.0b for Mac OS X, GraphPad Software, San Diego, California USA

2.2 Cell isolation and culture

Platelet-depleted blood samples were obtained from healthy human donors who had given informed consent to NHS Blood and Transplant at the time of donation for the use of their blood in research. The 10ml buffy coat samples were made up to 100 ml with Hank's buffered saline solution (HBSS, Lonza, BE10-543F), and 25 ml of diluted blood residue pipetted carefully onto 20 ml of Ficoll Paque (Cytiva, 17-440-03) in 50ml Falcon tubes, with care taken to preserve the interface between these two liquids. Peripheral blood mononuclear cells (PBMCs) were enriched by density gradient centrifugation by centrifuging the blood/Ficoll tubes at 430g for 40 min with the brake off after which the white blood cell fraction is visible as a cushion at the

interface between the two liquids. PBMCs were pipetted off, washed three times in HBSS (with centrifugation at 500g for 10 min), then the pellet re-suspended in 30 ml RMPI/1% FBS (%V/V). Monocytes were then purified by countercurrent centrifugal elutriation with the loading rate set to 13 ml/min, and stepwise increases in the flow rate performed after all cells were in the chamber. Forward and side scatter of elutriated cells were monitored by flow cytometry, and monocytes collected when the purity exceeded 80%, which typically occurred at flow rates of 18-22 ml/min. The number of live monocytes was estimated by manually counting with trypan blue using a haemocytometer, and plated at $1x10^6$ cells/ml in 20 ml/150 mm plate, in RPMI 1640 supplemented with 5% heat-inactivated FBS and 1% Penicillin-Streptomycin (Pen-Strep) (%V/V), and recombinant human M-CSF (100 ng/ml; Peprotech 300-25, or was a kind gift from Sir Marc Feldmann, University of Oxford) (Schubert et al., 2019). Cells were cultured for 5 days at 37 °C, 21% O_2, 5% CO_2, after which medium was aspirated and adherent cells were lifted by gentle scraping in 1 mM EDTA in PBS.

2.3 Inflammatory stimulation of macrophages

After lifting and counting, live cells were re-plated at 1 $x10^6$/ml in RPMI 1640/10% FBS/1%Pen-Strep (%V/V) and allowed to re-adhere overnight. The following morning, medium was aspirated and replaced with fresh medium or that containing LPS (100 ng/ml, InvivoGen, tlrl-3pelps) (Higuchi et al., 2016), and/or IFN-γ (50 ng/ml, Peprotech, 300-02) (Rey-Giraud et al., 2012), or IL-4 (Peprotech, 200-04) and IL-13 (Peprotech, 200-13) (both at 20 ng/ml) (Rogers et al., 2019) and incubated for 24 h.

2.4 Sodium chlorate treatment

Fresh blood monocytes were cultured with M-CSF for 5 days as described above but with the addition of 30 mM sodium chlorate (ThermoFisher Scientific 44408) in the culture medium (Baeuerle and Huttner, 1986; Lucas and Mazzone, 1996). For macrophage sodium chlorate treatment, cells were re-plated on day 5 of M-CSF treatment as usual, with the addition of sodium chlorate at 30 mM in the culture medium for 24 h, and then polarisation for a further 24 h in medium containing sodium chlorate plus IFN-γ and/or LPS and IL-4/IL-13 as in Section 2.3 above.

2.5 siRNA knockdown

At the point of re-plating, between 1 and 10 $x10^6$ M-CSF-differentiated macrophages were suspended in 200 µl nucleofector buffer (Amaxa Human Macrophage Nucleofector kit, Lonza, VVPA-1008) containing 10, 50, or 100 nM siRNA targeting *HS6ST1* (Ambion Silencer Select siRNA, 4390824), or non-targeting control (Ambion Silencer Select negative control siRNA, 4390844), or no siRNA as a buffer-only control. Cells were electroporated using the setting Y-001 on the Amaxa nucleofector II, then adjusted to 1 $x10^6$ cells/ml RPMI 1640/10% FBS/1% Pen-Strep and incubated for the desired time point, either in flat-bottomed multi-well plates or on gelatin-coated coverslips (Section 2.13).

2.6 Cell lines

The monocytic cell lines U937 and THP1 (laboratory stocks, from American Type Culture Collection) were maintained in RPMI 1640/ 10% FBS/ 1% Pen-Strep and split regularly. To induce maturation to a more mature macrophage-like phenotype, cells were stimulated with phorbol 12-myristate 13-acetate (PMA, 100 ng/ml, Sigma-

Aldrich P1585) overnight. After siRNA electroporation of THP1, cells were re-suspended in media with or without PMA and cultured for 24, 48, or 72 h.

2.7 Crystal violet viability assay

After electroporation with siRNA, primary cells were adjusted to 1 x10^6 cells/ml in 96-well flat-bottomed plates and cultured for 24, 48, or 72 h. Media were aspirated, cells washed in PBS, and incubated in crystal violet solution of 0.5% crystal violet (Sigma-Aldrich, C3886) and 20% methanol in H_2O for 20 min at room temperature. Cells were washed 4 times with 200 µl deionized water per well and the plates allowed to dry overnight before cells were solubilized with 100 µl methanol per well and absorbance at 570 nm quantified using a FluoSTAR Omega plate reader (BMG Labtech). Absorbance readings were averaged across three replicate wells per condition and expressed as a percentage of the untreated control for each donor.

2.8 MTS viability assay

At the relevant time point, 20 µl/well of (3-(4,5-dimethylthiazol-2-yl)-5-(3-carboxymethoxyphenyl)-2-(4-sulfophenyl)-2H-tetrazolium) (MTS) reagent (Promega, G109A) was added to 1 x10^5 cells grown in 96-well flat-bottomed plates. Plates were returned to the incubator for 30 min, then the absorbance at 495 nm read using a FLUOStar Omega plate reader (BMG Labtech). Absorbance readings were averaged across three replicate wells per condition and expressed as a percentage of the untreated control for each donor.

2.9 RNA isolation

RNA was isolated using the RNeasy minikit (QIAgen 74106) according to manufacturer's instructions, including the optional DNase digestion step using the RNase-free DNase set (Qiagen 79254). The eluted RNA was quantified on a Nanodrop 100 spectrophotometer (ThermoFisher Scientific). Purity and quality of the RNA samples were determined by assessing the concentration, and optical density ratio of 260/280 and 260/230 to indicate contamination by protein and salt, respectively. Yields were typically in excess of 30 ng/µl per 1 $x10^6$ primary macrophages, with 260/280 values between 1.6 and 2.0 being considered sufficiently pure.

2.10 Gene expression quantification by qPCR

100-500 ng total RNA was reverse transcribed to cDNA with a High-Capacity cDNA Reverse Transcription Kit (Applied Biosystems 4368814) according to manufacturer's instructions. For comprehensive profiling of HS-associated gene expression, cDNA was amplified on a custom-designed TaqMan array card (ThermoFisher Scientific, 4342253) (Table 1). The abundance of target genes was expressed as a fold change relative to the average expression level in monocyte samples using the delta delta Ct method, with the average of the housekeeping genes *18S* and *GAPDH* used for normalization. Hierarchical clustering of relative expression data to form a heatmap was performed in R using RColorBrewer and gplots β using Canberra distance as the clustering metric. Code was adapted from (Chanalaris et al., 2019). For individual qPCRs, cDNA was amplified in 384-well plates (Greiner Bio-One Sapphire 785290) with 2x Universal PCR mastermix (Applied Biosystems 4304437) and the relevant TaqMan probe (ThermoFisher

Scientific) (Table 2). Where genes from the array were run to confirm expression patterns, the same probe sets were used for individual qPCRs as had been included in the array (Table 1). *18S* and *GAPDH* were again used as normalizing control genes, with *RPLP0* additionally used in some experiments.

Table 1. Human primer/probe sets used in TaqMan array cards

Chain elongation		**6-O-sulfotransferases**	
EXT1	Hs00609162_m1	HS6ST1	Hs00757137_m1
EXT2	Hs00181158_m1	HS6ST2	Hs02925656_m1
EXTL1	Hs00184929_m1	HS6ST3	Hs00542178_m1
EXTL2	Hs01018237_m1	**Editing enzymes**	
EXTL3	Hs00918601_m1	HSPE	Hs00935036_m1
N-deacetylase/N-sulfotransferases		HSPE2	Hs00222435_m1
NDST1	Hs00925442_m1	SULF1	Hs00290918_m1
NDST2	Hs00234335_m1	SULF2	Hs01016476_m1
NDST3	Hs01128584_m1	**Core proteins**	
NDST4	Hs00224024_m1	AGRN	Hs00394748_m1
Glucuronyl C5-epimerase		GPC1	Hs00892476_m1
GLCE	Hs00392011_m1	GPC2	Hs00415099_m1
2-O-sulfotransferase		GPC3	Hs01018936_m1
HS2ST1	Hs00202138_m1	GPC4	Hs00155059_m1
3-O-sulfotransferases		GPC5	Hs00270114_m1
HS3ST1	Hs00245421_s1	GPC6	Hs00170677_m1
HS3ST2	Hs00428644_m1	HSPG2	Hs00194179_m1
HS3ST3A1	Hs00925624_s1	SDC1	Hs00896423_m1
HS3ST3B1	Hs00797512_s1	SDC2	Hs00299807_m1
HS3ST4	Hs00901124_s1	SDC3	Hs01568665_m1
HS3ST5	Hs00999394_m1	SDC4	Hs00161617_m1
HS3ST6	Hs03007244_m1	TGFBR3	Hs01114253_m1
Normalizing genes			
18S	Hs99999901_s1		
RPLP0	Hs99999902_m1		
GAPDH	Hs99999905_m1		

Table 2. TaqMan primer/probe sets used for individual qPCRs

Gene name	Primer/probe set	Gene name	Primer/probe set
CD206 (MRC1)	Hs00267207	CCL2	Hs00234140
CD209 (DC-SIGN)	Hs01588349	CXCL8	Hs00174103
VEGFA	Hs00900055	CXCL12	Hs02829207
CD274 (PD-L1)	Hs00204257	CXCL1	Hs00236937
TGFB1	Hs00998133	IL6	Hs00174131
IL1B	Hs01555410	NOS2	Hs01075529

2.11 Gel electrophoresis and immunoblotting

Cells were lysed in SDS buffer (0.2 g SDS, 5.0 ml 1M Tris.HCl pH 6.8, 1 ml bromophenol blue (0.1%), 4 ml glycerol, 880 µl of 0.5 M EDTA) containing a protease inhibitor cocktail (Sigma P8340) at 1:10 and 5% beta-mercaptoethanol (VWR 0482). For analysis of phosphorylated proteins, sodium orthovanadate (Sigma S6508) was also added (1:100) as a phosphatase inhibitor. Serum-free conditioned medium was collected from the same cells and soluble proteins concentrated by adding 100 µl trichloroacetic acid (TCA, Sigma 10699) and 1 µl FBS per 1 ml of conditioned medium. After incubation at 4 °C overnight, samples were centrifuged (13000 rpm, 15 min), the supernatant discarded and the pellet resuspended in 100 µl reducing SDS sample buffer. All samples were boiled for 5 min then briefly centrifuged before equal volumes were loaded into wells of 10 % Tris-Glycine gels (Table 3) and run at 125 V for 2.5 h. PageRuler prestained protein ladder (ThermoFisher Scientific 26616) was run simultaneously and used as a molecular weight marker. Following gel electrophoresis, proteins were transferred to PVDF membranes using the TransBlot Turbo apparatus (BioRad 10026938) and transfer kit (BioRad 170-4272) according to manufacturer's instructions with the 7 min mixed molecular weight setting. Membranes were blocked for at least 1 h in 5% milk

(VWR 84615) in PBS, or 5% BSA for analysis of phosphoproteins, then incubated in primary antibody at 1:1000 (except for pERK and pSTAT1 where 1:2000 was optimal) in relevant blocking buffer overnight at 4 °C on a shaker. The following morning, membranes were washed for 90 min with PBS/0.1% Tween-20 before incubation in the relevant secondary antibody (1:5000 or 1:10000 for anti-mouse) in blocking buffer for 1 h at room temperature on a shaker. Membranes were washed for 90 min with PBS-Tween then for 5 min with PBS before ECL substrate (Bio-Rad Clarity Western ECL substrate 170-5061) was applied for 5 min. Excess substrate was removed by gentle squeezing under plastic film then the membrane transferred to a cassette and exposed to photographic film (ThermoFisher CL-Xposure film 34090) in the dark room with a range of exposure times to determine the optimal signal. For antibodies against total STAT1 and STAT6 it was necessary to use Can Get Signal solution 1 for primary antibody and solution 2 for secondary antibody (2BScientific NKB-101T), which were used in place of blocking buffer for antibody incubation. Developed films were imaged on a scanner and the bands quantified using Phoretix 1D software (TotalLab Quant).

Table 3. Recipe for 10% Tris-glycine gels for SDS-PAGE.

Recipe for 10% Tris-glycine gels	
Lower gel	Volume (ml)
H_2O	15.90
30% acrylamide mix (Severn Biotech 20-2100-10)	13.30
1.5M Tris.HCl (pH 8.8) (made from Trizma base Sigma T1503)	10.00
10% SDS (Sigma L3771)	0.40
10% APS (Sigma A3678)	0.40
Tetramethylethylenediamine (TEMED) Sigma T9281	0.02
Upper gel	
H_2O	8.20
30% acrylamide mix	2.00
1.0M Tris.HCl (pH 6.8)	1.50
10% SDS	0.12
10% APS	0.12
TEMED	0.012

Table 4. Antibodies used for western blotting, immunocytochemistry, and flow cytometry

Antibody	Supplier	Catalogue number	Dilution
rabbit anti-HS6ST1	Abcam	ab106195	1:100
isotype control for rabbit anti-HS6ST1	Abcam	ab171870	1:100
mouse anti-actin	Abcam	ab3280	1:5000
mouse anti-pSTAT1	Invitrogen	33-3400	1:2000
rabbit anti-STAT1	Cell Signaling Technology	9172S	1:1000
rabbit anti-pSTAT6 (Y641)	Cell Signaling Technology	D859Y	1:1000
rabbit anti-STAT6	Cell Signaling Technology	9362S	1:1000
rabbit anti-p44/42 (pERK)	Cell Signaling Technology	4370S	1:2000
anti-mouse-HRP	Abcam	ab6728	1:400
anti-rabbit HRP	Abcam	ab6721	1:400
anti-CD16 APC-Vio770	Miltenyi biotech	130-098-102	1:100
anti-CD14 PerCP	Miltenyi biotech	130-094-969	1:100
anti-CD68-PE	Miltenyi biotech	130-099-685	1:100
anti-CD80-PE	Miltenyi biotech	130-117-795	1:100
anti-CD64-APC	BD Pharmingen	561189	1:100
anti-CD163-APC	Miltenyi biotech	130-100-612	1:100
anti-CD209-PE	Miltenyi biotech	130-099-707	1:100
anti-mouse IgM Alexafluor 488	Biolegend	406522	1:500
anti-mouse IgG Alexafluor 488	Biolegend	405319	1:500
anti-rabbit AlexaFluor488	Invitrogen	A11034	1:500
anti-heparan sulfate 3G10	amsbio	370260	1:100
anti-heparan sulfate 10E4	amsbio	370255	1:100

2.12 Flow cytometry

Conditioned medium was aspirated and cells incubated in 100 µl of 2 mM EDTA in PBS per well of a 12-well plate for 10 min at 37 °C before being gently scraped with a cell lifter and centrifuged (500g, 5 min). Cells were re-suspended in PBS containing 1:100 eFluor450 fixable viability dye (Invitrogen 65-0863-14) at 100 µl per $1x10^6$ cells and incubated on ice for 20 min. Cells were washed in PBS then centrifuged (500g, 5 min) and re-suspended in Fc-receptor blocking reagent (Miltenyi 130-059-901) diluted at 1:5 in the recommended buffer (0.5% BSA and 2 mM EDTA in PBS) and incubated on ice for 15 min. For intracellular staining, cells were washed in PBS, centrifuged (500g, 5 min) and re-suspended in 100 µl Cytofix/Cytoperm reagent (BD Biosciences 554715) for 20 min then washed in 1ml Cytofix/Cytoperm wash buffer before incubation with antibody (Table 4) at 1:100 in

Cytofix/Cytoperm wash buffer for 30 min on ice. Cells were washed again in 1ml Cytofix/Cytoperm wash buffer, centrifuged (500g, 5 min) and resuspended in 100 µl of PBS.

For cell-surface staining, after FcR blocking the cells were washed in 1ml of PBS then centrifuged (500g, 5 min) and re-suspended in PBS containing antibody (Table 4) at 1:100 with 100 µl per sample and incubated on ice for 30 min. Cells were washed again in PBS, then the pellet resuspended in 100 µl 4% paraformaldehyde solution (PFA, Sigma F8775) and incubated at room temperature for 10 minutes before a final wash in PBS and pellets resuspended in 100 µl PBS.

For unconjugated antibodies, a second antibody incubation step was included for the fluorescently-labelled secondary antibody (Table 4). Different concentrations of primary and secondary antibody were trialled for optimum results. Samples were stored at 4 °C before flow cytometry analysis on an LSR II (BD Biosciences). Data were analysed using FlowJo software (BD Biosciences, Version 10.7.1 for Mac).

2.13 Immunostaining and confocal microscopy

After 5 days culture in M-CSF, monocyte-derived macrophages were transferred to 12-well plates containing gelatin-coated 18 mm coverslips (VWR 631-0153). Gelatin coating was done by incubating coverslips on droplets of 0.1% w/v gelatin (Sigma G2625) dissolved in H_2O for 20 min at room temperature, and then transferring the coverslips to droplets of 1% glutaraldehyde in H_2O for a further 15 minutes. Coverslips were then transferred to droplets of 1 M ammonium chloride in H_2O and incubated for 15 minutes, before being placed gelatin face up in 12-well plates containing 70% ethanol to sterilise the coverslips and kept at 4 °C. When ready to use, ethanol was aspirated and coverslips washed several times in PBS and once in

RPMI before transferring to fresh 12-well plates and adding cells. Cells were allowed to re-adhere overnight, or were incubated for 24, 48, or 72 h time points, before medium was aspirated and cells were washed in ice-cold PBS. Coverslips were fixed in 4% PFA (Sigma F8775) for 10 minutes at room temperature, washed in PBS, then blocked in 5% goat serum (Sigma G6767) 3% BSA in PBS for 1 h at room temperature. Coverslips were washed again in PBS and cells permeabilised in 0.1% Triton-X (BDH 306324N) in PBS for 15 min at room temperature, then washed in PBS. Primary antibody targeting HS6ST1 (Abcam ab106195) was added at 1:100 in block (5% goat serum 3% BSA), or cells incubated in blocking solution alone for no-primary control staining, and incubated overnight at 4 °C. The following day, coverslips were washed in PBS and incubated with secondary antibody (goat anti-rabbit AlexaFluor 488 Invitrogen A11034) at 1:500 for 1 hour at room temperature. Slides were washed in PBS then stained with 4'6-diamidino-2-phenylindole, dihydrochloride (DAPI, Sigma-Aldrich, D9542) at 1:1000 and phalloidin-AlexaFluor568 (Invitrogen A12380) at 1:40 in blocking buffer for 1 hour at room temperature. Coverslips were washed in PBS and mounted on slides using 5 µl mounting medium (Vectashield anti-fade mounting medium H-1000) per coverslip and edges sealed with nail varnish. Slides were kept in the dark at room temperature until imaging.

Images were captured on an Olympus confocal microscope (FV1200) using the 60x objective lens under oil. For single plane images, scan speed was set at 10 µl/pixel and laser power set to minimize both background staining and photo bleaching, and kept consistent throughout each experiment. For z-stack images, the upper and lower bounds were set such that the phalloidin staining was strongest in the middle slices

and weaker at the extremes. Multiple slices were taken per field at consistent intervals in the z-plane.

Image analysis was performed using ImageJ software (Fiji Version 1.0 for Mac OS X). All quantification was performed on raw unadjusted images. For quantification of total cellular HS6ST1 staining, z-stacks were projected into a single image using the z-project tool in ImageJ and the sum slices setting. The freeform drawing tool was used to draw around the outline of each cell in the phalloidin-AlexaFluor568 channel, then the shortcut command-shift-E used to paste this outline to the corresponding position on the compressed image of the HS6ST1-AlexaFluor488 channel and the integrated density measured. The same outline was used to measure integrated density of an area the same size adjacent to the cell but not including parts of any other cells and this value subtracted for background correction.

2.14 Cytokine array

Conditioned media were collected from primary human macrophages 24 h after HS6ST1 knockdown by siRNA electroporation, and applied to Proteome Profiler Array XL (R&D systems ARY022B) according to manufacturer's instructions. For each donor, media from cells treated with 50 nM si*HS6ST1* and non-targeting siRNA were developed on the same film with a 5 min exposure. The films from all three donors were then scanned and quantified using TotalLab Quant software. The average of the two duplicate pixel intensity values was plotted on a dot-line graph. For the heatmap, the pixel intensity ratio was calculated by dividing the average si*HS6ST1* sample intensity value by the average non-targeting siRNA sample intensity value for each donor for each cytokine – these fold changes were then

logged to the power of 2 to more symmetrically distribute the values around 0. The heatmap was generated in GraphPad Prism.

2.15 Phagocytosis assays

Monocyte-derived macrophages were incubated at 37 °C with fluorescently-labelled *E. coli* BioParticles (Invitrogen E2861) or zymozan Bioparticles (Invitrogen Z23373), or latex beads (Polysciences 17154-10) that had been incubated in FBS for 24 h then washed and resuspended in PBS. For some experiments, corresponding control samples were incubated on ice. Media containing unbound particles were aspirated and cells lifted by 10 min incubation in 2 mM EDTA/PBS and gentle scraping with a cell lifter. Cells were centrifuged (500g, 5 min) and re-suspended in 100 µl PBS containing eFluor450 fixable viability dye (Invitrogen 65-0863-14) at 1:100, then incubated on ice for 20 minutes. Cells were washed in 1 ml PBS then resuspended in 100 µl 4% formaldehyde solution (PFA, Sigma F8775) for 15 min at room temperature. Cells were washed again and resuspended in 100 µl PBS and refrigerated until acquisition on an LSR II flow cytometer.

2.16 Migration assays using transwells and Celigo

THP1 cells were adjusted to 1 x10^6 cells/ml in culture media and 50 µl transferred to the upper chamber of HTS Transwell-96 inserts with 8.0 µm diameter pores (Corning 3374). The lower reservoir contained 235 µl media with or without MCP-1 (Peprotech 300-04). 50 µl cell suspension for each sample was added directly to 235 µl media for positive controls. Plates were incubated at 37 °C for 4 hours, with 10 µl Hoechst (Life Technologies, 33432) added to each of the lower reservoirs or positive control wells for the final 30 minutes. 150 µl from each of the lower reservoirs or positive control wells was transferred to optical bottomed plates (Griener 655090)

and the number of post-migratory cells per well quantified by the Celigo automated plate reader (Celigo Image Cytometer, Nexcelom Bioscience).

For primary human monocyte-derived macrophages, after 5 days in culture with M-CSF (100 ng/ml) the cells were lifted and adjusted to 1 x10^6 cells/ml in RPMI/1% FBS/1% Pen-Strep and 100 µl cell suspension transferred to the top well of transwell inserts. The lower reservoir contained 500 µl with or without 500 pM MCP-1. After 24 h incubation at 37 °C, the upper side of the transwell membrane was vigorously scraped with a cotton-tipped swab moistened in PBS to remove adherent but non-migrated cells, and then the post-migratory cells on the underside of the membrane were stained with 300 µl/well crystal violet solution for 20 mins. Inserts were rinsed under DI water until the water ran clear and then allowed to dry before being imaged on an optical microscope.

2.17 Enzyme-linked immunosorbent assay (ELISA)

For quantification of secreted proteins in conditioned media of macrophages, conditioned media collected at relevant time points was applied to sandwich ELISA kits for TNF (BD OptEIA 555212), and IL-10 (Biolegend ELISA Max Human IL-10 430604) according to manufacturers' instructions. Sandwich ELISAs for MCP-1 (CCL2) and IL-8 (CXCL8) were formed by coating 96-well MaxiSorp plates (Thermo Scientific 439454) with capture antibodies against MCP-1 (BD Pharmingen 555055) or IL-8 (BD Pharmingen 554716) at 1:500 at 4 °C overnight on a shaker. Wells were washed 3 times with 200 µl/well PBS-0.05% Tween-20 then blocked in 200 µl/well 2% BSA and incubated for 1 hour at room temperature on a shaker. Plates were washed 3 times in PBS-tween then diluted samples or dilution series of cytokine standards for MCP-1 (Peprotech 300-04) or IL-8 (Peprotech 200-08) in

0.5% BSA/PBS-tween applied and incubated for 2 hours. Plates were washed 3 times in PBS-tween then incubated with biotinylated detection antibodies against MCP-1 (BD Pharmingen 554664) and IL-8 (BD Pharmingen 554718) at 1:1000 in 0.5% BSA/PBS-tween. After washing 3 times in PBS-tween, plates were incubated with streptavidin-HRP at 1:400 in 0.5% BSA/PBS-tween for 1 hour at room temperature on a shaker. Plates were washed 3 times in PBS-tween before substrate was applied. All ELISAs were developed using the OptEIA TMB substrate reagent set (BD 555214) and the reaction stopped by addition of 2 N H_2SO_4, after which absorbance was immediately read at 450 nm and at 570 nm for plate correction using a FluoSTAR Omega plate reader from BMG Labtech. ELISAs were performed in duplicate for each sample and the average absorbance value used.

2.18 Statistical analysis

Data were analysed in Graphpad Prism software by either one-way unpaired ANOVA with multiple comparisons using the two-stage linear step-up procedure of Benjamini, Krieger and Yekutieli to correct for multiplicity, or paired t-tests, as indicated in the figure legentds. Data sets with 4 or more values were tested for normality using the Shapiro-Wilk normality test before performing these parametric tests; where data sets had 3 or fewer values, normality was assumed. For t-tests, a p-value of less than 0.05 was considered significant. For ANOVAs, the q values represent p values for each comparison that have been adjusted for the false discovery rate during multiplicity correction, and a value of less than 0.05 is considered significant.

Chapter 3: Polarisation of human macrophages and profiling of HS-associated gene expression

3.1 Introduction

Because of the key role of HS in regulating numerous cytokines and chemokines as well as growth factors, the expression of HS by immune cells is potentially of great importance to immune regulation. As discussed in Section 1.5.3 of the Introduction, macrophage heparan sulfate has not been thoroughly investigated but HS is known to be involved in the signalling of many cytokines and growth factors, and its biosynthesis in macrophages is regulated by inflammatory stimuli (Martinez et al., 2015; Sikora et al., 2016). However, these previous reports did not comprehensively profile expression of all the core proteins and enzymes required for HS biosynthesis so the full extent of HSPG expression and the potential myriad roles of these GAGs in macrophage function are unknown. My first aim was therefore to investigate which HS associated genes are expressed by primary human macrophages, and how these expression levels differ in macrophages exposed to different immunological stimuli. I felt it was important to do this in a primary cell rather than a cell line, which may not be representative of all aspects of physiological macrophage functions. Macrophage polarisation remains a contentious issue in the field, with a spectrum of activation states thought to be a more physiologically relevant model than the traditional M1/M2 dichotomy (Chapter 1.2.2), yet *in vitro* polarisation with defined combinations of stimuli remains a useful tool to interrogate macrophage functions. I chose to model two opposing ends of the macrophage activation spectrum from classically activated, pro-inflammatory M1-like macrophages, to

alternatively activated, anti-inflammatory M2-like macrophages (Figure 3.1). There are many published methods to generate macrophages from human blood monocytes *in vitro*, and here I used M-CSF, a process I will hereafter refer to as maturation. These macrophages can then be induced to form different phenotypes by the application of immunological stimuli including cytokines and bacterial products such as lipopolysaccharide (LPS), which I hereafter refer to as stimulation, after which the macrophages differ in measurable ways such as the abundance of various cell-surface molecules and expression of different genes. I refer to this process of phenotype change in response to stimuli as polarisation, and the differentially expressed genes and proteins as polarisation markers.

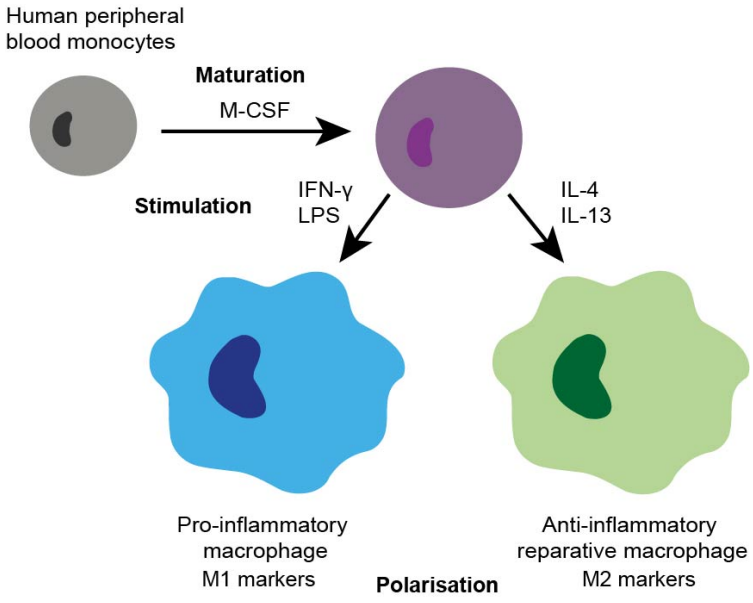

Figure 3.1 Schematic of experimental design.
Human peripheral blood monocytes were cultured in M-CSF to induce the change from non-adherent monocyte to adherent macrophage, a process I refer to as maturation, which models the process that would occur *in vivo* when these cells migrate from the bloodstream into tissues. Unpolarised M-CSF macrophages were then exposed to bacterial and endogenous molecules, which I describe as stimulation, an experimental step that represents exposure of macrophages *in vivo* to myriad molecules that may be secreted by other cells of the body, such as cytokines, or released from pathogens, such as LPS. Such molecules are detected by receptors on the macrophage surface and the signalling pathways they activate lead to expression of various genes and cell-surface protein molecules, which are quantifiable *in vitro*. This process by which stimulated macrophages acquire different effector phenotypes is here referred to as polarisation.

3.2 Monocyte-derived macrophage isolation and polarisation

I isolated monocytes from buffy coats from healthy human blood donors first by enriching the PBMC fraction by density gradient centrifugation, then further segregating the different white blood cell fractions by countercurrent centrifugal elutriation (Chapter 2.2). The monocyte fraction was collected and cultured in the presence of M-CSF for 5 days (Schubert et al., 2019). To investigate whether these cells displayed a phenotype typical of human macrophages, I stained them for the intracellular macrophage marker CD68 and found that in all three donors tested it was expressed in near 100% of the cells (Figure 3.2). These 'unpolarised' M-CSF-differentiated macrophages were then polarised by stimulation with IFN-γ (Rey-Giraud et al., 2012) and/or LPS (Higuchi et al., 2016) or IL-4/IL-13 (Rogers et al., 2019) for a further 24 h. Fresh medium without any stimuli was applied to the M-CSF-only unpolarised control.

3.2.1 Validation of macrophage phenotypes by flow cytometry staining for cell-surface markers

To validate my protocol for polarising M-CSF-differentiated macrophages to a pro- or anti-inflammatory phenotype, I quantified the expression levels of several cell-surface protein markers associated with IFN-γ/LPS or IL-4/IL-13 stimulation (Figure 3.3). While there is considerable debate as to which cell surface markers best describe pro- and anti-inflammatory macrophage phenotypes, I measured expression of CD64 and CD80 as markers of the pro-inflammatory phenotype, and CD209 and CD163 as markers of the anti-inflammatory phenotype (Ambarus et al., 2012; Bertani et al., 2017). CD64 was strongly upregulated by IFN-γ, whereas the co-

stimulatory molecule CD80 was most highly expressed on those cells treated with both IFN-γ and LPS. CD209 (DC-SIGN) was highly abundant on the surface of only those cells treated with IL-4 and IL-13, whereas CD163 showed variable expression between treatment conditions and substantial variation in staining between different blood donors.

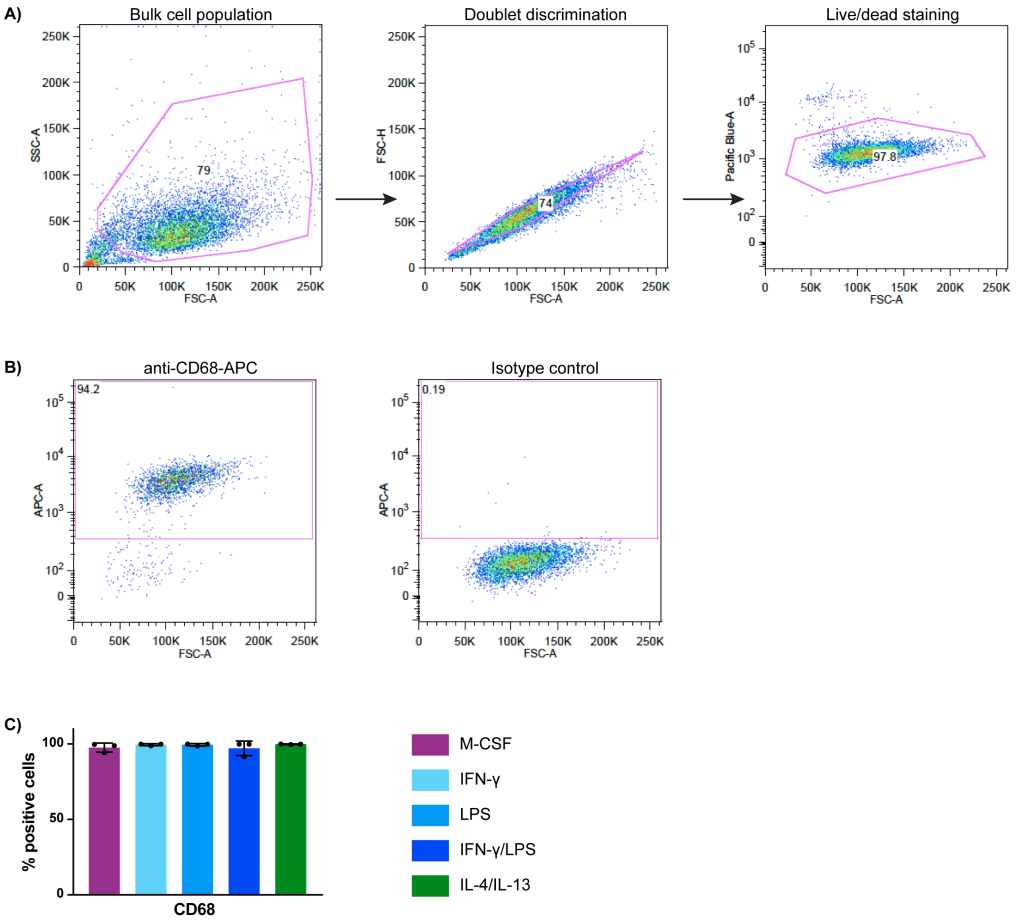

Figure 3.2 Human blood monocyte-derived macrophages were positive for the pan-macrophage marker CD68.
The monocyte population was purified from buffy coats from healthy human blood donors, and cultured with M-CSF (100 ng/ml) for 5 days. Adherent cells then received fresh medium either alone or containing IFN-γ (50 ng/ml) and/or LPS (100 ng/ml), separately or in combination, or IL-4 and IL-13 (both at 20 ng/ml). After 24 h stimulation, cells were lifted, fixed and permeabilised, and stained for the intracellular pan-macrophage marker CD68. A) Representative plots showing the gating strategy applied to all samples, indicating the gating of the bulk cell population, doublet discrimination based on forward scatter height and area, then live/dead discrimination by exclusion of viability dye. B) The position of the CD68-positive gate was defined by the position of the isotype control population for each donor, then applied across all samples. C) M-CSF-differentiated macrophages with or without 24 h further stimulation were uniformly positive for CD68 (n=3 donors). Error bars represent mean ± SD.

Parallel samples were stained with isotype control antibodies for CD68, CD64, CD80, CD163 and CD209, and all showed MFIs comparable to the unstained control samples, indicating limited non-specific binding.

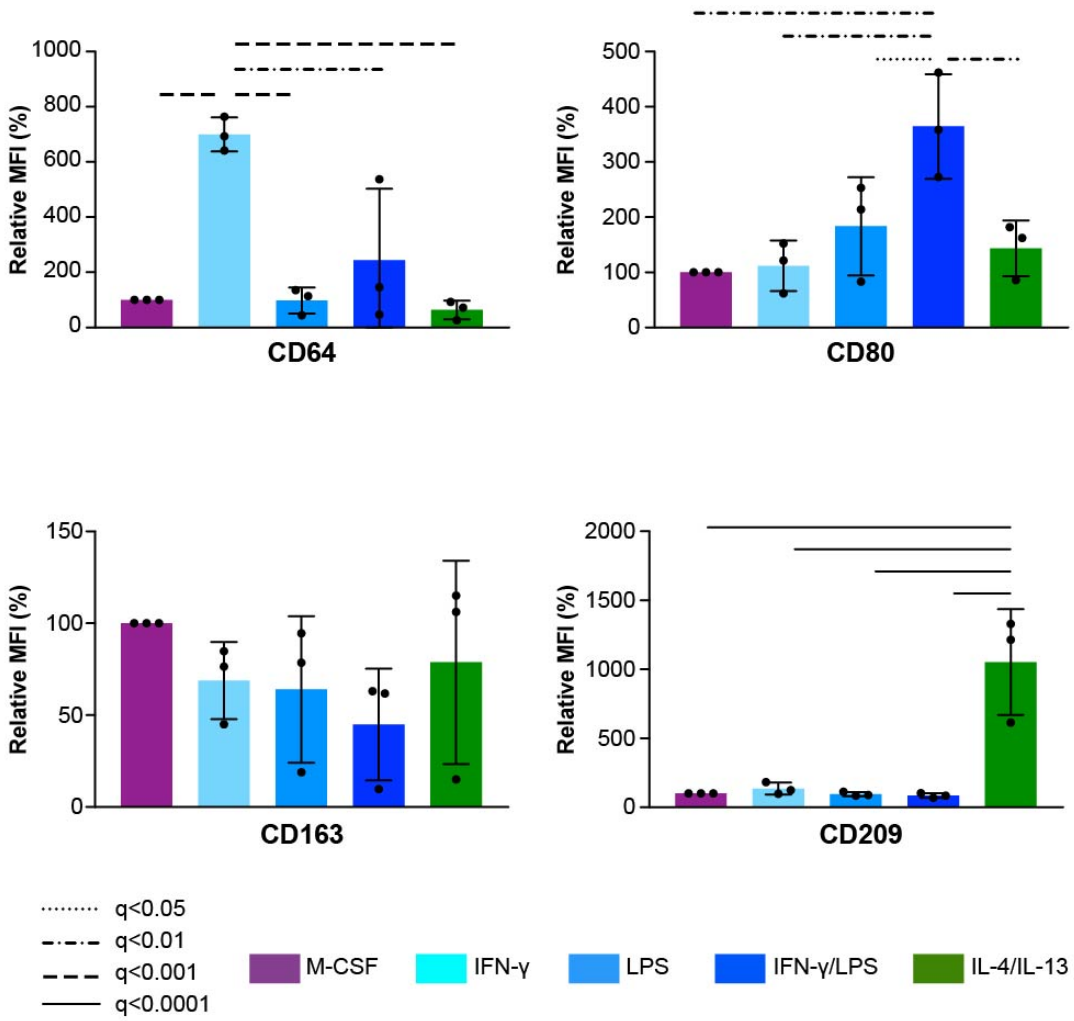

Figure 3.3 *In vitro* polarisation of macrophages induced expression of characteristic cell-surface markers.
The monocyte population was purified from buffy coats from healthy human blood donors, and cultured with M-CSF (100 ng/ml) for 5 days. Adherent cells then received fresh medium either alone or containing IFN-γ (50 ng/ml) and/or LPS (100 ng/ml), separately or in combination, or IL-4 and IL-13 (both at 20 ng/ml). After 24 h stimulation, cells were lifted and stained without permeabilisation with antibodies against CD64, CD80, CD163, and CD209. The same gating strategy was applied to exclude doublets and dead cells as in Figure 3.2. The median fluorescence intensity (MFI) of all single live cells was recorded for each sample and expressed as a percentage relative to the MFI of M-CSF-only cells from the same donor (N=3 donors). Error bars represent mean ± SD. Data were analysed by one-way unpaired ANOVA with multiple comparisons.

3.2.2 Macrophages expressed messenger RNA for markers associated with their polarisation

To further profile the different macrophage phenotypes I had generated, I quantified the mRNA levels of several genes known to be induced by my chosen stimuli (Martinez et al., 2006) in macrophages and monocytes from the same donors (Figure 3.4). In terms of markers for the pro-inflammatory phenotype, transcription of *IL6* was moderately induced by stimulation with LPS, and significantly upregulated by IFN-γ and LPS together, whereas *IL1B* was induced most strongly by LPS alone. Inducible nitric oxide synthase (*NOS2*) was significantly upregulated by IFN-γ and LPS together relative to all other treatment conditions. Finally, expression of the macrophage mannose receptor (*CD206),* a marker of the anti-inflammatory phenotype (Mia et al., 2014), was strongly and significantly upregulated only in the IL-4/IL-13-treated samples, with LPS or IFN-γ/LPS treatment depressing transcription relative to M-CSF-only macrophages.

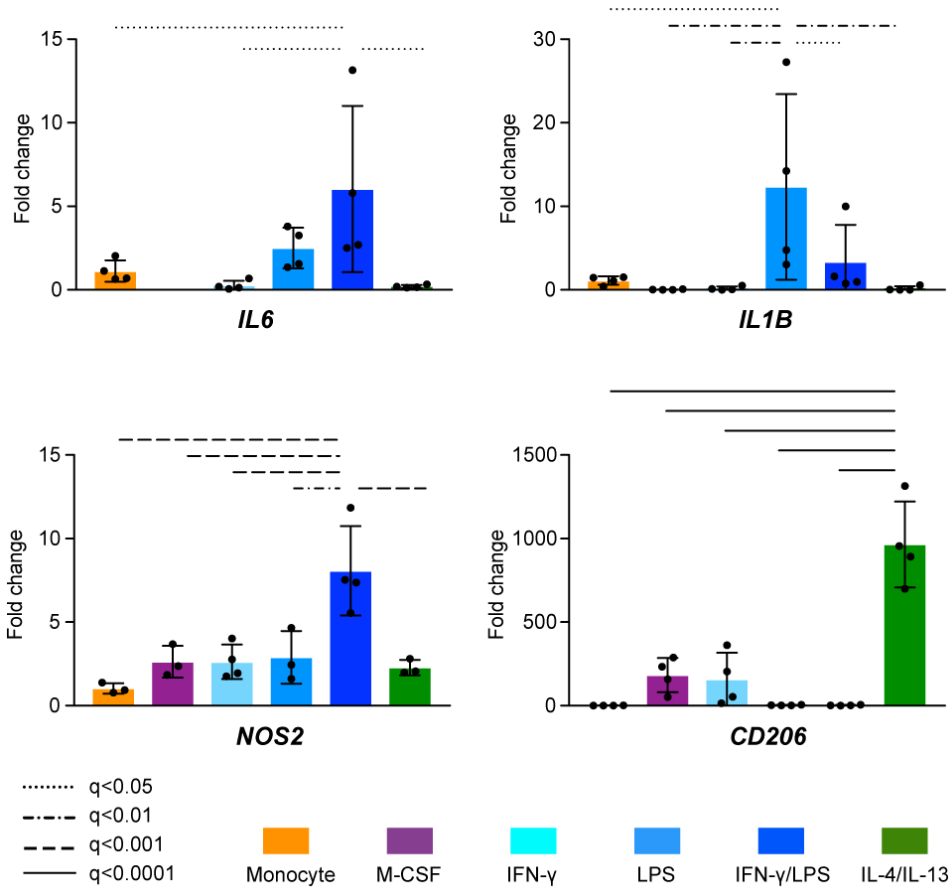

Figure 3.4 *In vitro* stimulation of macrophages induced mRNA expression of characteristic polarisation markers.
The monocyte population was purified from buffy coats from healthy human blood donors, and cultured with M-CSF (100 ng/ml) for 5 days. Adherent cells then received fresh medium either alone or containing IFN-γ (50 ng/ml) and/or LPS (100 ng/ml), separately or in combination, or IL-4 and IL-13 (both at 20 ng/ml). After 24 h stimulation, cells were lysed for RNA isolation and generation of cDNA by reverse transcription. The relative mRNA expression levels of interleukin-6 (*IL6*), interleukin-1β (*IL1B*), nitric oxide synthase 2 (*NOS2*) and macrophage mannose receptor (*CD206)* were quantified and analysed using the ΔΔCt method. Data are presented as fold changes relative to the average expression level in donor-matched monocytes. n=4 blood donors. Error bars represent mean ± SD. Data were analysed using an unpaired one-way ANOVA with multiple comparisons.

3.2.3 ELISAs for secreted cytokines to confirm macrophage activation

To complete profiling of the macrophage phenotypes I had generated, I quantified secretion of the cytokines TNF and interleukin-10 (IL-10) into the culture medium of M-CSF-differentiated macrophages stimulated for 24 hours (Figure 3.5). I found that high levels of TNF were secreted by cells exposed to LPS, as expected, and that IL-10 was also most abundant in the conditioned medium of IFN-γ/LPS- and LPS-treated samples at this time point.

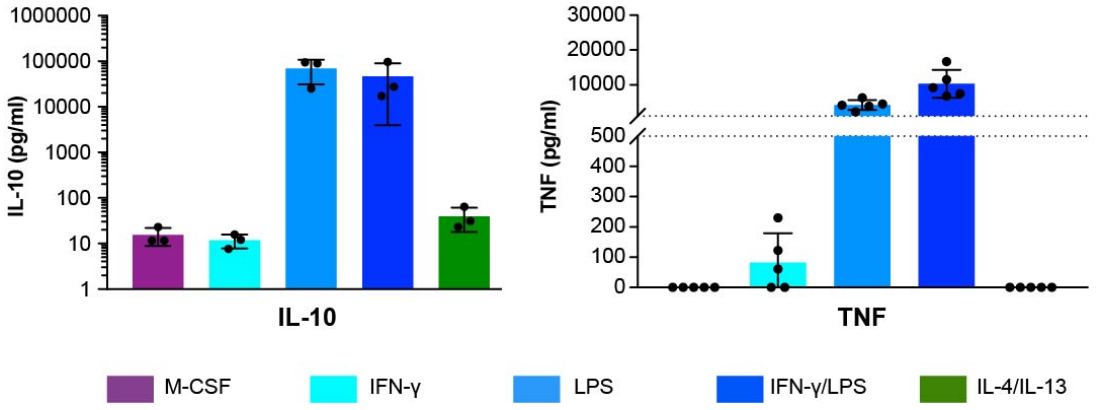

Figure 3.5 Macrophages secreted IL-10 and TNF dependent on applied stimuli.
The monocyte population was purified from buffy coats from healthy human blood donors, and cultured with M-CSF (100 ng/ml) for 5 days. Adherent cells then received fresh medium either alone or containing IFN-γ (50 ng/ml) and/or LPS (100 ng/ml), separately or in combination, or IL-4 and IL-13 (both at 20 ng/ml). After 24 h stimulation, conditioned media were subjected to ELISA analyses to quantify secretion of IL-10 and TNF. n=3 donors for IL-10 and n=5 for TNF. Error bars represent mean ± SD.

3.3 Comprehensive profiling of HS-associated genes by microfluidic real-time quantitative PCR array

Having confirmed that my protocols for monocyte isolation and culture yielded a macrophage population that polarised to a range of different phenotypes in response to applied stimuli, I set out to quantify the relative expression levels of all heparan sulfate core proteins, and biosynthetic and modifying enzymes. To achieve this, I used a custom-designed microfluidic qPCR array card containing primers for these genes of interest and three housekeeping genes (Table 5). Because I found RPLP0 to be significantly LPS-responsive (Figure 3.6) I used only the average of 18S and GAPDH, which were not regulated by any of the stimuli used. Expression levels of HS-associated genes were calculated relative to the average expression level in monocytes.

Table 5. HS-associated genes included in Taqman microfluidic array for qPCR.

HS core proteins	**HS N-deacetylase/N-sulfotransferases**	**3-O-sulfotransferases**
Perlecan (HSPG2)	NDST1	HS3ST1
Syndecan-1 (SDC1)	NDST2	HS3ST2
Syndecan-2 (SDC2)	NDST3	HS3ST3A
Syndecan-3 (SDC3)	NDST4	HS3ST3B
Syndecan-4 (SDC4)		HS3ST4
Glypican-1 (GPC1)	**Glucuronyl C5 epimerase**	HS3ST5
Glypican-2 (GPC2)	GLCE	HS3ST6
Glypican-3 (GPC3)		
Glypican-4 (GPC4)	**2-O-sulfotransferase**	**Editing**
Glypican-5 (GPC5)	HS2ST1	SULF1
Glypican-6 (GPC6)		SULF2
TGFβ receptor 3 (TGFBR3)	**6-O-sulfotransferases**	HPSE
Agrin (AGRN)	HS6ST1	HPSE2
	HS6ST2	
Chain elongation	HS6ST3	**Housekeeping genes**
EXT1		18S
EXT2		GAPDH
EXTL1		RPLP0
EXTL2		
EXTL3		

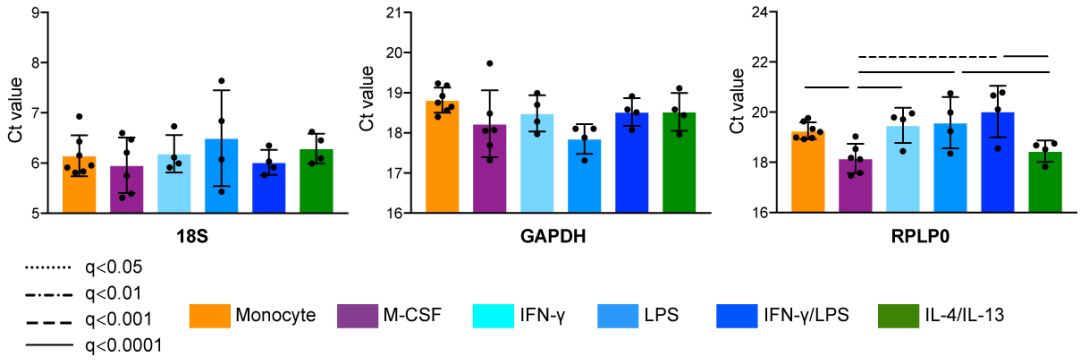

Figure 3.6. Ct values of housekeeping genes in monocytes and polarised macrophages.
The monocyte population was purified from buffy coats from healthy human blood donors, and cultured with M-CSF (100 ng/ml) for 5 days. Adherent cells then received fresh medium either alone or containing IFN-γ (50 ng/ml) and/or LPS (100 ng/ml), separately or in combination, or IL-4 and IL-13 (both at 20 ng/ml). After 24 h stimulation, cells were lysed for RNA isolation and generation of cDNA by reverse transcription. The Ct values for the housekeeping genes 18S, GAPDH and RPLP0 were analysed by one-way ANOVA with multiple comparisons, and all significant comparisons are indicated. n = 7 donors for monocytes, n = 6 for M-CSF macrophages, and n = 4 for all other treatment conditions.

The relative expression levels were subjected to cluster analysis according to the most similar patterns of gene expression and displayed as a heatmap (Figure 3.7). Where expression of genes was undetectable in monocytes, or was present in some macrophage samples but not others, data were not included in the heatmap. The monocytes were found clustered together, as were the M-CSF-differentiated macrophages, while samples that had received IFN-γ and LPS, either separately or in combination, were mostly clustered together, and all but one of the IL-4/IL-13-treated samples clustered together, and sat between monocytes and M-CSF macrophages in terms of HS-associated gene expression patterns. The majority of genes were upregulated by maturation from monocyte to macrophage, while a smaller subset of genes were downregulated by M-CSF.

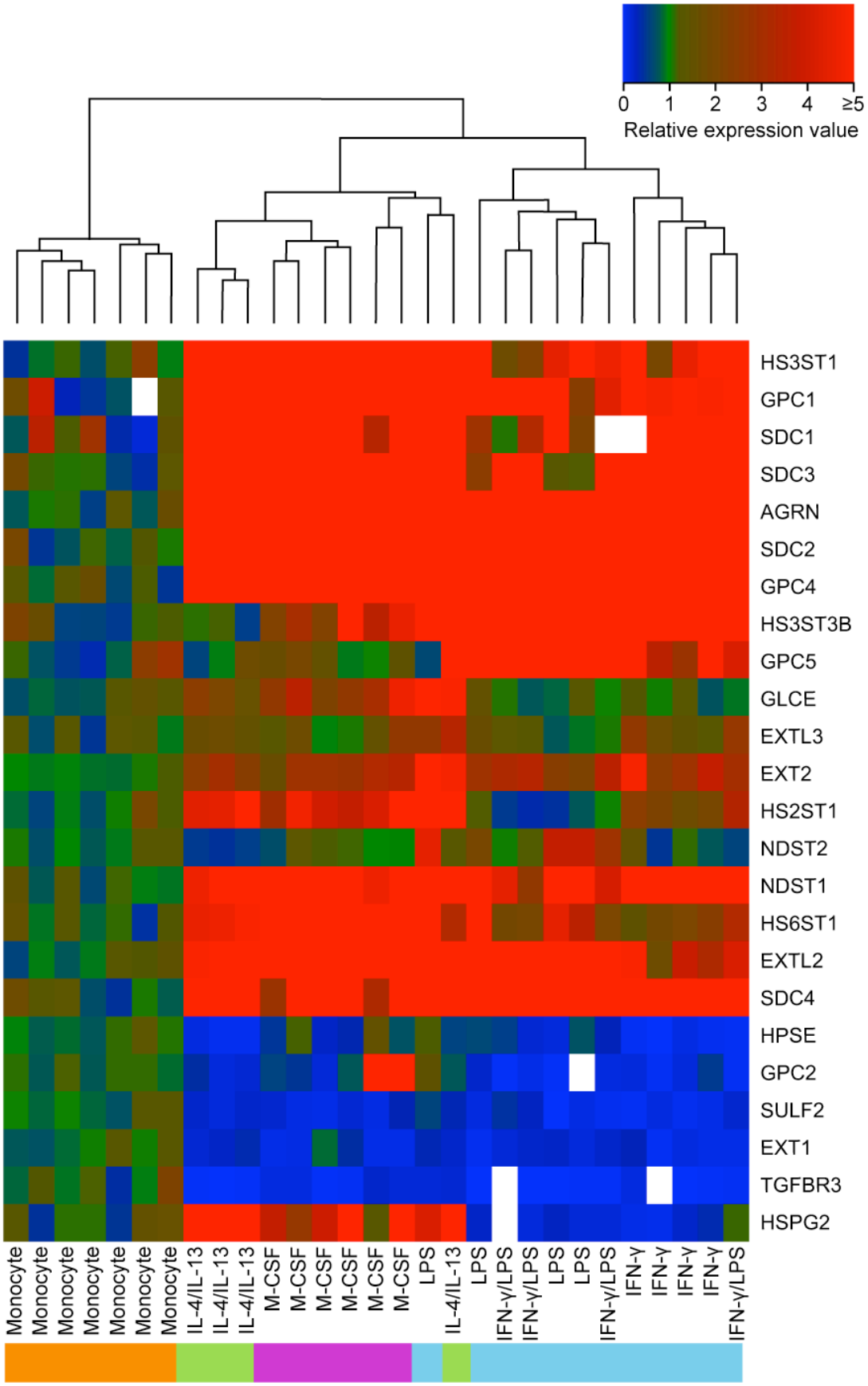

Figure 3.7. Expression of heparan sulfate-associated genes altered with macrophage maturation and polarisation. **Legend on page 85.**

3.3.1 Macrophages differentially expressed heparan sulfate core proteins after inflammatory stimulation

Comparing the Ct values for each of the core protein genes in M-CSF-differentiated macrophages to the average Ct of the housekeeping genes 18S and GAPDH in each sample enabled me to determine which core proteins were most abundantly expressed in unpolarised macrophages at the mRNA level (Figure 3.8). The four syndecans were in the top half of core protein genes for level of expression, whereas the glypican family were generally less abundant. Out of the 13 heparan sulfate core protein genes, only glypican-6 (*GPC6*) was not expressed in monocytes or macrophages. Glypican-3 (*GPC3*) was not detectable in any monocyte samples but was detectable in some macrophage samples. The relative expression levels of each gene compared to the average in monocytes were plotted on individual graphs (Figure 3.9). Of the 11 core proteins expressed in monocytes and macrophages, the majority showed low expression in monocytes and subsequent upregulation after maturation to macrophages by M-CSF.

Figure 3.7 Expression of heparan sulfate-associated genes altered with macrophage maturation and polarisation.
The monocyte population was purified from buffy coats from healthy human blood donors, and cultured with M-CSF (100 ng/ml) for 5 days. Adherent cells then received fresh medium either alone or containing IFN-γ (50 ng/ml) and/or LPS (100 ng/ml), separately or in combination, or IL-4 and IL-13 (both at 20 ng/ml). After 24 h stimulation, RNA was extracted and the relative expression levels of heparan sulfate-associated genes quantified using Taqman microfluidic arrays. Fold change in gene expression for each sample was determined using the ΔΔCt method relative to the average level in the monocyte samples, and the samples subjected to cluster analysis based on most similar patterns of gene expression. The heatmap shows all HS-associated genes that were expressed in the majority of samples; white squares indicate that the gene was undetectable in that sample. Increased expression relative to monocytes is shown in red, no change shown in green, and downregulation relative to the monocyte average shown in blue. n = 7 donors for monocytes, n = 6 for M-CSF macrophages without further polarisation, and n = 4 for each of the stimulated conditions.

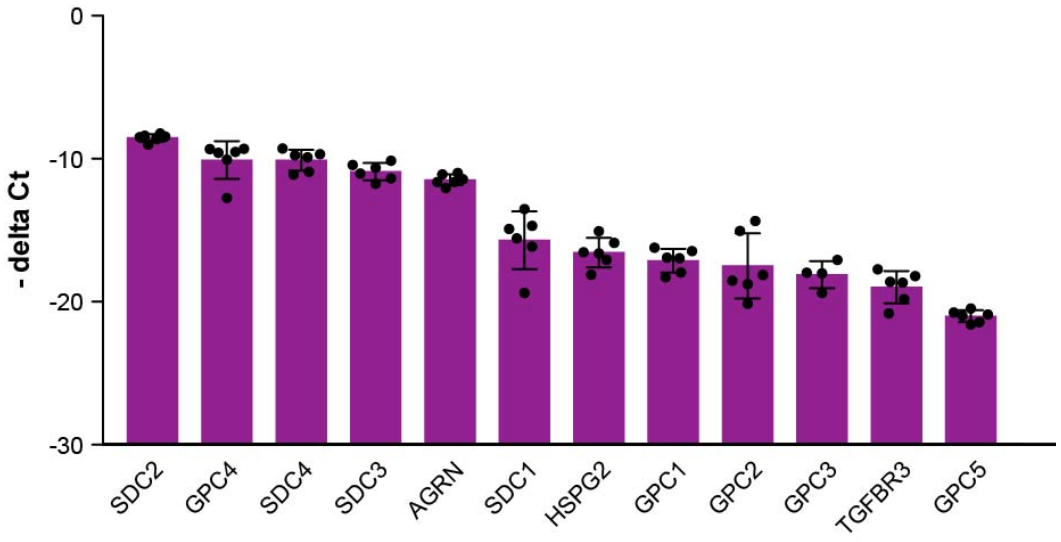

Figure 3.8 Expression of heparan sulfate core proteins in M-CSF macrophages in order of relative message abundance.
Ct values of HS-associated gene expression in M-CSF-matured macrophages were normalised to the expression levels of the housekeeping genes 18S and GAPDH in each sample, yielding delta Ct values. The negative of each delta Ct value has been plotted here, such that a greater bar height indicates a higher average expression level in M-CSF macrophages. Where data points are absent, expression of that gene was undetectable in one or more samples. n = 6 donors. Error bars represent mean ± SD.

Transforming growth factor receptor 3 (*TGFBR3*) was unique in showing significant downregulation from monocyte to all other types of macrophage (Figure 3.9). Agrin and perlecan showed reciprocal regulation, with agrin being induced by pro-inflammatory stimuli and perlecan (*HSPG2*) being highly and significantly upregulated only in the IL-4/IL-13-treated samples. Syndecan-1 and -2 showed similar patterns of regulation, with highest expression in M-CSF-only and IL-4/IL-13-treated samples. Syndecan-3 was not significantly regulated between different types of macrophage, whereas syndecan-4 was strongly regulated by all stimuli with a highest average fold change after LPS treatment. Glypican-1 and -4 showed similar patterns of gene regulation, with the highest average fold change in M-CSF and IL-4/IL-13-treated samples, whereas glypican-5 showed greatest induction by LPS and IFN-γ/LPS.

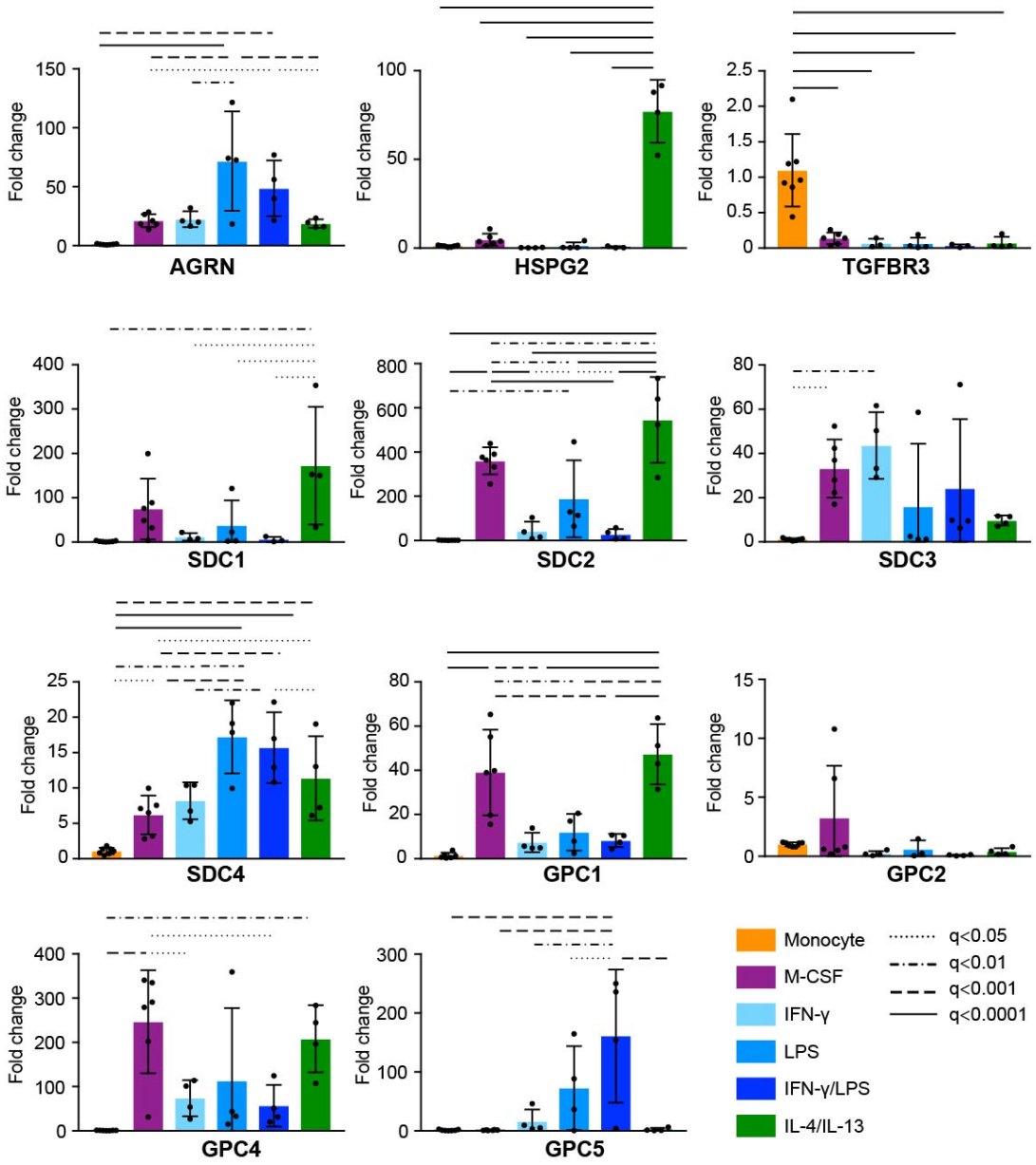

Figure 3.9 Heparan sulfate core proteins were differentially regulated according to inflammatory stimuli in macrophages.
Expression of heparan sulfate core proteins in human monocytes, M-CSF macrophages, and those further stimulated with IFN-γ, and/or LPS, or IL-4 and IL-13, was quantified by qPCR using microfluidic arrays. Data were analysed using the ΔΔCt method relative to the average expression level in monocytes, and plotted on individual graphs for each core protein gene.. n = 7 donors for monocytes, n = 6 for M-CSF macrophages, and n = 4 for all other treatment conditions. Error bars represent mean ± SD. Data were tested for normality using the Shapiro-Wilk normality test, then analysed by one-way unpaired ANOVA with multiple comparisons.

3.3.2 Macrophages differentially expressed heparan sulfate biosynthetic enzymes after inflammatory stimulation

The fold change in expression of HS biosynthetic enzymes relative to the average level in monocytes was compared between macrophages treated only with M-CSF and those with additional stimulation (Figure 3.10). Of the family of enzymes responsible for biosynthesis of the heparan sulfate backbone, both protein isoforms of extostosin (*EXT*) were expressed, and two of the three isoforms of exostosin-like (*EXTL*) were expressed. *EXT1* and *EXT2* showed reciprocal regulation, with *EXT1* being downregulated during maturation from monocyte to macrophage, whereas *EXT2* was significantly upregulated. *EXTL2* showed significant upregulation from monocyte to macrophage, and was highly induced by IFN-γ/LPS in some donors. Of the four N-deacetylase N-sulfotransferase (*NDST*) enzymes, isoforms 1 and 2 were expressed in monocytes and macrophages, whereas isoforms 3 and 4 were undetectable in all samples. *NDST1* showed significant upregulation during maturation from monocyte to macrophage, whereas the average level of *NDST2* expression remained consistent between monocyte and M-CSF macrophage but then showed significant induction by LPS. The epimerase (*GLCE*) showed significant upregulation from monocyte to macrophage, then was generally downregulated again after exposure of cells to IFN-γ and/or LPS. Only one of the two protein isoforms of mammalian heparanase (*HPSE*) was expressed and showed no significant change during maturation from monocyte to macrophage but was downregulated after exposure to inflammatory stimuli, most dramatically after IFN-γ treatment.

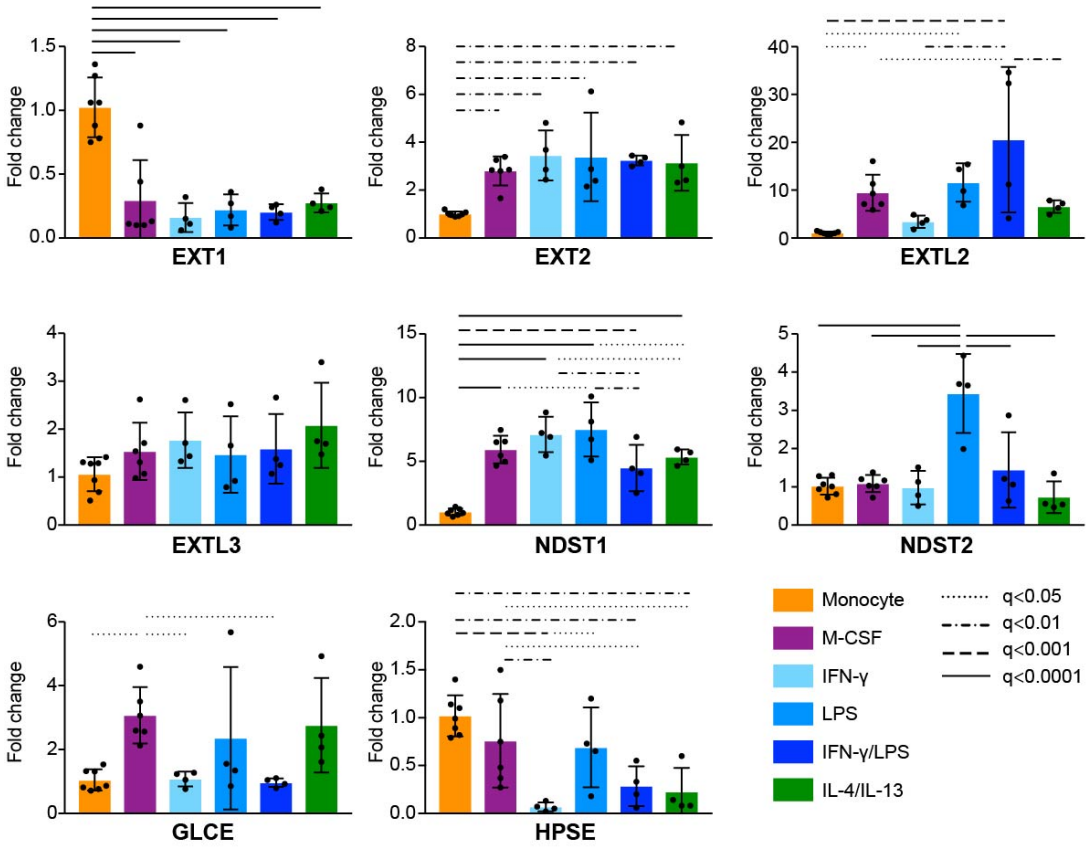

Figure 3.10 Heparan sulfate biosynthetic enzymes were differentially regulated according to macrophage maturation and polarisation.
Expression of heparan sulfate biosynthetic enzymes in human monocytes, M-CSF macrophages, and those further stimulated with IFN-γ, and/or LPS, or IL-4 and IL-13, was quantified by qPCR using microfluidic arrays. Data were analysed using the ΔΔCt method, relative to the average expression level in monocytes, and plotted on individual graphs for each gene. n = 7 donors for monocytes, n = 6 for M-CSF macrophages, and n = 4 for all other treatment conditions. Error bars represent mean ± SD. Data were tested for normality using the Shapiro-Wilk normality test, then analysed by one-way unpaired ANOVA with multiple comparisons.

3.3.3 Macrophages differentially expressed sulfotransferase enzymes after inflammatory stimulation

The fold changes of expression level of the heparan sulfate O-sulfotransferases in each of the different macrophage types relative to the average in monocytes were plotted on individual graphs for each gene (Figure 3.11). The 2-O-sulfotransferase (*HS2ST1*) was significantly upregulated during maturation from monocyte to macrophage in response to M-CSF, and showed some further changes after additional stimulation but this was variable between donors. Of the seven protein isoforms of heparan sulfate 3-O-sulfotransferases, *HS3ST1*, *HS3ST3A*, and *HS3ST3B* were expressed in the majority of samples, although *HS3ST3A* was not detectable in all donors. *HS3ST1* showed a high fold induction during M-CSF-induced maturation of monocytes, whereas there were no significant differences between monocytes and macrophages in the other two isoforms detected. *HS3ST3B* showed strong upregulation in response to LPS although this was highly variable between donors. Of the four protein isoforms of heparan sulfate 6-O-sulfotransferase, only *HS6ST1* was detectable in monocytes or macrophages and showed significant upregulation in response to M-CSF, with varying degrees of further downregulation in response to additional inflammatory stimuli. Of the two sulfatase enzymes that act to remove 6-O-sulfate groups from HS chains on the cell surface, *SULF1* was not detectable in any samples, while *SULF2* showed significant downregulation from monocyte to all types of macrophage.

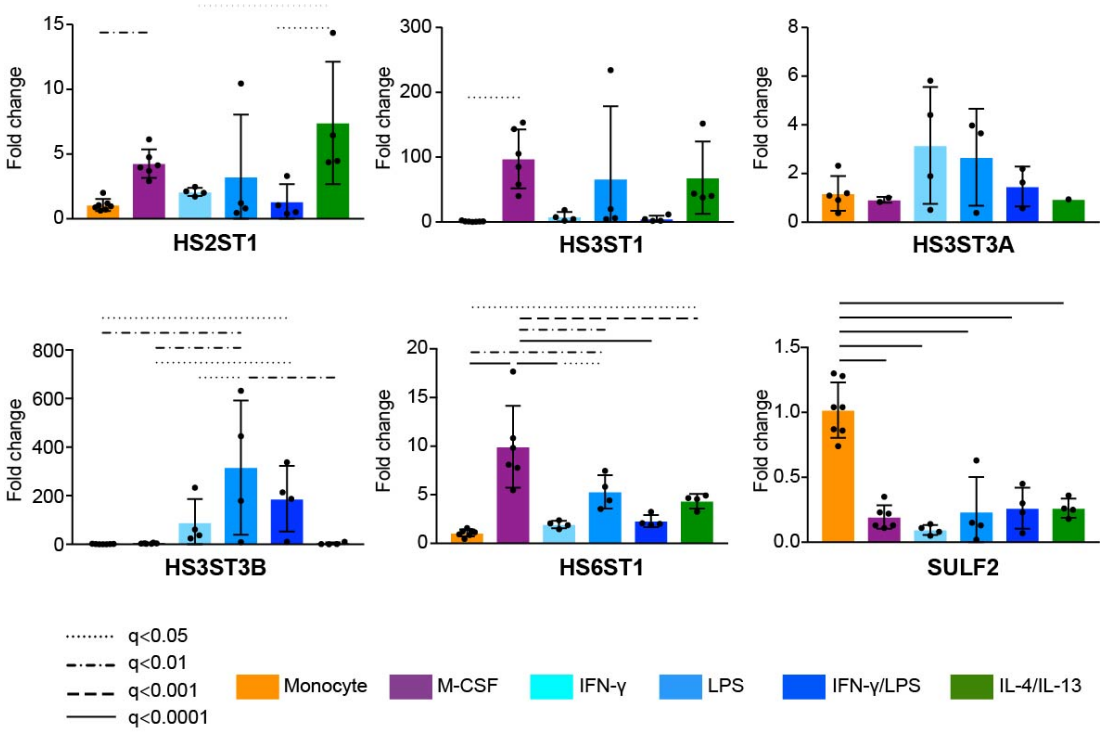

Figure 3.11 Heparan sulfate sulfotransferases were differentially regulated according to macrophage maturation and polarisation.
Expression of heparan sulfate sulfotransferases and de-sulfatases in human monocytes, M-CSF macrophages, and those further stimulated with IFN-γ, and/or LPS, or IL-4 and IL-13, was quantified by qPCR using microfluidic arrays. Data were analysed using the ΔΔCt method relative to the average expression level in monocytes, and plotted on individual graphs for each core protein gene. n = 7 donors for monocytes, n = 6 for M-CSF macrophages, and n = 4 for all other treatment conditions. Error bars represent mean ± SD. Data were tested for normality using the Shapiro-Wilk normality test, then analysed by one-way unpaired ANOVA with multiple comparisons.

3.3.4 The monocytic cell lines THP1 and U937 express many of the HS-associated genes detected in primary monocyte-derived M-CSF macrophages

I also profiled expression of HS-associated genes in the monocytic cell lines THP1 and U937, to evaluate whether these could model the responses seen in primary cells. THP1 and U937 were stimulated overnight with PMA to induce maturation to a pseudo-macrophage phenotype including adhesion to the plastic cell culture plates. The same Taqman microfluidic array cards were used to quantify relative expression of HS-associated genes in these cells, and showed that all of the genes detected in primary M-CSF-differentiated macrophages were expressed in at least one of the two cell lines (Figure 3.12), indicating they could be useful as a model for macrophage HS biosynthesis and functions in future experiments.

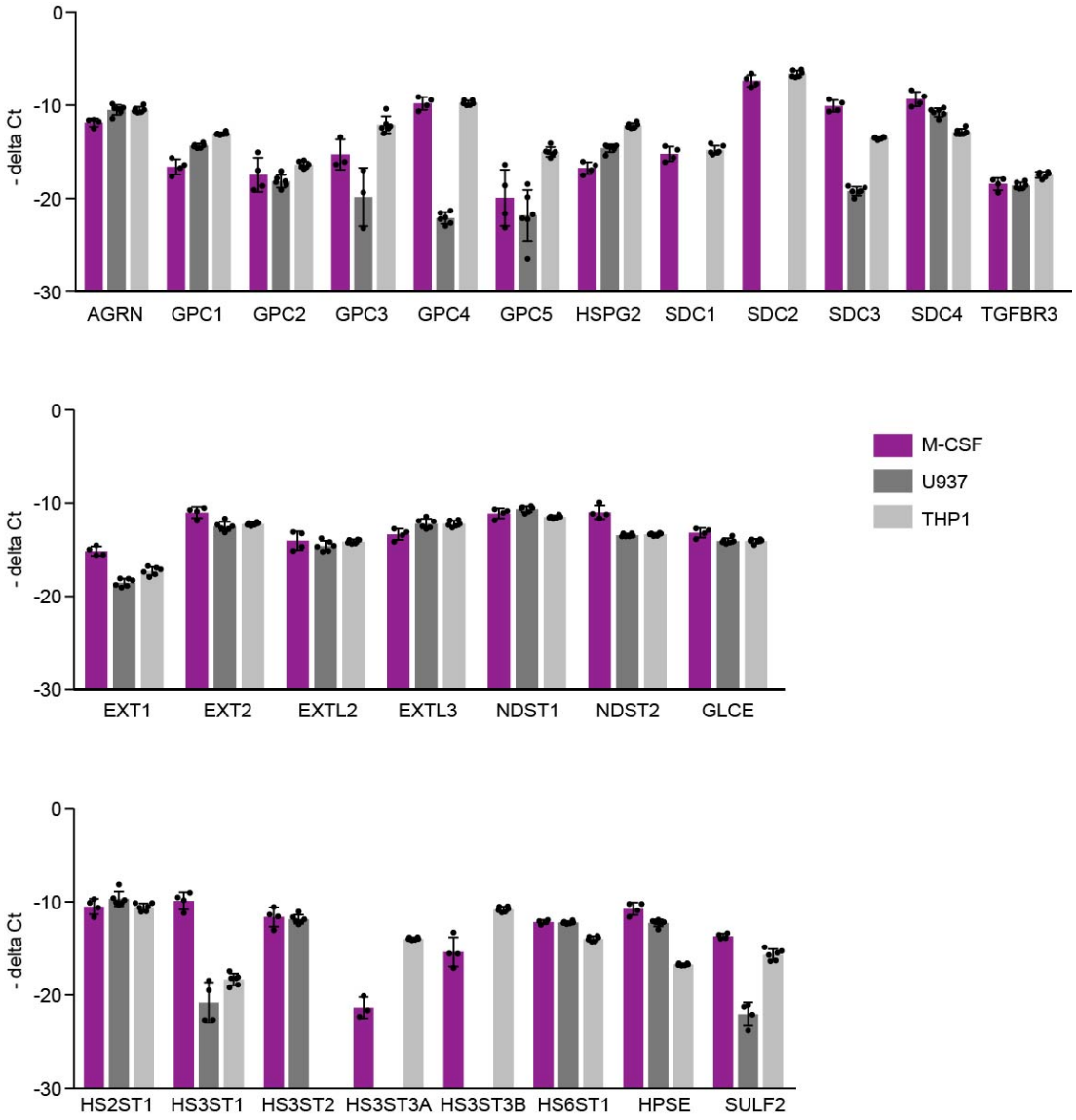

Figure 3.12 The monocytic cell lines THP1 and U937 showed similar expression levels of HS-associated genes to primary M-CSF-differentiated macrophages.
THP1 and U937 cells were stimulated with 100 ng/ml of PMA overnight to induce maturation to a macrophage phenotype, and primary human monocytes were cultured for 5 days with M-CSF. Adherent cells were lysed for RNA isolation and generation of cDNA. The relative expression levels of HS-associated genes were quantified using the same microfluidic qPCR array cards as for primary monocyte-derived macrophages and compared to the average Ct of the two housekeeping genes *18S* and *GAPDH* for each sample to yield delta Ct values. Negative delta Ct values are plotted here so that a higher bar on the bar graph represents a higher relative level of expression of that gene. Where bars are missing, the gene was undetectable in that cell type. n = 4 blood donors for primary monocyte-derived macrophages; n = 6 independent samples for the cell lines. Error bars represent mean ± SD.

3.4 Detection of cell-surface heparan sulfate using antibodies

Based on the transcriptome analysis of HS-associated gene expression in monocytes and polarised M-CSF macrophages and the strong differential regulation seen for many of the biosynthetic enzymes and sulfotransferases, I predicted that the structure and quantity of HS on the cell surface might differ between different phenotypes of macrophage. To detect cell-surface heparan sulfate directly, I stained primary M-CSF macrophages with the antibodies 3G10, which recognises the stub of HS remaining after digestion with bacterial heparinase III (amsbio 370260), and 10E4, which recognises a poorly defined epitope of the HS backbone (David et al., 1992) (Figure 3.13). Thus, quantification of the staining with these antibodies by flow cytometry should act as a surrogate measure of the number of HS chains, and the total quantity of HS, respectively. However, my staining with 3G10 was on average higher without heparinase III treatment, when epitope recognised by the antibody is unlikely to have been produced. Moreover, the isotype control primary antibody yielded strong staining compared to the unstained and no-primary controls, suggesting there are non-specific interactions between the IgG2b class of antibody and the macrophage surface. Similarly, 10E4 staining resulted in a fluorescence signal as strong as the no-primary control, and heparinase III treatment, which should destroy the epitope recognised by this antibody, did not abolish staining and in fact increased it in one donor tested. These antibodies were thus not used further for analysing macrophage heparan sulfate levels.

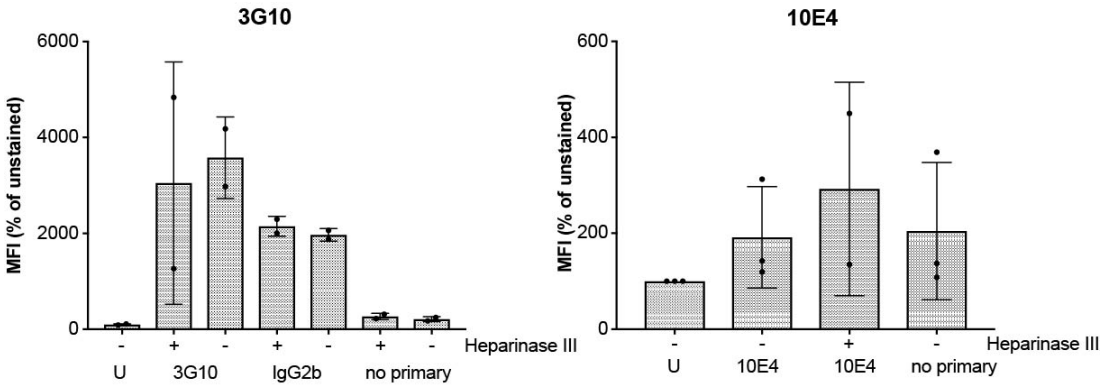

Figure 3.13 Commercial anti-HS antibodies were ineffective at detecting macrophage cell-surface HS chains.
M-CSF-differentiated human monocyte-derived macrophages were stained with the commercial antibodies 3G10 and 10E4 and appropriate secondary antibodies, with or without heparinase III pre-treatment (50 mU/ml, 100 µl/10^6 cells, 20 min, 37 °C) that should expose the epitope recognised by 3G10 and abolish the epitope recognised by 10E4. The median fluorescence intensity of all single live cells for each sample was compared to that of the unstained control for each donor and expressed as a percentage. Error bars represent mean ± SD. n = 2 or 3 donors.

3.5 Maturation and polarisation of monocyte-derived macrophages after sodium chlorate treatment

Given the general upregulation of HS core proteins and biosynthetic enzymes I observed upon maturation of primary human monocytes to macrophages in the presence of M-CSF, I sought to determine whether an increase in cell-surface HS expression is necessary for this maturation process to occur. Furthermore, the strong and significant differences seen in HS biosynthetic enzyme expression between macrophages polarised to M1-like or M2-like phenotypes led me to hypothesise that different HS sulfation patterns might be involved in the polarisation process, perhaps by acting as a co-receptor for the polarising cytokines IFN-γ and IL-4, which can both bind HS (Ori et al., 2011).

3.5.1 M-CSF maturation of monocytes in the presence of sodium chlorate

To test the role of HS sulfation in monocyte to macrophage maturation, I cultured fresh blood monocytes in M-CSF for 5 days, with or without the addition of 30 mM sodium chlorate, to inhibit sulfation of HS chains (Baeuerle and Huttner, 1986; Safaiyan et al., 1999). Cells were then lifted and stained for the pan-macrophage marker CD68, the monocytic marker CD14, and the macrophage marker CD16 (Figure 3.14). There was no significant difference in CD68 expression between untreated and sodium chlorate-treated macrophages in four donors, indicating that these cells have not lost their macrophage phenotype in the absence of HS sulfation. There were also no apparent differences in CD14 and CD16 expression between treated and untreated cells in two donors. However, because I did not confirm that sodium chlorate had abolished HS sulfation in these cells, I cannot conclude that M-CSF maturation of monocytes to macrophages is not dependent on sulfated HS.

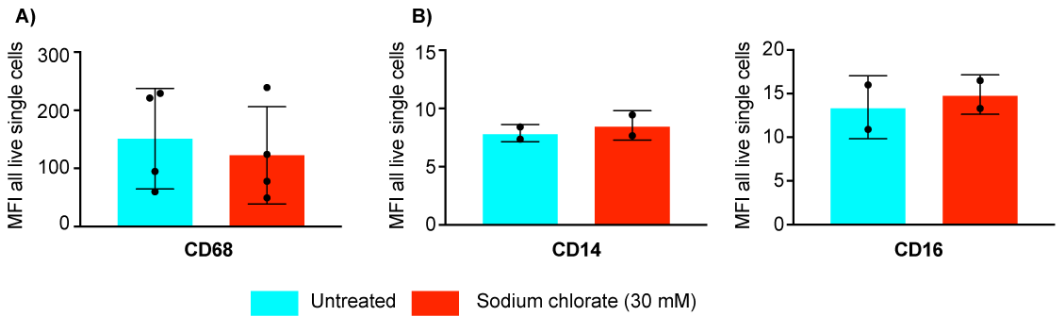

Figure 3.14 Staining for protein markers of macrophage phenotype after sodium chlorate treatment of monocytes. Human blood-derived monocytes were cultured with M-CSF (100 ng/ml) for 5 days as before, but with or without the addition of 30 mM sodium chlorate. Cells were then lifted and stained for analysis of marker expression by flow cytometry. A) Cells were fixed and permeabilised before staining for the intracellular macrophage marker CD68 (n=4 donors). Control versus sodium chlorate treated groups were not significantly different by paired t-test. B) Cell-surface staining of macrophages for CD14 and CD16 (n=2 donors). Gating to select for live single cells was performed as in Figure 3.2. Error bars represent mean ± SD.

3.5.2 Polarisation of monocyte-derived macrophages after sodium chlorate treatment

To investigate whether the upregulation of HS biosynthetic enzymes during monocyte to macrophage maturation with M-CSF, and the predicted increase in cell-surface HS, is required for subsequent stimulation to induce a change in polarisation, I incubated monocyte-derived macrophages with sodium chlorate for 24 h to abolish sulfation of newly synthesized HS chains, then stimulated for a further 24 h with IFN-γ and or LPS, or IL-4 and IL-13 in the presence of sodium chlorate, or fresh medium only as an unpolarised control. Sodium chlorate was retained during the polarisation step to prevent re-expression of sulfated HS on the cell-surface during this time. I then quantified the upregulation of prototypic pro- and anti-inflammatory markers in these cells to determine whether cell surface HS contributes to the ability of polarising stimuli to induce measurable phenotypic changes. By flow cytometry, the pro-inflammatory markers CD80 and CD64 were detectable in all samples, being most strongly induced by IFN-γ/LPS or IFN-γ alone, respectively (Figure 3.15). There was no significant difference in the expression level CD80 when the MFI of untreated cells was compared to that of sodium chlorate treated cells for each polarising condition, but there was a significant decrease in the surface level of CD64 in the chlorate-treated cells after IFN-γ stimulation compared to the non-chlorate treated IFN-γ stimulated cells. The anti-inflammatory macrophage markers CD163 and CD209 showed a trend towards reduced expression in chlorate-treated cells regardless of the applied stimuli, which was significant for several stimuli but also true of the unpolarised M-CSF control (Figure 3.15).

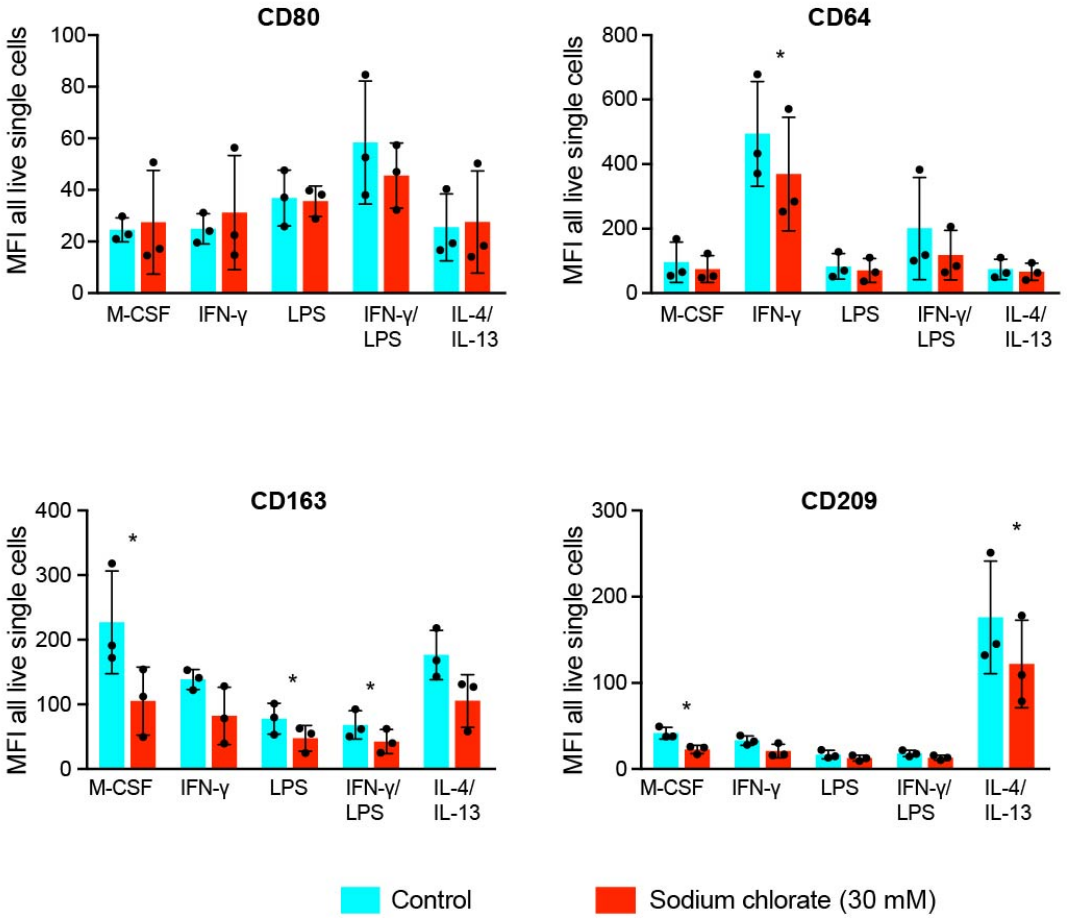

Figure 3.15 Staining for protein markers of macrophage polarisation in stimulated sodium chlorate-treated cells. Monocyte-derived macrophages were re-plated after 5 days culture in M-CSF (100 ng/ml) as before, but with the addition of 30 mM sodium chlorate in the cell culture medium. After 24 h, media were aspirated and replaced with fresh media containing IFN-γ (50 ng/ml), LPS (100 ng/ml) or IL-4 and IL-13 (both 20 ng/ml), or non-polarising control (labelled M-CSF) for a further 24 h. Those cells cultured with sodium chlorate for 24 h also had sodium chlorate in the medium for this polarising step, whereas the non-chlorate-treated control cells had only the polarising stimuli. Cells were then lifted and stained for analysis of marker expression by flow cytometry, with gating for live single cells performed as in Figure 3.2. n=3 donors. Error bars represent mean ± SD. All control versus sodium chlorate samples for each polarisation condition were analysed by paired t-test, and all significant comparisons are shown where $p<0.05$ (*).

By qPCR, the sodium chlorate-treated cells upregulated the expected polarisation markers associated with pro- and anti-inflammatory polarisation (Figure 3.16) with no significant differences between treated and untreated cells except for an increase in TNF message in response to IFN-γ/LPS.

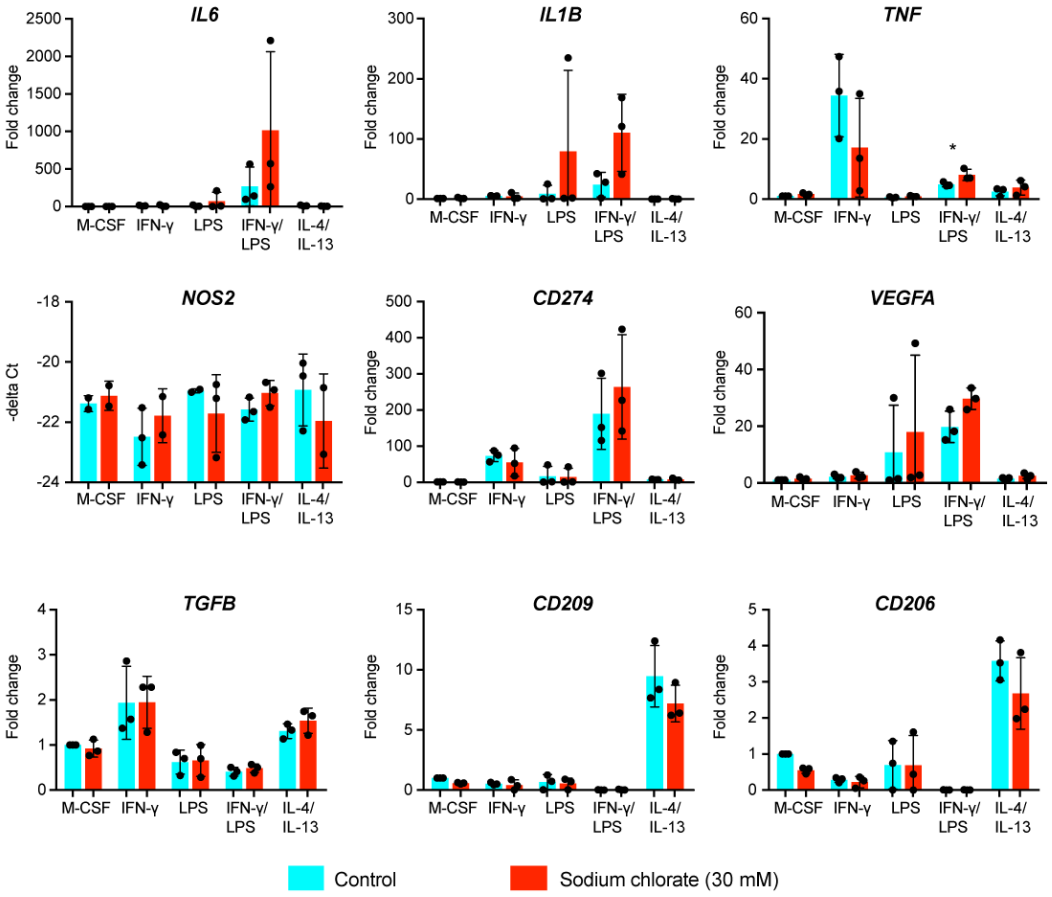

Figure 3.16 Quantification of polarisation markers in stimulated sodium chlorate-treated cells. Monocyte-derived macrophages were re-plated after 5 days culture in M-CSF (100 ng/ml) as before, but with the addition of 30 mM sodium chlorate in the cell culture medium. After 24 h, media were aspirated and replaced with fresh media containing IFN-γ (50 ng/ml), LPS (100 ng/ml) or IL-4 and IL-13 (20 ng/ml), or non-polarising control (labelled M-CSF) for a further 24 h. Those cells cultured with sodium chlorate for 24 h also had sodium chlorate in the medium for this polarising step, whereas the non-chlorate-treated control cells had only the polarising stimuli as in Figure 3.2. Message levels of polarisation markers were quantified by qPCR, normalized to the housekeeping genes 18S and GAPDH, and data expressed as a fold change relative to the expression level in non-sodium chlorate-treated M-CSF macrophages. n=3 donors. Error bars represent mean ± SD. Control versus sodium chlorate samples were analysed by paired t-test, and all significant comparisons are shown where $p<0.05$ (*).

However, a trend became more evident when the expression of pro-inflammatory macrophage markers in response to IFN-γ/LPS and of anti-inflammatory macrophage markers in response to IL-4/IL-13 were plotted separately (Figure 3.17). In all 3 donors, the upregulation of the M1 polarisation markers *IL-6, IL-1β, TNF, CD274,* and *VEGFA* in response to IFN-γ/LPS stimulation was greater in the

chlorate pre-treated samples than in the controls (Figure 3.17A). In contrast, the upregulation of the anti-inflammatory markers *CD209* and *CD206* following IL-4/IL-13 stimulation was lower in all 3 donors following chlorate treatment than in controls (Figure 3.17B). *TGFβ* was an exception to this trend in that its upregulation in response to IL-4/IL-13 was increased by chlorate pre-treatment rather than decreased. However, since this gene was also upregulated by IFN-γ (Figure 3.16) it is not an exclusive marker of anti-inflammatory macrophages.

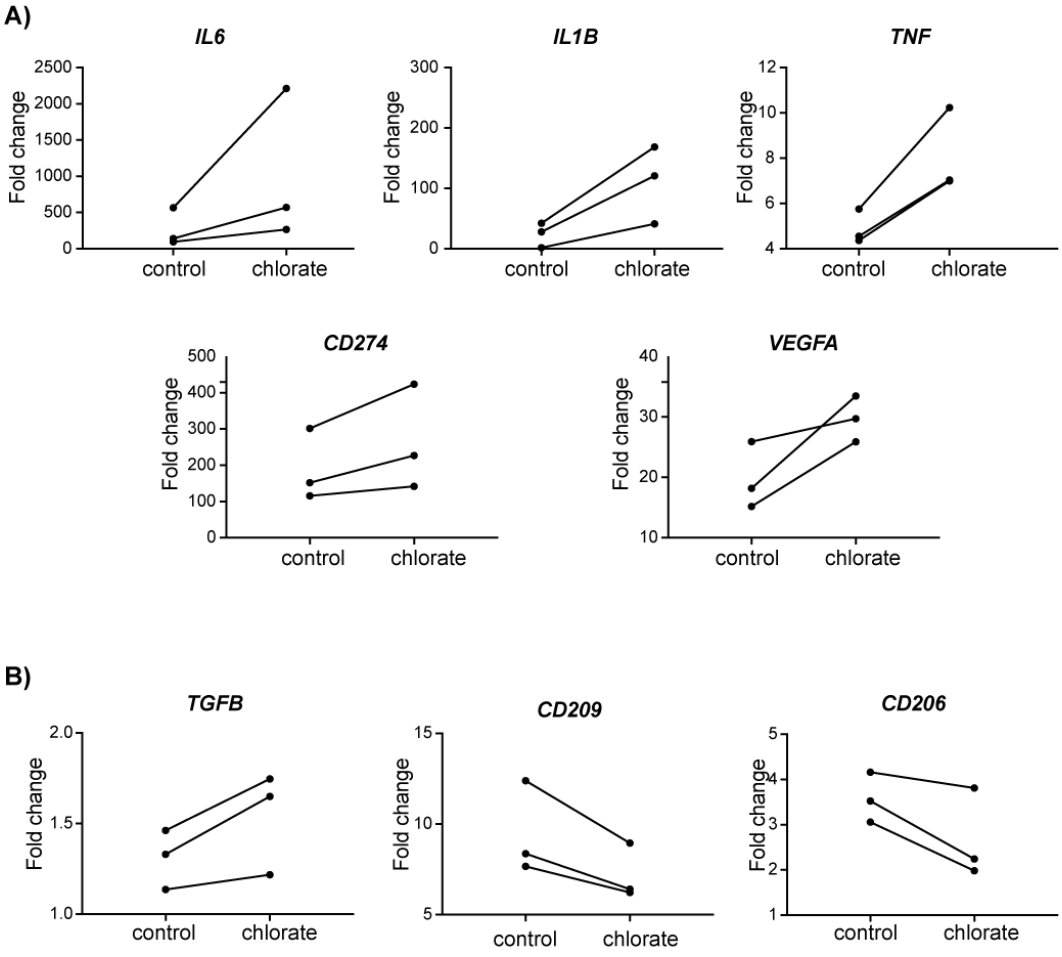

Figure 3.17 Pro- and anti-inflammatory polarisation markers were differentially affected by sodium chlorate treatment. Selected data from the qPCR analysis of polarisation marker expression in Figure 3.15 were plotted on individual graphs showing the relative expression of each marker in control and chlorate-treated samples for each donor relative to the untreated M-CSF control (n=3). A) Fold change in expression of pro-inflammatory markers *IL6, IL1B, TNF, CD274,* and *VEGFA* after stimulation with IFN-γ and LPS. B) Fold change in expression of anti-inflammatory markers *TGFB, CD209* and *CD206* after stimulation with IL-4 and IL-13.

3.6 Discussion

It is now common practice to purify white blood cell fractions using beads and positive or negative selection. However, given the large numbers of monocyte-derived macrophages I would need to perform the planned transcriptome analysis and subsequent functional studies looking at the effect of manipulating HS expression on macrophage functions, I decided to use the older method of countercurrent centrifugal elutriation that gives a higher yield of less pure cells (Turpin et al., 1986). Because monocytes but not lymphocytes adhere to plastic in response to M-CSF, the maturation step provided a way to select for myeloid cells as the small number of lymphocytes that may be present after elutriation are washed away at the re-plating stage after 5 days. I found that the methods I used to mature and polarise monocyte-derived macrophages successfully yielded populations of cells with substantially different and polarised phenotypes, indicated by the differential expression of pro- and anti-inflammatory markers that I measured.

Comprehensive profiling of HS-associated genes by microfluidic array card revealed that many HS core proteins are expressed by monocytes and macrophages, and that at least one isoform of enzymes in each step of the biosynthetic pathway was expressed, indicating that macrophages have the potential to elaborate fully modified HS. I found that the most abundant HS core proteins at the message level in M-CSF-differentiated macrophages were syndecans-2 and -4, and glypican-4, which is consistent with previous data showing abundant transcript for syndecan-2 in monocyte-derived macrophages (Clasper et al., 1999), and that phospholipase-C

treatment released sulfated GAGs from macrophages (Wegrowski et al., 2006), indicating the presence of GPI-anchored core proteins.

When the transcriptome data were represented as a heatmap such that most similar patterns of gene expression were clustered together, I found that all monocyte samples from multiple donors clustered together and were most similar to the unpolarised M-CSF-differentiated macrophages and the anti-inflammatory IL-4/IL-13-polarised macrophages, consistent with previous reports that these M2-like cells are similar to unpolarised macrophages (Martinez et al., 2006). Unexpectedly, the IL-4/IL-13 sample from one donor segregated further away in the region of IFN-γ and/or LPS-stimulated samples. The reason for this is unclear, but as this donor on the array was not among those used for polarisation marker quantification, it is possible that macrophages from this donor did not polarise properly. This may be due to cells being hyporesponsive to stimulation, perhaps due to previous activation during acute infection of the donor, or because of chronic inflammatory disease (Papoutsopoulou et al., 2019) or age of the donor, which in mice has been demonstrated to reduce macrophage responsiveness (Yoon et al., 2004).

The majority of HS-associated genes were upregulated from monocyte to M-CSF macrophage, suggesting that maturation is associated with a global increase in cell-surface HS. This is consistent with a previous study of macrophage HSPGs showing low levels of sulfated GAG in monocytes and increased GAG synthesis upon maturation to macrophages (Wegrowski et al., 2006). Curiously, I found that the message level of *EXT1* decreased from monocyte to macrophage, whereas *EXT2*

expression increased, which is surprising given that these two enzymes are thought to act as a heterodimeric complex (McCormick et al., 2000). However, downregulation of *EXT1* from monocyte to macrophage has previously been reported in response to GM-CSF (Trottein et al., 2009) so may represent a feature of macrophage maturation.

Polarisation resulted in significant differences in the expression levels of many genes, indicating that macrophages may alter their cell-surface HS in response to the stimuli they encounter in the microenvironment. The core protein agrin was most highly upregulated by LPS stimulation, whereas perlecan was strongly induced by IL-4/IL-13, suggesting the existence of a pro/anti-inflammatory switch in the type of HS core proteins expressed, although the relevance of such a switch to macrophage functions has not been explored.

As previously seen in other cell types (Krenn et al., 2008), protein isoforms of the same enzyme were regulated differently in macrophages by the stimuli used. Expression of HS sulfotransferase protein isoforms has been shown to correlate with variation in ligand binding (Ford-Perriss et al., 2002; Huynh et al., 2012), suggesting that the isoforms may generate specific HS motifs with different ligand-binding properties. It may be the case that the different HS structures produced assist in the effector functions of macrophages required by a particular immunological challenge. I observed a strong and significant upregulation of *NDST1* upon maturation of monocytes to macrophages, which suggests that maturation is associated with an increase in N-sulfation of HS and thus the potential for increased downstream

modifications such as O-sulfation as well. N-sulfated HS has previously been shown to maintain macrophages in a quiescent state by inhibiting IFN-β signalling (Gordts et al., 2014), suggesting it may play an anti-inflammatory role by suppressing activation of macrophages.

Inflammatory stimuli such as LPS and IFN-γ have previously been shown to induce upregulation of some enzymes in the HS biosynthetic pathway, such as *HS3ST3B* (Sikora et al., 2016), and I observed similar increases in some but not all 3-O-sulfotransferases with IFN-γ and/or LPS stimulation. In contrast, the 2-O-sulfotransferase *(HS2ST1)* was most highly expressed in IL-4/IL-13-polarised macrophages in my hands, whereas 6-O-sulfotransferase-1 *(HS6ST1)* was most highly expressed in unpolarised M-CSF macrophages and its functional partner sulfatase-2 *(SULF2)* was most abundant in monocytes. Overall it seems likely that macrophages polarised with different stimuli have substantially different HS structures.

I attempted to detect HS on the surface of M-CSF macrophages with antibodies, with a view to subsequently comparing the binding of epitope-specific antibodies to pro- and anti-inflammatory cells. However, the antibody 3G10 that recognises the stub of HS left behind on the core protein after heparinase III treatment (David et al., 1992) did not show the expected increase in staining after heparinase digestion of macrophages. Moreover, the isotype control antibody resulted in substantially higher fluorescence than for unstained or no-primary control samples, suggesting this antibody type may be binding to something other than the HS epitope on

macrophages. It seems unlikely that this would be the Fc-receptor however, as an FcR blocking step was included in the staining protocol. I encountered similar problems with the antibody 10E4 that recognises N-sulfated HS (David et al., 1992): the fluorescence of stained cells was not much stronger than for unstained, was not abolished by heparinase treatment, and was comparably strong in the no-primary control cells. Further optimisation with the dilutions of primary and secondary antibodies may have helped to improve detection of macrophage HS. Others have reported an increase in 3G10 staining between monocytes and macrophages (Clasper et al., 1999), indicating a greater number of HS chains, which is consistent with the increased expression of biosynthetic enzymes I observed. Epitope-specific antibodies have also shown differences in HS structure between pro- and anti-inflammatory macrophages: the 2-O-sulfate specific antibody AO4B08 showed stronger staining of anti-inflammatory macrophages than pro-inflammatory (Martinez et al., 2015), which is consistent with my transcriptome data showing highest expression of *HS2ST1* message in IL-4/IL-13-stimulated macrophages. In the same study, disaccharide composition analysis by HPLC confirmed the increased abundance of 2-O-sulfated disaccharides in anti-inflammatory versus pro-inflammatory macrophages, correlating with the increased message level of *HS2ST1* they reported. At time of writing, samples of M-CSF-differentiated and polarised (IFN-γ/LPS and IL-4/IL-13) macrophages have been sent to a collaborator for disaccharide composition analysis by mass spectrometry (Antia et al., 2018). It is hoped that these data will reveal differences in pro- and anti-inflammatory HS structure and increase our understanding of the correlation between the expression level of different HS biosynthetic enzymes and the abundance of different sulfated motifs.

Given the upregulation I observed for the majority of HS-associated genes during monocyte to macrophage, it seemed plausible that monocyte to macrophage maturation requires increased cell-surface HS. To test whether M-CSF-induced maturation relies on sulfated HS, I cultured monocytes in sodium chlorate for the 5 day M-CSF period to inhibit sulfation of GAGs (Baeuerle and Huttner, 1986; Safaiyan et al., 1999), and then stained for markers associated with monocyte to macrophage transition. CD14 is a marker of the monocytic lineage whose expression is maintained or slightly increased by M-CSF maturation (Asakura et al., 1996), and CD16 is upregulated in M-CSF macrophages relative to monocytes (Ambarus et al., 2012). I saw no obvious differences in the expression level of these markers in M-CSF macrophages cultured in sodium chlorate relative to normal controls, indicating that the ability of macrophages to mature in the presence of M-CSF was not compromised by loss of GAG sulfation. Moreover, CD68 expression was not significantly affected by sodium chlorate, showing that the cells were still committed to the monocytic lineage. These results are not surprising as M-CSF is not thought to bind to HS (Ori et al., 2011) and therefore its signalling should not be affected by loss of HS sulfation.

I then hypothesised that the increased expression of HS-associated genes and presumed increase in cell-surface HSPGs in M-CSF macrophages reflected a requirement for HS for macrophage functions after maturation, such as the ability to respond to immunological signals in the microenvironment. Indeed, IFN-γ and IL-4, which I had used to generate pro- and anti-inflammatory macrophages, respectively,

have both been reported to bind HS (Ori et al., 2011). I therefore tested whether pre-treating cells with sodium chlorate to abolish HS sulfation affected the response to polarising stimuli. I found that chlorate treatment significantly reduced IFN-γ-induced CD64 protein expression, but appeared to increase the upregulation of pro-inflammatory markers at the message level. The reason for this discrepancy is not clear, but may be because samples for flow and for qPCR were collected at the same time point of 24 h after stimulation, but changes in protein expression would be expected to take longer than changes in mRNA levels. Further investigation is required as to the effect of chlorate treatment on IFN-γ signalling, but as heparin inhibits the interaction of IFN-γ with its receptor (Sadir et al., 1998) it seems likely that sulfated HS is inhibitory for IFN-γ signalling and therefore that chlorate treatment would increase it.

Chlorate-treated cells showed reduced upregulation of the anti-inflammatory markers CD163, CD209, and CD206 at protein and message levels, suggesting that IL-4 signalling is compromised in HS-deficient cells. This is consistent with a previous study showing reduced IL-4-induced upregulation of CD209 (DC-SIGN) in chlorate-treated dendritic cells (den Dekker et al., 2008). However, M-CSF only controls also showed decreased staining for CD163 and CD209, suggesting that chlorate treatment may have altered macrophage phenotype more globally than just the responsiveness to IL-4. I did not perform viability assays on chlorate-treated macrophages so it remains possible that decreased cell viability can account for some of the reduced marker expression.

Overall I have shown that stimulation of human monocyte-derived macrophages with different inflammatory stimuli leads to distinct phenotypes with associated profiles of HS-associated gene expression. Treatment of macrophages with sodium chlorate to inhibit HS sulfation appeared to alter the upregulation of polarisation markers, but as I was unable to reliably detect HS with antibodies and other methods such as HPLC were not available I cannot be sure that the time point or concentration of sodium chlorate were sufficient to abolish sulfation of macrophage HS. Moreover, I did not perform viability assays such as MTS, meaning that chlorate treatment could have resulted in cell death or altered other cellular processes independent of the HS sulfation status. Furthermore, these experiments were performed in only 3 donors and no functional validation of changes in cytokine signalling was carried out. The altered induction of polarisation markers in chlorate-treated cells suggests that macrophage HS may be involved in regulating responsiveness to polarising cytokines and calls for further investigation to illuminate this area.

Chapter 4: The role of 6-O-sulfation of HS in macrophage functions

4.1 Introduction

Following my initial qPCR screen of HS-associated gene expression in human monocytes and polarised macrophages, I selected one gene in particular for further study: heparan sulfate 6-O-sulfotransferase 1 (HS6ST1). Along with its protein isoforms (HS6ST2 and HS6ST3), this enzyme can add a sulfate group to the 6th carbon position of GlcNAc residues (Habuchi et al., 1995). This is unique among heparan sulfate modifications in that it can be removed after the HSPGs have been trafficked to the cell surface, a reaction catalysed by the sulfatase enzymes (SULF1 and SULF2) (Morimoto-Tomita et al., 2002). Expression of the sulfatase enzymes is tightly regulated during development (Ohto et al., 2002; Ratzka et al., 2010) by morphogens such as sonic hedgehog (Shh) (Dhoot et al., 2001), where they switch the function of HS between activatory or inhibitory for a number of morphogens, including members of the Wnt/β-catenin and TGF-β/BMP families (Figure 4.1). The proposed mechanism of activity of the morphogen Wnt is that it binds with high affinity to 6-O-sulfated HS, which precludes binding to its signalling receptor Frizzled. Removal of 6-O-sulfate groups by the SULF enzymes reduces the affinity of Wnt for HS and thus enables interaction with its receptor, Frizzled (Ai et al., 2003). Similarly, the BMP inhibitor Noggin binds to 6-O-sulfated HS, so expression of SULFs and consequent reduction of 6-O-sulfation releases Noggin and enables BMP to signal (Viviano et al., 2004). As discussed in Chapter 1.4, 6-O-sulfation has also been identified as a particularly important HS modification for the signalling of

many chemokines, cytokines, and growth factors. For example, the signalling of FGF-2 requires an HS motif containing a 6-O-sulfate group (Rusnati et al., 1994) and their removal via SULF2 digestion decreased signalling (Seffouh et al., 2013). The binding site for IFN-γ is also known to contain an abundance of 6-O-sulfate groups (Vanhaverbeke et al., 2004). However, very little is known about the requirements for 6-O-sulfation of macrophage HS and whether a similar 6-O-sulfate switch regulates aspects of inflammation as it does development.

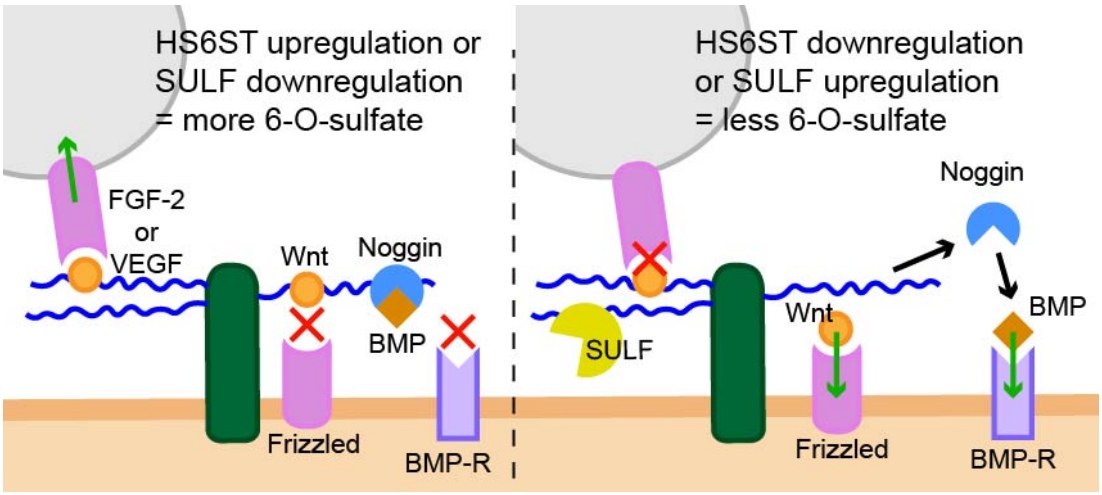

Figure 4.1 HS6STs and SULFs play reciprocal roles in regulating growth factor signalling. 6-O-sulfate groups of HS facilitate binding of factors including FGF-2 and VEGF and promotes their signalling, so decreased biosynthesis of 6-O-sulfated HS or increased SULF activity would be expected to decrease the activity of these growth factors. In contrast, 6-O-sulfated HS binds and sequesters both Wnt and BMP bound to its inhibitor Noggin so desulfatase activity frees these ligands to interact with their receptors.

4.2 HS6ST1 as a target gene for further study

According to my microfluidic array transcriptome analysis (Chapter 3.3.3), *HS6ST1* and *SULF2* were abundantly expressed in monocytes and macrophages, whereas the other protein isoforms *HS6ST2*, *HS6ST3*, and *SULF1*, were not detectable. This means that I can be fairly confident that the overall level of 6-O-sulfation of macrophage HS is solely under the control of *HS6ST1* and *SULF2* in my

experimental conditions. Moreover, 6-O-sulfotransferases act near the end of the biosynthetic pathway so the consequences of abolishing HS6ST1 expression for other aspects of HS biosynthesis should be minimal, making this gene a suitable target for mechanistic studies of HS function in macrophages.

4.2.1 Validation of changes in *HS6ST1* expression upon macrophage maturation and stimulation

To confirm the reciprocal regulation of *HS6ST1* and *SULF2* mRNA observed in the qPCR screens in Chapter 3 (Chapter 3.3.3), I performed individual qPCRs with the same TaqMan probes as used on the array, with samples from other donors not previously run on the array cards **(**Figure 4.2**).** These assays confirmed strong and significant upregulation of *HS6ST1* during maturation from monocyte to macrophage, and the subsequent downregulation of its expression upon further stimulation. *SULF2* was expressed in monocytes and significantly downregulated by M-CSF and all other polarising stimuli. As before with the microfluidic array cards, expression of *HS6ST2*, *HS6ST3*, and *SULF1* were undetectable. These strong and reproducible differences in separate qPCR settings and with a different subset of donors validated my choice of *HS6ST1* as a candidate gene for further study. Given that *HS6ST1* was most highly expressed in M-CSF-differentiated macrophages without further stimulation, I decided to focus on these 'unpolarised' macrophages for further experiments.

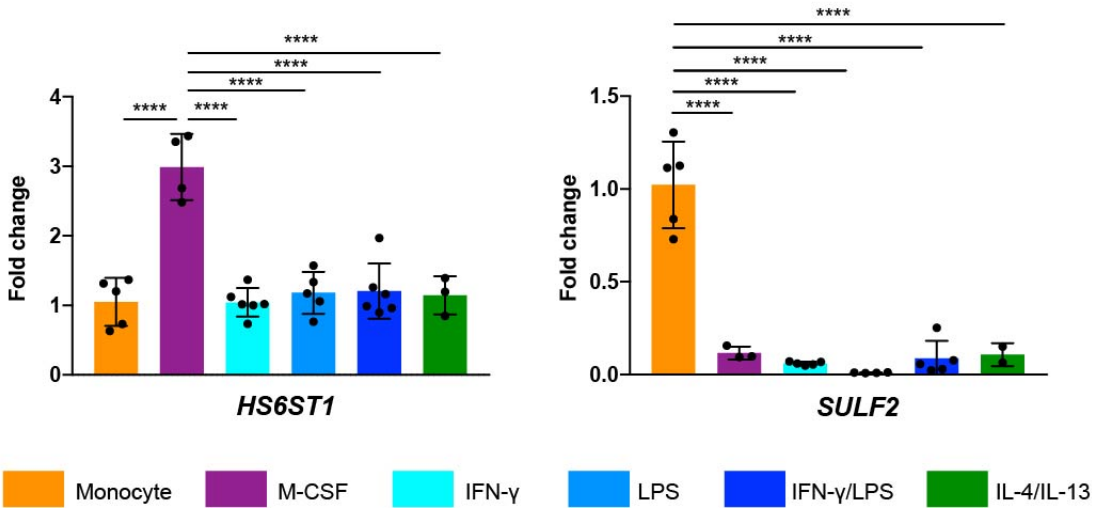

Figure 4.2 *HS6ST1* and *SULF2* showed reciprocal regulation during monocyte to macrophage maturation.
Manual qPCR of *HS6ST1* and *SULF2* in primary human monocytes and M-CSF-differentiated macrophages with or without further polarisation. Where indicated, cells were polarised by treatment for 24 h with LPS (100 ng/ml), IFN-γ (50 ng/ml), or IL-4 and IL-13 (both at 20 ng/ml). Data were analysed using the ΔΔCt method using the housekeeping genes 18S and GAPDH and expressed as a fold change relative to the average expression level in monocytes. Error bars represent mean ± SD. Data were analysed by one-way ANOVA with multiple comparisons. All significant comparisons are indicated, where q<0.0001 (****). Samples from 3 to 5 donors were analysed per condition.

4.2.2 Knockdown of *HS6ST1*

To begin investigating the role of 6-O-sulfation of heparan sulfate in macrophage functions, I first optimized the knockdown of *HS6ST1* in primary human M-CSF-differentiated macrophages. Initial attempts using transfection reagents such as jetPRIME and DharmaFECT were unsuccessful due to the low cell numbers stipulated in the protocol, and therefore I was unable to extract sufficient RNA for qPCR. I also predicted that I would not have sufficient cells using this method for subsequent experiments. Given the quantities of siRNA required by this method, scaling up the quantities to knock down HS6ST1 in more cells would have been prohibitively expensive. Thus I turned to an alternative method of siRNA transfection: electroporation using an Amaxa nucleofector apparatus with a buffer

designed specifically for macrophages (Warwick and Usachev, 2017). The major advantage of this method is that it is more cost-effective, as the cells are electroporated in a cuvette in solution, meaning that knockdown can be performed in up to 10 million cells in only 200 µl of nucleofector buffer and thus requiring only a small quantity of siRNA. To investigate whether this method was sufficient to reduce *HS6ST1* at the message level, I tested three different concentrations of siRNA: 10, 50, and 100 nM, with non-targeting siRNA controls at the same concentrations (Figure 4.3). I obtained significant knockdown by 24 h at all three concentrations tested, and this was consistent across 6 independent experiments each using monocyte-derived macrophages from different blood donors. The knockdown was sustained at 48 and 72 h, although knockdown achieved with 10 nM siRNA was not significant at 72 h. To investigate whether there were off-target effects of si*HS6ST1* treatment, or whether there were compensatory changes in the expression levels of other genes controlling 6-O-sulfation, such as the other HS6ST protein isoforms or the sulfatase enzymes, I also quantified the relative expression levels of these genes by qPCR. There were no significant changes in the expression levels of *SULF2* (Figure 4.3), while *HS6ST2*, *HS6ST3*, and *SULF1* remained undetectable. In the absence of upregulation of the other enzymes controlling the 6-O-sulfation, knockdown of *HS6ST1* is expected to lead to a reduction in 6-O-sulfation, provided that macrophages turn over their cell-surface HS to replace it with newly synthesised HS within this timeframe.

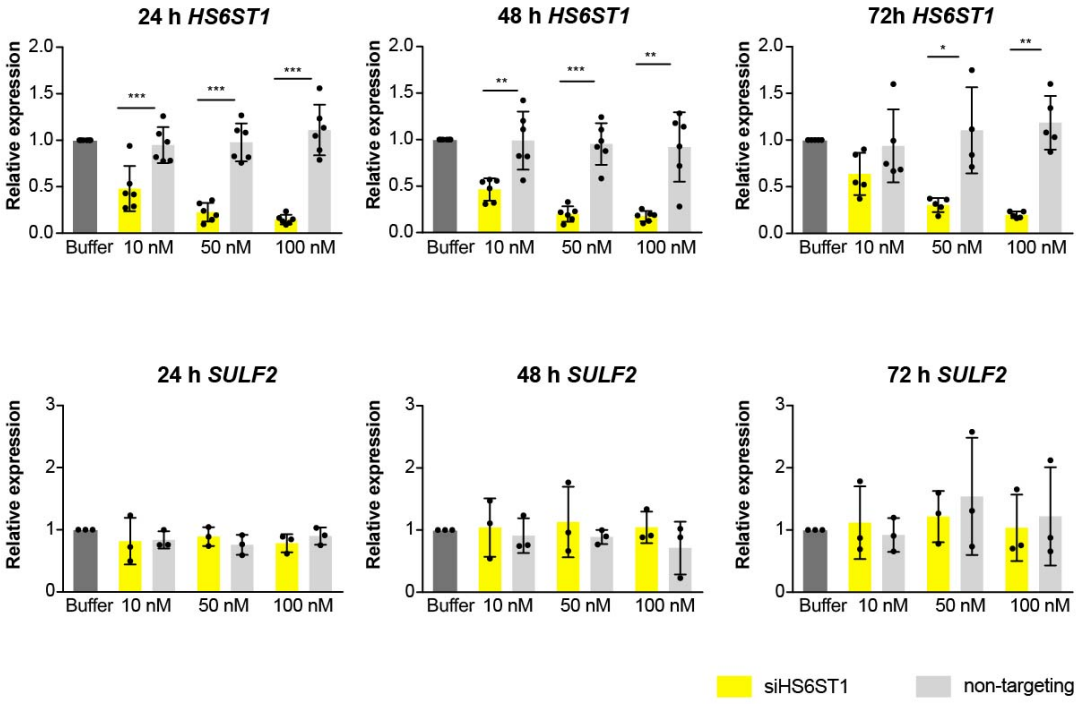

Figure 4.3 Expression of *HS6ST1* was reduced by siRNA transfection of primary human monocyte-derived macrophages.
After 5 days of culture in M-CSF, monocyte-derived macrophages were re-suspended in nucleofector buffer containing siRNA (10, 50, or 100 nM) targeting *HS6ST1*, or non-targeting control, and the mixtures electroporated in an Amaxa nucleofector apparatus. Cells were diluted to 1 million cells/ml with RPMI/10% FBS/1% Pen-Strep and cultured for 24, 48, or 72 h. Media were aspirated and the adherent cells washed in PBS before RNA was isolated and reverse transcribed to cDNA. Relative expression of *HS6ST1* and *SULF2* were quantified by qPCR using the ΔΔCt method relative to the three housekeeping genes 18S, GAPDH, and RPLP0 and as a fold change compared to the buffer control for each donor at each time point. ($n \geq 3$ blood donors). Error bars represent mean ± SD. Groups were tested for normality using the Shapiro-Wilk normality test, and si*HS6ST1* groups compared to the non-targeting siRNA controls using a two-tailed paired student's t-test. All significant comparisons are shown where $p<0.05$ (*), $p<0.01$ (**), $p<0.005$ (***), and $p<0.0001$ (****).

The human monocytic cell line THP1 is a widely-used model for many monocyte and macrophage functions. These cells grow in suspension like primary blood monocytes, but can be activated by stimuli such as PMA that will induce them to mature to a more macrophage-like phenotype, becoming larger and more adherent. Because both forms of THP1 cell might be useful for functional studies, I tested whether I could successfully knock down *HS6ST1* using the same method of electroporation I had successfully applied in the primary macrophages (Figure 4.4). THP1 cells were re-suspended in media with or without PMA to induce them to mature and adhere after knockdown. I again tested different concentrations of siRNA, and found that the knockdown was maintained over time by collecting samples at 24, 48, and 72 h post-electroporation.

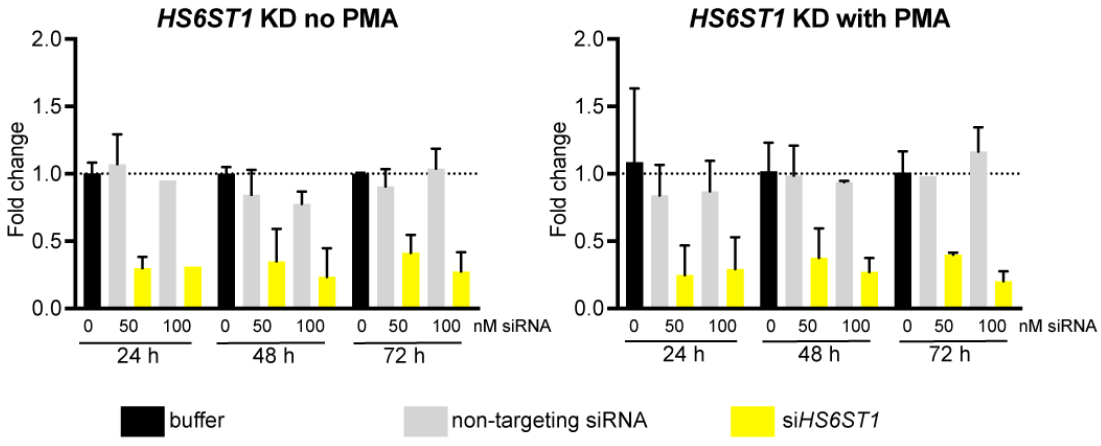

Figure 4.4 Knockdown of *HS6ST1* was achieved in THP1 cells.
THP1 cells were electroporated with 50 or 100 nM siRNA targeting *HS6ST1*, or non-targeting control siRNA, then re-suspended at 1 million cells/ml in media with or without 100ng/ml PMA. After 24, 48, or 72 h incubation, cells were collected for RNA extraction and qPCR. 18S and GAPDH were used as the housekeeping genes, and relative gene expression assessed by the ΔΔCt method, with fold changes expressed relative to the average in the buffer control samples at each time point. n=1 to 5 replicates per condition. Error bars represent mean ± SD.

4.2.3 siRNA treatment did not affect cell viability

To determine whether knockdown of *HS6ST1* in primary macrophages had a measurable effect on cell viability, I performed crystal violet assays to quantify the proportions of adherent, and thus viable, macrophages in the different treatment conditions at the three time points (Figure 4.5). In three donors, these assays showed no significant effect of knockdown on cell viability, and also no significant effect of electroporation in the nucleofector buffer compared to untreated control cells.

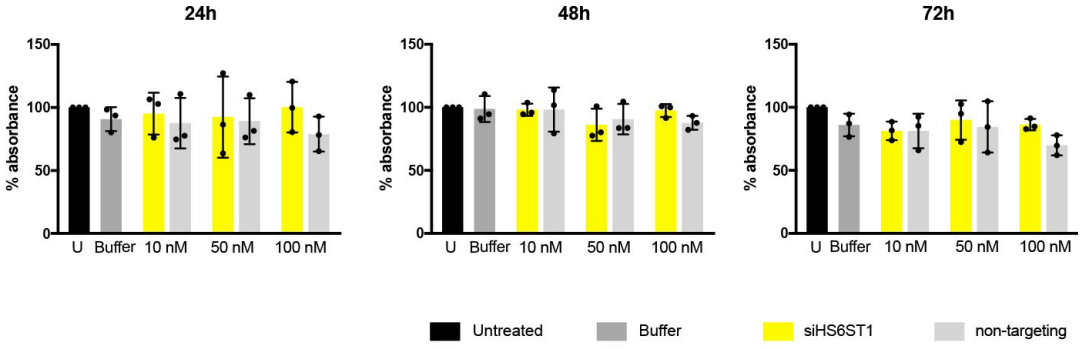

Figure 4.5 Knockdown of *HS6ST1* did not affect macrophage viability.
After electroporation with siRNA, cells were cultured for 24, 48, or 72 h in RPMI/10% FBS/1% Pen-Strep before incubation with crystal violet dye, followed by methanol solubilisation and quantification of absorbance at 490 nm. Average absorbance per condition was expressed as a percentage of the absorbance of untreated control cells (U) for each donor (n=3) at each time point. Error bars represent mean ± SD. Data were tested by one-way ANOVA with multiple comparisons, and no comparisons were significant.

4.3 Detection of HS6ST1 protein

After knockdown of *HS6ST1* by siRNA transfection, the reduction in *HS6ST1* message was strong and significant by 24 h. However, it is possible that the turnover time of the protein is much slower than this, and that knockdown would have no meaningful effect on enzyme abundance and thus 6-O-sulfation of HS until later time points. To quantify the relative amounts of HS6ST1 protein I tried several techniques, including immunoblotting and immunocytochemistry.

4.3.1 Detection of HS6ST1 protein by immunoblotting

Cell lysates and TCA-precipitated conditioned media from monocyte-derived macrophages were run on SDS-PAGE gels, transferred to PVDF membranes, and probed with several anti-HS6ST1 antibodies. However, neither colourimetric (alkaline phosphatase, using Western Blue stabilised substrate for alkaline phosphatase, Promega S3841) nor chemiluminescent (horseradish peroxidase) detection produced specific bands at the expected molecular weight of 48.2 kDa. SantaCruz mouse anti-HS6ST1 (sc-398231) resulted in no staining at all by chemiluminescent detection, and R&D sheep anti-HS6ST1 (AF5057) produced high background staining by chemiluminescent detection. An abcam rabbit anti-HS6ST1 antibody (ab106195) produced faint bands at approximately 48 kDa by colourimetric detection, albeit with high background (Figure 4.6A). It has been reported that HS6ST1 can be shed into the extracellular space (Habuchi et al., 1995) so to prevent potential loss of protein from the cells I treated PMA-activated THP1 cells with an inhibitor of exocytosis, GolgiStop (BD Biosciences 554715), for 4 h. However, no specific band was detectable from the lysates of these cells (Figure 4.6B) Lysing cells in RIPA buffer (50 mM Tris-HCl, pH 7.4, 150 mM NaCl, 1% Triton X-100, 0.5% sodium deoxycholate, 0.1% SDS), reducing (R) SDS buffer, or non-reducing (NR) SDS buffer gave similar results, with no strong, specific HS6ST1 bands.

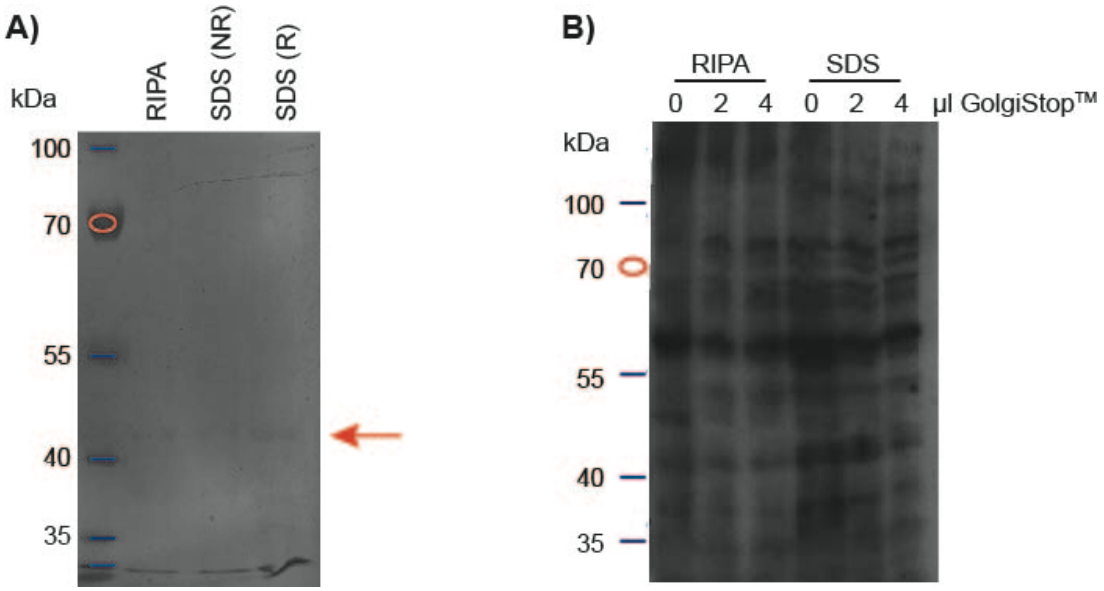

Figure 4.6 Attempts to detect HS6ST1 protein by immunoblotting.
Cell lysates from human monocyte-derived macrophages or THP1 cells were analyzed by SDS-PAGE electrophoresis and immunoblotting for HS6ST1. A) M-CSF-differentiated macrophages were lysed in equal volumes of RIPA or SDS buffer with (R) or without (NR) 5% beta-mercaptoethanol as a reducing agent. Detection was performed with alkaline phosphatase and colourimetric detection. B) THP1 cells were treated with PMA overnight before 4 h treatment with GolgiStop at 0, 2, or 4 µl per million cells, and lysed in RIPA buffer or non-reducing SDS buffer. Detection was performed by chemiluminescence.

4.2.2 Detection of HS6ST1 protein by flow cytometry with intracellular staining

I hypothesized that the antibody may not recognise the denatured HS6ST1 protein on an SDS-PAGE gel so I thus tried methods in which the protein may be preserved in a more native conformation, namely flow cytometry and immunocytochemistry. The abcam rabbit anti-HS6ST1 antibody I used (ab106195) was not directly conjugated so to perform flow cytometry I first tested different concentrations of primary and an AlexaFluor488-conjugated anti-rabbit secondary antibody (see Table 4, Chapter 2.11 for antibody details), using THP1 cells as a convenient model cell (Figure 4.7A). The results from my initial antibody titration assay indicated that dilutions of 1:100 for the primary antibody and 1:500 for the secondary antibody gave strong staining, with all cells showing as positive and a high median fluorescence intensity (MFI), while

the no-primary control showed minimal staining. However, when I repeated the staining using these antibody dilutions and including an isotype control antibody (ab171870) matched to the anti-HS6ST1 primary, I found that all cells fell within the positive gate whether they had full staining, isotype control antibody, or even no primary antibody (Figure 4.7B). Additionally, the MFI of cells stained with the isotype control was much higher than that of the cells stained with anti-HS6ST1. This suggested that these antibodies bind to the THP1 surface in an antigen-independent manner. A step to block Fc receptors was included as part of sample preparation, so interaction of the Fc region with these cell-surface receptors seems unlikely to be the problem. I repeated the experiment with additional washes between each staining step to remove any non-specifically bound antibody but with the same results.

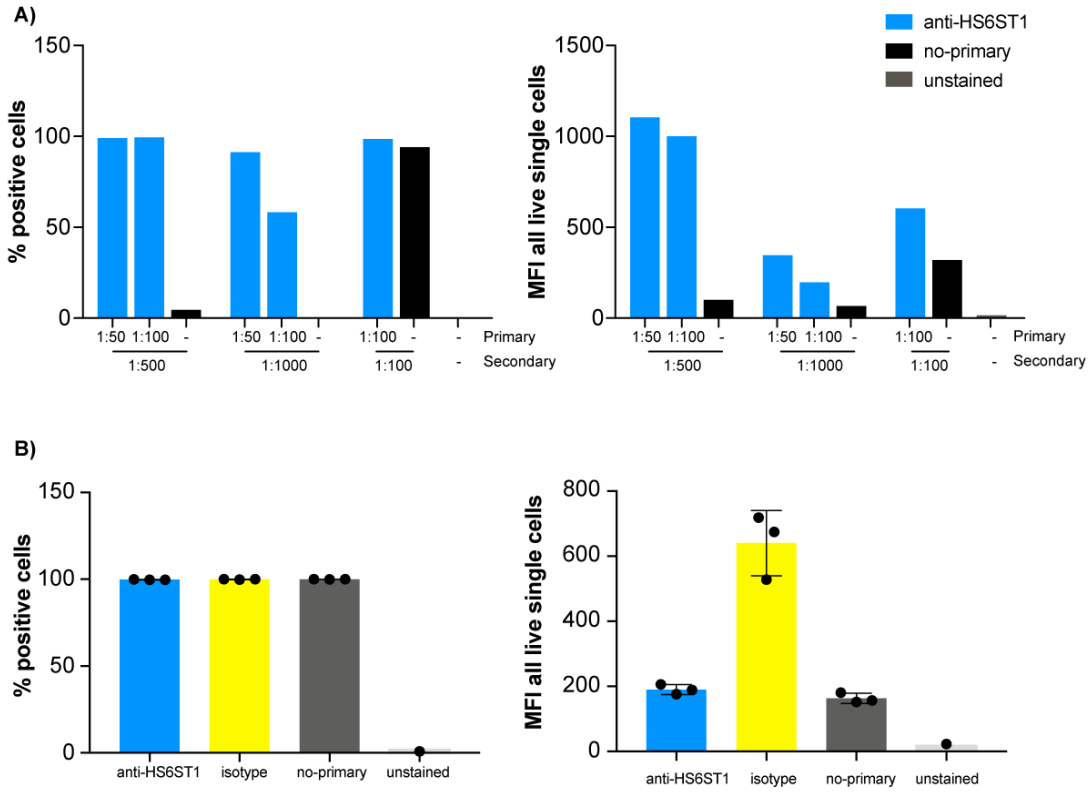

Figure 4.7 Intracellular staining of THP1 cells for HS6ST1 by flow cytometry.
THP1 cells were fixed and permeabilised before staining with anti-HS6ST1 primary antibody and AlexaFluor488-conjugated secondary antibody, then staining quantified by flow cytometry. A) Titration of different primary and secondary antibody concentrations, n=1 sample per condition. B) Primary antibody or isotype control at 1:100 dilution and secondary antibody at 1:500 dilution (n=3). Error bars represent mean ± SD.

4.3.3 HS6ST1 immunocytochemistry optimization

I decided to try another method for detection of HS6ST1 protein. Macrophages, being strongly adherent cells, are ideal candidates for visualization by microscopy, as they will grow on glass coverslips, which can then be stained and mounted on microscope slides. I coated the coverslips with gelatin before seeding the macrophages to encourage the formation of cell-matrix interactions and cell spreading to mimic their morphology in physiological settings. After allowing the M-CSF-differentiated macrophages to adhere to the coverslips for 24 h after seeding, they were washed, fixed, permeabilised and stained with abcam rabbit anti-HS6ST1 (ab106195) and fluorescently labelled anti-rabbit secondary antibody, and DAPI and phalloidin for visualization of the nucleus and cytoskeleton, respectively. Images were then acquired in a single plane on an Olympus confocal microscope with 60x magnification (Figure 4.8). Although there was high background staining in the HS6ST1 channel, the no-primary control showed minimal staining indicating there is limited non-specific interaction of the secondary antibody in this context, unlike the similar fluorescence intensities observed between stained and no-primary controls by flow cytometry (Figure 4.7B). The staining in cell areas, defined by phalloidin staining, was much stronger than the background staining, suggesting that immunofluorescence microscopy might present a way of quantifying HS6ST1 protein if background correction were performed.

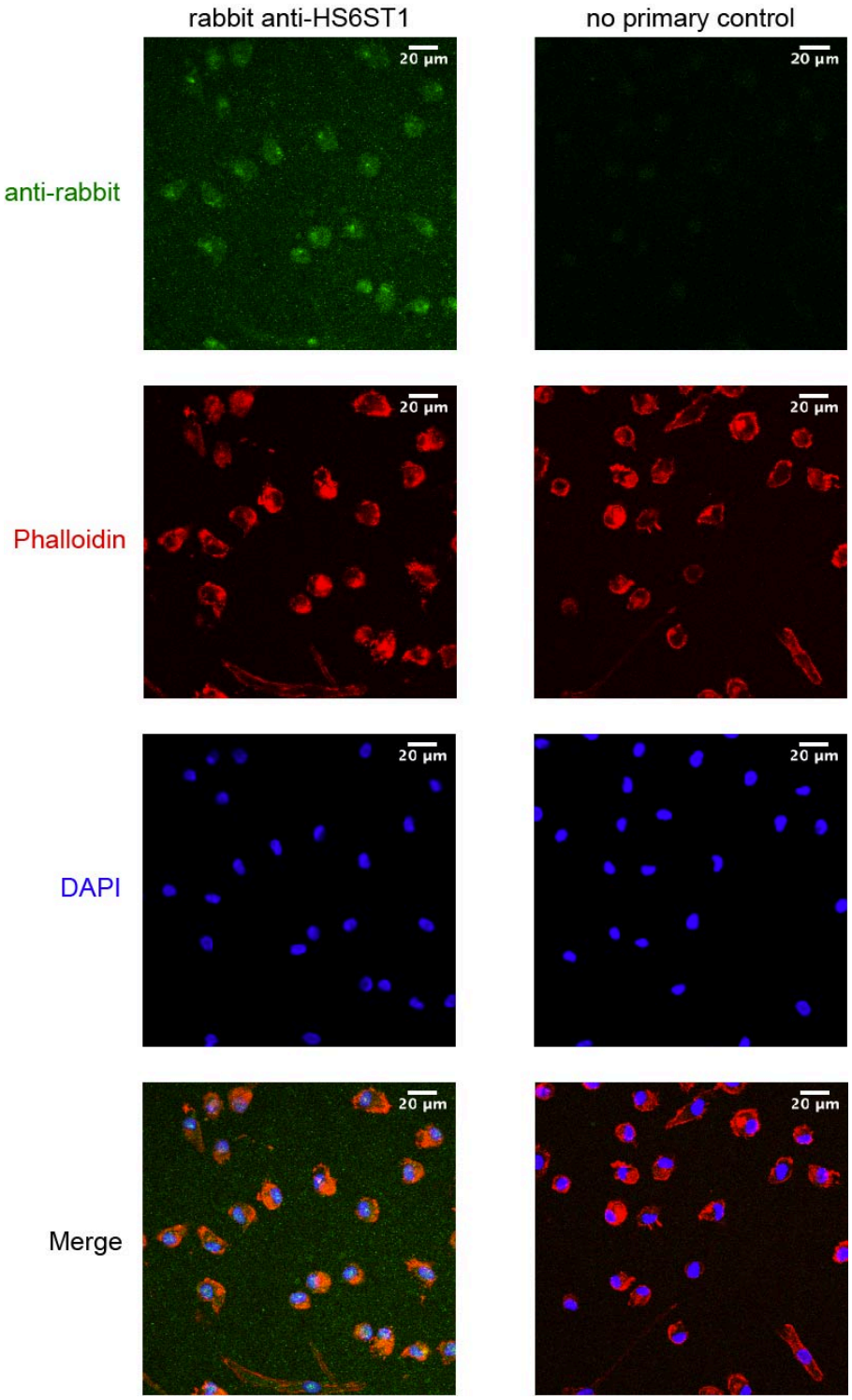

Figure 4.8 Staining of HS6ST1 protein in primary human macrophages visualised by confocal microscopy.
After 5 days in culture with M-CSF, human monocyte-derived macrophages were seeded at 1 million cells/ml on gelatin-coated coverslips and cultured for 24 h. Coverslips were washed in PBS, fixed, and the cells permeabilized before intracellular staining of HS6ST1 protein with rabbit primary antibody at 1:100 and AlexaFluor488-labelled anti-rabbit secondary antibody at 1:500. Nuclei were stained with DAPI and the actin cytoskeleton with phalloidin-568. Images were captured on an Olympus confocal microscope with the 60x objective.

To more accurately quantify total intracellular HS6ST1 protein, several slices in the Z plane were taken through the macrophage cell layer in each of the three channels (Figure 4.9A). Each z-stack was the compressed into a single image representing the total staining intensity, which could then be quantified. The boundary of each cell was defined in the phalloidin channel then copied across to the same location in the HS6ST1 channel, and integrated density measured. The same area was quantified adjacent to the cell but not overlapping with any other cells, and this value was subtracted for background correction (Figure 4.9B). All whole cells in at least 10 fields of view were quantified for both HS6ST1 staining and no-primary control samples. This revealed a strong and significant difference between the mean integrated density of stained samples and that of the no-primary control (Figure 4.9C). However, although this result suggests there is negligible non-specific binding of the secondary antibody, it does not prove the specificity of the anti-HS6ST1 primary antibody. To investigate the antibody's specificity, I applied this same method of staining and image capture and quantification to samples that had been electroporated with si*HS6ST1*, non-targeting control siRNA, or buffer alone, 24, 48, or 72 h prior to staining (Figure 4.10). Despite successful knockdown of *HS6ST1* by siRNA electroporation confirmed by qPCR (Figure 4.10C), there was no change in staining intensity with the HS6ST1 antibody in si*HS6ST1*-treated samples compared to non-targeting or buffer control samples. This result indicates that either macrophage HS6ST1 protein is not turned over and therefore loss of *HS6ST1* mRNA has no effect on its abundance, or the anti-HS6ST1 antibody binds non-specifically to something other than the target enzyme.

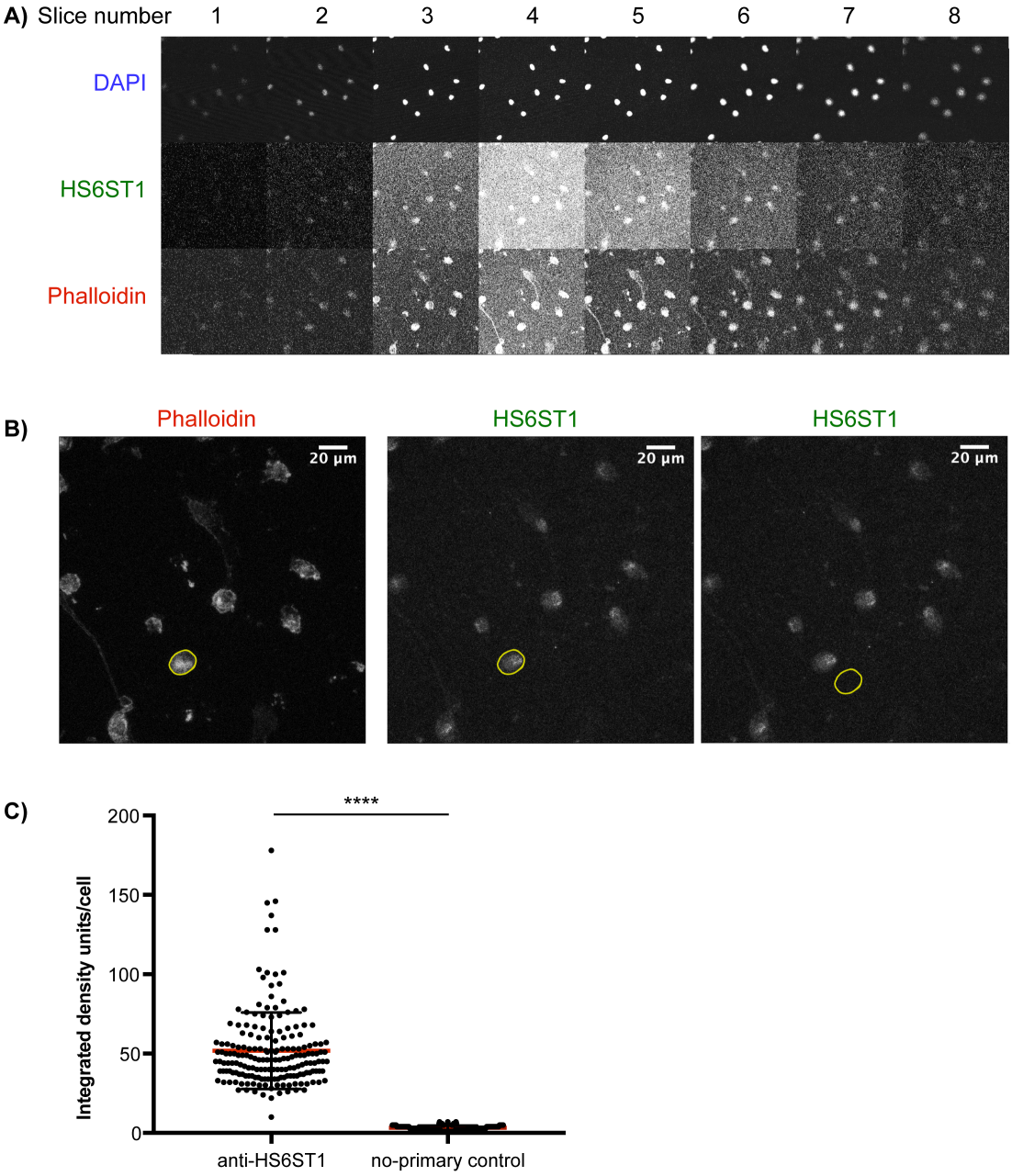

Figure 4.9 Maximum intensity Z-projections from confocal imaging were quantified for total intracellular HS6ST1 protein staining.
M-CSF-differentiated macrophages plated on gelatin-coated coverslips and stained intracellularly for HS6ST1 were visualised by confocal microscopy, taking 8 slices at 5 µm apart per channel. These z-slices were then projected into one image using the Sum Slices tool in ImageJ for quantification of total intracellular staining. A) Representative images obtained from one field of view showing the 8 slices in the three different channels. B) Representative images demonstrating gating strategy applied to all z-stacks: cell outline drawn in the phalloidin channel (AlexaFluor568), then transferred to the same position in the HS6ST1 channel (AlexaFluor488) and integrated density of the cell area measured. Integrated density of an adjacent area not including any other cells was subtracted from each cell reading for background correction. C) Z-stack images from a minimum of 10 fields of view were quantified for cells stained with anti-HS6ST1 or no-primary controls. Each dot represents the background-corrected integrated density of a single cell. Data sets did not pass the Shapiro-Wilk normality test so the two groups were analysed by two-tailed Mann-Whitney test. $P<0.0001$ (****). N=1 donor. Error bars represent mean ± SD.

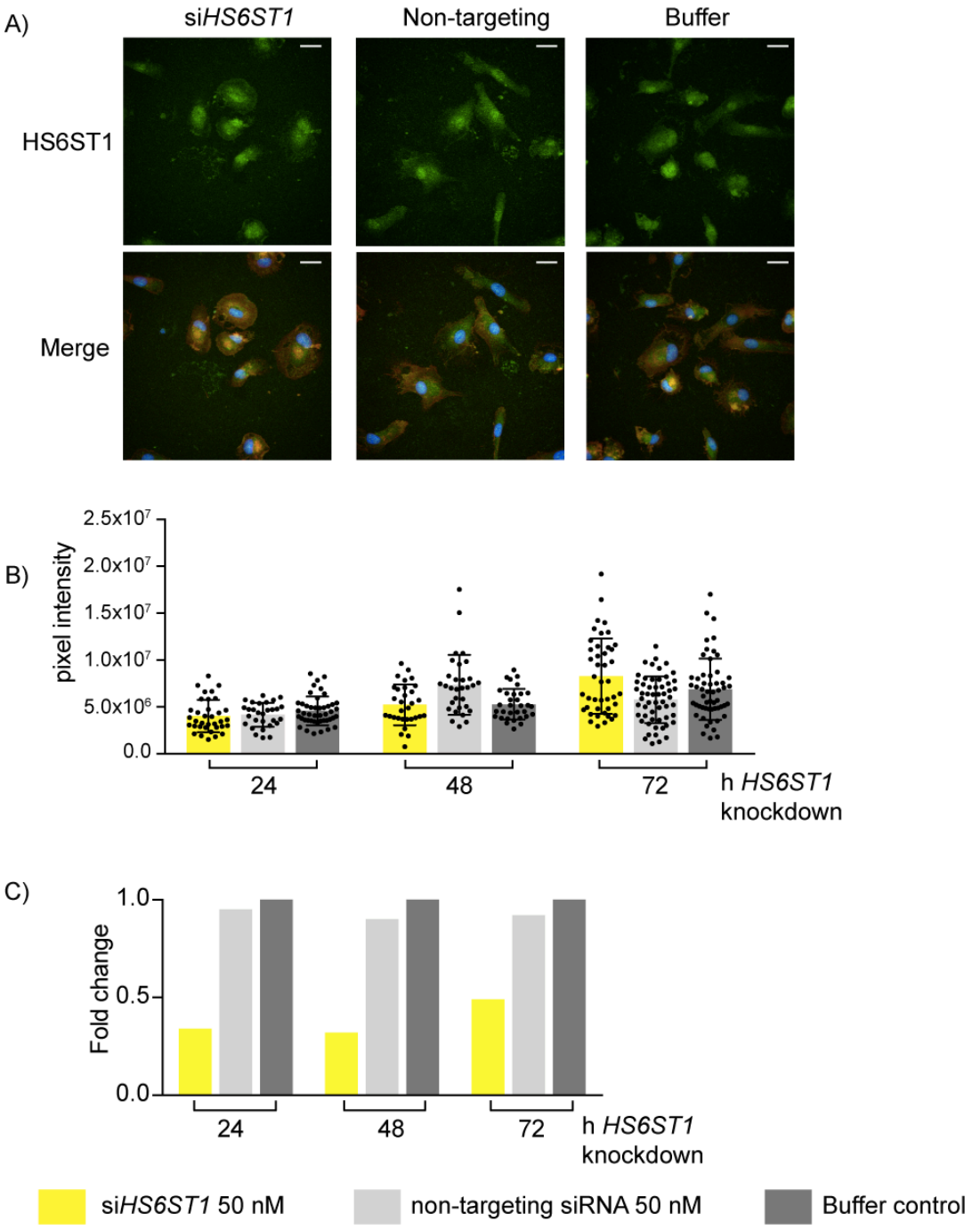

Figure 4.10 Quantification of confocal images after *HS6ST1* knockdown in primary macrophages.
M-CSF macrophages from one blood donor were electroporated with 50 nM siRNA targeting HS6ST1, a non-targeting control siRNA, or buffer-only control, and plated on gelatin-coated coverslips at $1x10^5$/ml. After 24, 48, or 72 h in culture, the coverslips were washed and the cells fixed, permeabilised, and stained, then images captured on an Olympus confocal microscope with z-slices at 1 µm intervals. A minimum of 5 fields of view was quantified for each sample condition. Scale bars 20 µm A) Representative maximum intensity z-projections from 24 h time point showing HS6ST1 staining only and merged image with DAPI (blue) and phalloidin (red). B) Quantification of z-stacks was performed as in Figure 4.9 with background subtraction, where each dot represents the background-adjusted integrated density for one cell. Error bars represent mean ± SD. C) *HS6ST1* quantified by qPCR. n=1 donor.

4.4 Contribution of HS6ST1 to phagocytosis by macrophages

I next considered functions of macrophages in which 6-O-sulfation of HS might be involved. Phagocytosis of pathogens is an essential macrophage function, and there is some evidence that heparan sulfate is involved in this process (Chapter 1.5.2.1). HS may act as a co-receptor for the conventional phagocytic receptors, perhaps capturing pathogens on the surface through electrostatic attraction. Alternatively, it is possible that HS inhibits the uptake of some pathogens by blocking access to their receptor. I thus optimised phagocytosis assays to investigate the role of 6-O-sulfation in phagocytosis by macrophages.

4.4.1 Optimization of phagocytosis assays

I first optimised an assay using flow cytometry that would enable me to quantify the uptake of fluorescently labelled substrates. M-CSF-differentiated monocyte-derived macrophages were incubated with FITC-labelled *E. coli* or zymozan bioparticles to represent bacterial and fungal pathogens, respectively, and samples acquired by flow cytometry (Figure 4.11). Representative images of the gating strategy used are shown in Figure 4.11A: debris were gated out using forward and side scatter, then live cells selected on the basis of viability dye exclusion. The position of the positive gate was defined by the fluorescence of control cells that had not been exposed to fluorescently labelled particles, such that less than 1% of live cells fell within the positive gate. To investigate whether the particles were being internalized by macrophages or simply adhering to the cell surface, control samples were placed on ice for the same time period (Figure 4.11B) as the colder temperature should prevent active internalization by the cells. The majority of cells were still positive for

fluorescently labelled bioparticles even when they had been incubated on ice, suggesting that there is a substantial contribution to the total signal of non-internalized particles adhering to the cell surface. Measuring the MFI however yielded greater separation between the samples incubated at 37 °C and their on ice control (Figure 4.11C), indicating that MFI might be a better measure of phagocytosis than the percentage of cells falling within the positive gate.

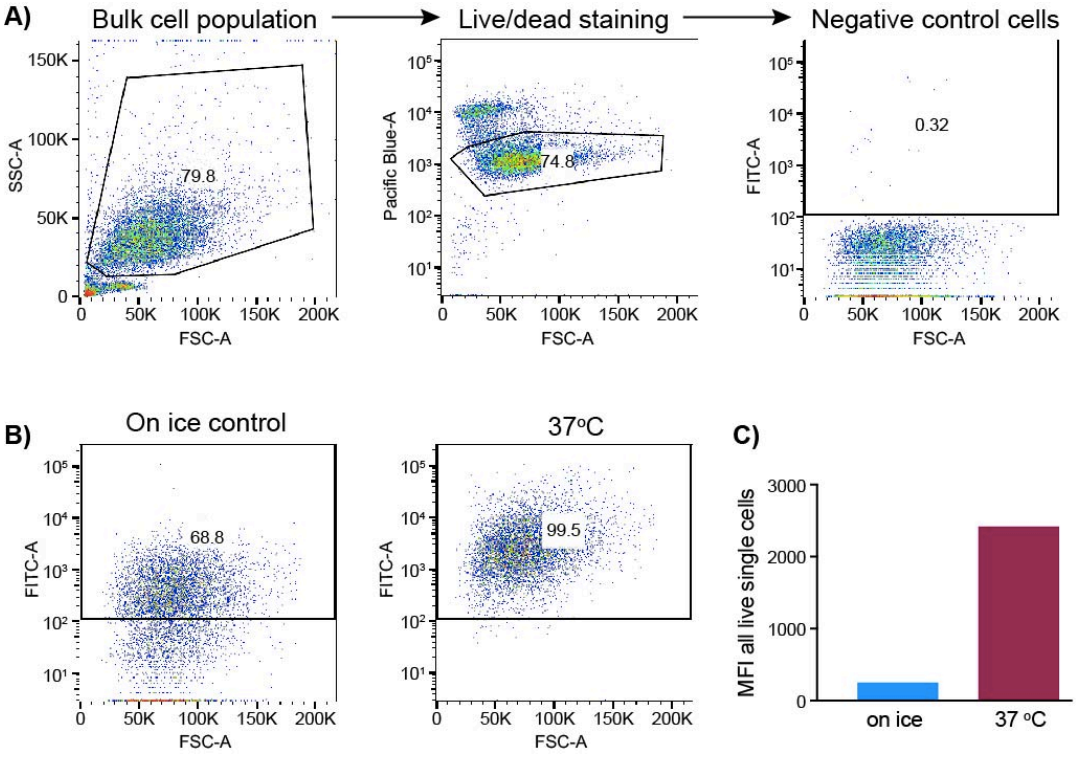

Figure 4.11 Gating strategy for phagocytosis assays in primary human macrophages.
M-CSF-differentiated macrophages from one donor were incubated with fluorescently labelled *E. coli* bioparticles then stained with viability dye and fixed before samples were acquired on an LSR II flow cytometer. A) Dot plots of negative control samples not incubated with bioparticles showing gating strategy applied to all samples. The position of the positive gate was defined by the negative control population, such that the percentage of cells falling in the positive gate was less than 1. B) Dot plots of representative samples incubated for 30 min with MOI of 10 *E. coli* particles, either on ice or at 37 °C. C) MFI of the same two samples: 10 bioparticles per cell incubated for 30 min on ice or at 37 °C.

To determine the optimal time point for uptake of *E. coli* or zymozan particles, and the ideal number of particles per cell (multiplicity of infection, or MOI), I performed a time course of uptake of different particle MOIs in macrophages from one blood donor (Figure 4.12). As zymozan particles are much bigger than *E. coli* particles, I used lower MOIs. Controls on ice were included for some time points in the *E. coli* uptake experiment (Figure 4.12 A). All MOIs of *E. coli* at almost all time points resulted in a universally positive population, and even the on-ice controls showed substantial positivity, especially at higher MOIs. The differences between the MFI of each MOI at 37 °C and on ice, however, were substantially different, further supporting the use of MFI as a measure of phagocytosis rather than percentage positive. Cells incubated with zymozan particles showed a much lower proportion of positive cells (Figure 4.12B), but a high MFI was achieved by 60 min, especially at higher MOIs. I decided on MOI 10 to reduce reagent consumption, and the time point of 45 min.

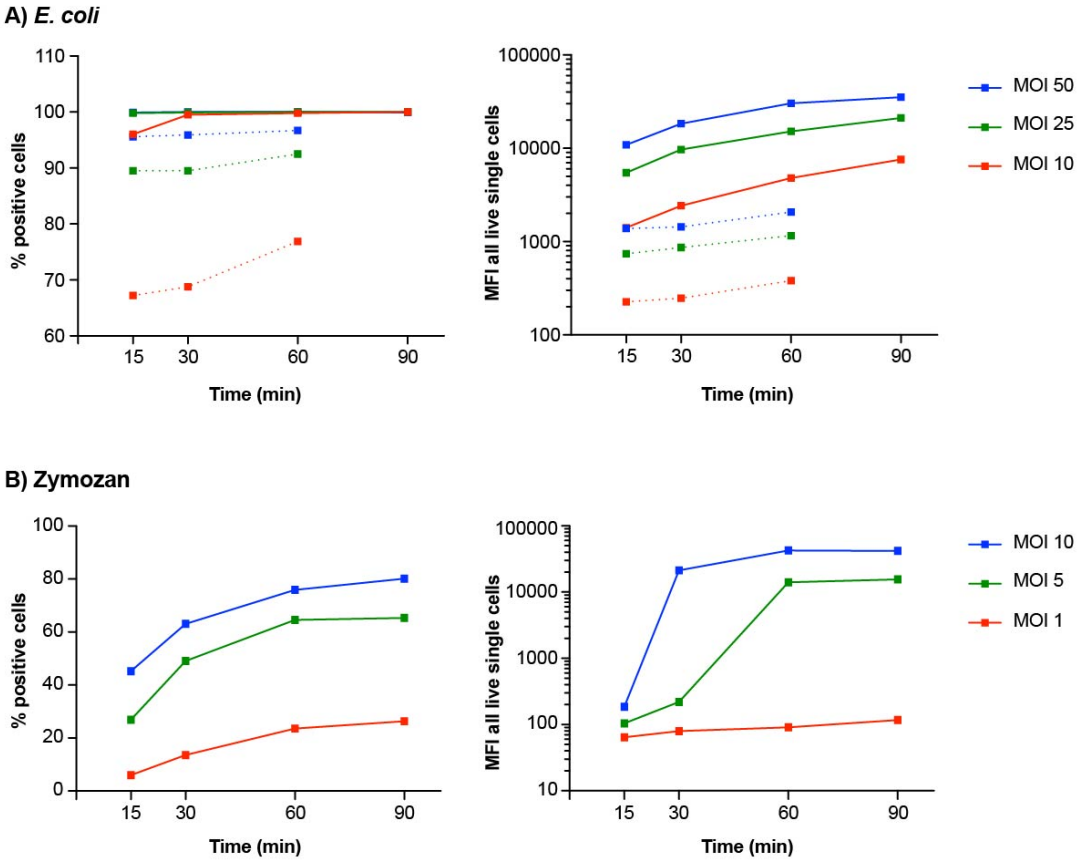

Figure 4.12 Primary macrophage phagocytosis of *E. coli* and zymozan changes over time and with concentration.
After 5 days culture in M-CSF, monocyte-derived macrophages (n=1) were lifted and re-plated at 1 million cells/ml media and allowed to re-adhere overnight. Fluorescently-labelled *E. coli* or zymozan bioparticles were then added to the media and cells cultured for 15, 30, 60, or 90 min at 37 °C (solid lines) or on ice (dotted lines). Media were aspirated and cells lifted and stained with viability dye then fixed before samples were acquired on an LSR II flow cytometer. Gating was done as in Figure 4.11. A) *E. coli* bioparticles at MOIs of 10, 25, or 50 particles per cell. B) Zymozan bioparticles at MOIs of 1, 5 or 10 particles per cell.

I then tested the uptake of *E. coli* and zymozan in primary macrophages 24 h after electroporation with 10, 50, or 100 nM siRNA targeting *HS6ST1*, using MFI as a measure of phagocytosis rather than the percentage of cells that fell within the positive gate. The three biological repeats on three donors were performed at different times, so to account for differences in laser brightness and sample storage time I normalized the MFI values to that of the buffer control for each donor (Figure 4.13A). There was an apparent increase in uptake of *E. coli* in cells after electroporation with 50 nM siRNA targeting *HS6ST1* compared to the non-targeting control, although this difference was non-significant, whereas there was no effect of knockdown on the uptake of zymozan. Knockdown was confirmed at the message level in these donors by qPCR (Figure 4.13B) and was significant in all three donors. Plotting the expression level of *HS6ST1* mRNA against uptake of *E. coli*, both relative to the uptake by buffer control from each donor, showed no significant correlation when linear regression analysis was performed, with an R-squared value of 0.03425 being not significantly different from zero (Figure 4.13C). It may be the case that loss of 6-O-sulfation does not affect the uptake of *E. coli* or zymozan and that heparan sulfate is not involved in phagocytosis of these substrates. Alternatively, more than 24 h between siRNA electroporation and phagocytosis assay may be necessary for the cell-surface HS to have been turned over sufficiently that the loss of 6-O-sulfation becomes manifest, so I decided to repeat the *E. coli* uptake assay after longer time points of *HS6ST1* knockdown. In addition, I added an alternative form of phagocytic substrate to test alternative receptor pathways: fluorescent beads that had been opsonised in FBS to represent antibody-dependent uptake of pathogens.

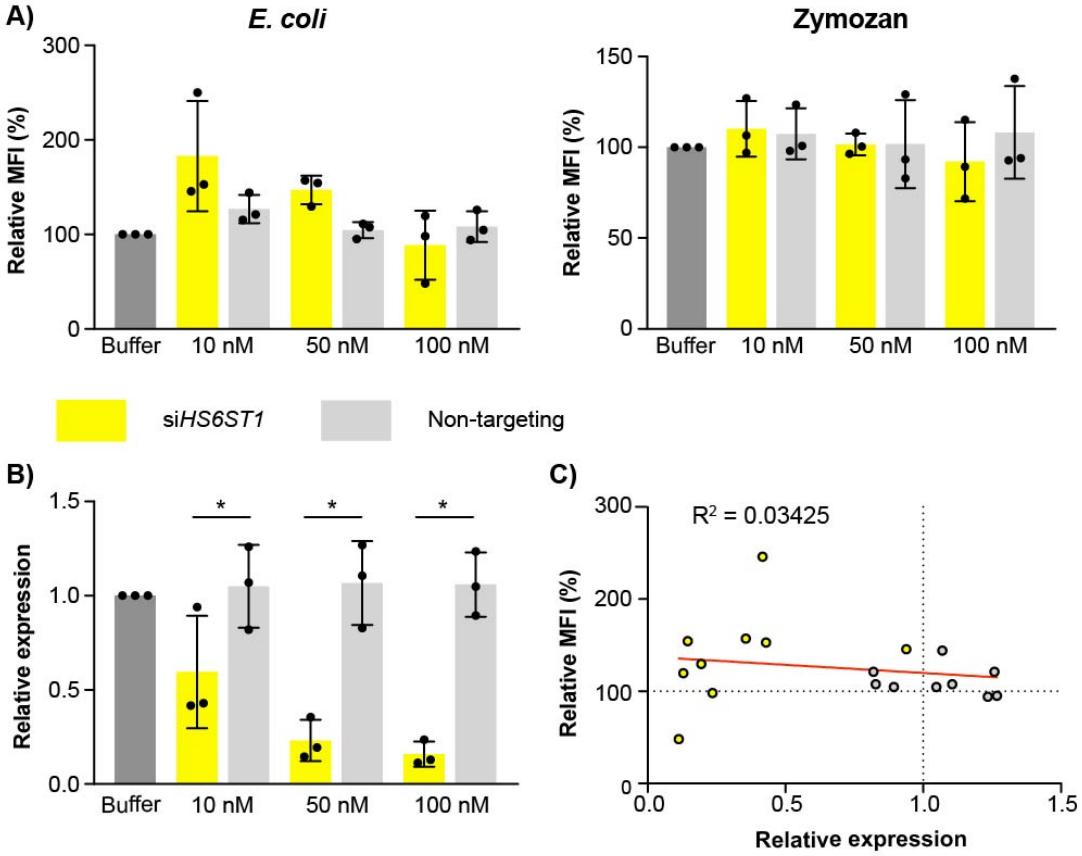

Figure 4.13 Phagocytosis of *E. coli* and zymozan bioparticles was not significantly altered by *HS6ST1* knockdown.
24 h after electroporation with 10, 50, or 100 nM si*HS6ST1*, non-targeting siRNA, or buffer alone, monocyte-derived macrophages were incubated with fluorescently labelled *E. coli* or zymozan particles at 10 particles per cell for 45 min before staining with viability dye, fixing, and sample acquisition and analysis as in Figure 4.11. A) Relative MFI of all single live cells as a percentage of the buffer control sample for each donor. There were no statistically significant differences in uptake of *E. coli* or zymozan particles between si*HS6ST1* and non-targeting samples by paired t-test. B) qPCR of message levels of *HS6ST1* to confirm knockdown in these three donors (data also shown in Figure 4.3) using the ΔΔCt method. Error bars represent mean ± SD. C) For all siHS6ST1 (yellow dots) and non-targeting siRNA (grey dots) samples from the three donors, relative MFI was plotted against relative expression of *HS6ST1* and linear regression analysis performed. The R squared value was 0.03425 and this was not significantly different from zero. n=3 donors.

4.4.2 Range-finding for FBS-opsonised beads

To determine the optimal MOI and time point for incubation of primary human macrophages with FBS-opsonised beads, I incubated cells with different MOIs of the bioparticles for 45 or 90 minutes before fixing the cells and quantifying cellular fluorescence by flow cytometry as in Figure 4.11. To control for beads adhering to

the surface but not being internalized, I placed one sample at 37 °C and a corresponding control at 4 °C (Figure 4.14). There was some uptake of beads at all MOIs, with greater uptake relative to surface adherence at higher MOIs. Once again, MFI appeared a better measure of phagocytosis than percentage positivity, as the difference between staining at 37 °C and 4 °C was generally greater. For further experiments, I chose an MOI of 50 particles per cell at a time point of 45 minutes because there was a strong but not maximal signal; this is important because any effect of knockdown on phagocytic capacity may be masked if detection is not within the linear range, and because it may be the case that knockdown increases rather than decreases phagocytosis.

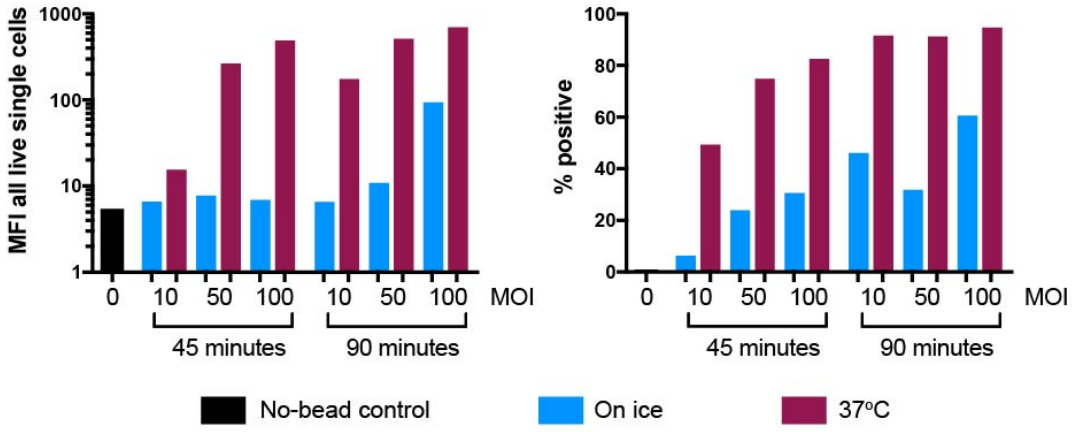

Figure 4.14 FBS-opsonised bead phagocytosis by primary human macrophages.
Fluorescent bioparticles were opsonised with FBS overnight then washed in PBS before being added to M-CSF-differentiated human monocyte-derived macrophages (n=1) at 10, 50 or 100 particles per cell and incubated for 45 or 90 minutes at 37 °C (pink) or on ice (blue) then cellular fluorescence measured by flow cytometry. Gating to select for live single cells was performed as in Figure 4.11. The median fluorescence intensity and percentage of live single cells that were positive are shown, with cells not exposed to fluorescent beads (0 min, black bar) as a control for autofluorescence.

4.4.3 Time courses of uptake of *E. coli* and opsonised beads after *HS6ST1* knockdown in primary macrophages.

Because of the slight but not significant increase in *E. coli* uptake I observed after 24 h *HS6ST1* knockdown with 50 nM siRNA (Figure 4.13A), I repeated this experiment in three further donors and at additional time points of 48 and 72 h. Experiments were also performed with FBS-opsonised beads to test the role of 6-O-sulfated HS in an additional phagocytic pathway. 24, 48 or 72 h after electroporation with si*HS6ST1*, non-targeting siRNA, or nucleofector buffer alone, there were no significant differences in the uptake of fluorescently labelled *E. coli* or FBS-opsonised beads (Figure 4.15), suggesting that HS, or at least 6-O-sulfation of HS, is not involved in phagocytosis of these substrates.

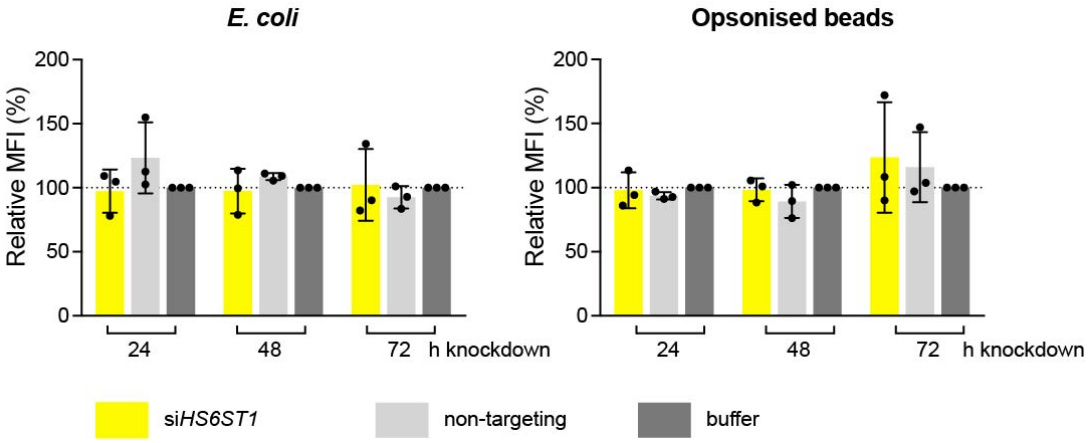

Figure 4.15 Phagocytosis of *E. coli* and opsonised beads over time after knockdown.
24, 48, or 72h after electroporation with 50 nM siRNA targeting *HS6ST1* or a non-targeting control, or with buffer alone, cells were incubated with *E. coli* or FBS-opsonised beads at MOIs 10 and 50, respectively. After 45 min cells were lifted, stained with viability dye and fixed before median fluorescence intensity measured on flow cytometer. Gating to select for live single cells was performed as in Figure 4.11. Data are expressed relative to the MFI of the buffer control for each donor at each time point. n=3 donors. Error bars represent mean ± SD. Data were analysed by one-way ANOVA with multiple comparisons but no comparisons were significant.

4.5 Effect of *HS6ST1* knockdown on macrophage migration

Many chemokines are known to bind HS, and many have been reported to require this interaction for maximum chemotactic efficacy as described in Chapter 1 (Chapter 1.5.2.1). However, chemokines have thus far been almost exclusively studied as binding to the HS on the vascular endothelium, which immobilizes chemokines in a gradient and affects migrating leukocytes *in trans*. Whether or not leukocyte HS is involved in chemokine signalling *in cis* remains unexplored. I thus optimized assays to investigate whether loss of *HS6ST1* expression affects the ability of monocyte cells to migrate towards chemokines.

4.5.1 THP1 migration towards MCP-1 and the effect of HS6ST1 knockdown

I first optimized an assay in THP1 cells using a transwell migration system with the prototypic chemokine MCP-1 (CCL2) as the chemoattractant. I used an available automated system (Celigo Image Cytometer, Nexcelom Bioscience) in which the number of fluorescently labelled cells that has migrated across the insert with a pore-containing membrane is quantified in a 96-well plate with an optical base. Because this system counts cells in suspension in the lower well, and is not able to count those adhering to the underside of the transwell insert, I used suspension-cultured THP1 cells rather than adherent primary macrophages. My trial experiment showed some random migration in the absence of chemokine but much stronger migration with MCP-1, particularly at the higher concentration tested (Figure 4.16).

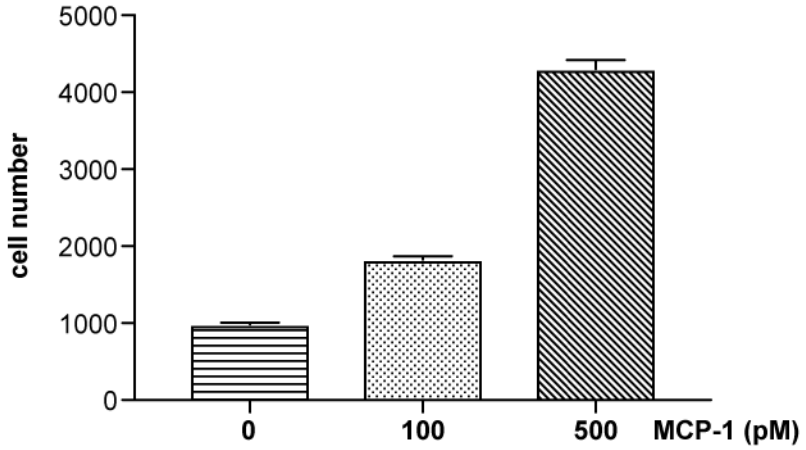

Figure 4.16 Automated quantification of THP1 migration towards MCP-1.
50000 THP1 cells were transferred to the upper chamber of 96-well transwell inserts with 8.0 μm diameter pores, with the lower chamber containing 500, 100, or 0 pM MCP-1 (CCL2), and incubated at 37 ^{o}C for 4 h. Inserts were then removed and post-migratory cells in the bottom chamber labelled with Hoechst 33342 and transferred to a 96-well plate with an optical base for automated cell counting using the Celigo image cytometer. n=3 replicates per condition. Error bars represent mean ± SD.

I then performed this assay on THP1 cells that had been electroporated with siRNA targeting *HS6ST1*, a non-targeting control, or buffer but no siRNA, for 24, 48, or 72 h prior to the 4 h transwell migration experiment. The number of cells counted per well by the Celigo plate reader showed no significant differences in migration towards MCP-1, or in random migration, upon HS6ST1 knockdown (Figure 4.17A). However, the same volume of cell suspension from each sample was loaded into the top well of the transwell plate, rather than the same number of cells, so it is possible that differences in the amounts of cell death between conditions or between replicate samples may have resulted in different numbers of cells being loaded. To account for these possible differences, I made a positive control for each sample in which the same volume of cell suspension was pipetted directly into the optical plate without having to go through a transwell membrane, giving a reading equivalent to the number of cells that would be detected per sample if 100% of them had migrated. I then normalized all the migrated samples to these positive controls for each

condition, and found that there were some significant differences (Figure 4.17B). After 24 h knockdown, the relative migration of cells treated with siRNA targeting *HS6ST1* was slightly but significantly higher than the non-targeting controls, with no change in the random migration observed in the absence of MCP-1. In contrast, after 72 h knockdown, the migration towards MCP-1 and the random migration were both significantly lower in the si*HS6ST1*-treated samples than the non-targeting controls, suggesting that knockdown of *HS6ST1* and thus loss of 6-O-sulfation reduces the ability of THP1 cells to migrate by a mechanism not involving the binding or activity of MCP-1.

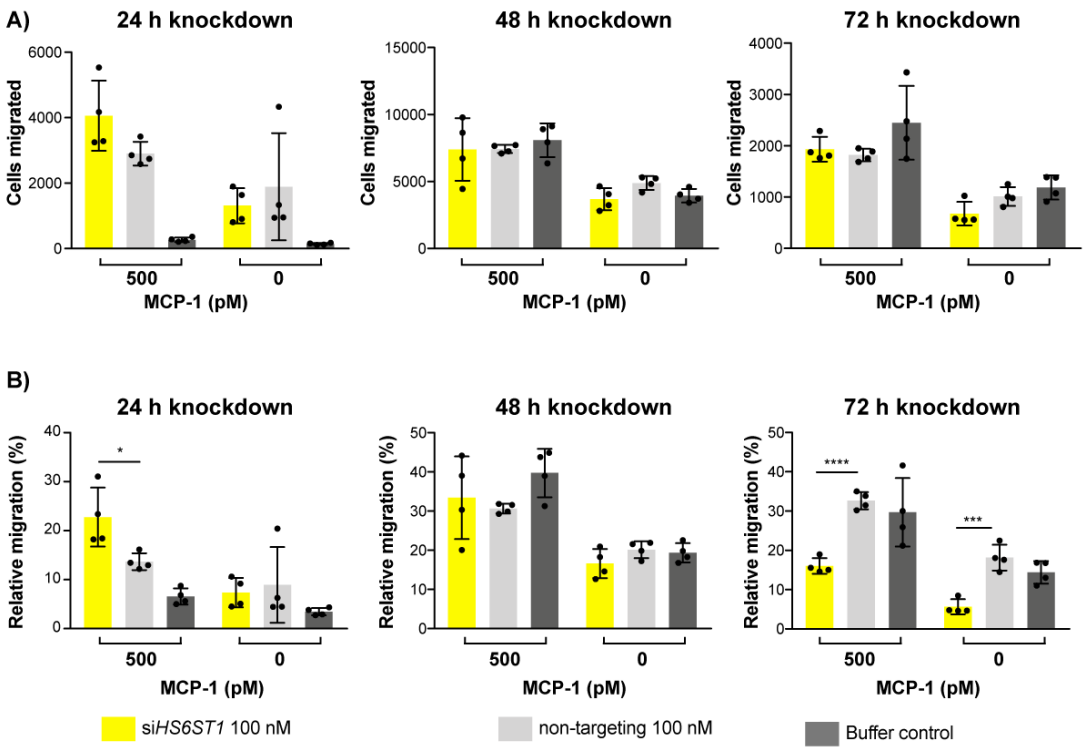

Figure 4.17 Migration of THP1 towards MCP-1 after *HS6ST1* knockdown.
After 24, 48, or 72 h knockdown with 100 nM siRNA targeting *HS6ST1*, or a non-targeting control, THP1 cells were tested for transwell migration towards 500 or 0 pM MCP-1 (CCL2) as described in Figure 4.16. Each sample was divided between four replicate wells per condition for the transwell assay. A) The absolute cell count per well as determined by the Celigo automated cell counter. B) Relative migration calculated by normalizing to the average cell count in the positive control wells for each condition. si*HS6ST1* samples were compared to non-targeting samples of the same time point by unpaired student t-test. All significant comparisons are shown, where $p < 0.05$ (*), $p < 0.001$ (***) and $p < 0.0001$ (****). Error bars represent mean ± SD.

My initial experiment involved one sample per electroporation condition per time point which was then split between 4 wells of the transwell plate to give the replicate readings. To increase the power of these experiments, I repeated the transwell assay with four independent samples (electroporated separately and cultured in separate wells) and did not get the same result: with normalization to the positive controls for each sample there was no difference between the MCP-1-dependent or random migration of knockdown and control cells at any time point (Figure 4.18). This finding suggests that knockdown of *HS6ST1* does not affect the ability of THP1 cells to migrate towards MCP-1 under these experimental conditions.

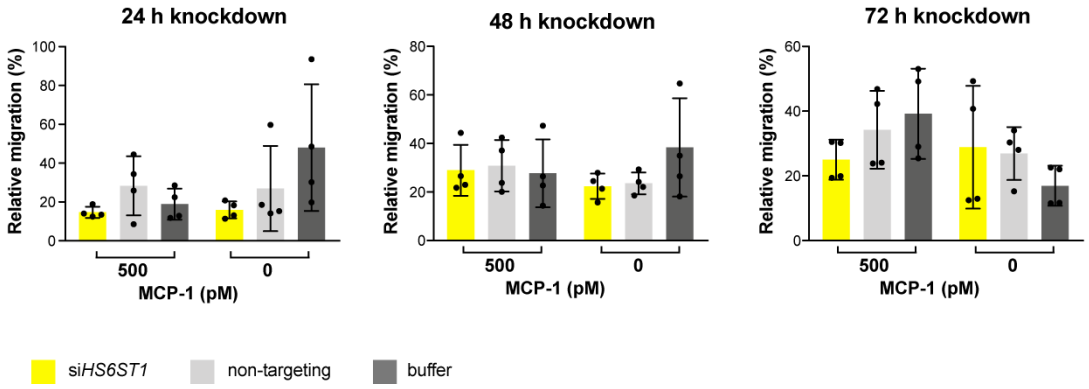

Figure 4.18 Migration of THP1 towards MCP-1 after *HS6ST1* knockdown.
After 24, 48, or 72 h knockdown with 100 nM siRNA targeting *HS6ST1*, or a non-targeting control, THP1 cells were tested for transwell migration towards 500 or 0 pM MCP-1 (CCL2) as described in Figure 4.16 then normalized to the positive control for each sample. n=4 independent samples per condition. Error bars represent mean ± SD.

4.5.2 Migration of M-CSF macrophages

THP1 cells without PMA stimulation are more representative of monocytes than of macrophages, whereas my gene of interest, *HS6ST1*, is more highly expressed in macrophages than in monocytes. Therefore I tried optimizing the transwell migration assay with primary human M-CSF macrophages. There are several challenges to overcome with this approach, including the fact that macrophages are adherent and will not be found in suspension in the lower chamber, meaning automated counting with the Celigo was not possible. I thus attempted to manually quantify the transwell migration of human monocyte-derived M-CSF macrophages towards MCP-1 (CCL2). I initially stained migrated cells on the underside of the transwell membrane with DAPI before cutting the membrane out of its insert and mounting on a glass slide for visualization of the cells by fluorescence microscopy. However, having removed the membrane from the insert meant it was no longer perfectly flat and along one optical plane, meaning cells could not accurately be counted (data not shown). I then stained cells with crystal violet and viewed the whole transwell inserts under an optical microscope (Figure 4.19). However, it was difficult to discern individual cells, and the pores in the membrane also retained some crystal violet dye making them look similar to cells (Figure 4.19A). Even at the higher magnification of 40x (Figure 4.19B) it was impossible to accurately count the cells by eye, but no gross changes in migration were evident. Because *HS6ST1* is most highly expressed in M-CSF macrophages not in monocytes (Figure 4.2), and because migration is more of a monocyte than a macrophage function, I decided this line of inquiry was not relevant enough to justify further investigation.

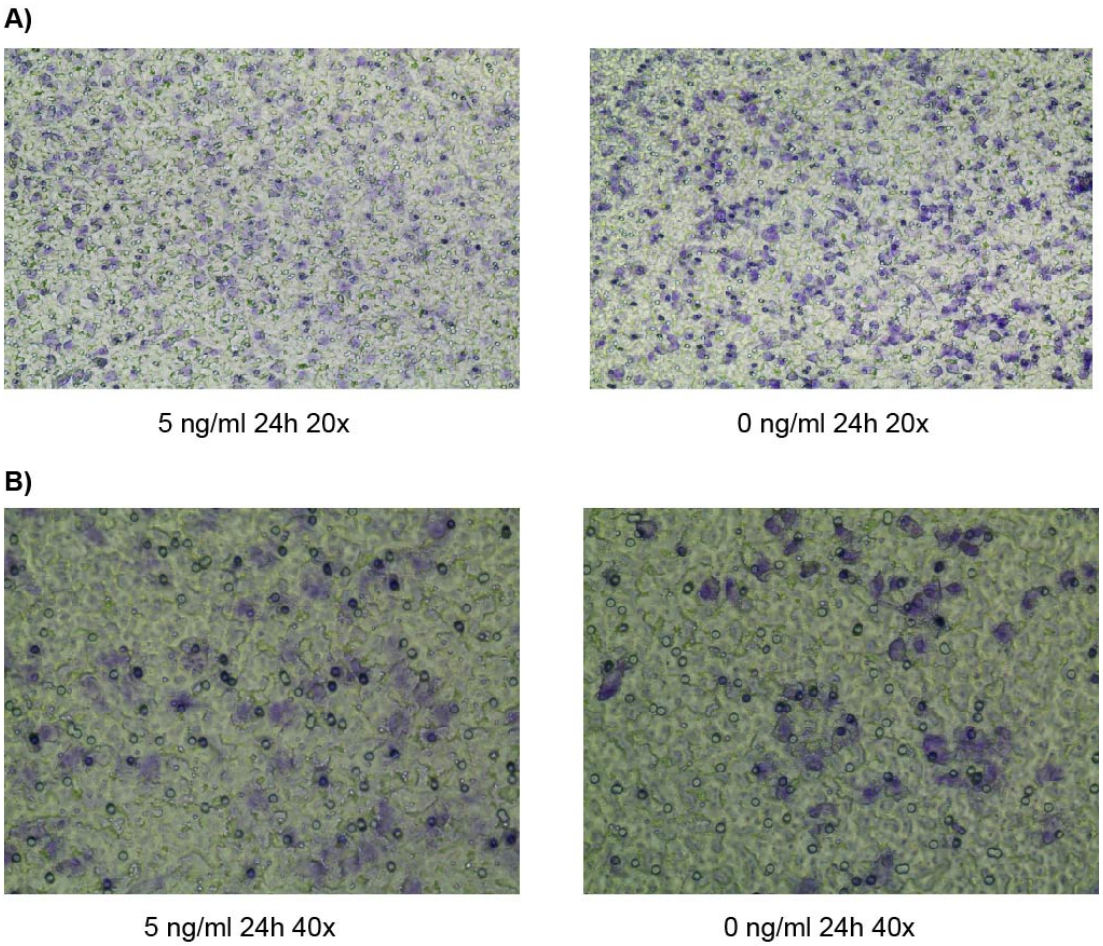

Figure 4.19 Migration of M-CSF-differentiated macrophages towards MCP-1.
M-CSF-differentiated monocyte-derived macrophages were lifted and counted then equal numbers transferred to the upper chamber of 8.0um pore-size transwell inserts, with 5 or 0 ng/ml MCP-1 (CCL2) in the lower chamber. After 24 h incubation at 37 °C, inserts were removed, washed, and cells on the upper surface of the membrane removed by vigorous scrubbing with cotton bud. Lower surface of membranes were stained with crystal violet solution, and membranes within intact inserts visualized under an optical microscope. Images were captured at A) 20x and B) 40x magnification.

4.6 Discussion

The results from my multifluidic qPCR array card (Chapter 3.3) indicated reciprocal regulation of *HS6ST1* and *SULF2* during maturation from monocyte to macrophage, and in this chapter I confirmed this result in other blood donors by individual qPCRs. As these enzymes add and remove, respectively, the 6-O-sulfate groups from HS chains, these changes in message level of the two enzymes suggest that increased 6-O-sulfation of cell surface HS is a feature of macrophage maturation. To investigate the contribution of *HS6ST1* to macrophage functions I used siRNA electroporation to knock it down in M-CSF macrophages, with the consistent levels of *SULF2* expression I observed making it likely that *HS6ST1* knockdown leads to reduced 6-O-sulfation of HS chains. I also tested knocking down *HS6ST1* in THP1 cells as this monocytic cell line might present a useful alternative to primary macrophages in some assays. PMA stimulation induces adherence of THP1 cells and development of a phenotype more representative of primary macrophages. I thought that THP1 cells in culture may continue replicating and thus the efficiency of the knockdown in the cell population would be less, although this did not seem to be the case when the knockdown efficiency in THP1 cells with or without PMA pre-treatment was compared.

A major limitation of my results in this chapter is that I was unable to detect HS6ST1 protein and thus could not be confident that the reduction in message I observed after siRNA electroporation resulted in reduced expression of the enzyme at the protein level. Effective antibodies to detect many of the HS biosynthetic enzymes are lacking, and my inability to detect a specific HS6ST1 band by immunoblotting is

consistent with the absence of successful immunoblots for this protein in the literature. It may be the case that the abundance of the protein is insufficient for detection by these antibodies on western blots: protein isoforms of HS6STs have previously been detected by overexpressing tagged forms of the protein (Habuchi et al., 2000), but introducing expression vectors successfully into macrophages is technically challenging. If abundance is not the issue then the problem may be the specificity of the antibody. My confocal images suggest that the high background staining is due to non-specific binding of the abcam anti-HS6ST1 antibody, as staining was minimal in the no-primary control. THP1 cells also showed strong staining by flow cytometry with the isotype control antibody, suggesting that this antibody is binding to something other than HS6ST1.

If reliable quantification of HS6ST1 protein is not possible, a surrogate indicator of effective knockdown would be to perform disaccharide composition analysis on the HS from knockdown and control macrophages and quantify the difference in 6-O-sulfated disaccharides. This is particularly important given that macrophages are terminally differentiated cells and may not turn over their HS very quickly, if at all, meaning that loss of enzyme expression might still have little effect on disaccharide composition at the cell surface. One of the original aims of the project was to carry out disaccharide composition analysis by HPLC, but this did not occur for various reasons including COVID-19 laboratory closures, and difficulties in accessing training for this specialist technique.

Without knowing whether and at what time point electroporation with si*HS6ST1* leads to reduced HS6ST1 protein and thus decreased 6-O-sulfation of HS, selecting the best time point for functional studies was difficult. I initially tested the phagocytosis of two substrates, *E. coli* and zymozan particles, 24 h after electroporation with siRNA, but there were no significant differences between si*HS6ST1* and non-targeting siRNA samples, although there was a non-significant trend towards increased uptake after *HS6ST1* knockdown in the case of *E. coli*. I therefore tested the uptake of *E. coli* at longer time points post-electroporation with the hypothesis that 24 h knockdown may be insufficient time for a decrease in 6-O-sulfation at the cell surface to become manifest. However, the previously observed increase in *E. coli* uptake after knockdown was not evident, and there were no changes in the uptake of FBS-opsonised beads. Given that the evidence linking HS to phagocytosis (Chapter 1.5.2.1) comes mainly from studies of cell lines which are non-professional phagocytes, it is perhaps unsurprising that professional phagocytes such as macrophages with an array of specific phagocytic receptors (Stuart and Ezekowitz, 2005) are not compromised in their ability to internalise pathogens by a possible reduction in HS 6-O-sulfation.

While a role for HS in phagocytosis may remain speculative, more well established is the role of HS in chemokine activity. However, it is generally HS on the presenting cell such as an endothelial cell, rather than on the migrating leukocyte, that is involved in potentiating chemokine activity such that the HS regulates chemokine activity *in trans* rather than *in cis*. Nevertheless, I sought to determine whether knockdown of *HS6ST1* had any effect on chemotaxis: I chose THP1 cells as

a model cell line and the chemokine MCP-1 (CCL2) because of its known interaction with 6-O-sulfated HS (Miller et al., 2016). Since THP1 cells are non-adherent in the absence of stimuli such as PMA, they were ideal candidates for transwell migration assays in which the migrated cells in the bottom chamber are counted by an automated cell counter. Despite promising results in my first experiment that suggested decreased migration after HS6ST1 knockdown in THP1, a repeated experiment with four independent samples did not recapitulate this initial finding. As the initial experiment had been one sample split between four replicate wells, the second experiment was scientifically more rigorous and I thus concluded that the loss of *HS6ST1* expression has no effect on the migration of THP1 cells towards MCP-1 (CCL2). Moreover, in addition to the technical problems in reliably quantifying cells and normalizing from different conditions, there were conceptual problems with this line of inquiry. As my gene of interest, HS6ST1, displays highest message level after M-CSF-induced monocyte maturation to macrophages, it is unclear how relevant 6-O-sulfation can be to the migration of monocytes, here modelled by THP1, unless the presence of 6-O-sulfation is inhibitory *in cis* to MCP-1-dependent migration. Macrophages are considered to be less migratory than monocytes; *in vivo* the cell would mature as it migrated towards the site of inflammation in response to stimuli it encountered, and would acquire a mature macrophage phenotype in the tissue where its activity is required. However, it has been reported that monocyte-derived macrophages lose responsiveness to MCP-1 as they mature due to receptor downregulation (Fantuzzi et al., 1999), which is also the case for PMA-activated THP1 cells (Denholm and Stankus, 1995), meaning that an alternative chemoattractant would be required in order to test macrophage migration after

HS6ST1 knockdown. However, numerous functions have been reported for MCP-1 (CCL2) in regulating monocyte and macrophage behaviour, including polarisation and priming for response to infection (Gschwandtner et al., 2019) so it may be the case that changes in HS 6-O-sulfation state affect macrophage responses to MCP-1 other than migration.

Chapter 5: The role of 6-O-sulfation of HS in macrophage signalling

5.0 Introduction

6-O-sulfate groups are unique modifications of HS in that they can be post-synthetically removed by extracellular enzymes, the SULFs (Chapter 1.3.2). Many macrophage-relevant immunological molecules bind to HS in a manner dependent on 6-O-sulfate groups, including cytokines, chemokines, and growth factors (Ori et al., 2011). IFN-γ, for example, is known to bind 6-O-sulfated HS (Vanhaverbeke et al., 2004), although it remains unresolved whether this interaction promotes or inhibits signalling through its receptor (Chapter 1.4.1). IL-4, another macrophage-polarising cytokine, has also been shown to bind to the highly sulfated domains of HS (Lortat-Jacob et al., 1997) which may promote its signalling (den Dekker et al., 2008), but the role of 6-O-sulfate groups specifically is unknown. Therefore I sought to test the role of 6-O-sulfate in the signalling of macrophage-polarising cytokines using the *HS6ST1* siRNA knockdown model I had optimised, and to identify further potential candidate proteins whose activity might be regulated by macrophage HSPGs.

5.1 FGF-2 signalling as a positive control for altered 6-O-sulfation state

FGF-2 is well known to require HS for formation of the receptor-ligand complex, and the HS sulfation requirements have been defined, involving both 6-O- and 2-O-sulfation for full mitogenic activity (Chapter 1.4.2). Therefore quantifying FGF-2 signalling in my macrophage *HS6ST1* knockdown model should provide a positive control for the loss of 6-O-sulfation. To that end, I stimulated M-CSF differentiated monocyte-derived macrophages with a low concentration of FGF-2 (0.1 ng/ml) for a range of time points, 48 h after electorporation with si*HS6ST1* or non-targeting control (both 50 nM) and then quantified ERK1/2 (p44/42 MAPK) phosphorylation by western blotting (Figure 5.1). The blot was stripped and re-probed for actin to demonstrate equal loading in all lanes and enable normalization of the band intensities for p44 and p42. The phosphorylation of ERK was visually reduced for the si*HS6ST1* samples compared to the non-targeting control, and quantification revealed the relative intensity of ERK phosphorylation to be between ½ and ⅓ of that seen for the control, indicating that the 6-O-sulfation status had been sufficiently altered by knockdown of *HS6ST1* as to reduce FGF-2 signalling.

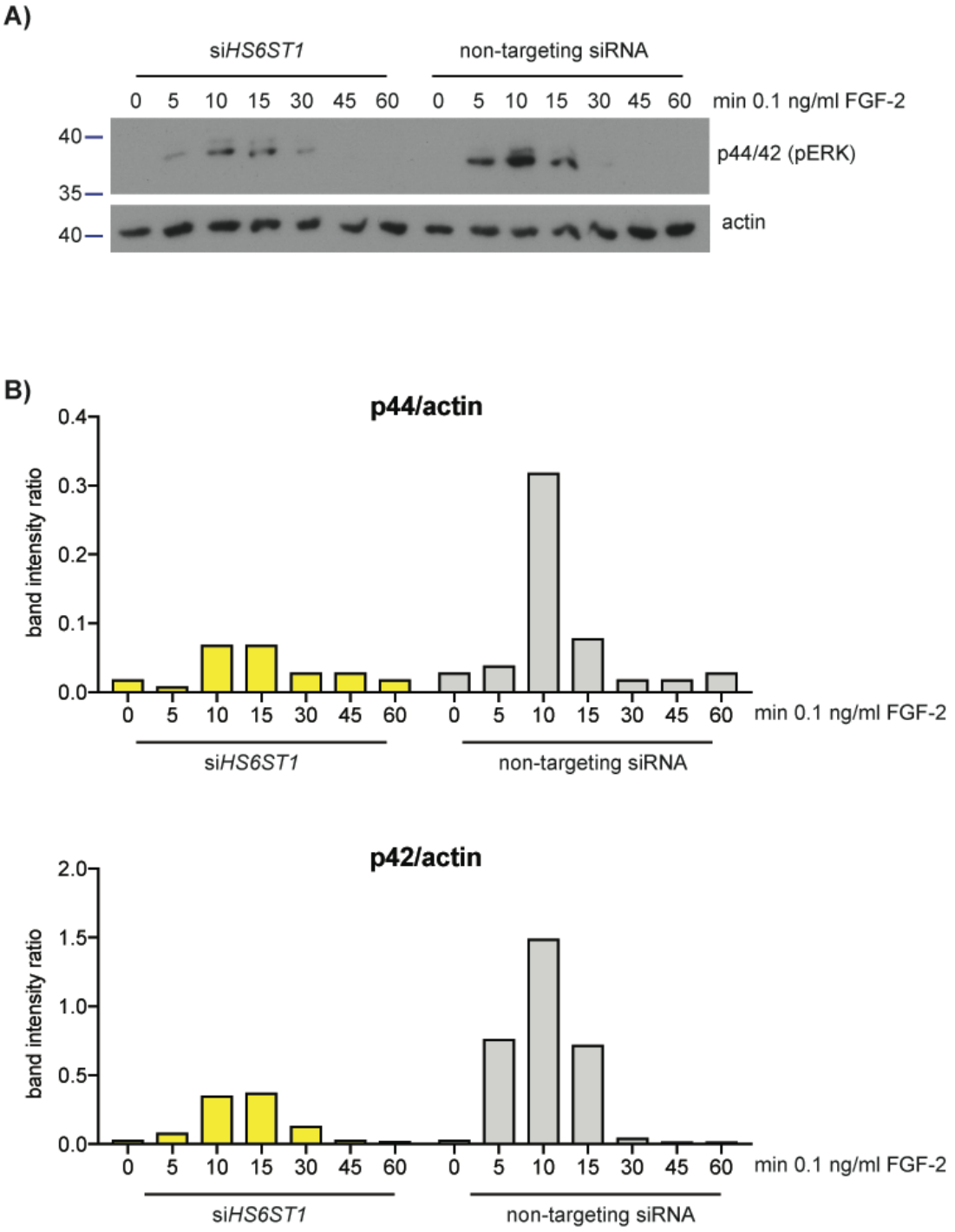

Figure 5.1 Phosphorylation of ERK1/2 by knockdown or control macrophages in response to FGF-2. 48 h after electroporation with 50 nM siRNA targeting *HS6ST1* or a non-targeting control, M-CSF-differentiated monocyte-derived macrophages were treated with 0.1 ng/ml FGF-2 for a range of time points including a 0 min untreated control. Cell lysates were subjected to gel electrophoresis and immunoblotting for p44/42 MAPK (pERK1/2) and the membrane stripped and re-probed for actin as a loading control. A) Scanned images of the blot for pERK1/2 and re-probe for actin. B) Quantification of the p44 and p42 band intensities normalized to the actin loading control for each lane.

5.2 The effect of HS6ST1 knockdown on upregulation of macrophage polarisation markers

Given the effect of HS6ST1 knockdown on FGF-2 signalling, and the upregulation of HS6ST1 during maturation from monocyte to macrophage (Chapter 3.3.3) I next sought to determine whether the ability of HS-binding cytokines such as IFN-γ and IL-4 to induce macrophage polarisation to M1 and M2-like phenotypes, respectively, was also affected by knockdown. M-CSF-differentiated macrophages were incubated for 48 h after electroporation with 50 nM si*HS6ST1* or non-targeting control, or nucleofector buffer alone, before stimulation with IFN-γ, IFN-γ and LPS, or IL-4 and IL-13 for a further 24 h as in Chapter 3.

For all donors used in this chapter for experiments on the effects of HS6ST1 knockdown, I confirmed effective knockdown of HS6ST1 message, and that SULF2 message levels were not significantly affected, by qPCR (Figure 5.2A). For some donors I also measured viablity of the cells by comparing the MTS assay absorbance for electroporated cells to that of untreated control cells for each donor at each time point (Figure 5.2B).

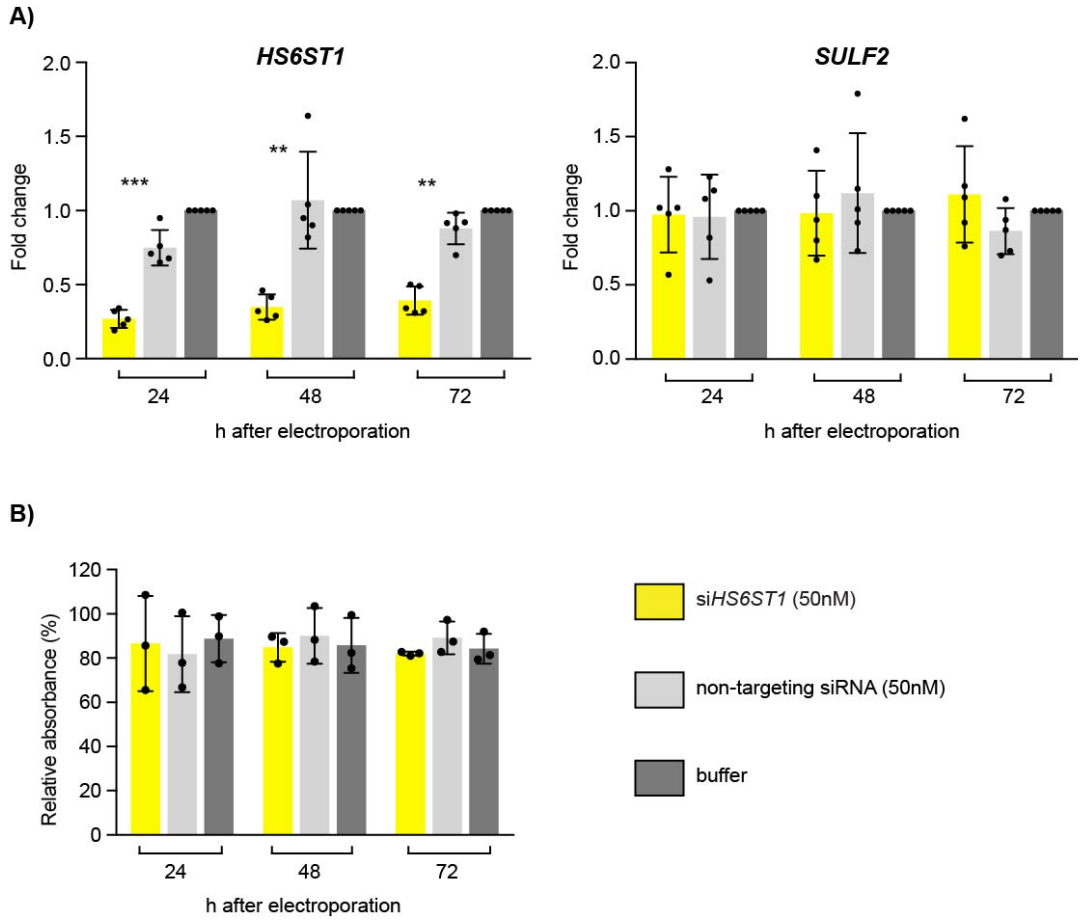

Figure 5.2 Confirmation of HS6ST1 knockdown and cell viability in primary macrophages. M-CSF differentiated macrophages electroporated with siHS6ST1, non-targeting control siRNA (both 50 nM), or nucleofector buffer alone were incubated for 24, 48, or 72 h. A) Expression levels of HS6ST1 and SULF2 quantified by qPCR were normalized to the housekeeping genes 18S and GAPDH and expressed as a fold change relative to the expression level in buffer control samples for each donor at each time point. N=5 donors. B) Viability of electroporated cells was determined by MTS assay and the measured absorbance expressed as a percentage of that for the non-electroporated cells from the same donor at the same time point. Each data point is the average of 3 replicate wells. N=3 donors. Error bars represent mean ± SD. Data were analysed by paired t-test to compare siHS6ST1 samples against non-targeting controls. All significant comparisons are shown, where $p<0.01$ (**) and $p<0.001$ (***).

5.2.1 Quantification of polarisation markers by qPCR after HS6ST1 knockdown

After 24 h knockdown and a further 24 h polarisation, macrophage samples were lysed and RNA extracted for qPCR analysis of polarisation markers. The M1 markers *IL6* and *IL1B* were strongly induced by stimulation with IFN-γ and LPS, whereas *TNF* was upregulated in response to both IFN-γ alone and IFN-γ in combination with LPS (Figure 5.3). Upregulation was seen regardless of whether the cells had been electroporated with siRNA targeting *HS6ST1*, a non-targeting control siRNA, or nucleofector buffer alone. *NOS2* was not detectable in all samples but showed a trend towards higher expression in the IFN-γ/LPS treated cells. The M2 markers *CD206* and *CD209* were both induced by IL-4/IL-13 stimulation in all three electroporation conditions. When si*HS6ST1* and non-targeting siRNA samples were compared for each polarisation condition, there were no significant differences in the upregulation of these markers.

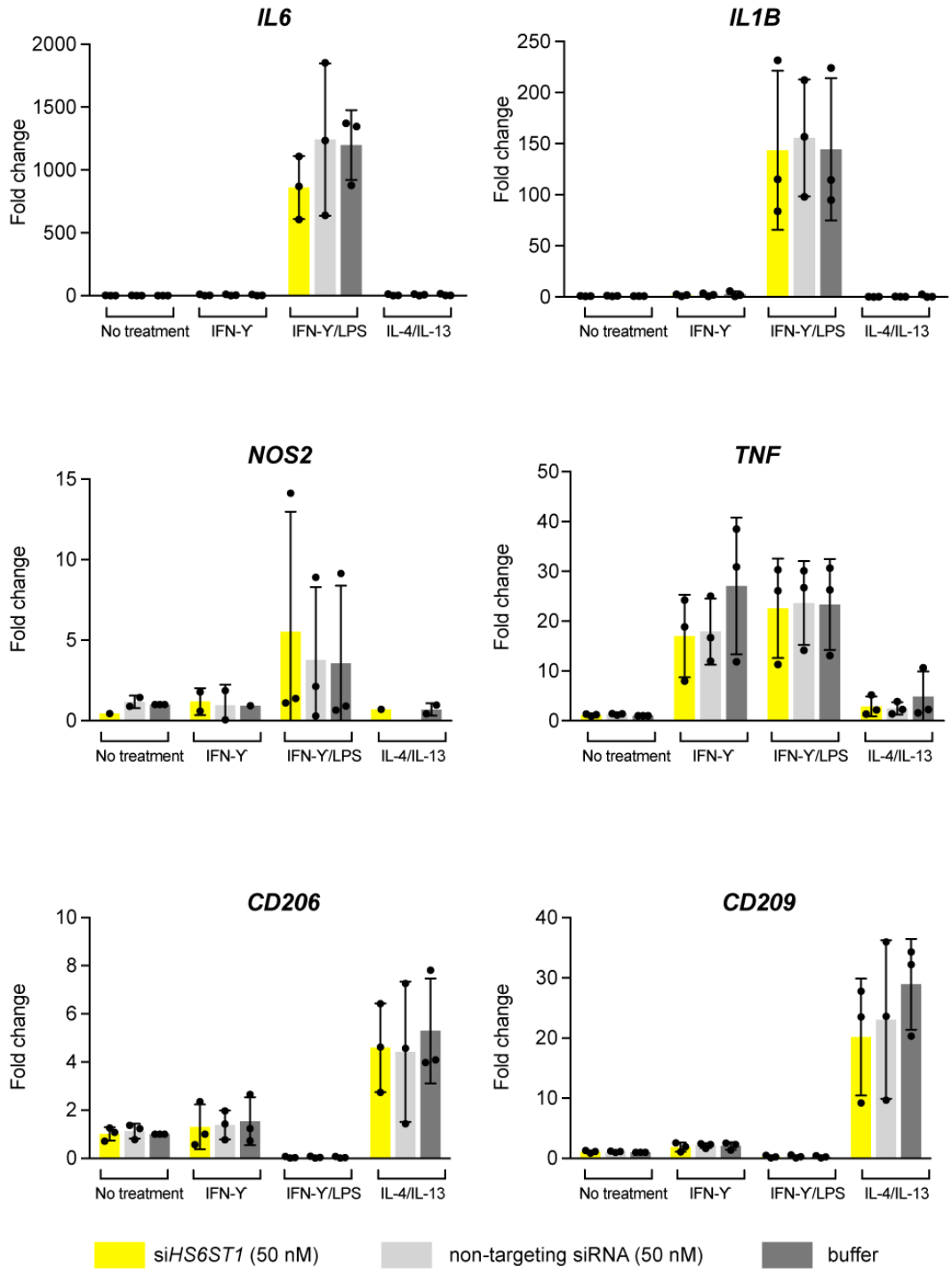

Figure 5.3 Upregulation of polarisation markers induced by cytokine stimulation of knockdown or control cells was quantified by qPCR. 24 h after electroporation with siHS6ST1 or non-targeting siRNA (50 nM) or nucleofector buffer alone, monocyte-derived macrophages were cultured for a further 24 h with fresh medium only (no treatment) or IFN-γ (50 ng/ml), IFN-γ and LPS (100 ng/ml) or IL-4 and IL-13 (both 20 ng/ml). The relative expression levels of the M1 markers *IL6*, *IL1B*, *NOS2* and *TNF*, and of the M2 markers *CD206* and CD209, were quantified by qPCR. Data were normalized to the housekeeping genes 18S and GAPDH and expressed as a fold change relative to the expression level in the no treatment buffer control sample for each donor. N=3 donors. Error bars represent mean ± SD. All si*HS6ST1* vs non-targeting pairs were analysed by paired t-test but no comparisons were significant.

5.2.2 Quantification of polarisation markers by flow cytometry after *HS6ST1* knockdown

After 24 h knockdown and a further 24 h polarisation, macrophage samples were lifted and stained for quantification of the cell-surface polarisation markers CD64, CD80, CD163 and CD209 by flow cytometry in 2 donors (Figure 5.4). As I observed previously (Chapter 3.2.1), CD64 was most strongly upregulated by IFN-γ, while CD80 was more strongly induced by IFN-γ LPS, while CD163 showed high expression in the unstimulated cells with variable expression between polarisation conditions and CD209 was highly expressed following IL-4/IL-13 stimulation. There were no clear differences between samples electroporated with si*HS6ST1* or non-targeting siRNA, and more conclusive results would require repeated experiments on cells from more blood donors.

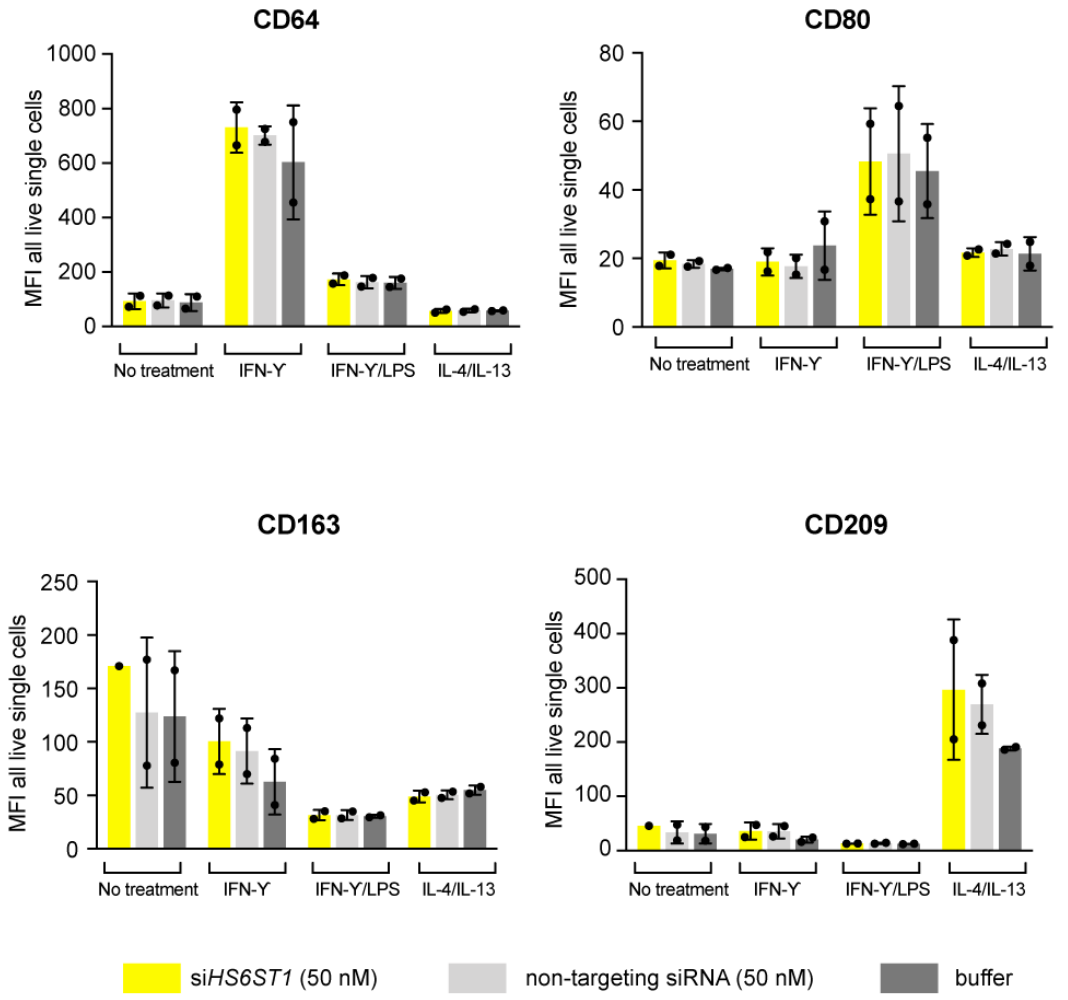

Figure 5.4 Quantification of macrophage cell-surface markers after HS6ST1 knockdown and polarisation. 24 h after electroporation with siHS6ST1 or non-targeting siRNA (50 nM) or nucleofector buffer alone, monocyte-derived macrophages were cultured for a further 24 h with fresh medium only (no treatment) or IFN-γ (50 ng/ml), IFN-γ and LPS (100 ng/ml) or IL-4 and IL-13 (both 20 ng/ml). Cells were then lifted and stained for flow cytometry quantification of the cell-surface pro-inflammatory macrophage markers CD80 and CD64, and the anti-inflammatory macrophage markers CD163 and CD209. Gating to select for live, single cells was performed as previously. N=2 donors. Error bars represent mean ± SD.

5.3 Effect of *HS6ST1* knockdown on signalling downstream of IFN-γ and IL-4

A possible reason for the inability to detect a difference in the polarisation response of siHS6ST1 and control macrophages is that the 24 h incubation period offered sufficient time to mask any possible difference in kinetics of the signalling event resulting from loss of HS6ST1 expression. To more directly test the effects of HS6ST1 knockdown on the signalling of IFN-γ and IL-4 in isolation, I aimed to quantify the phosphorylation of proteins downstream in their respective pathways: STAT1 and STAT6, respectively.

5.3.1 Optimization of cytokine concentrations for phospho-STAT westerns.

I began by testing the phosphorylation of STAT1 and STAT6 in response to a dilution series of IFN-γ and IL-4, respectively, with the aim of finding the lowest concentration of cytokine that still yielded detectable STAT phosphorylation (Figure 5.5). A low concentration is preferable for testing the role of HS as a high concentration may flood the system and mask any effect of knockdown. Based on immunoblotting for pSTAT1 and pSTAT6, I selected 1 ng/ml IFN-γ and 0.1 ng/ml IL-4 as appropriate concentrations for use in the knockdown experiments.

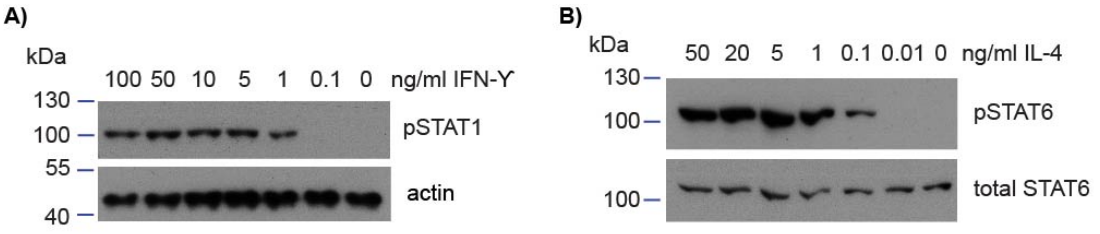

Figure 5.5 Optimisation of IFN-γ and IL-4 concentrations for STAT westerns.
M-CSF-differentiated macrophages were stimulated with various concentrations of IFN-γ or IL-4 for 15 min before cells were lysed in reducing SDS buffer containing protease and phosphatase inhibitors and run on 10% SDS-page gels. Membranes were initially probed for phosphorylated forms of STAT1 and STAT6 (pSTAT1 and pSTAT6, respectively) before they were stripped and re-probed for loading controls.

5.3.2 Quantification of pSTAT1 and pSTAT6 in stimulated cells after knockdown

The phosphorylation of STAT1 in response to IFN-γ stimulation was quantified in two donors, 48 or 72 h after electroporation with si*HS6ST1*, non-targeting siRNA, or nucleofector buffer alone. Phosphorylated STAT1 was only detectable in IFN-g-stimulated samples (Figure 5.6). When the band intensities were quantified and normalized to those for total STAT1, there were small differences between si*HS6ST1* and non-targeting siRNA-treated samples for both donors. However, one donor (Figure 5.6A) showed slightly reduced pSTAT1 band intensity in si*HS6ST1* versus non-targeting siRNA-treated samples, whereas the other (Figure 5.6B) showed the opposite. While analysis of additional donors would be required to perform statistical analysis, it appears from these data that 6-O-sulfation does not substantially affect IFN-γ signalling.

Similarly, I quantified the phosphorylation of STAT6 in response to IL-4 stimulation in one donor 48 or 72 h after electroporation with siHS6ST1, non-targeting siRNA, or nucleofector buffer alone. Phosphorylated STAT6 was only detectable in IL-4-stimulated samples (Figure 5.7). The band intensities of pSTAT6 were normalized to those of actin and showed slightly higher relative intensity of pSTAT6 in knockdown versus non-targeting samples at both 48 and 72 h post-electroporation. Experiments on further donors would be required to draw conclusions about the contribution of 6-O-sulfation to macrophage IL-4 signalling, but it appears from these data that 6-O-sulfation does not substantially affect IL-4 signalling.

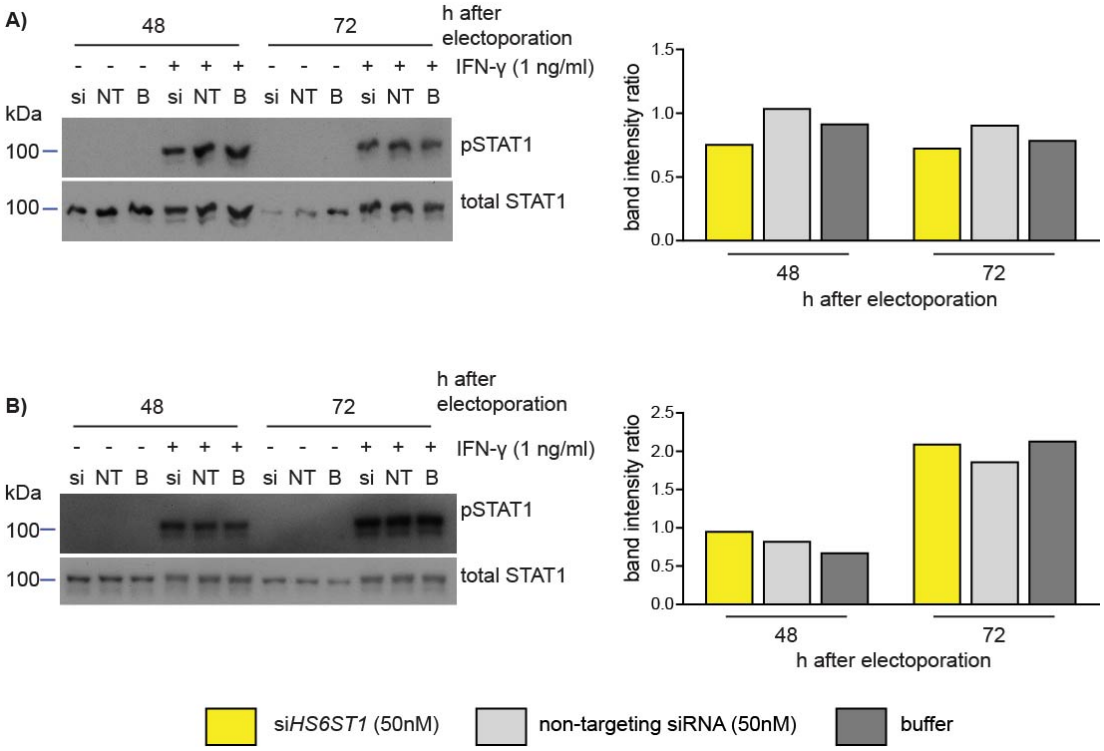

Figure 5.6 Phosphorylation of STAT1 after IFN-γ stimulation was evaluated after HS6ST1 knockdown. 48 or 72 h after electroporation with siHS6ST1 (si) or non-targeting siRNA (NT) (50 nM) or nucleofector buffer alone (B), monocyte-derived macrophages from two donors, A and B, were treated with 1 ng/ml of IFN-γ for 15 min before lysis for SDS-PAGE and immunoblotting for phosphorylated STAT1 (pSTAT1). The membrane was stripped and reprobed for total STAT1 protein as a loading control. Band intensity ratio was calculated by dividing the measured pixel volume for each pSTAT1 band by that of the total STAT1 band for the same lane. N=2 donors (A and B).

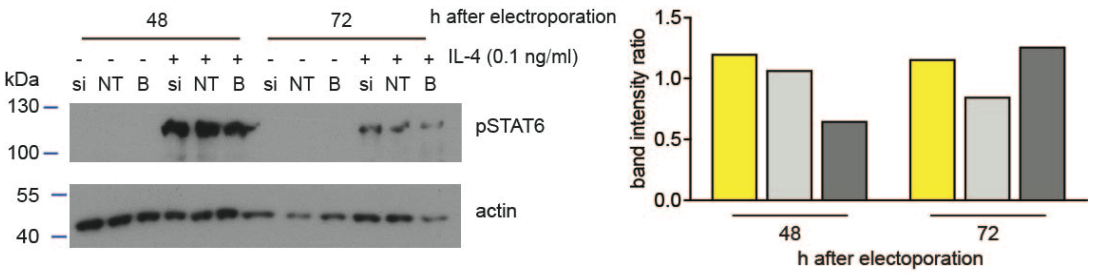

Figure 5.7 Phosphorylation of STAT6 after IL-4 stimulation was evaluated after HS6ST1 knockdown. 48 or 72 h after electroporation with siHS6ST1 (si) or non-targeting siRNA (NT) (50 nM) or nucleofector buffer alone (B), monocyte-derived macrophages were treated with 0.1 ng/ml of IL-4 for 15 min before lysis for SDS-PAGE. Equal volumes of sample were loaded per lane of two gels, with one membrane probed for phosphorylated STAT6 (pSTAT6) and the other for actin as a loading control. Band intensity ratio was calculated by dividing the measured pixel volume for each pSTAT6 band by that of the actin band for the same lane. N=1 donor.

5.4 Cytokine array detection of other HS-dependent cell-surface ligands

Many other cytokines bind to HS apart from IFN-γ and IL-4 and this binding may require 6-O-sulfation, in which case it would be expected that loss of 6-O-sulfation on the cell surface would lead to a reduction in cytokine bound to the cell-surface and thus an increase in cytokine levels in the conditioned medium. To investigate whether knockdown of *HS6ST1* and the predicted decrease in cell-surface 6-O-sulfation had an effect on the binding of a wide range of cytokines and chemokines, I used a multiplex cytokine array printed with duplicate spots of capture antibodies for a number of different cytokines (Chapter 2.14). The conditioned media from three donors 24 h after electroporation with si*HS6ST1* or non-targeting control at 50 nM were incubated on these arrays which were then washed and the bound antibodies detected with a cocktail of detection antibodies by chemiluminescence. Each pair of samples from different donors was exposed together on the same film, but the absolute pixel intensity differed between donors analysed on the arrays at different times. To account for these differences, the data were presented as a fold change by dividing the average pixel intensity of the two siHS6ST1 spots by that of the corresponding non-targeting spots for each cytokine. These values were then logged to base 2 to more symmetrically distribute the data around 0, such that upregulation is a positive value and downregulation a negative value (Figure 5.8A). Many cytokines were not detectable in all three donors (white squares) but the chemokines CCL2 (MCP-1), CXCL1 (GROa), IL-8 (CXCL8) and CXCL12 were among those proteins detectable in the conditioned medium from all three donors under both si and NT conditions. When the original pixel values for each donor were plotted for these four chemokines, some trends were evident with the amount of CCL2 and IL-8

being higher in the conditioned medium of knockdown samples than non-targeting controls (Figure 5.8B), although these differences were not significant. CXCL1 and CXCL12 showed decreased abundance in the conditioned medium of knockdown samples compared to controls in two out of the three donors.

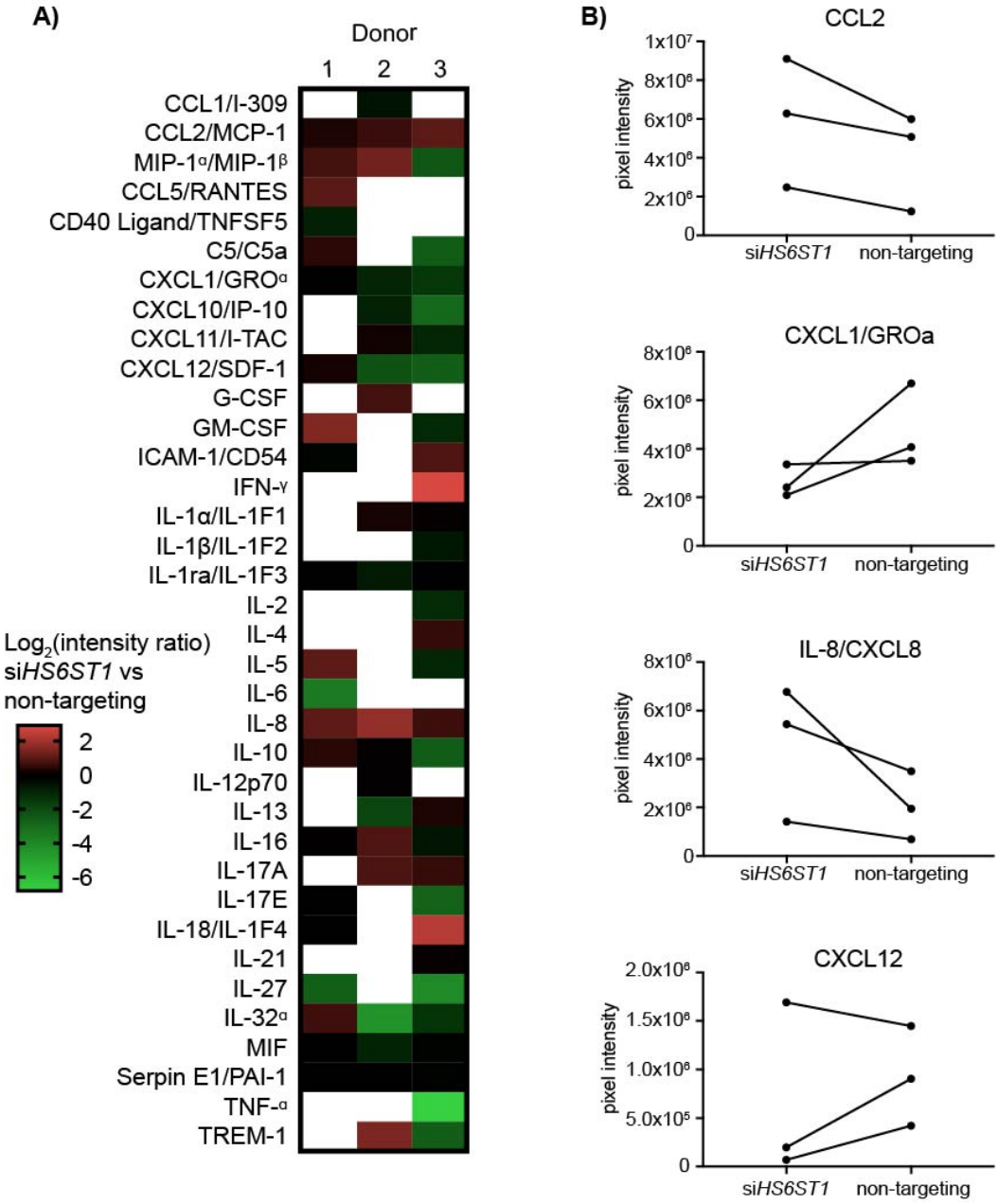

Figure 5.8 Differential abundance of cytokines in the conditioned media of knockdown and non-targeting cells. A) Heatmap of the log2 of the average pixel intensity of the two si*HS6ST1* spots divided by that of the two non-targeting control spots (log2(intensity ratio)). B) Pixel intensities of four shortlisted cytokines/chemokines where each data point represents the average pixel intensity of the two duplicate cytokine spots on the array per donor per condition. N=3 donors.

To investigate whether these observed differences in chemokine abundance could be explained by differences in gene transcription between si*HS6ST1* and non-targeting siRNA samples, I performed qPCR 24, 48 and 72 h after electroporation (Figure 5.9A). There were no significant differences in message level of *CCL2*, *CXCL8*, *CXCL12*, or *CXCL1* between si*HS6ST1* and non-targeting groups at any time point.

I analysed the concentration of CCL2 and CXCL8 in the conditioned media of further donors by ELISA and at the additional time points of 48 and 72 h (Figure 5.9B). There was a trend towards elevated CCL2 in the conditioned medium of siHS6ST1 samples versus non-targeting controls, which was significant at 48 h post-knockdown. There were no significant differences in the concentrations of CXCL8 detected in the conditioned medium of knockdown or control samples at any time point. These results support CCL2 as a target for further study into the role of HS6ST1 and 6-O-sulfation in the regulation of chemokine activity.

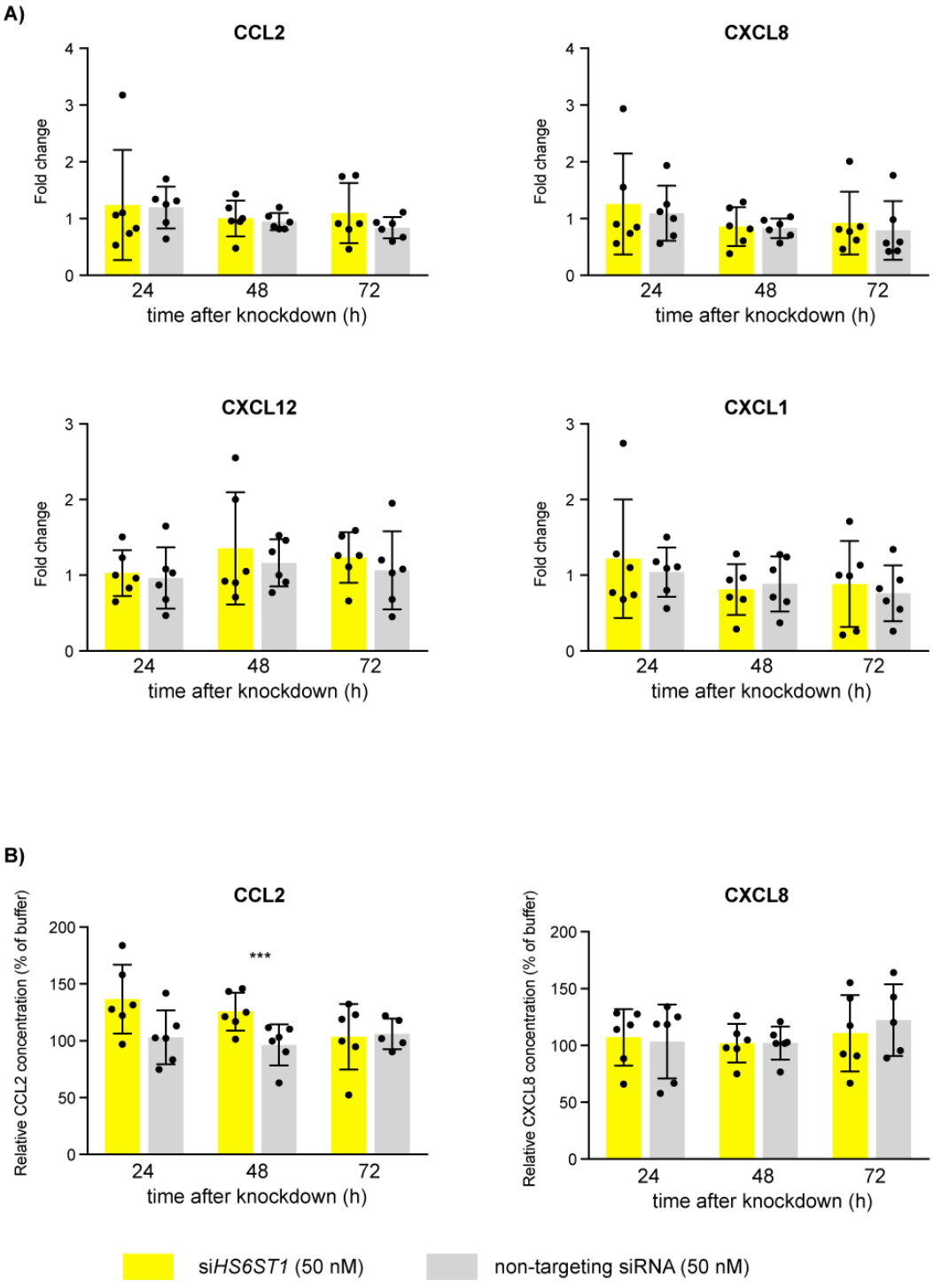

Figure 5.9 Quantification of mRNA and secreted protein levels for shortlisted cytokines. Samples were collected from monocyte-derived macrophages 24, 48, and 72 h after electroporation with 50 nM siRNA targeting *HS6ST1* or a non-targeting control, or nucleofector buffer alone. A) Message levels for the cytokines *CCL2 (MCP-1), CXCL8 (IL-8), CXCL12 and CXCL1* were determined by qPCR normalized to the housekeeping genes *18S* and *GAPDH* and expressed as a fold change relative to the expression level in buffer control samples for each donor at each time point. B) CCL2 and CXCL8 protein in the conditioned medium was quantified by ELISA and the concentrations expressed as a percentage of that detected in the buffer control samples for each donor at each time point. N=6 donors. Error bars represent mean ± SD. All si*HS6ST1* vs NT pairs were analysed by paired t-test and all significant comparisons shown. P<0.001 (***).

5.5 Discussion

In this chapter, I aimed to investigate the role of 6-O-sulfated macrophage HS in regulating the signalling or retention of bioactive molecules such as chemokines and cytokines. Because of the well-established role of HS containing 6-O-sulfate groups in promoting the formation of the FGF-2 receptor-ligand complex (Chapter 1.4.2) I chose to test the effect of my HS6ST1 knockdown on phosphorylation of ERK after stimulation of macrophages with FGF-2. I tested a time course of FGF-2 stimulation because ERK activation shows a biphasic response (Zhu et al., 2010) that is decreased in both intensity and duration by complete ablation of HS sulfation with sodium chlorate (Delehedde et al., 2002). I found that 48 h after electroporation, the siHS6ST1 samples showed substantially reduced phosphorylation of both ERK 1 (p44) and ERK 2 (p42) compared to the non-targeting control samples. Quantification of pERK bands relative to actin showed that ERK phosphorylation is elevated above baseline at 5 mins, peaks at 10 mins, and then returns to baseline after 15 min, whereas ERK phosphorylation in the knockdown samples showed a smaller peak at 10 and 15 minutes. These findings are consistent with studies showing significantly reduced phosphorylation of ERK in response to FGF-2 after HS6ST1 knockdown in chondrocytes (Chanalaris et al., 2019) and in fibroblasts from Hs6st1/2-null murine embryos (Sugaya et al., 2008). As I have not performed disaccharide composition analysis to verify the loss of 6-O-sulfation of macrophage HS post-knockdown, this measurable change in a signalling event known to be dependent on 6-O-sulfated HS provides a surrogate marker for successful knockdown and validates other experiments testing changes to macrophage phenotype after HS6ST1 knockdown.

Some of the stimuli I used to polarise macrophages to M1-like and M2-like phenotypes, namely IFN-γ and IL-4, respectively, bind to HS (Ori et al., 2011). Therefore I tested whether the ability of macrophages to polarise to different phenotypes in response to stimuli was affected by HS6ST1 knockdown by measuring the upregulation of polarisation markers, as in Chapter 3. I found no significant differences between knockdown and control samples in the expression levels of pro- or anti-inflammatory macrophage markers by qPCR and no obvious trend by flow cytometry. I hypothesised that this lack of detectable difference may be due to the long time point (24 h) and high concentrations of cytokines used, which may both contribute to a masking of any effect of altered HS structure on cytokine signalling. I therefore decided to more directly interrogate IFN-γ and IL-4 signalling by quantifying the phosphorylation of their downstream signalling proteins, STAT1 and STAT6, respectively. After determining suboptimal concentrations of cytokine to make the potential co-receptor role of HS more important for signalling, I tested knockdown and control cells for differences in the phosphorylation responses to IFN-γ and IL-4. There were some slight differences but in the case of IFN-γ the trend was not consistent between the two donors tested, and only one donor was tested for IL-4. A number of technical issues made accurate quantification of STAT phosphorylation difficult and thus I am unable to provide any conclusive evidence as to the effect of HS6ST1 knockdown on IFN-γ and IL-4 signalling. These limitations included use of enzymatic chemiluminescence (ECL) that can saturate at higher band intensities high variability of the signal depending on multiple factors including temperature of the substrate and the time after substrate application that a film is exposed. Moreover, this method does not enable simultaneous detection with more

than one antibody, meaning membranes required chemical stripping and re-probing for loading controls. As I experienced carry-over of phospho-STAT signal into the loading control, I had to resort to running equal volumes of sample simultaneously on two gels for some antigens, which makes subsequent quantification less reliable. To more accurately and consistently quantify STAT phosphorylation relative to total STAT in multiple donors, I would have liked to use two antibodies from different species detected simultaneously using a digital fluorescence imager (Pillai-Kastoori et al., 2020).

To potentially discover other candidates whose activity is regulated by 6-O-sulfated macrophage HS, I broadened my investigations of the effect of HS6ST1 knockdown on macrophage signalling and considered the issue of cell-surface retention of ligands by HS. Binding to HS may promote or inhibit signalling in *cis* by regulating interaction with receptors also expressed on the macrophage surface, or in *trans* by presentation to other cells. I hypothesised that changes to the sulfation state of macrophage HS might lead to changes in the ability to retain immune mediators and thus changes in the amount of soluble molecule detectable in the conditioned medium. I thus applied conditioned medium from macrophages 24 h after electroporation with siHS6ST1 or non-targeting siRNA to cytokine array membranes that are printed with capture antibodies specific for a number of chemokines, cytokines, and growth factors. When I compared the relative intensity of staining for spots on the siHS6ST1 versus non-targeting arrays across 3 blood donors, I found considerable variation between donors, but there were some candidates present in the CM of all three donors and differed between knockdown and control samples.

Because loss of HS6ST1 expression could lead to compensatory changes in expression of other genes, I quantified message levels of the four shortlisted chemokines (CCL2, CXCL8, CXCL12 and CXCL1), and found no significant differences, indicating that the changes in abundance in the conditioned medium are due to protein localization and not gene transcription. Because the array is not quantitative and the affinity of the capture antibodies for their target proteins may vary substantially, there is no guarantee that differences observed in spot intensity on the array correspond to biologically relevant differences in cytokine concentration. I thus carried out ELISAs for CCL2 and CXCL8 with standards of known concentration to quantify their abundance in the conditioned medium of knockdown and control macrophages. At 48 h post-electroporation there was a significant increase in the concentration of CCL2 in knockdown versus control samples, and a non-significant trend in the same direction at 24 h (Figure 5.9). Previous studies into the sulfate requirements for CCL2 to bind to HS demonstrated that a 6-O-sulfated hexamer had 200-fold greater affinity for CCL2 than its 2-O-sulfated isomer (Miller et al., 2016). This requirement for 6-O-sulfated HS for high-affinity binding is consistent with the higher concentration of free CCL2 in the conditioned medium I observed after HS6ST1 knockdown. It remains to be determined whether interaction of secreted CCL2 with cell-surface HS might regulate macrophage activity in an autocrine manner, or whether presentation of CCL2 by macrophages serves to coordinate the activities of other immune cells.

The increase in CXCL8 with knockdown I observed in the cytokine array was not recapitulated in ELISA analysis with more donors and at additional time points,

suggesting this may have been a false positive. CXCL8 has been shown to bind to HS (Frevert et al., 2003), and truncating its HS-binding region did not affect receptor binding but reduced its ability to induce neutrophil chemotaxis *in vivo* (Middleton et al., 1997). However, binding to HS may not require a 6-O-sulfate group, as de-6-O-sulfated heparin was only slightly less effective than unmodified heparin in competition assays, whereas de-N- and de-2-O-sulfated heparins were much less effective (Spillmann et al., 1998).

The cytokine arrays also showed changes in the abundance of CXCL12 and CXCL1 in conditioned media after HS6ST1 knockdown. CXCL12 is known to bind HS (Amara et al., 1999) which enables it to be presented to leukocytes on the surface of endothelial cells (Connell et al., 2016; Rueda et al., 2012). Recombinant SULF2 reduced binding of CXCL12 to heparin (Uchimura et al., 2006), suggesting that binding does require 6-O-sulfate groups, yet of the 3 donors I tested on the cytokine array, 2 showed reduced abundance in the CM of si*HS6ST1* samples. ELISA quantification in more donors would be required to determine whether decreased CXCL12 and CXCL1 in the soluble phase is a consistent feature of HS6ST1 knockdown samples and thus whether binding of these chemokines to HS is likely to involve 6-O-sulfate groups.

Among the more than 400 HS- or heparin-binding proteins (Ori et al., 2011), there are undoubtedly others that are produced by or act on macrophages whose binding is affected by changes to the 6-O-sulfation state. In order to screen for more potential ligands, I have sent conditioned medium samples from knockdown and non-targeting

control cells for label-free quantitative mass spectrometry in a collaborating laboratory (Yang et al., 2020). Samples were collected after an initial 48 h incubation with serum as a source of potential HS ligands, then multiple washes with PBS to remove BSA and unbound protein, and a further 24 h incubation in serum-free medium with or without heparin to displace HS-bound ligands into the conditioned medium. It is hoped that by comparing the peptides detected in the various conditions we might identify proteins whose abundance in the conditioned medium is affected by knockdown of *HS6ST1*, and that by running the peptides through both the human and bovine protein databases we might be able to identify HS ligands involved in both autocrine and paracrine signalling.

Chapter 6: Final Discussion

6.1 Roles of heparan sulfate in leukocyte biology are poorly understood

HS is potentially one of the most information-dense structures in nature, due to the number of enzymatic modifications the HS chains experience and the huge combinatorial diversity of these modifications (Turnbull and Field, 2007). A substantial proportion of the biological activity of HS is due to its ability to regulate the activity of myriad soluble ligands that are believed to bind selectively to sulfated motifs on the HS chain. Among the more than 400 ligands of HS are numerous chemokines, cytokines, and growth factors (Ori et al., 2011), suggesting this proteoglycan could have a central role in regulating immune responses. Despite the near-ubiquitous expression of HS, its functions in inflammation and immunity have mainly been studied in the context of endothelial and stromal cells, focusing on aspects such as leukocyte recruitment via chemokine presentation on the vascular endothelium. However, leukocytes themselves also express HSPGs and the few published studies in this area indicate they regulate a number of aspects of leukocyte function, including cytokine signalling (reviewed in (Collins and Troeberg, 2019)).

HS structure is thought to be regulated by changes in expression of the enzymes that drive its biosynthesis and modification, as genetic manipulation of the HS biosynthesis machinery results in changes to the sulfated disaccharide composition (Qiu et al., 2018). Moreover, in addition to spatial and temporal regulation of HS biosynthesis during development, it has been shown that inflammatory stimuli such as bacterial LPS and cytokines alter the expression levels of HS biosynthetic

enzymes and consequently change the abundance of different HS sulfated motifs in cell types such as endothelial cells (Carter et al., 2003; Krenn et al., 2008). I thus hypothesised that macrophage HS biosynthesis would be regulated during inflammation and that this would alter macrophage functions such as responsiveness to chemokines and cytokines. I aimed to profile these changes during maturation and polarisation of primary human macrophages, and to investigate possible functional effects of a selected candidate gene, the 6-O-sulfotransferase *HS6ST1*.

6.2 Macrophages regulate expression of HS biosynthesis machinery in response to environmental stimuli

To model the spectrum of macrophage activation states thought to occur *in vivo*, I polarised monocyte-derived primary human macrophages towards pro-inflammatory M1-like and anti-inflammatory M2-like phenotypes using IFN-γ/LPS and IL-4/IL-13, respectively. The resulting populations showed significant differences in the expression of typical M1 and M2 markers, many of which are receptors, suggesting that polarisation had successfully generated the expected functionally different macrophage activation states. I used a custom-designed microfluidic array card to profile mRNA expression of all the full-time HS core proteins and biosynthetic/modifying enzymes in monocytes, M-CSF-differentiated macrophages, and pro-inflammatory and anti-inflammatory polarised macrophages. This comprehensive analysis revealed significant changes in HS-associated gene expression when monocytes mature to macrophages in the presence of M-CSF, and also upon their subsequent polarisation to pro- and anti-inflammatory phenotypes.

6.2.1 Maturation is associated with increased capacity for HS biosynthesis

I found that the majority of HS-associated genes were upregulated during M-CSF maturation from monocyte to macrophage, while a smaller subset of genes (HPSE, SULF2, EXT1, TGFBR3) was downregulated, indicating that maturation may be associated with a general increase in the capacity of myeloid cells to synthesise heparan sulfate proteoglycans. This is supported by previous reports showing that macrophage maturation is associated with increased biosynthesis of sulfated GAGs in monocyte-derived macrophages cultured with GM-CSF (Trottein et al., 2009; Wegrowski et al., 2006) or simply in serum-containing medium (Martinez et al., 2015). My observation that M-CSF-induced maturation also leads to increased expression of many HS-associated genes indicates that the increased capacity for HS biosynthesis is a general feature of macrophage maturation and not specifically linked to just one stimulus.

This increase in HS synthesis may reflect increases in the number, length, and/or sulfation of HS chains. The chain elongation enzymes EXT1 and EXT2 showed reciprocal regulation between monocyte and macrophage, with EXT1 being downregulated during maturation and EXT2 being upregulated. This is curious, as these two enzymes are believed to act as a heterodimeric complex and it has been reported that EXT1 is the rate-limiting enzyme (McCormick et al., 2000), meaning that the upregulation of EXT2 I observed may not lead to increased polymerisation of the HS backbone in M-CSF macrophages due to the decreased expression of EXT1. However, EXT1-deficient cells do synthesise some HS provided that EXT2 and EXTL2 are both expressed (Okada et al., 2010), so downregulation of EXT1

may not necessarily indicate that macrophages have significantly decreased ability to polymerise HS. The role of EXT2 upregulation in macrophages may be to determine HS chain length, as it has been reported that knockdown of EXT2 leads to shorter HS chains being produced (Busse et al., 2007). Similarly, EXT2 knockdown resulted in reduced binding of 3G10, the antibody recognising HS stubs remaining on the core protein after heparanase digestion (Nadanaka and Kitagawa, 2018), indicating that one role for EXT2 in HS biosynthesis might be to determine the number of HS chains that are synthesised. If EXT2 does serve these regulatory functions in macrophages it may be the case that maturation is associated with increased length and/or number of HS chains.

The broadly increased expression I observed may also have reflected an increase in HS sulfation upon macrophage maturation. GM-CSF-induced maturation has been shown to upregulate enzymes such as GLCE and HS2ST1 (Trottein et al., 2009), and consistent with this study I also found that GLCE and HS2ST1 were significantly upregulated by monocyte maturation to macrophages. In parallel, I saw that NDST1, HS3ST1 and HS6ST1 were significantly upregulated during M-CSF maturation. These can be reasonably expected to increase HS sulfation, supporting the hypothesis that macrophage maturation is associated with increased modification of HS chains. N-sulfation is a pre-requisite for other downstream modifications, such as epimerisation (Li et al., 1997), epimerisation promotes subsequent 2-O-sulfation (Pinhal et al., 2001), and 6-O-sulfotransferases preferentially act on 2-O-sulfated disaccharides (Jemth et al., 2003; Smeds et al., 2003). Thus, coordinated

upregulation may enable cooperative interaction between these enzymes to elaborate a more highly sulfated HS chain.

Most core proteins were upregulated by M-CSF maturation, meaning that macrophages have more potential attachment sites for new HS chains. TGFBR3 (betaglycan) was the exception, being most highly expressed in monocytes, but this core protein is a part-time HSPG meaning it is only decorated with HS chains under certain conditions. CD44 (the hyaluronan receptor) is also a part-time HSPG but was not included in the transcriptome analysis; it has been reported that monocyte to macrophage maturation is associated with upregulation of the isoform of CD44 containing the attachment sites for HS chains, resulting in the ability of macrophages to present FGF-2 (Jones et al., 2000). The biological relevance of this apparent reciprocal regulation between TGFBR3 and CD44 and the role of TGFBR3 in monocyte/macrophage functions remains to be determined.

6.2.2 Polarising stimuli initiate differential expression of HS-associated genes

In addition to the substantial changes in HS-associated gene expression during monocyte maturation, many genes showed significant differential expression between samples stimulated with pro-inflammatory stimuli (IFN-γ and/or LPS) or anti-inflammatory stimuli (IL-4 and IL-13), and any one of these would have been a good candidate for further study (Figure 6.1). *SDC2* was the most highly expressed HS core protein at the transcript level in M-CSF macrophages, and showed significant downregulation in the presence of IFN-γ, consistent with previous reports (Martinez et al., 2006), and significant upregulation in response to IL-4 and IL-13,

suggesting it plays more of a role in M2 macrophages. The HS chains of SDC2 may be important for reparative functions, as SDC2 upregulation was shown to enable macrophages to present FGF-2 to target cells and induce their proliferation, but this ability was lost if cells were heparinase treated (Clasper et al., 1999). Similarly, Sdc2-null mice have reduced VEGF-dependent angiogenesis that could be rescued by re-expression of wild-type Sdc2 but not a mutant construct lacking the HS attachment sites (Corti et al., 2019). *SDC1* was also downregulated by M1 stimuli and upregulated in response to M2 stimuli, as has previously been reported for murine macrophages (Angsana et al., 2015). In the same study, Sdc1-null murine macrophages showed reduced motility and enhanced adhesion, indicating that the role of SDC1 might be in regulating macrophage interactions with extracellular matrix molecules rather than regulating growth factor signalling. Whether this role requires GAG chains has not been established. In contrast, I found that *SDC3* and *SDC4*, while similarly abundant in M-CSF macrophages, were strongly induced by IFN-γ or LPS as has previously been reported for human endothelial cells (Vuong et al., 2015) and murine macrophages (Tanino et al., 2012).

The glypicans showed similar differences in regulation between protein isoforms, with *GPC1* showing strong induction by IL-4 and IL-13, and *GPC5* being strongly upregulated by LPS with and without IFN-γ. *GPC4* was the second most abundant core protein transcript in M-CSF unpolarised macrophage and was downregulated by M1 stimuli, consistent with previous reports (Martinez et al., 2006) but the significance of its expression is not clear. *GPC3*, which I found was only expressed in M-CSF macrophages, has previously been implicated in hematopoiesis due to the

impaired production of monocyte/macrophage progenitors in Gpc3-null mice (Viviano et al., 2005). Whether the requirement for glypican-3 is cell intrinsic or part of the bone marrow niche would require bone marrow transfer experiments between Gpc3-null and wild-type mice.

My finding that *AGRN* (agrin) was upregulated by LPS alone (and to a lesser extent by LPS with IFN-γ), but not by IL-4/IL-13, suggests that an abundance of agrin is a feature of pro-inflammatory macrophages. Consistent with this hypothesis, a previous study found that another pro-inflammatory stimulus, IFN-α, induced agrin upregulation in T cells (Jury et al., 2007). Although mainly studied for its role in formation of the neuromuscular junction, functions for immune cell agrin have also been reported. Mice genetically lacking agrin showed reduced numbers of monocytes and macrophages (Mazzon et al., 2012), indicating that agrin is required for survival of monocyte progenitor cells and the subsequent maturation of monocytes. These agrin-deficient macrophages also showed impaired phagocytic ability due to defective F-actin rearrangement, consistent with the purported role for agrin in linking the extracellular matrix to the cytoskeleton via its receptor alpha-dystroglycan. My finding that pro-inflammatory stimuli induce upregulation of agrin could indicate that these M1-like cells are primed for phagocytosis of pathogens. Agrin was shown to promote actin rearrangement in T cells (Jury et al., 2007) and has been proposed to be involved in forming the immunological synapse (Jury and Kabouridis, 2010), so it is possible that agrin serves a similar function in macrophages during formation of the phagocytic synapse. Whether M1 macrophages do indeed show greater phagocytic capacity to which agrin contributes could be

investigated by comparing phagocytosis by M1 and M2 polarised macrophages and testing whether bead uptake is affected by agrin knockdown.

In contrast to agrin, which was most highly expressed in pro-inflammatory macrophages, the HS core protein perlecan (HSPG2) showed similar levels of expression in monocytes, unpolarised macrophages and pro-inflammatory macrophages, but was strongly and significantly upregulated in macrophages stimulated with IL-4/IL-13. Perlecan has been best studied in the ECM, where its ability to bind growth factors and modulate the adhesion of cells plays an important role in wound healing, angiogenesis, and tumour growth (Knox and Whitelock, 2006). The modular nature of the HSPG2 gene enables translation of different proteins by inclusion or exclusion of domains by alternative splicing (Gubbiotti et al., 2017): it is not known which isoform of perlecan is expressed in anti-inflammatory macrophages, or where it is localised. Perlecan had previously been reported to be upregulated by hypoxia in macrophages (Asplund et al., 2010), and was recently shown to contribute to the ability of macrophages to bind LDL (Ng et al., 2021), arguably consistent with a role for perlecan in M2 macrophage functions such as scavenging debris and in pathologies associated with hypoxia and LDL such as atherosclerosis. In other cell types, perlecan has previously been shown to be downregulated by IFN-γ (Sharma and Iozzo, 1998) and upregulated by TGF-β (Dodge et al., 1990), further supporting a role for this HS core protein in tissue repair and resolution of immune responses. To my knowledge this thesis presents the first data demonstrating IL-4/IL-13-induced upregulation of perlecan transcript.

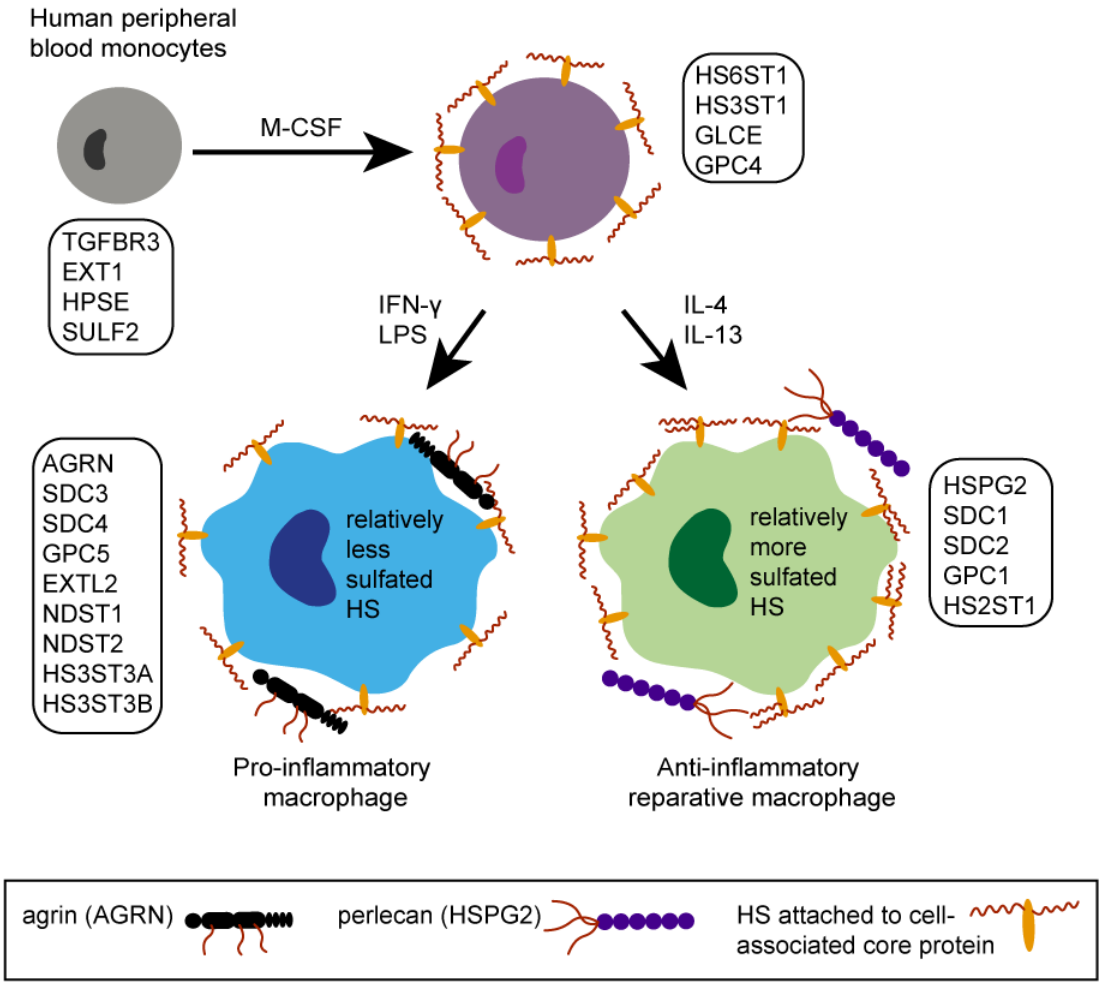

Figure 6.1 Schematic of regulated HS-associated genes in monocyte maturation and macrophage polarisation.
Monocyte to macrophage maturation with M-CSF was associated with downregulation of TGFBR3, EXT1, HPSE, and SULF2, and upregulation of most other HS-associated genes. Subsequent polarisation to pro- or anti-inflammatory macrophages resulted in further significant changes to HS-associated gene expression, and these changes suggested that the HS in anti-inflammatory macrophages is more highly sulfated. Gene names are positioned to indicate the cell type in which they were most highly expressed.

As with the core proteins, HS biosynthetic enzymes also showed differential expression between unpolarised, pro-inflammatory, and anti-inflammatory macrophages. I found that EXT1 and EXT2 showed minimal regulation in M-CSF macrophages further stimulated with IFN-γ and/or LPS or IL-4/IL-13, indicating that the capacity to synthesise the HS backbone is unaffected by macrophage polarisation. However, biosynthesis of HS is also regulated by the exostosin-like

enzymes EXTL1-3, and I found isoforms 2 and 3 were expressed in monocytes and macrophages, with EXTL2 being significantly upregulated by IFN-γ+LPS, as previously reported (Martinez et al., 2006), and EXTL3 showing no regulation in expression. EXTL2 and EXTL3 have previously been suggested to regulate termination of HS chain elongation, as decreased expression of either resulted in longer HS chains (Busse et al., 2007; Katta et al., 2015). Therefore the increased expression of EXTL2 I observed in pro-inflammatory macrophages might lead to these cells synthesising shorter HS chains than their anti-inflammatory counterparts, which could affect the availability of binding sites on HS for ligands, and conversely the accessibility of transmembrane receptors.

The N-deactylase N-sulfotransferases 1 and 2 showed different patterns of expression, with NDST1 showing modest differences between unpolarised, pro-inflammatory and anti-inflammatory macrophages, whereas NDST2 was expressed at similar levels in all samples except LPS-treated in which it was significantly upregulated. The implications for the changes in expression of these enzymes are not clear, but NDST1 was previously implicated in maintaining macrophages in a quiescent state through inhibiting IFN-β signalling via HS binding (Gordts et al., 2014). As N-sulfation is known to be a pre-requisite for further downstream modifications, it may be the case that upregulation of NDSTs in pro-inflammatory macrophages facilitates increased activity of other sulfotransferases. Ndst2 knockout mice appear normal (Ledin et al., 2004) but the role of this isoform in inflammatory settings has not been explored.

GLCE expression was significantly lower in response to pro-inflammatory stimuli, with the exception of LPS which showed a non-significant trend towards downregulation, likely due to the high level of variability in LPS-responsive gene regulation seen between donors, but was maintained in response to IL-4/IL-13. This potential decrease in epimerisation of pro-inflammatory macrophage HS could lead to reduced overall sulfation, as epimerisation promotes subsequent 2-O- and 6-O-sulfation (Smeds et al., 2003). *HS2ST1* and *HS6ST1* both showed downregulation with pro-inflammatory stimuli, suggesting that pro-inflammatory macrophage polarisation is associated with reduced 2-O- and 6-O-sulfation relative to anti-inflammatory macrophages and therefore that these HS modifications are involved in reparative rather than pro-inflammatory functions of macrophages.

Only 3 of the 7 3-O-sulfotransferase protein isoforms were expressed in monocytes and macrophages, and all showed striking patterns of regulation in response to stimuli. *HS3ST1* was downregulated more by IFN-γ and/or LPS than by IL-4/IL-13, suggesting that its activity might be higher in anti-inflammatory macrophages. In contrast, *HS3ST3A* and *HS3ST3B* showed similar levels of expression in monocytes and M-CSF macrophages but both were upregulated in response to IFN-γ and/or LPS, which in the case of *HS3ST3B* was significant and with a large effect size in some donors. These data are in accordance with previous reports that LPS activation of monocytes induced a 2-fold increase in *HS3ST3B* transcript (Sikora et al., 2016), and that there was a 65-fold increase in the expression of this gene in M1 macrophages relative to M2 (Martinez et al., 2015). Due to the paucity of standards for 3-O-sulfated disaccharides, this modification has not been much studied so the

significance of these findings is not clear. However, improved standards are being developed for HPLC (Mochizuki et al., 2020) so detailed analysis of the HS motifs synthesised by the different protein isoforms of the HS3STs and their biological functions may be possible in the near future.

6.2.3 Effects on HS structure require direct investigation

Based on the differential expression of enzymes I observed in monocytes and macrophages, one might predict that maturation in the presence of M-CSF is associated with an increase in cell-surface HS and that it is moderately N-, 2-O- and 6-O-sulfated. Pro-inflammatory stimuli induced changes in HS enzyme expression that might lead to reduced epimerization and reduced 2-O- and 6-O-sulfation, but increased 3-O-sulfation. In contrast, anti-inflammatory macrophage HS may well retain a similar pattern of HS composition to unpolarised macrophages, with a possible switch to different core proteins including perlecan, whereas pro-inflammatory macrophages might be using more agrin. However, there are many levels at which HS structure can be regulated in addition to transcription of the HS-associated genes, including translation of protein, enzyme localization, relative activity, and cooperative interactions. The strength of correlation between enzyme expression and associated HS modification is not well established, and I had hoped to increase our understanding of the regulation of HS structure by comparing the HS transcriptome profiles in polarised macrophages to the disaccharide composition of each population. However, carrying out such analyses by HPLC was delayed by such an extent as to preclude inclusion in this thesis. As an alternative, I sent samples to a collaborator lab for disaccharide composition analysis by liquid chromatography

mass spectrometry, a more recently developed technique that has shown substantial differences in the proportions of HS disaccharides present in different cell lines (Antia et al., 2018), which may reasonably be expected to also be true of primary cells. At time of writing, these samples had still not been analysed and so the HS composition of unpolarised, pro-inflammatory, and anti-inflammatory macrophages in my experimental system is unknown, but can be predicted based on other similar studies comparing disaccharide composition with enzyme expression. For example, upregulated HS2ST1 in human monocyte-derived macrophages correlated with increased abundance of 2-O-sulfated disaccharides (Martinez et al., 2015), suggesting that my IL-4/IL-13-stimulated macrophages are likely to have more of this modification than the pro-inflammatory macrophages. Moreover, a mutant cell library with selective deletions of HS biosynthetic enzymes demonstrated strong correlation between enzyme expression and their resulting HS structure (Qiu et al., 2018). In addition, previous studies have demonstrated differences in the immunoreactivity of HS after changes in biosynthetic enzyme expression: LPS-induced upregulation of HS3ST3B in endothelial cells resulted in increased binding of an antibody that recognises 3-O-sulfated motifs (Krenn et al., 2008) for example. However, validation of the effects of the observed changes in gene expression on HS composition would strengthen the impact of my findings.

6.2.4 Sulfated HS supports macrophage polarisation

The increased capacity for HS biosynthesis I observed upon M-CSF maturation led me to hypothesise that the presence of cell-surface HS chains is important for macrophage maturation or effector functions. Monocytes differentiated with M-CSF

in the presence of sodium chlorate showed no apparent differences in the expression levels of CD68, CD14 and CD16 compared to controls, indicating that abolishing HS sulfation does not impair macrophage maturation. This finding is unsurprising, given that M-CSF is not reported to be an HS-binding protein (Ori et al., 2011). However, other immune mediators associated with polarisation of macrophages are known to bind to HS, including IFN-γ (Lortat-Jacob and Grimaud, 1991) and IL-4 (Lortat-Jacob et al., 1997), so it is expected that abolishing HS sulfation of macrophages would affect upregulation of the M1 and M2 polarisation markers associated with these cytokines. My data showing greater upregulation of M1 polarisation markers in response to IFN-γ/LPS in chlorate-treated cells suggests that HS does have a negative regulatory role for the signalling of pro-inflammatory stimuli. LPS is not known to require HS for signalling and its pathway via TLR4 has been well studied, so it is most likely that lack of sulfated HS affected IFN-γ signalling. Since the HS-binding and receptor-binding sites overlap it is plausible that interacting with HS inhibits IFN-γ signalling, and thus that normally sulfated macrophage HS serves to maintain macrophages in a quiescent state by decreasing their responsiveness to pro-inflammatory stimuli, as has previously been demonstrated for IFN-β (Gordts et al., 2014). In contrast, sodium chlorate-mediated mediated desulfation of macrophage HS led to decreased IL-4/IL-13-induced upregulation of *CD209* (DC-SIGN) and *CD206* (MRC1), and is consistent with the decreased cell-surface level of CD209 protein I also observed. IL-4 but not IL-13 has been reported to be an HS-binding protein (Ori et al., 2011), making it most likely that the effect of altered HS sulfation on polarisation occurs via IL-4 signalling. My data suggest that sulfated HS promotes IL-4 signalling, which is consistent with a previous report that sodium

chlorate treatment of dendritic cells reduced IL-4-induced upregulation of DC-SIGN (CD209) (den Dekker et al., 2008) and indicates that macrophage HS skews the phenotype towards M2.

6.3 What are the functions of HS6ST1 and 6-O-sulfation in macrophages?

The highly significant downregulation of the endosulfatase *SULF2* during monocyte to macrophage maturation was of interest because of the reciprocal expression pattern it showed to its functional partner, the 6-O-sulfotransferase (*HS6ST1*). This pattern of regulation is likely to increase levels of 6-O-sulfated HS between monocyte and macrophage. The signalling of developmental molecules such as Wnt and the BMP inhibitor Noggin are regulated by a switch in 6-O-sulfation status controlled by HS6STs and SULFs (Ai et al., 2003; Viviano et al., 2004), and it is possible that a similar molecular switch operates in an immune context. For example, TGF-β signalling is promoted by 6-O-sulfation, and overexpression of HS6STs in idiopathic pulmonary fibrosis results in hyperresponsiveness to TGF-β and may contribute to the excessive fibrotic response (Lu et al., 2014). Sulf1 knockdown also increased TGF-β signalling, and TGF-β stimulation of fibroblasts induced Sulf1 expression and reduced 6-O-sulfation of HS (Yue et al., 2008), suggesting that TGF-β regulates its own activity via a negative feedback loop affecting HS sulfation. If a similar 6-O-sulfate switch operates in macrophages, further agnostic investigation into the ligands it regulates is warranted.

6-O-sulfation is a unique modification of HS in that it can be removed post-synthetically on the cell surface by desulfatase enzymes (SULFs). I found that only

one of the three protein isoforms of 6-O-sulfotrasferases, HS6ST1, was expressed in monocyte-derived macrophages, and that its expression was upregulated by M-CSF and down-regulated by further polarising stimuli, whether pro- or anti-inflammatory. In addition to its unique property of being post-synthetically edited, I chose HS6ST1 over other potential candidates because it is at or near the end of the HS biosynthetic pathway and thus its loss should have minimal knock-on effects on other HS modifications. In contrast, knocking down an enzyme earlier in the pathway such as NDST or GLCE would have multiple effects on HS structure including changes in the affinity of various subsequent enzymes for HS and thus different O-sulfate modifications, meaning any potential phenotype observed would be more difficult to attribute to one particular modification.

6.3.1 6-O-sulfated HS had no effect on phagocytosis or migration

I hypothesised that 6-O-sulfated HS is required for some of the immune functions of macrophages, such as phagocytosis, migration, and the ability to respond to polarising signals by upregulation of genes and acquiring an appropriate effector phenotype. The evidence implicating HS in phagocytosis is circumstantial and not specific to professional phagocytes (Section 1.5.2.1) having been mainly conducted in epithelial cells and fibroblasts. However, as it is a renowned function of macrophages, I tested phagocytosis of three different substrates that use different pathways for uptake (Freeman and Grinstein, 2014). To represent bacterial pathogens I used *E. coli*, which can be recognised by phagocytic receptors such as scavenger receptor A (CD204) and MARCO, in addition to TLRs. In contrast, zymozan would be taken up by C-type lectins such as Dectin-1 and the macrophage mannose

receptor (CD206) that recognise fungal polysaccharides. Coating the latex beads with FBS was a model for pathogen opsonisation by antibodies, which would be taken up by macrophage Fc-receptors such as FcγRI (CD64) and FcγRIIIa (CD16a). However, in the time points and conditions I tested, loss of HS6ST1 expression had no significant effect on macrophage phagocytosis of these substrates, suggesting that none of these receptor pathways require sulfated GAGs for their activity. Ectopically expressing individual receptors in cells whilst manipulating their HS structure might help to unpick whether any of these receptors require HS as part of their PAMP recognition process.

Another important function of leukocytes is their ability to home in on a site of inflammation in response to directional cues such as chemokines, many of which require interactions with endothelial HS for maximum activity. CCL2 (MCP-1) is known to bind HS on the endothelium with the effect of potentiating its activity, and binding is substantially increased by the presence of a 6-O-sulfate group (Miller et al., 2016), yet in my transwell experiments there was no significant effect of *HS6ST1* knockdown on the migration of THP1 cells. This could suggest that leukocyte HS is not required for signalling of this chemokine.

6.3.2 Agnostic methods are required to establish the effects of 6-O-sulfated HS on macrophage signalling

A major limitation throughout my project was not knowing that *HS6ST1* knockdown had affected the level of 6-O-sulfation on the macrophage cell-surface and at what time point after electroporation this occurs. Pulse-chase experiments have shown that

HS turnover in some cells takes between 4 and 24 h (Carter et al., 2003). However, macrophages are terminally differentiated cells so it may be the case that they do not change their HS structure once they have matured, but I would argue that the significant changes I observed in HS enzyme expression after polarisation make this unlikely. An encouraging observation was that FGF-2 signalling was decreased in knockdown macrophages relative to controls, with phosphorylation of ERK1/2 in response to a suboptimal concentration of FGF-2 being decreased in the absence of HS6ST1 (Chapter 5.1). As the role of 6-O-sulfated HS in facilitating FGF signalling is well established (Chapter 1.4.2), this finding demonstrates that knockdown resulted in a biologically relevant degree of change to the disaccharide composition of HS. It is also in accordance with previous work from our group in which HS6ST1 knockdown in chondrocytes led to reduced FGF-2 signalling (Chanalaris et al., 2019). I had hoped to more definitively show that 6-O-sulfated HS was less abundant after HS6ST1 knockdown by HPLC or mass spectrometry, but at time of writing these experiments had not been performed and thus responsiveness to FGF-2 provided a surrogate measure of changes in HS sulfation.

To determine whether 6-O-sulfated HS is involved in the signalling of polarising cytokines and whether it is this group specifically whose loss during chlorate treatment alters upregulated of polarisation markers, I polarised macrophages with IFN-γ with or without LPS, or with IL-4/IL-13, and measured polarisation marker upregulation by qPCR and flow cytometry. In contrast to my previous results with chlorate-treated cells, there were no significant differences or conserved trends between polarisation marker expression in knockdown and control cells, suggesting

that the sulfate groups required for IFN-γ and IL-4 binding to HS are not 6-O-sulfates. Consistent with this conclusion, phosphorylation of STAT1 in response to IFN-γ was only slightly affected by HS6ST1 knockdown and the effect showed different directions in the two donors. Similarly, the effect size of pSTAT6 in response to IL-4 was very small. However, the n numbers from these experiments are too low to draw any meaningful conclusions from these data, and had time not been restricted I would have repeated these experiments on more donors. Testing different combinations of antibodies to ensure target and control were from different species would have enabled me to use simultaneous fluorescent detection, overcoming difficulties I experienced with reliably quantifying band intensities from chemiluminescent detection.

To more definitively test whether 6-O-sulfated HS is required for IFN-γ and IL-4 binding, an array of modified heparinoids on a chip or using an ELISA method may have enabled me to quantify the relative affinities of these cytokines for different HS motifs, as has been performed for other proteins such as Tau (Rauch et al., 2018). Other methods to measure affinity include SPR: immobilising 6-O-sufficient and -deficient HS on the chip would enable me to test the effect on cytokine binding and dissociation. It is important to note however that measurable binding in isolation does not necessarily mean a relevant physiological interaction *in vivo* in the presence of other mediators, where the relative affinities are presumably important.

When I screened the conditioned medium of control versus knockdown cells for differences in the abundance of cytokine ligands, I found a reproducible increase in

CCL2 in the conditioned medium after knockdown. This was confirmed in multiple donors and after several time points by ELISA, showing significance at 48 h post-knockdown, and was not due to changes in transcription of this gene. These data suggest that non-6-O-sulfated HS cannot support binding of CCL2 to the macrophage cell surface, which is consistent with previous reports that CCL2 binds 6-O-sulfated HS with 200-fold higher affinity than an isomer lacking 6-O-sulfate (Miller et al., 2016). The purpose of this interaction is unclear, since macrophages are generally less migratory than monocytes, having reached their destination concurrent with their maturation. It may be the case that macrophages can present CCL2 to other cells, as is known for FGF-2, or that macrophage HS serves to regulate the availability of CCL2 to indirectly affect the migration of other cells. It is also possible that the binding of CCL2 to macrophage HS is not biologically relevant and is a side-effect of the ability of CCL2 to bind to endothelial HS. Alternatively, the CCL2 in a mature macrophage context may be serving some function other than inducing migration (Gschwandtner et al., 2019), such as promoting survival or priming for subsequent responses to stimuli.

Another shortlisted cytokine from the array was CXCL8 (IL-8), but subsequent ELISAs did not reproduce the trend towards increased abundance in the conditioned medium after *HS6ST1* knockdown. IL-8 binding to HS is thought to require N-, 2-O- and 6-O-sulfate groups (Spillmann et al., 1998) so I would have predicted that *HS6ST1* knockdown would result in increased abundance of this cytokine in the conditioned medium. However, it has previously been reported that removal of 2-O-sulfate groups had a larger effect on IL-8 binding than removal of 6-O-sulfate groups

(Spillmann et al., 1998) so knockdown of *HS6ST1* may have had too small an effect for me to quantify. The consequences for altered interaction with macrophage HS are unclear: the receptor-binding and GAG-binding sites on IL-8 are spatially distinct so simultaneous binding is theoretically possible (Pichert et al., 2012), but it may be the case that HS is not required for IL-8 signalling, only for its localisation on the apical surface of endothelial cells (Middleton et al., 1997).

Effects of HS 6-O-sulfation on protein levels of a limited number of cytokines were tested using a commercially available cytokine array, but it is likely that the relative abundance of many other ligands in the conditioned medium is also affected by HS6ST1 knockdown in macrophages. Agnostic approaches are thus required to establish the role of 6-O-sulfated HS in macrophages. With this in mind, I designed an experiment in which cells were cultured with serum for 48 h following electroporation with si*HS6ST1* or non-targeting control siRNA, which would provide a source of exogenous, potentially HS-binding, ligands (Figure 6.2). These could be distinguished from endogenous macrophage-produced ligands by comparison of the human and bovine sequence databases. It would be expected that any ligands requiring 6-O-sulfate for binding to cell-surface HS would be more abundant in the medium of si*HS6ST1*-treated cells due to their decreased affinity for less sulfated HS. It is possible that some ligands may interact more strongly with HS in the absence of 6-O-sulfate and therefore would be less abundant. To discriminate between proteins whose abundance is altered by changes in binding to HS and other possible secondary effects of knockdown, duplicate samples would be incubated with heparin for a further 24 h to displace any HS-binding ligands from the cell-

surface, and any candidates from these samples could be compared with their corresponding non-heparin-treated controls. At time of writing, these conditioned medium samples were awaiting analysis by our collaborator.

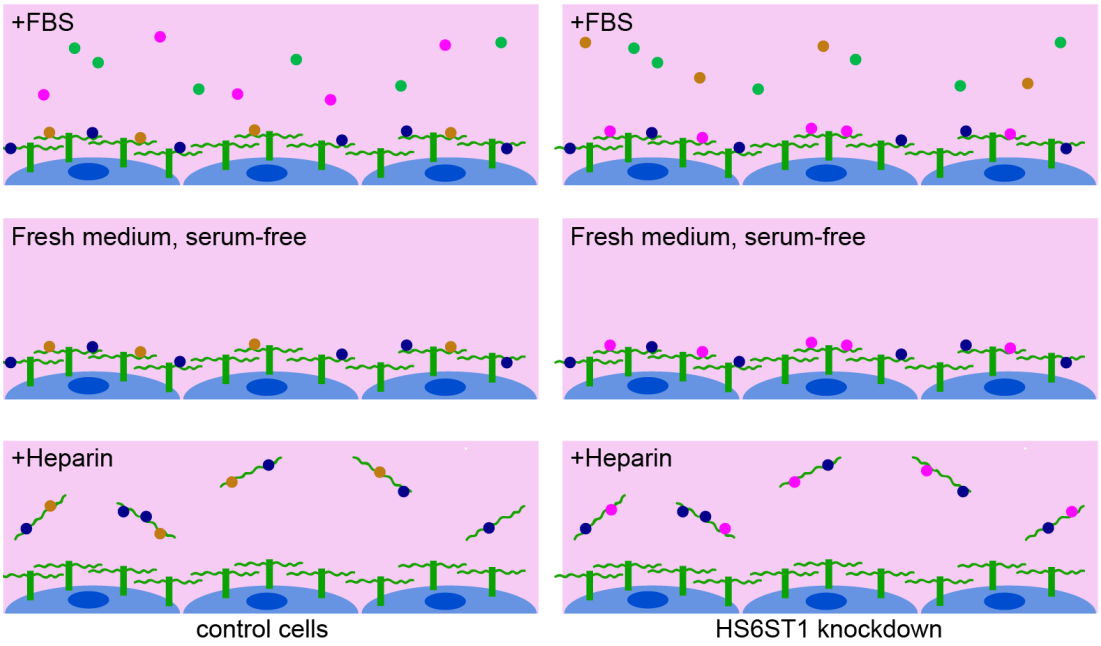

Figure 6.2. Design schematic of the mass spectrometry experiment to discover novel HS ligands affected by loss of 6-O-sulfation.
Culturing monocyte-derived macrophages in serum-containing medium provides a source of exogenous (bovine) ligands to supplement the endogenous (human) ligands secreted by macrophages. Unbound ligands are removed by aspiration of the medium, and replacement with serum-free medium containing heparin ensures HS-bound ligands will be displaced from the surface and collected in the conditioned medium for detection by mass spectrometry. Comparing the proteome of control and HS6ST1 knockdown cells should reveal those ligands whose binding to HS is affected by loss of 6-O-sulfation.

Another way to determine the role of HS6ST1 and 6-O-sulfated HS in macrophages *in vivo* might be to make a conditional knockout mouse. Global deficiency of Hs6sts is usually embryonically or perinatally lethal due to multiple morphological defects, although severity appears to depend on the background mouse strain (Habuchi et al., 2007; Izvolsky et al., 2008). Selectively deleting Hs6st1 in myeloid cells might help to elucidate the function of 6-O-sulfated macrophage HS *in vivo*, a methodology that has been successfully applied to other enzymes of the HS biosynthetic pathway. For

example, conditional deletion of Ndst1 in monocytes resulted in increased susceptibility of mice to atherosclerosis and obesity and a corresponding increase in the inflammatory activation of macrophages, with elevated STAT1 signalling downstream of IFN-β (Gordts et al., 2014), indicating that N-sulfated HS negatively regulates the activity of this cytokine on macrophages. To my knowledge, a selective knockout of *Hs6st1* has not yet been generated in any murine tissue type.

6.4 Therapeutic implications

Heparin has been used clinically as an anticoagulant since 1935, and has since been shown to have anti-inflammatory effects that are presumed to be due to disruption of HS-ligand interactions (Paschoa, 2016). For example, intravenous heparin was shown to reduce leukocyte recruitment to sites of acute inflammation in mice through blocking P- and L-selectins (Wang et al., 2002), suggesting that interrupting the binding of HS ligands might present a therapeutic strategy. Although heparin is unsuitable for prolonged use due to increased risk of bleeding and possible heparin-induced thrombocytopenia, its anti-inflammatory effects have been shown to be independent of its anti-coagulant effects (Sy et al., 1983), leading to the development of modified heparinoids with reduced anti-coagulant activity (Mulloy, 2019). As an alternative to intravenous administration, nebulised heparin or heparinoids can be administered to the lung and have shown efficacy in murine asthma models (Ghonim et al., 2018) and patients with chronic obstructive pulmonary disease (COPD) (Shute et al., 2018), and are currently being explored as treatment or prophylaxis for COVID-19 (Tandon et al., 2020; Wilkinson et al., 2020; Yu et al., 2020).

To avoid global disruption of all HS-ligand interactions by heparin, specific ligands and their HS motifs must be targeted, to which end a few different strategies are possible (Figure 6.3). The first is to modify endogenous HS structure by regulating the activity of biosynthetic enzymes, which is an attractive strategy in diseases where HS biosynthesis is known to be dysregulated, such as cancer (Nagarajan et al., 2018). It is unclear how HS biosynthetic enzyme activity might be promoted, but inhibitors of selected enzymes in the biosynthetic pathway have been reported, such as the SULF inhibitor OKN-007 (Zheng et al., 2013) and a modified iminosugar related to L-iduronic acid that acts as an inhibitor of HS2ST1 (Brown et al., 2006). However, problems remain with how the inhibitor would be delivered, and how its activity would be restricted to only target cells: genetic manipulation of the HS biosynthetic pathway has demonstrated that lack of HS results in severe phenotypes (Habuchi and Kimata, 2010; Habuchi et al., 2007; Izumikawa and Kitagawa, 2010; Ringvall and Kjellen, 2010), so disrupting all HS biosynthesis in patients seems risky. Thus this strategy is a long way from being clinically useful.

A second strategy for disrupting HS-ligand interactions is competitive inhibition with HS mimetics or HS derivatives, which have the advantage over heparin of having more consistent sulfate structures and thus more direct ligand targeting with potentially fewer off-target effects, in addition to minimal anticoagulant activity. HS mimetics that were initially developed as heparanase inhibitors have been found to have anti-inflammatory effects independent of heparanase-inhibitory ability due to competition with endogenous HS for the binding of pro-inflammatory cytokines and growth factors. The HS mimetic PI-88 (muparfostat), for example, was the first

heparanase inhibitor to enter clinical trials for cancer (Kudchadkar et al., 2008) and has been shown to competitively inhibit HS binding and signalling of FGF-1, -2, and VEGF (Cochran et al., 2003; Francis et al., 2003). Another HS mimetic, PG545 (pixatimod) has similarly been shown to inhibit angiogenesis and metastasis in several pre-clinical cancer models and has entered clinical trials (Dredge et al., 2018). It appears to have several immunomodulatory activities including inhibiting Wnt signalling and thus suppresses tumour growth (Jung et al., 2015).

HS derivatives have also been selected to promote signalling of ligands in diseases where angiogenesis and wound healing would be beneficial. For example, an HS fraction affinity-isolated for VEGF165 binding was shown to promote the affinity of VEGF for its receptor (Rouet et al., 2005) and angiogenic potential in vessel formation assays (Wang et al., 2014). Furthermore, it promoted neovascularisation, resolution of inflammation and wound healing in rat wound healing models (Tong et al., 2009; Tong et al., 2012), and promoted healing of treatment-resistant diabetic foot ulcers in patients (Papanas et al., 2016). HS fractions could theoretically be selected for high affinity binding to any HS-dependent ligand in order to modulate signalling. However, the available data make it clear that high-affinity HS mimetics could either promote or inhibit ligand activity, underlining the importance of greater understanding of the role of HS in signalling for the future development of therapeutics.

A third strategy is to make small molecules that will occupy and thus block ligand-binding motifs on endogenous HS chains, thus inhibiting ligand activity. Surfen (vis-

2-methyl-4-amino-quinolyl-carbamide), for example, interacts electrostatically with heparin and HS and was shown to inhibit FGF-2 and VEGF signalling *in vitro* (Schuksz et al., 2008). However, in the same study, surfen also inhibited heparanase digestion, the antagonistic effect of heparin on blood clotting, and binding of the HS-binding glycoprotein from herpes simplex virus 1 (HSV-1), suggesting that it binds to a common HS motif present in the binding site of multiple ligands, and therefore that its effects are likely too broad for clinical application. A more targeted approach is to use peptides derived from the HS-binding region of the target ligand, such as the synthetic peptide derived from VEGF that has been shown to inhibit signalling *in vitro* and inhibit tumour growth *in vivo* (Lee et al., 2010). Similarly, synthetic peptides based on the HS-binding regions of chemokines (CCL5, CXCL8, CXCL12) were able to inhibit chemokine-induced transendothelial migration *in vitro*, and the CXCL8-derived peptide reduced the severity of disease and inflammatory infiltrate in antigen-induced arthritis, a murine model of rheumatoid arthritis (McNaughton et al., 2018).

Alternatively, the whole HS-binding protein may be mutated to form a dominant-negative competitor of endogenous protein. This was demonstrated with a mutant form of CCL2 that had increased affinity for HS but strongly reduced receptor activation, and was shown to competitively inhibit endogenous native CCL2 activity (Piccinini et al., 2010) and thus inhibit inflammation *in vivo* (Gschwandtner et al., 2016). Collectively these studies provide evidence that HS-ligand interactions can be selectively targeted for therapeutic benefit, and support the need for greater understanding of the specificity of HS-ligand binding motifs.

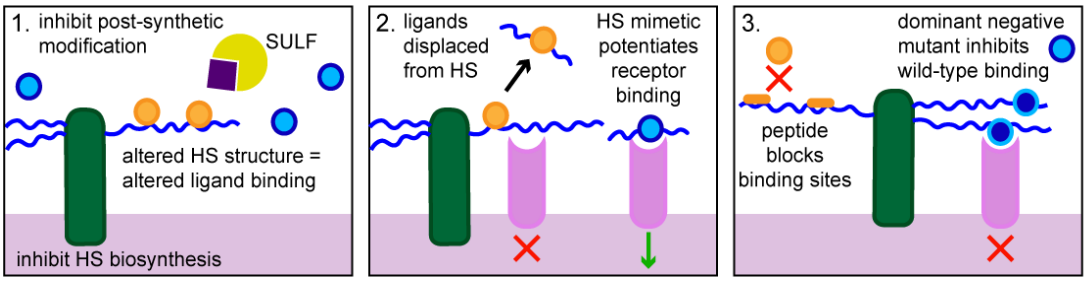

Figure 6.3. Therapeutic strategies targeting HS-ligand interactions.
The first strategy is to alter the structure of endogenous HS by pharmacologically inhibiting enzymes in the biosynthetic pathway, such as the SULF inhibitor (OKN-007), to change the availability of binding sites for HS ligands. A second strategy is to design or isolate HS mimetics that bind to the target ligand and either competitively inhibit its binding to endogenous HS, or promote signalling by interacting with both the ligand and its receptor. The third strategy is to synthesise proteins or peptide fragments that bind to HS and mask the binding sites, making them unavailable for endogenous ligand.

Whether we will ever be able to target the HS on individual cell types, such as macrophages, is much harder to predict and will require further study of the HS-biosynthetic machinery and resulting sulfated motifs expressed by different cell types, and a greater understanding of their role in regulating the many components of inflammation.

6.5 Conclusions and future perspectives

In this project, I have demonstrated significant changes occurring in the HS-associated gene transcriptome during monocyte maturation with M-CSF and subsequent polarisation of these macrophages with IFN-γ and/or LPS, or IL-4/IL-13. Disaccharide composition analysis of the HS from these cell types would confirm whether the differences in enzyme expression level are reflected in the relative abundance of sulfated motifs: from my transcriptome data it seems likely that IL-4/IL-13-polarised macrophages generally have more HS with a higher degree of

sulfation, whereas pro-inflammatory macrophages may selectively increase 3-O-sulfate groups. Maturation and polarisation also induced changes in the core proteins expressed, although whether the actions of these core proteins in macrophages are dependent on their HS chains remains to be established and would require systematic evaluation of mutant proteins lacking the HS attachment region.

My data on the use of sodium chlorate before macrophage polarisation (Chapter 3.5) suggest that sulfated HS is required for IL-4 activity and inhibits IFN-γ activity, but it may not be the 6-O-sulfate group that is responsible as the signalling data after *HS6ST1* knockdown were inconclusive (Chapter 5.3). However, a reduction in 6-O-sulfated HS due to *HS6ST1* knockdown did affect the distribution of CCL2 between the cell-membrane-bound and free forms, and it is likely that other immune functions of macrophages were also affected. Knockdown had no significant effect in the phagocytosis assays I performed, but I did not test efferocytosis (uptake of apoptotic cells) or uptake of lipoproteins, and it is possible that HS is involved in these processes. For example, it has been reported that macrophages exposed to hypoxia synthesised longer and more sulfated GAG chains with a higher affinity for LDL (Asplund et al., 2011), while heparinase digestion reduced internalisation and degradation of LDL (Kaplan et al., 1998). Whether HS contributes to lipoprotein metabolism by macrophages *in vivo*, and whether specific HS modifications such as 6-O-sulfate are required, will require further investigation.

Chondroitin sulfate/dermatan sulfate (CS/DS) is a structurally similar GAG to HS and shares the same tetrasaccharide linkage region on the core protein but is

synthesised by a distinct set of enzymes. Expression levels of the xylosyl transferases responsible for initiating the tetrasaccharide linkage region, and of the CS enzymes, were not quantified in this project, but it is likely they would also be relevant to macrophage functions because the selective sulfation at various positions may regulate ligand binding in a similar manner to HS. Digesting human macrophages with heparinises or chondroitinases indicates that CS/DS makes up more than half of the total GAG content (Martinez et al., 2015), so this proteoglycan may compete with the relatively less abundant HS for binding of ligands, with as-yet unknown consequences. Comprehensive profiling of CS biosynthesis, such as that shown here for HS, would help illuminate this area.

There are several mechanisms by which macrophage HSPGs could regulate immune responses, and all may occur in different conditions and for different ligands. The highly sulfated HS of M2-polarised macrophages has already been established to facilitate presentation of FGF-2 to target cells and form a signalling-competent trimolecular complex with the receptor (Clasper et al., 1999). This presenting function may be true for other bioactive molecules and would thus give HS a role for regulating interactions between macrophages and stromal cells, which in the case of growth factors would be expected to be especially important for wound healing and tissue repair. In addition to direct presentation, macrophage HSPGs may indirectly regulate the signalling of surrounding cells by regulating the availability of ligands. For example, the changes in abundance of cytokines such as CCL2 I observed in the conditioned medium of HS6ST1 knockdown macrophages indicate that changing HS sulfation status might shift the distribution of ligands between cell-bound and soluble

states and thus affect their ability to bind their receptor. Another dimension to HS in inflammation that I did not explore in this project is heparanase-mediated release of bioactive molecules by cleaving off sections of the HS chain. Macrophages may secrete heparanase themselves or may have their HS cleaved by heparanases from other cellular sources, with a variety of possible consequences including release of HS-bound growth factors (Goldberg et al., 2013).

In addition to regulating ligands acting on other cells, macrophage HS may serve a cell-intrinsic function. Macrophage HS may regulate the basal activation state of the macrophage by determining how sensitive it is to signals in the microenvironment. For example, the available evidence indicates that HS promotes signalling of anti-inflammatory cytokines such as IL-10 (Salek-Ardakani et al., 2000) and IL-4 (den Dekker et al., 2008), whereas it inhibits signalling of IFN-β (Gordts et al., 2014) and IFN-γ (Sadir et al., 1998). Macrophages in murine models of chronic inflammatory disease show changes in HS biosynthesis (Swart and Troeberg, 2019): it may therefore be the case that dysregulated HS structure underlies many chronic inflammatory diseases due to aberrant macrophage signalling and inappropriate immune activity. Selective knockouts in murine disease models and comparisons of HS structure in healthy versus diseased human tissue are warranted.

An important function of macrophages is acting as a bridge between the innate and adaptive immune systems by processing and presenting foreign antigen to T and B cells with appropriate costimulation to activate them. It has been suggested that agrin may function in the immunological synapse between T cells and antigen-presenting

cells (Khan et al., 2001), and it has also been reported that interaction with HSPGs on the antigen-presenting cell surface potentiates antigen uptake, processing, and MHC class II-restricted antigen presentation, leading to more potent activation of T cells (Leonetti et al., 2010). The HS sulfation requirements for these processes remain to be determined, as does the importance of such HSPG-dependent mechanisms *in vivo*.

HS synthesised by other immune cells is also likely to be important for the regulation of immune responses. Like macrophages, maturation of dendritic cells is associated with increased biosynthesis of sulfated GAGs (Wegrowski et al., 2006) that regulate IL-4 signalling (den Dekker et al., 2008) and likely other mediators too. Similarly, HS biosynthesis is regulated at different stages of B cell maturation (Bret et al., 2009) and by inflammatory stimuli (Jarousse et al., 2011), with consequences for the signalling of B cell activating factors such as APRIL (Kimberley et al., 2009) and IL-7 (Borghesi et al., 1999).

In addition to the monocyte-derived macrophage population recruited during inflammation, tissue-resident macrophages are found throughout the body where they play homeostatic and sentinel roles as well as contributing to inflammation. Investigation of resident macrophage HS is much more challenging due to difficulty isolating them from human tissues, but studies in mice have indicated that HS-associated gene expression changes significantly in murine models of chronic inflammatory diseases (Swart and Troeberg, 2019).

The available evidence overwhelmingly indicates that regulation of HS biosynthesis is a common feature of inflammatory stimulation of many cell types, and that HS is likely to regulate the activity of multiple immune mediators. In this thesis I have demonstrated significant changes to HS biosynthesis upon maturation of primary human monocytes to macrophages and their subsequent polarisation to pro- and anti-inflammatory phenotypes. This polarisation was affected by ablation of HS sulfation by sodium chlorate treatment, implicating macrophage HS in the responsiveness of macrophages to polarising stimuli. Future investigation of how specific changes to macrophage HS structure affect the immune functions of these cells will help increase our understanding of the role of sulfated GAGs in regulating inflammation.

The End

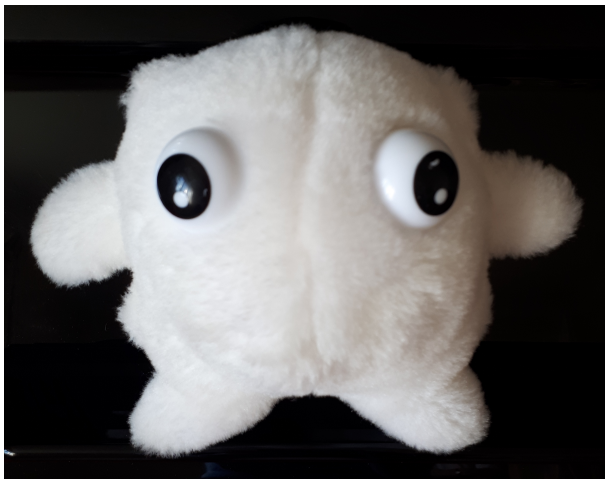

Montgomery the Macrophage

Bibliography

Ai, X., A.T. Do, O. Lozynska, M. Kusche-Gullberg, U. Lindahl, and C.P. Emerson, Jr. 2003. QSulf1 remodels the 6-O sulfation states of cell surface heparan sulfate proteoglycans to promote Wnt signaling. *J Cell Biol*. 162:341-351.

Amara, A., O. Lorthioir, A. Valenzuela, A. Magerus, M. Thelen, M. Montes, J.L. Virelizier, M. Delepierre, F. Baleux, H. Lortat-Jacob, and F. Arenzana-Seisdedos. 1999. Stromal cell-derived factor-1alpha associates with heparan sulfates through the first beta-strand of the chemokine. *J Biol Chem*. 274:23916-23925.

Ambarus, C.A., S. Krausz, M. van Eijk, J. Hamann, T.R. Radstake, K.A. Reedquist, P.P. Tak, and D.L. Baeten. 2012. Systematic validation of specific phenotypic markers for in vitro polarized human macrophages. *J Immunol Methods*. 375:196-206.

Angsana, J., J. Chen, S. Smith, J. Xiao, J. Wen, L. Liu, C.A. Haller, and E.L. Chaikof. 2015. Syndecan-1 modulates the motility and resolution responses of macrophages. *Arterioscler Thromb Vasc Biol*. 35:332-340.

Annaval, T., R. Wild, Y. Cretinon, R. Sadir, R.R. Vives, and H. Lortat-Jacob. 2020. Heparan Sulfate Proteoglycans Biosynthesis and Post Synthesis Mechanisms Combine Few Enzymes and Few Core Proteins to Generate Extensive Structural and Functional Diversity. *Molecules*. 25.

Antia, I.U., K. Mathew, D.R. Yagnik, F.A. Hills, and A.J. Shah. 2018. Analysis of procainamide-derivatised heparan sulphate disaccharides in biological samples using hydrophilic interaction liquid chromatography mass spectrometry. *Anal Bioanal Chem*. 410:131-143.

Arnold, L., A. Henry, F. Poron, Y. Baba-Amer, N. van Rooijen, A. Plonquet, R.K. Gherardi, and B. Chazaud. 2007. Inflammatory monocytes recruited after skeletal muscle injury switch into antiinflammatory macrophages to support myogenesis. *J Exp Med*. 204:1057-1069.

Asakura, E., T. Hanamura, A. Umemura, K. Yada, T. Yamauchi, and T. Tanabe. 1996. Effects of macrophage colony-stimulating factor (M-CSF) on lipopolysaccharide (LPS)-induced mediator production from monocytes in vitro. *Immunobiology*. 195:300-313.

Ashikari-Hada, S., H. Habuchi, Y. Kariya, N. Itoh, A.H. Reddi, and K. Kimata. 2004. Characterization of growth factor-binding structures in heparin/heparan sulfate using an octasaccharide library. *J Biol Chem*. 279:12346-12354.

Asplund, A., V. Friden, P. Stillemark-Billton, G. Camejo, and G. Bondjers. 2011. Macrophages exposed to hypoxia secrete proteoglycans for which LDL has higher affinity. *Atherosclerosis*. 215:77-81.

Asplund, A., G. Ostergren-Lunden, G. Camejo, P. Stillemark-Billton, and G. Bondjers. 2009. Hypoxia increases macrophage motility, possibly by decreasing the heparan sulfate proteoglycan biosynthesis. *J Leukoc Biol*. 86:381-388.

Asplund, A., P. Stillemark-Billton, E. Larsson, E.K. Rydberg, J. Moses, L.M. Hulten, B. Fagerberg, G. Camejo, and G. Bondjers. 2010. Hypoxic regulation of secreted proteoglycans in macrophages. *Glycobiology*. 20:33-40.

Atri, C., F.Z. Guerfali, and D. Laouini. 2018. Role of Human Macrophage Polarization in Inflammation during Infectious Diseases. *Int J Mol Sci*. 19.

Baeuerle, P.A., and W.B. Huttner. 1986. Chlorate--a potent inhibitor of protein sulfation in intact cells. *Biochem Biophys Res Commun*. 141:870-877.

Bartlett, M.R., P.A. Underwood, and C.R. Parish. 1995. Comparative analysis of the ability of leucocytes, endothelial cells and platelets to degrade the subendothelial basement membrane: evidence for cytokine dependence and detection of a novel sulfatase. *Immunol Cell Biol*. 73:113-124.

Bashir, S., Y. Sharma, A. Elahi, and F. Khan. 2016. Macrophage polarization: the link between inflammation and related diseases. *Inflamm Res*. 65:1-11.

Bashkin, P., S. Doctrow, M. Klagsbrun, C.M. Svahn, J. Folkman, and I. Vlodavsky. 1989. Basic fibroblast growth factor binds to subendothelial extracellular matrix and is released by heparitinase and heparin-like molecules. *Biochemistry*. 28:1737-1743.

Bertani, F.R., P. Mozetic, M. Fioramonti, M. Iuliani, G. Ribelli, F. Pantano, D. Santini, G. Tonini, M. Trombetta, L. Businaro, S. Selci, and A. Rainer. 2017. Classification of M1/M2-polarized human macrophages by label-free hyperspectral reflectance confocal microscopy and multivariate analysis. *Sci Rep*. 7:8965.

Bonvin, P., F. Gueneau, V. Buatois, M. Charreton-Galby, S. Lasch, M. Messmer, U. Christen, A.D. Luster, Z. Johnson, W. Ferlin, M. Kosco-Vilbois, A. Proudfoot, and N. Fischer. 2017. Antibody Neutralization of CXCL10 in Vivo Is Dependent on Binding to Free and Not Endothelial-bound Chemokine: IMPLICATIONS FOR THE DESIGN OF A NEW GENERATION OF ANTI-CHEMOKINE THERAPEUTIC ANTIBODIES. *J Biol Chem*. 292:4185-4197.

Borghesi, L.A., Y. Yamashita, and P.W. Kincade. 1999. Heparan sulfate proteoglycans mediate interleukin-7-dependent B lymphopoiesis. *Blood*. 93:140-148.

Bret, C., D. Hose, T. Reme, A.C. Sprynski, K. Mahtouk, J.F. Schved, P. Quittet, J.F. Rossi, H. Goldschmidt, and B. Klein. 2009. Expression of genes encoding for proteins involved in heparan sulphate and chondroitin sulphate chain synthesis and modification in normal and malignant plasma cells. *Br J Haematol*. 145:350-368.

Brown, J.R., Y. Nishimura, and J.D. Esko. 2006. Synthesis and biological evaluation of gem-diamine 1-N-iminosugars related to L-iduronic acid as inhibitors of heparan sulfate 2-O-sulfotransferase. *Bioorg Med Chem Lett*. 16:532-536.

Buscher, K., E. Ehinger, P. Gupta, A.B. Pramod, D. Wolf, G. Tweet, C. Pan, C.D. Mills, A.J. Lusis, and K. Ley. 2017. Natural variation of macrophage activation as disease-relevant phenotype predictive of inflammation and cancer survival. *Nat Commun*. 8:16041.

Busse, M., A. Feta, J. Presto, M. Wilen, M. Gronning, L. Kjellen, and M. Kusche-Gullberg. 2007. Contribution of EXT1, EXT2, and EXTL3 to heparan sulfate chain elongation. *J Biol Chem*. 282:32802-32810.

Bystrom, J., I. Evans, J. Newson, M. Stables, I. Toor, N. van Rooijen, M. Crawford, P. Colville-Nash, S. Farrow, and D.W. Gilroy. 2008. Resolution-phase macrophages possess a unique inflammatory phenotype that is controlled by cAMP. *Blood*. 112:4117-4127.

Carlsson, P., J. Presto, D. Spillmann, U. Lindahl, and L. Kjellen. 2008. Heparin/heparan sulfate biosynthesis: processive formation of N-sulfated domains. *J Biol Chem*. 283:20008-20014.

Carmeliet, P., Y.S. Ng, D. Nuyens, G. Theilmeier, K. Brusselmans, I. Cornelissen, E. Ehler, V.V. Kakkar, I. Stalmans, V. Mattot, J.C. Perriard, M. Dewerchin, W.

Flameng, A. Nagy, F. Lupu, L. Moons, D. Collen, P.A. D'Amore, and D.T. Shima. 1999. Impaired myocardial angiogenesis and ischemic cardiomyopathy in mice lacking the vascular endothelial growth factor isoforms VEGF164 and VEGF188. *Nat Med*. 5:495-502.

Carter, N.M., S. Ali, and J.A. Kirby. 2003. Endothelial inflammation: the role of differential expression of N-deacetylase/N-sulphotransferase enzymes in alteration of the immunological properties of heparan sulphate. *J Cell Sci*. 116:3591-3600.

Celie, J.W., E.D. Keuning, R.H. Beelen, A.M. Drager, S. Zweegman, F.L. Kessler, R. Soininen, and J. van den Born. 2005. Identification of L-selectin binding heparan sulfates attached to collagen type XVIII. *J Biol Chem*. 280:26965-26973.

Chakravarty, L., L. Rogers, T. Quach, S. Breckenridge, and P.E. Kolattukudy. 1998. Lysine 58 and histidine 66 at the C-terminal alpha-helix of monocyte chemoattractant protein-1 are essential for glycosaminoglycan binding. *J Biol Chem*. 273:29641-29647.

Chanalaris, A., H. Clarke, S.E. Guimond, T.L. Vincent, J.E. Turnbull, and L. Troeberg. 2019. Heparan Sulfate Proteoglycan Synthesis Is Dysregulated in Human Osteoarthritic Cartilage. *Am J Pathol*. 189:632-647.

Chen, J., and J. Liu. 2005. Characterization of the structure of antithrombin-binding heparan sulfate generated by heparan sulfate 3-O-sulfotransferase 5. *Biochim Biophys Acta*. 1725:190-200.

Chistiakov, D.A., A.A. Melnichenko, V.A. Myasoedova, A.V. Grechko, and A.N. Orekhov. 2017. Mechanisms of foam cell formation in atherosclerosis. *J Mol Med (Berl)*. 95:1153-1165.

Chmiela, M., B. Paziak-Domanska, and T. Wadstrom. 1995. Attachment, ingestion and intracellular killing of Helicobacter pylori by human peripheral blood mononuclear leukocytes and mouse peritoneal inflammatory macrophages. *FEMS Immunol Med Microbiol*. 10:307-316.

Christianson, H.C., and M. Belting. 2014. Heparan sulfate proteoglycan as a cell-surface endocytosis receptor. *Matrix Biol*. 35:51-55.

Clarke, D., O. Katoh, R.V. Gibbs, S.D. Griffiths, and M.Y. Gordon. 1995. Interaction of interleukin 7 (IL-7) with glycosaminoglycans and its biological relevance. *Cytokine*. 7:325-330.

Clasper, S., S. Vekemans, M. Fiore, M. Plebanski, P. Wordsworth, G. David, and D.G. Jackson. 1999. Inducible expression of the cell surface heparan sulfate proteoglycan syndecan-2 (fibroglycan) on human activated macrophages can regulate fibroblast growth factor action. *J Biol Chem*. 274:24113-24123.

Cochran, S., C. Li, J.K. Fairweather, W.C. Kett, D.R. Coombe, and V. Ferro. 2003. Probing the interactions of phosphosulfomannans with angiogenic growth factors by surface plasmon resonance. *J Med Chem*. 46:4601-4608.

Coillard, A., and E. Segura. 2019. In vivo Differentiation of Human Monocytes. *Front Immunol*. 10:1907.

Collins, L.E., and L. Troeberg. 2019. Heparan sulfate as a regulator of inflammation and immunity. *J Leukoc Biol*. 105:81-92.

Connell, B.J., R. Sadir, F. Baleux, C. Laguri, J.P. Kleman, L. Luo, F. Arenzana-Seisdedos, and H. Lortat-Jacob. 2016. Heparan sulfate differentially controls CXCL12alpha- and CXCL12gamma-mediated cell migration through differential presentation to their receptor CXCR4. *Sci Signal*. 9:ra107.

Corti, F., Y. Wang, J.M. Rhodes, D. Atri, S. Archer-Hartmann, J. Zhang, Z.W. Zhuang, D. Chen, T. Wang, Z. Wang, P. Azadi, and M. Simons. 2019. N-terminal syndecan-2 domain selectively enhances 6-O heparan sulfate chains sulfation and promotes VEGFA165-dependent neovascularization. *Nat Commun*. 10:1562.

David, G., X.M. Bai, B. Van der Schueren, J.J. Cassiman, and H. Van den Berghe. 1992. Developmental changes in heparan sulfate expression: in situ detection with mAbs. *J Cell Biol*. 119:961-975.

de Agostini, A.I., S.C. Watkins, H.S. Slayter, H. Youssoufian, and R.D. Rosenberg. 1990. Localization of anticoagulantly active heparan sulfate proteoglycans in vascular endothelium: antithrombin binding on cultured endothelial cells and perfused rat aorta. *J Cell Biol*. 111:1293-1304.

Dehio, C., E. Freissler, C. Lanz, O.G. Gomez-Duarte, G. David, and T.F. Meyer. 1998. Ligation of cell surface heparan sulfate proteoglycans by antibody-

coated beads stimulates phagocytic uptake into epithelial cells: a model for cellular invasion by Neisseria gonorrhoeae. *Exp Cell Res*. 242:528-539.

Delehedde, M., M. Lyon, J.T. Gallagher, P.S. Rudland, and D.G. Fernig. 2002. Fibroblast growth factor-2 binds to small heparin-derived oligosaccharides and stimulates a sustained phosphorylation of p42/44 mitogen-activated protein kinase and proliferation of rat mammary fibroblasts. *Biochem J*. 366:235-244.

Dementiev, A., M. Petitou, J.M. Herbert, and P.G. Gettins. 2004. The ternary complex of antithrombin-anhydrothrombin-heparin reveals the basis of inhibitor specificity. *Nat Struct Mol Biol*. 11:863-867.

den Dekker, E., S. Grefte, T. Huijs, G.B. ten Dam, E.M. Versteeg, L.C. van den Berk, B.A. Bladergroen, T.H. van Kuppevelt, C.G. Figdor, and R. Torensma. 2008. Monocyte cell surface glycosaminoglycans positively modulate IL-4-induced differentiation toward dendritic cells. *J Immunol*. 180:3680-3688.

Denholm, E.M., and G.P. Stankus. 1995. Changes in the expression of MCP-1 receptors on monocytic THP-1 cells following differentiation to macrophages with phorbol myristate acetate. *Cytokine*. 7:436-440.

Dennissen, M.A., G.J. Jenniskens, M. Pieffers, E.M. Versteeg, M. Petitou, J.H. Veerkamp, and T.H. van Kuppevelt. 2002. Large, tissue-regulated domain diversity of heparan sulfates demonstrated by phage display antibodies. *J Biol Chem*. 277:10982-10986.

Dhoot, G.K., M.K. Gustafsson, X. Ai, W. Sun, D.M. Standiford, and C.P. Emerson, Jr. 2001. Regulation of Wnt signaling and embryo patterning by an extracellular sulfatase. *Science*. 293:1663-1666.

Dideberg, V., G. Kristjansdottir, L. Milani, C. Libioulle, S. Sigurdsson, E. Louis, A.C. Wiman, S. Vermeire, P. Rutgeerts, J. Belaiche, D. Franchimont, A. Van Gossum, V. Bours, and A.C. Syvanen. 2007. An insertion-deletion polymorphism in the interferon regulatory Factor 5 (IRF5) gene confers risk of inflammatory bowel diseases. *Hum Mol Genet*. 16:3008-3016.

Dieguez-Gonzalez, R., M. Calaza, E. Perez-Pampin, A.R. de la Serna, B. Fernandez-Gutierrez, S. Castaneda, R. Largo, B. Joven, J. Narvaez, F. Navarro, J.L. Marenco, J.L. Vicario, F.J. Blanco, J.C. Fernandez-Lopez, R. Caliz, M.D. Collado-Escobar, L. Carreno, J. Lopez-Longo, J.D. Canete, J.J. Gomez-Reino, and A. Gonzalez. 2008. Association of interferon regulatory factor 5

haplotypes, similar to that found in systemic lupus erythematosus, in a large subgroup of patients with rheumatoid arthritis. *Arthritis Rheum*. 58:1264-1274.

Dodge, G.R., I. Kovalszky, J.R. Hassell, and R.V. Iozzo. 1990. Transforming growth factor beta alters the expression of heparan sulfate proteoglycan in human colon carcinoma cells. *J Biol Chem*. 265:18023-18029.

Dredge, K., T.V. Brennan, E. Hammond, J.D. Lickliter, L. Lin, D. Bampton, P. Handley, F. Lankesheer, G. Morrish, Y. Yang, M.P. Brown, and M. Millward. 2018. A Phase I study of the novel immunomodulatory agent PG545 (pixatimod) in subjects with advanced solid tumours. *Br J Cancer*. 118:1035-1041.

Dunay, I.R., R.A. Damatta, B. Fux, R. Presti, S. Greco, M. Colonna, and L.D. Sibley. 2008. Gr1(+) inflammatory monocytes are required for mucosal resistance to the pathogen Toxoplasma gondii. *Immunity*. 29:306-317.

Dyer, D.P. 2020. Understanding the mechanisms that facilitate specificity, not redundancy, of chemokine-mediated leukocyte recruitment. *Immunology*. 160:336-344.

Dyer, D.P., C.L. Salanga, B.F. Volkman, T. Kawamura, and T.M. Handel. 2016. The dependence of chemokine-glycosaminoglycan interactions on chemokine oligomerization. *Glycobiology*. 26:312-326.

Elkin, M., N. Ilan, R. Ishai-Michaeli, Y. Friedmann, O. Papo, I. Pecker, and I. Vlodavsky. 2001. Heparanase as mediator of angiogenesis: mode of action. *FASEB J*. 15:1661-1663.

Epelman, S., K.J. Lavine, and G.J. Randolph. 2014. Origin and functions of tissue macrophages. *Immunity*. 41:21-35.

Esko, J.D., and R.J. Linhardt. 2009. Proteins that Bind Sulfated Glycosaminoglycans. *In* Essentials of Glycobiology. nd, A. Varki, R.D. Cummings, J.D. Esko, H.H. Freeze, P. Stanley, C.R. Bertozzi, G.W. Hart, and M.E. Etzler, editors, Cold Spring Harbor (NY).

Esko, J.D., and S.B. Selleck. 2002. Order out of chaos: assembly of ligand binding sites in heparan sulfate. *Annu Rev Biochem*. 71:435-471.

Fang, F.C. 2004. Antimicrobial reactive oxygen and nitrogen species: concepts and controversies. *Nat Rev Microbiol*. 2:820-832.

Fantuzzi, L., P. Borghi, V. Ciolli, G. Pavlakis, F. Belardelli, and S. Gessani. 1999. Loss of CCR2 expression and functional response to monocyte chemotactic protein (MCP-1) during the differentiation of human monocytes: role of secreted MCP-1 in the regulation of the chemotactic response. *Blood*. 94:875-883.

Feehan, K.T., and D.W. Gilroy. 2019. Is Resolution the End of Inflammation? *Trends Mol Med*. 25:198-214.

Fellgett, S.W., R.J. Maguire, and M.E. Pownall. 2015. Sulf1 has ligand-dependent effects on canonical and non-canonical Wnt signalling. *J Cell Sci*. 128:1408-1421.

Ferreras, C., G. Rushton, C.L. Cole, M. Babur, B.A. Telfer, T.H. van Kuppevelt, J.M. Gardiner, K.J. Williams, G.C. Jayson, and E. Avizienyte. 2012. Endothelial heparan sulfate 6-O-sulfation levels regulate angiogenic responses of endothelial cells to fibroblast growth factor 2 and vascular endothelial growth factor. *J Biol Chem*. 287:36132-36146.

Feyzi, E., T. Saldeen, E. Larsson, U. Lindahl, and M. Salmivirta. 1998. Age-dependent modulation of heparan sulfate structure and function. *J Biol Chem*. 273:13395-13398.

Filippi, M.D. 2019. Neutrophil transendothelial migration: updates and new perspectives. *Blood*. 133:2149-2158.

Firestein, G.S., and I.B. McInnes. 2017. Immunopathogenesis of Rheumatoid Arthritis. *Immunity*. 46:183-196.

Ford-Perriss, M., S.E. Guimond, U. Greferath, M. Kita, K. Grobe, H. Habuchi, K. Kimata, J.D. Esko, M. Murphy, and J.E. Turnbull. 2002. Variant heparan sulfates synthesized in developing mouse brain differentially regulate FGF signaling. *Glycobiology*. 12:721-727.

Francis, D.J., C.R. Parish, M. McGarry, F.S. Santiago, H.C. Lowe, K.J. Brown, J.A. Bingley, I.P. Hayward, W.B. Cowden, J.H. Campbell, G.R. Campbell, C.N. Chesterman, and L.M. Khachigian. 2003. Blockade of vascular smooth muscle cell proliferation and intimal thickening after balloon injury by the sulfated oligosaccharide PI-88: phosphomannopentaose sulfate directly binds

FGF-2, blocks cellular signaling, and inhibits proliferation. *Circ Res*. 92:e70-77.

Franklin, B.S., M.S. Mangan, and E. Latz. 2016. Crystal Formation in Inflammation. *Annu Rev Immunol*. 34:173-202.

Freeman, S.A., and S. Grinstein. 2014. Phagocytosis: receptors, signal integration, and the cytoskeleton. *Immunol Rev*. 262:193-215.

Frevert, C.W., J. Felgenhauer, M. Wygrecka, M.V. Nastase, and L. Schaefer. 2018. Danger-Associated Molecular Patterns Derived From the Extracellular Matrix Provide Temporal Control of Innate Immunity. *J Histochem Cytochem*. 66:213-227.

Frevert, C.W., M.G. Kinsella, C. Vathanaprida, R.B. Goodman, D.G. Baskin, A. Proudfoot, T.N. Wells, T.N. Wight, and T.R. Martin. 2003. Binding of interleukin-8 to heparan sulfate and chondroitin sulfate in lung tissue. *Am J Respir Cell Mol Biol*. 28:464-472.

Fujiwara, N., and K. Kobayashi. 2005. Macrophages in inflammation. *Curr Drug Targets Inflamm Allergy*. 4:281-286.

Fukasawa, M., F. Sekine, M. Miura, M. Nishijima, and K. Hanada. 1997. Involvement of heparan sulfate proteoglycans in the binding step for phagocytosis of latex beads by Chinese hamster ovary cells. *Exp Cell Res*. 230:154-162.

Gallina, G., L. Dolcetti, P. Serafini, C. De Santo, I. Marigo, M.P. Colombo, G. Basso, F. Brombacher, I. Borrello, P. Zanovello, S. Bicciato, and V. Bronte. 2006. Tumors induce a subset of inflammatory monocytes with immunosuppressive activity on CD8+ T cells. *J Clin Invest*. 116:2777-2790.

Gangavarapu, P., L. Rajagopalan, D. Kolli, A. Guerrero-Plata, R.P. Garofalo, and K. Rajarathnam. 2012. The monomer-dimer equilibrium and glycosaminoglycan interactions of chemokine CXCL8 regulate tissue-specific neutrophil recruitment. *J Leukoc Biol*. 91:259-265.

Ghonim, M.A., J. Wang, S.V. Ibba, H.H. Luu, K. Pyakurel, I. Benslimane, S. Mousa, and A.H. Boulares. 2018. Sulfated non-anticoagulant heparin blocks Th2-induced asthma by modulating the IL-4/signal transducer and activator of transcription 6/Janus kinase 1 pathway. *J Transl Med*. 16:243.

Gitay-Goren, H., S. Soker, I. Vlodavsky, and G. Neufeld. 1992. The binding of vascular endothelial growth factor to its receptors is dependent on cell surface-associated heparin-like molecules. *J Biol Chem*. 267:6093-6098.

Giuffre, L., A.S. Cordey, N. Monai, Y. Tardy, M. Schapira, and O. Spertini. 1997. Monocyte adhesion to activated aortic endothelium: role of L-selectin and heparan sulfate proteoglycans. *J Cell Biol*. 136:945-956.

Goldberg, R., A. Meirovitz, N. Hirshoren, R. Bulvik, A. Binder, A.M. Rubinstein, and M. Elkin. 2013. Versatile role of heparanase in inflammation. *Matrix Biol*. 32:234-240.

Gordon, S. 2016. Phagocytosis: The Legacy of Metchnikoff. *Cell*. 166:1065-1068.

Gordts, P., E.M. Foley, R. Lawrence, R. Sinha, C. Lameda-Diaz, L. Deng, R. Nock, C.K. Glass, A. Erbilgin, A.J. Lusis, J.L. Witztum, and J.D. Esko. 2014. Reducing macrophage proteoglycan sulfation increases atherosclerosis and obesity through enhanced type I interferon signaling. *Cell Metab*. 20:813-826.

Graham, G.J., T.M. Handel, and A.E.I. Proudfoot. 2019. Leukocyte Adhesion: Reconceptualizing Chemokine Presentation by Glycosaminoglycans. *Trends Immunol*. 40:472-481.

Graham, G.J., P.C. Wilkinson, R.J. Nibbs, S. Lowe, S.O. Kolset, A. Parker, M.G. Freshney, M.L. Tsang, and I.B. Pragnell. 1996. Uncoupling of stem cell inhibition from monocyte chemoattraction in MIP-1alpha by mutagenesis of the proteoglycan binding site. *EMBO J*. 15:6506-6515.

Griffiths, H.R., D. Gao, and C. Pararasa. 2017. Redox regulation in metabolic programming and inflammation. *Redox Biol*. 12:50-57.

Gschwandtner, M., R. Derler, and K.S. Midwood. 2019. More Than Just Attractive: How CCL2 Influences Myeloid Cell Behavior Beyond Chemotaxis. *Front Immunol*. 10:2759.

Gschwandtner, M., A.M. Piccinini, T. Gerlza, T. Adage, and A.J. Kungl. 2016. Interfering with the CCL2-glycosaminoglycan axis as a potential approach to modulate neuroinflammation. *Neurosci Lett*. 626:164-173.

Gubbiotti, M.A., T. Neill, and R.V. Iozzo. 2017. A current view of perlecan in physiology and pathology: A mosaic of functions. *Matrix Biol*. 57-58:285-298.

Guilliams, M., I. De Kleer, S. Henri, S. Post, L. Vanhoutte, S. De Prijck, K. Deswarte, B. Malissen, H. Hammad, and B.N. Lambrecht. 2013. Alveolar macrophages develop from fetal monocytes that differentiate into long-lived cells in the first week of life via GM-CSF. *J Exp Med*. 210:1977-1992.

Guimond, S., M. Maccarana, B.B. Olwin, U. Lindahl, and A.C. Rapraeger. 1993. Activating and inhibitory heparin sequences for FGF-2 (basic FGF). Distinct requirements for FGF-1, FGF-2, and FGF-4. *J Biol Chem*. 268:23906-23914.

Habuchi, H., O. Habuchi, and K. Kimata. 1995. Purification and characterization of heparan sulfate 6-sulfotransferase from the culture medium of Chinese hamster ovary cells. *J Biol Chem*. 270:4172-4179.

Habuchi, H., and K. Kimata. 2010. Mice deficient in heparan sulfate 6-O-sulfotransferase-1. *Prog Mol Biol Transl Sci*. 93:79-111.

Habuchi, H., N. Nagai, N. Sugaya, F. Atsumi, R.L. Stevens, and K. Kimata. 2007. Mice deficient in heparan sulfate 6-O-sulfotransferase-1 exhibit defective heparan sulfate biosynthesis, abnormal placentation, and late embryonic lethality. *J Biol Chem*. 282:15578-15588.

Habuchi, H., M. Tanaka, O. Habuchi, K. Yoshida, H. Suzuki, K. Ban, and K. Kimata. 2000. The occurrence of three isoforms of heparan sulfate 6-O-sulfotransferase having different specificities for hexuronic acid adjacent to the targeted N-sulfoglucosamine. *J Biol Chem*. 275:2859-2868.

Hannoodee, S., and D.N. Nasuruddin. 2021. Acute Inflammatory Response. *In* StatPearls, Treasure Island (FL).

Hao, C., H. Xu, L. Yu, and L. Zhang. 2019. Heparin: An essential drug for modern medicine. *Prog Mol Biol Transl Sci*. 163:1-19.

Haschemi, A., P. Kosma, L. Gille, C.R. Evans, C.F. Burant, P. Starkl, B. Knapp, R. Haas, J.A. Schmid, C. Jandl, S. Amir, G. Lubec, J. Park, H. Esterbauer, M. Bilban, L. Brizuela, J.A. Pospisilik, L.E. Otterbein, and O. Wagner. 2012. The sedoheptulose kinase CARKL directs macrophage polarization through control of glucose metabolism. *Cell Metab*. 15:813-826.

Hashimoto, D., A. Chow, C. Noizat, P. Teo, M.B. Beasley, M. Leboeuf, C.D. Becker, P. See, J. Price, D. Lucas, M. Greter, A. Mortha, S.W. Boyer, E.C. Forsberg, M. Tanaka, N. van Rooijen, A. Garcia-Sastre, E.R. Stanley, F. Ginhoux, P.S. Frenette, and M. Merad. 2013. Tissue-resident macrophages self-maintain locally throughout adult life with minimal contribution from circulating monocytes. *Immunity*. 38:792-804.

Higuchi, H., T. Shoji, S. Iijima, and K. Nishijima. 2016. Constitutively expressed Siglec-9 inhibits LPS-induced CCR7, but enhances IL-4-induced CD200R expression in human macrophages. *Biosci Biotechnol Biochem*. 80:1141-1148.

Holmborn, K., J. Ledin, E. Smeds, I. Eriksson, M. Kusche-Gullberg, and L. Kjellen. 2004. Heparan sulfate synthesized by mouse embryonic stem cells deficient in NDST1 and NDST2 is 6-O-sulfated but contains no N-sulfate groups. *J Biol Chem*. 279:42355-42358.

Holscher, C., B. Arendse, A. Schwegmann, E. Myburgh, and F. Brombacher. 2006. Impairment of alternative macrophage activation delays cutaneous leishmaniasis in nonhealing BALB/c mice. *J Immunol*. 176:1115-1121.

Hoogewerf, A.J., G.S. Kuschert, A.E. Proudfoot, F. Borlat, I. Clark-Lewis, C.A. Power, and T.N. Wells. 1997. Glycosaminoglycans mediate cell surface oligomerization of chemokines. *Biochemistry*. 36:13570-13578.

Horsnell, W.G., and F. Brombacher. 2010. Genes associated with alternatively activated macrophages discretely regulate helminth infection and pathogenesis in experimental mouse models. *Immunobiology*. 215:704-708.

Hossain, M.M., T. Hosono-Fukao, R. Tang, N. Sugaya, T.H. van Kuppevelt, G.J. Jenniskens, K. Kimata, S.D. Rosen, and K. Uchimura. 2010. Direct detection of HSulf-1 and HSulf-2 activities on extracellular heparan sulfate and their inhibition by PI-88. *Glycobiology*. 20:175-186.

Huang, Z., Q. Luo, Y. Guo, J. Chen, G. Xiong, Y. Peng, J. Ye, and J. Li. 2015. Mycobacterium tuberculosis-Induced Polarization of Human Macrophage Orchestrates the Formation and Development of Tuberculous Granulomas In Vitro. *PLoS One*. 10:e0129744.

Hub, E., and A. Rot. 1998. Binding of RANTES, MCP-1, MCP-3, and MIP-1alpha to cells in human skin. *Am J Pathol*. 152:749-757.

Huntington, J.A., S.T. Olson, B. Fan, and P.G. Gettins. 1996. Mechanism of heparin activation of antithrombin. Evidence for reactive center loop preinsertion with expulsion upon heparin binding. *Biochemistry*. 35:8495-8503.

Huynh, M.B., J. Villares, J.E. Diaz, S. Christiaans, G. Carpentier, M.O. Ouidja, L. Sissoeff, R. Raisman-Vozari, and D. Papy-Garcia. 2012. Glycosaminoglycans from aged human hippocampus have altered capacities to regulate trophic factors activities but not Abeta42 peptide toxicity. *Neurobiol Aging*. 33:1005 e1011-1022.

Iniesta, V., J. Carcelen, I. Molano, P.M. Peixoto, E. Redondo, P. Parra, M. Mangas, I. Monroy, M.L. Campo, C.G. Nieto, and I. Corraliza. 2005. Arginase I induction during Leishmania major infection mediates the development of disease. *Infect Immun*. 73:6085-6090.

Irie, A., H. Habuchi, K. Kimata, and Y. Sanai. 2003. Heparan sulfate is required for bone morphogenetic protein-7 signaling. *Biochem Biophys Res Commun*. 308:858-865.

Ivetic, A., H.L. Hoskins Green, and S.J. Hart. 2019. L-selectin: A Major Regulator of Leukocyte Adhesion, Migration and Signaling. *Front Immunol*. 10:1068.

Izumikawa, T., and H. Kitagawa. 2010. Mice deficient in glucuronyltransferase-I. *Prog Mol Biol Transl Sci*. 93:19-34.

Izvolsky, K.I., J. Lu, G. Martin, K.H. Albrecht, and W.V. Cardoso. 2008. Systemic inactivation of Hs6st1 in mice is associated with late postnatal mortality without major defects in organogenesis. *Genesis*. 46:8-18.

Izvolsky, K.I., D. Shoykhet, Y. Yang, Q. Yu, M.A. Nugent, and W.V. Cardoso. 2003. Heparan sulfate-FGF10 interactions during lung morphogenesis. *Dev Biol*. 258:185-200.

Jackson, D.G., J.I. Bell, R. Dickinson, J. Timans, J. Shields, and N. Whittle. 1995. Proteoglycan forms of the lymphocyte homing receptor CD44 are alternatively spliced variants containing the v3 exon. *J Cell Biol*. 128:673-685.

Jaguin, M., N. Houlbert, O. Fardel, and V. Lecureur. 2013. Polarization profiles of human M-CSF-generated macrophages and comparison of M1-markers in classically activated macrophages from GM-CSF and M-CSF origin. *Cell Immunol*. 281:51-61.

Jakobsson, L., J. Kreuger, K. Holmborn, L. Lundin, I. Eriksson, L. Kjellen, and L. Claesson-Welsh. 2006. Heparan sulfate in trans potentiates VEGFR-mediated angiogenesis. *Dev Cell*. 10:625-634.

Jakubzick, C., E.L. Gautier, S.L. Gibbings, D.K. Sojka, A. Schlitzer, T.E. Johnson, S. Ivanov, Q. Duan, S. Bala, T. Condon, N. van Rooijen, J.R. Grainger, Y. Belkaid, A. Ma'ayan, D.W. Riches, W.M. Yokoyama, F. Ginhoux, P.M. Henson, and G.J. Randolph. 2013. Minimal differentiation of classical monocytes as they survey steady-state tissues and transport antigen to lymph nodes. *Immunity*. 39:599-610.

Janeway, C.A., Jr., and R. Medzhitov. 2002. Innate immune recognition. *Annu Rev Immunol*. 20:197-216.

Jarousse, N., D.L. Trujillo, S. Wilcox-Adelman, and L. Coscoy. 2011. Virally-induced upregulation of heparan sulfate on B cells via the action of type I IFN. *J Immunol*. 187:5540-5547.

Jayatilleke, K.M., and M.D. Hulett. 2020. Heparanase and the hallmarks of cancer. *J Transl Med*. 18:453.

Jemth, P., E. Smeds, A.T. Do, H. Habuchi, K. Kimata, U. Lindahl, and M. Kusche-Gullberg. 2003. Oligosaccharide library-based assessment of heparan sulfate 6-O-sulfotransferase substrate specificity. *J Biol Chem*. 278:24371-24376.

Jenniskens, G.J., T. Hafmans, J.H. Veerkamp, and T.H. van Kuppevelt. 2002. Spatiotemporal distribution of heparan sulfate epitopes during myogenesis and synaptogenesis: a study in developing mouse intercostal muscle. *Dev Dyn*. 225:70-79.

Jiao, X., P.C. Billings, M.P. O'Connell, F.S. Kaplan, E.M. Shore, and D.L. Glaser. 2007. Heparan sulfate proteoglycans (HSPGs) modulate BMP2 osteogenic bioactivity in C2C12 cells. *J Biol Chem*. 282:1080-1086.

Johnston, B., and E.C. Butcher. 2002. Chemokines in rapid leukocyte adhesion triggering and migration. *Semin Immunol*. 14:83-92.

Jones, M., L. Tussey, N. Athanasou, and D.G. Jackson. 2000. Heparan sulfate proteoglycan isoforms of the CD44 hyaluronan receptor induced in human inflammatory macrophages can function as paracrine regulators of fibroblast growth factor action. *J Biol Chem*. 275:7964-7974.

Josephson, K., N.J. Logsdon, and M.R. Walter. 2001. Crystal structure of the IL-10/IL-10R1 complex reveals a shared receptor binding site. *Immunity*. 15:35-46.

Juhas, U., M. Ryba-Stanislawowska, P. Szargiej, and J. Mysliwska. 2015. Different pathways of macrophage activation and polarization. *Postepy Hig Med Dosw (Online)*. 69:496-502.

Jung, D.B., M. Yun, E.O. Kim, J. Kim, B. Kim, J.H. Jung, E. Wang, D. Mukhopadhyay, E. Hammond, K. Dredge, V. Shridhar, and S.H. Kim. 2015. The heparan sulfate mimetic PG545 interferes with Wnt/beta-catenin signaling and significantly suppresses pancreatic tumorigenesis alone and in combination with gemcitabine. *Oncotarget*. 6:4992-5004.

Jury, E.C., J. Eldridge, D.A. Isenberg, and P.S. Kabouridis. 2007. Agrin signalling contributes to cell activation and is overexpressed in T lymphocytes from lupus patients. *J Immunol*. 179:7975-7983.

Jury, E.C., and P.S. Kabouridis. 2010. New role for Agrin in T cells and its potential importance in immune system regulation. *Arthritis Res Ther*. 12:205.

Kaplan, M., K.J. Williams, H. Mandel, and M. Aviram. 1998. Role of macrophage glycosaminoglycans in the cellular catabolism of oxidized LDL by macrophages. *Arterioscler Thromb Vasc Biol*. 18:542-553.

Kato, M., H. Wang, V. Kainulainen, M.L. Fitzgerald, S. Ledbetter, D.M. Ornitz, and M. Bernfield. 1998. Physiological degradation converts the soluble syndecan-1 ectodomain from an inhibitor to a potent activator of FGF-2. *Nat Med*. 4:691-697.

Katta, K., T. Imran, M. Busse-Wicher, M. Gronning, S. Czajkowski, and M. Kusche-Gullberg. 2015. Reduced Expression of EXTL2, a Member of the Exostosin (EXT) Family of Glycosyltransferases, in Human Embryonic Kidney 293 Cells Results in Longer Heparan Sulfate Chains. *J Biol Chem*. 290:13168-13177.

Khan, A.A., C. Bose, L.S. Yam, M.J. Soloski, and F. Rupp. 2001. Physiological regulation of the immunological synapse by agrin. *Science*. 292:1681-1686.

Kim, Y.G., N. Kamada, M.H. Shaw, N. Warner, G.Y. Chen, L. Franchi, and G. Nunez. 2011. The Nod2 sensor promotes intestinal pathogen eradication via

the chemokine CCL2-dependent recruitment of inflammatory monocytes. *Immunity*. 34:769-780.

Kimberley, F.C., L. van Bostelen, K. Cameron, G. Hardenberg, J.A. Marquart, M. Hahne, and J.P. Medema. 2009. The proteoglycan (heparan sulfate proteoglycan) binding domain of APRIL serves as a platform for ligand multimerization and cross-linking. *FASEB J*. 23:1584-1595.

Kitagawa, H., H. Shimakawa, and K. Sugahara. 1999. The tumor suppressor EXT-like gene EXTL2 encodes an alpha1, 4-N-acetylhexosaminyltransferase that transfers N-acetylgalactosamine and N-acetylglucosamine to the common glycosaminoglycan-protein linkage region. The key enzyme for the chain initiation of heparan sulfate. *J Biol Chem*. 274:13933-13937.

Kjellen, L., and U. Lindahl. 2018. Specificity of glycosaminoglycan-protein interactions. *Curr Opin Struct Biol*. 50:101-108.

Knox, S.M., and J.M. Whitelock. 2006. Perlecan: how does one molecule do so many things? *Cell Mol Life Sci*. 63:2435-2445.

Koenig, A., K. Norgard-Sumnicht, R. Linhardt, and A. Varki. 1998. Differential interactions of heparin and heparan sulfate glycosaminoglycans with the selectins. Implications for the use of unfractionated and low molecular weight heparins as therapeutic agents. *J Clin Invest*. 101:877-889.

Korkmaz, B., M.S. Horwitz, D.E. Jenne, and F. Gauthier. 2010. Neutrophil elastase, proteinase 3, and cathepsin G as therapeutic targets in human diseases. *Pharmacol Rev*. 62:726-759.

Krausgruber, T., K. Blazek, T. Smallie, S. Alzabin, H. Lockstone, N. Sahgal, T. Hussell, M. Feldmann, and I.A. Udalova. 2011. IRF5 promotes inflammatory macrophage polarization and TH1-TH17 responses. *Nat Immunol*. 12:231-238.

Krenn, E.C., I. Wille, B. Gesslbauer, M. Poteser, T.H. van Kuppevelt, and A.J. Kungl. 2008. Glycanogenomics: a qPCR-approach to investigate biological glycan function. *Biochem Biophys Res Commun*. 375:297-302.

Kreuger, J., and L. Kjellen. 2012. Heparan sulfate biosynthesis: regulation and variability. *J Histochem Cytochem*. 60:898-907.

Kudchadkar, R., R. Gonzalez, and K.D. Lewis. 2008. PI-88: a novel inhibitor of angiogenesis. *Expert Opin Investig Drugs*. 17:1769-1776.

Kumar, A., S. Das, A. Mandal, S. Verma, K. Abhishek, A. Kumar, V. Kumar, A.K. Ghosh, and P. Das. 2018a. Leishmania infection activates host mTOR for its survival by M2 macrophage polarization. *Parasite Immunol*. 40:e12586.

Kumar, H., T. Kawai, and S. Akira. 2011. Pathogen recognition by the innate immune system. *Int Rev Immunol*. 30:16-34.

Kumar, V., A. Kumar, S. Das, A. Kumar, K. Abhishek, S. Verma, A. Mandal, R.K. Singh, and P. Das. 2018b. Leishmania donovani Activates Hypoxia Inducible Factor-1alpha and miR-210 for Survival in Macrophages by Downregulation of NF-kappaB Mediated Pro-inflammatory Immune Response. *Front Microbiol*. 9:385.

Kuschert, G.S., A.J. Hoogewerf, A.E. Proudfoot, C.W. Chung, R.M. Cooke, R.E. Hubbard, T.N. Wells, and P.N. Sanderson. 1998. Identification of a glycosaminoglycan binding surface on human interleukin-8. *Biochemistry*. 37:11193-11201.

Lamanna, W.C., M.A. Frese, M. Balleininger, and T. Dierks. 2008. Sulf loss influences N-, 2-O-, and 6-O-sulfation of multiple heparan sulfate proteoglycans and modulates fibroblast growth factor signaling. *J Biol Chem*. 283:27724-27735.

Lambaerts, K., S.A. Wilcox-Adelman, and P. Zimmermann. 2009. The signaling mechanisms of syndecan heparan sulfate proteoglycans. *Curr Opin Cell Biol*. 21:662-669.

Lane, D.A., G. Kunz, R.J. Olds, and S.L. Thein. 1996. Molecular genetics of antithrombin deficiency. *Blood Rev*. 10:59-74.

Laurence, J.S., C. Blanpain, A. De Leener, M. Parmentier, and P.J. LiWang. 2001. Importance of basic residues and quaternary structure in the function of MIP-1 beta: CCR5 binding and cell surface sugar interactions. *Biochemistry*. 40:4990-4999.

Ledin, J., M. Ringvall, M. Thuveson, I. Eriksson, M. Wilen, M. Kusche-Gullberg, E. Forsberg, and L. Kjellen. 2006. Enzymatically active N-deacetylase/N-sulfotransferase-2 is present in liver but does not contribute to heparan sulfate N-sulfation. *J Biol Chem*. 281:35727-35734.

Ledin, J., W. Staatz, J.P. Li, M. Gotte, S. Selleck, L. Kjellen, and D. Spillmann. 2004. Heparan sulfate structure in mice with genetically modified heparan sulfate production. *J Biol Chem*. 279:42732-42741.

Lee, T.Y., J. Folkman, and K. Javaherian. 2010. HSPG-binding peptide corresponding to the exon 6a-encoded domain of VEGF inhibits tumor growth by blocking angiogenesis in murine model. *PLoS One*. 5:e9945.

Leonetti, M., A. Gadzinski, and G. Moine. 2010. Cell surface heparan sulfate proteoglycans influence MHC class II-restricted antigen presentation. *J Immunol*. 185:3847-3856.

Levy-Adam, F., S. Feld, V. Cohen-Kaplan, A. Shteingauz, M. Gross, G. Arvatz, I. Naroditsky, N. Ilan, I. Doweck, and I. Vlodavsky. 2010. Heparanase 2 interacts with heparan sulfate with high affinity and inhibits heparanase activity. *J Biol Chem*. 285:28010-28019.

Ley, K., C. Laudanna, M.I. Cybulsky, and S. Nourshargh. 2007. Getting to the site of inflammation: the leukocyte adhesion cascade updated. *Nat Rev Immunol*. 7:678-689.

Li, J., A. Hagner-McWhirter, L. Kjellen, J. Palgi, M. Jalkanen, and U. Lindahl. 1997. Biosynthesis of heparin/heparan sulfate. cDNA cloning and expression of D-glucuronyl C5-epimerase from bovine lung. *J Biol Chem*. 272:28158-28163.

Li, J.P., and M. Kusche-Gullberg. 2016. Heparan Sulfate: Biosynthesis, Structure, and Function. *Int Rev Cell Mol Biol*. 325:215-273.

Li, L., W.C. Xiong, and L. Mei. 2018. Neuromuscular Junction Formation, Aging, and Disorders. *Annu Rev Physiol*. 80:159-188.

Li, W., D.J. Johnson, C.T. Esmon, and J.A. Huntington. 2004. Structure of the antithrombin-thrombin-heparin ternary complex reveals the antithrombotic mechanism of heparin. *Nat Struct Mol Biol*. 11:857-862.

Libby, P. 2007. Inflammatory mechanisms: the molecular basis of inflammation and disease. *Nutr Rev*. 65:S140-146.

Lind, T., F. Tufaro, C. McCormick, U. Lindahl, and K. Lidholt. 1998. The putative tumor suppressors EXT1 and EXT2 are glycosyltransferases required for the biosynthesis of heparan sulfate. *J Biol Chem*. 273:26265-26268.

Lindahl, U., G. Backstrom, and L. Thunberg. 1983. The antithrombin-binding sequence in heparin. Identification of an essential 6-O-sulfate group. *J Biol Chem*. 258:9826-9830.

Locati, M., G. Curtale, and A. Mantovani. 2020. Diversity, Mechanisms, and Significance of Macrophage Plasticity. *Annu Rev Pathol*. 15:123-147.

Loke, P., M.G. Nair, J. Parkinson, D. Guiliano, M. Blaxter, and J.E. Allen. 2002. IL-4 dependent alternatively-activated macrophages have a distinctive in vivo gene expression phenotype. *BMC Immunol*. 3:7.

Lortat-Jacob, H., F. Baltzer, and J.A. Grimaud. 1996. Heparin decreases the blood clearance of interferon-gamma and increases its activity by limiting the processing of its carboxyl-terminal sequence. *J Biol Chem*. 271:16139-16143.

Lortat-Jacob, H., P. Garrone, J. Banchereau, and J.A. Grimaud. 1997. Human interleukin 4 is a glycosaminoglycan-binding protein. *Cytokine*. 9:101-105.

Lortat-Jacob, H., and J.A. Grimaud. 1991. Interferon-gamma binds to heparan sulfate by a cluster of amino acids located in the C-terminal part of the molecule. *FEBS Lett*. 280:152-154.

Lortat-Jacob, H., H.K. Kleinman, and J.A. Grimaud. 1991. High-affinity binding of interferon-gamma to a basement membrane complex (matrigel). *J Clin Invest*. 87:878-883.

Lortat-Jacob, H., J.E. Turnbull, and J.A. Grimaud. 1995. Molecular organization of the interferon gamma-binding domain in heparan sulphate. *Biochem J*. 310 (Pt 2):497-505.

Lowe-Krentz, L.J., and J.G. Joyce. 1991. Venous and aortic porcine endothelial cells cultured under standardized conditions synthesize heparan sulfate chains which differ in charge. *Anal Biochem*. 193:155-163.

Lu, J., L. Auduong, E.S. White, and X. Yue. 2014. Up-regulation of heparan sulfate 6-O-sulfation in idiopathic pulmonary fibrosis. *Am J Respir Cell Mol Biol*. 50:106-114.

Lucas, M., and T. Mazzone. 1996. Cell surface proteoglycans modulate net synthesis and secretion of macrophage apolipoprotein E. *J Biol Chem*. 271:13454-13460.

Lumeng, C.N., J.L. Bodzin, and A.R. Saltiel. 2007. Obesity induces a phenotypic switch in adipose tissue macrophage polarization. *J Clin Invest*. 117:175-184.

Maccarana, M., B. Casu, and U. Lindahl. 1993. Minimal sequence in heparin/heparan sulfate required for binding of basic fibroblast growth factor. *J Biol Chem*. 268:23898-23905.

Maccarana, M., Y. Sakura, A. Tawada, K. Yoshida, and U. Lindahl. 1996. Domain structure of heparan sulfates from bovine organs. *J Biol Chem*. 271:17804-17810.

MacMicking, J., Q.W. Xie, and C. Nathan. 1997. Nitric oxide and macrophage function. *Annu Rev Immunol*. 15:323-350.

Majumdar, R., M. Sixt, and C.A. Parent. 2014. New paradigms in the establishment and maintenance of gradients during directed cell migration. *Curr Opin Cell Biol*. 30:33-40.

Mantovani, A., A. Sica, S. Sozzani, P. Allavena, A. Vecchi, and M. Locati. 2004. The chemokine system in diverse forms of macrophage activation and polarization. *Trends Immunol*. 25:677-686.

Martinez, F.O., and S. Gordon. 2014. The M1 and M2 paradigm of macrophage activation: time for reassessment. *F1000Prime Rep*. 6:13.

Martinez, F.O., S. Gordon, M. Locati, and A. Mantovani. 2006. Transcriptional profiling of the human monocyte-to-macrophage differentiation and polarization: new molecules and patterns of gene expression. *J Immunol*. 177:7303-7311.

Martinez, F.O., A. Sica, A. Mantovani, and M. Locati. 2008. Macrophage activation and polarization. *Front Biosci*. 13:453-461.

Martinez, P., A. Denys, M. Delos, A.S. Sikora, M. Carpentier, S. Julien, J. Pestel, and F. Allain. 2015. Macrophage polarization alters the expression and sulfation pattern of glycosaminoglycans. *Glycobiology*. 25:502-513.

Mattila, J.T., O.O. Ojo, D. Kepka-Lenhart, S. Marino, J.H. Kim, S.Y. Eum, L.E. Via, C.E. Barry, 3rd, E. Klein, D.E. Kirschner, S.M. Morris, Jr., P.L. Lin, and J.L. Flynn. 2013. Microenvironments in tuberculous granulomas are delineated by

distinct populations of macrophage subsets and expression of nitric oxide synthase and arginase isoforms. *J Immunol*. 191:773-784.

Mazzon, C., A. Anselmo, C. Soldani, J. Cibella, C. Ploia, F. Moalli, S.J. Burden, M.L. Dustin, A. Sarukhan, and A. Viola. 2012. Agrin is required for survival and function of monocytic cells. *Blood*. 119:5502-5511.

McCormick, C., G. Duncan, K.T. Goutsos, and F. Tufaro. 2000. The putative tumor suppressors EXT1 and EXT2 form a stable complex that accumulates in the Golgi apparatus and catalyzes the synthesis of heparan sulfate. *Proc Natl Acad Sci U S A*. 97:668-673.

McNaughton, E.F., A.D. Eustace, S. King, R.B. Sessions, A. Kay, M. Farris, R. Broadbridge, O. Kehoe, A.J. Kungl, and J. Middleton. 2018. Novel Anti-Inflammatory Peptides Based on Chemokine-Glycosaminoglycan Interactions Reduce Leukocyte Migration and Disease Severity in a Model of Rheumatoid Arthritis. *J Immunol*. 200:3201-3217.

Medzhitov, R. 2008. Origin and physiological roles of inflammation. *Nature*. 454:428-435.

Melrose, J. 2020. Perlecan, a modular instructive proteoglycan with diverse functional properties. *Int J Biochem Cell Biol*. 128:105849.

Meyers, J.R., J. Planamento, P. Ebrom, N. Krulewitz, E. Wade, and M.E. Pownall. 2013. Sulf1 modulates BMP signaling and is required for somite morphogenesis and development of the horizontal myoseptum. *Dev Biol*. 378:107-121.

Mia, S., A. Warnecke, X.M. Zhang, V. Malmstrom, and R.A. Harris. 2014. An optimized protocol for human M2 macrophages using M-CSF and IL-4/IL-10/TGF-beta yields a dominant immunosuppressive phenotype. *Scand J Immunol*. 79:305-314.

Middleton, J., S. Neil, J. Wintle, I. Clark-Lewis, H. Moore, C. Lam, M. Auer, E. Hub, and A. Rot. 1997. Transcytosis and surface presentation of IL-8 by venular endothelial cells. *Cell*. 91:385-395.

Miller, R.L., A.B. Dykstra, W. Wei, C. Holsclaw, J.E. Turnbull, and J.A. Leary. 2016. Enrichment of Two Isomeric Heparin Oligosaccharides Exhibiting Different Affinities toward Monocyte Chemoattractant Protein-1. *Anal Chem*. 88:11551-11558.

Mills, C.D., K. Kincaid, J.M. Alt, M.J. Heilman, and A.M. Hill. 2000. M-1/M-2 macrophages and the Th1/Th2 paradigm. *J Immunol*. 164:6166-6173.

Mills, C.D., and K. Ley. 2014. M1 and M2 macrophages: the chicken and the egg of immunity. *J Innate Immun*. 6:716-726.

Mitroulis, I., V.I. Alexaki, I. Kourtzelis, A. Ziogas, G. Hajishengallis, and T. Chavakis. 2015. Leukocyte integrins: role in leukocyte recruitment and as therapeutic targets in inflammatory disease. *Pharmacol Ther*. 147:123-135.

Mochizuki, H., H. Futatsumori, E. Suzuki, and K. Kimata. 2020. A quantitative method to detect non-antithrombin-binding 3-O-sulfated units in heparan sulfate. *J Biol Chem*:100115.

Mohrs, M., K. Shinkai, K. Mohrs, and R.M. Locksley. 2001. Analysis of type 2 immunity in vivo with a bicistronic IL-4 reporter. *Immunity*. 15:303-311.

Monneau, Y., F. Arenzana-Seisdedos, and H. Lortat-Jacob. 2016. The sweet spot: how GAGs help chemokines guide migrating cells. *J Leukoc Biol*. 99:935-953.

Montaner, L.J., R.P. da Silva, J. Sun, S. Sutterwala, M. Hollinshead, D. Vaux, and S. Gordon. 1999. Type 1 and type 2 cytokine regulation of macrophage endocytosis: differential activation by IL-4/IL-13 as opposed to IFN-gamma or IL-10. *J Immunol*. 162:4606-4613.

Moore, K.L., K.D. Patel, R.E. Bruehl, F. Li, D.A. Johnson, H.S. Lichenstein, R.D. Cummings, D.F. Bainton, and R.P. McEver. 1995. P-selectin glycoprotein ligand-1 mediates rolling of human neutrophils on P-selectin. *J Cell Biol*. 128:661-671.

Morimoto-Tomita, M., K. Uchimura, Z. Werb, S. Hemmerich, and S.D. Rosen. 2002. Cloning and characterization of two extracellular heparin-degrading endosulfatases in mice and humans. *J Biol Chem*. 277:49175-49185.

Mosser, D.M., and J.P. Edwards. 2008. Exploring the full spectrum of macrophage activation. *Nat Rev Immunol*. 8:958-969.

Mulloy, B. 2019. The non-anticoagulant promise of heparin and its mimetics. *Curr Opin Pharmacol*. 46:50-54.

Munder, M., H. Schneider, C. Luckner, T. Giese, C.D. Langhans, J.M. Fuentes, P. Kropf, I. Mueller, A. Kolb, M. Modolell, and A.D. Ho. 2006. Suppression of T-cell functions by human granulocyte arginase. *Blood*. 108:1627-1634.

Murphy, K.J., C.L. Merry, M. Lyon, J.E. Thompson, I.S. Roberts, and J.T. Gallagher. 2004. A new model for the domain structure of heparan sulfate based on the novel specificity of K5 lyase. *J Biol Chem*. 279:27239-27245.

Murray, L.A., Q. Chen, M.S. Kramer, D.P. Hesson, R.L. Argentieri, X. Peng, M. Gulati, R.J. Homer, T. Russell, N. van Rooijen, J.A. Elias, C.M. Hogaboam, and E.L. Herzog. 2011. TGF-beta driven lung fibrosis is macrophage dependent and blocked by Serum amyloid P. *Int J Biochem Cell Biol*. 43:154-162.

Murray, P.J., and T.A. Wynn. 2011. Protective and pathogenic functions of macrophage subsets. *Nat Rev Immunol*. 11:723-737.

Nadanaka, S., and H. Kitagawa. 2018. Exostosin-like 2 regulates FGF2 signaling by controlling the endocytosis of FGF2. *Biochim Biophys Acta Gen Subj*. 1862:791-799.

Nagarajan, A., P. Malvi, and N. Wajapeyee. 2018. Heparan Sulfate and Heparan Sulfate Proteoglycans in Cancer Initiation and Progression. *Front Endocrinol (Lausanne)*. 9:483.

Nathan, C. 2002. Points of control in inflammation. *Nature*. 420:846-852.

Nathan, C., and A. Ding. 2010. Nonresolving inflammation. *Cell*. 140:871-882.

Ng, C.Y., J.M. Whitelock, H. Williams, H.N. Kim, H.J. Medbury, and M.S. Lord. 2021. Macrophages bind LDL using heparan sulfate and the perlecan protein core. *J Biol Chem*:100520.

Norrby, K. 2000. 2.5 kDa and 5.0 kDa heparin fragments specifically inhibit microvessel sprouting and network formation in VEGF165-mediated mammalian angiogenesis. *Int J Exp Pathol*. 81:191-198.

Ohto, T., H. Uchida, H. Yamazaki, K. Keino-Masu, A. Matsui, and M. Masu. 2002. Identification of a novel nonlysosomal sulphatase expressed in the floor plate, choroid plexus and cartilage. *Genes Cells*. 7:173-185.

Okada, M., S. Nadanaka, N. Shoji, J. Tamura, and H. Kitagawa. 2010. Biosynthesis of heparan sulfate in EXT1-deficient cells. *Biochem J*. 428:463-471.

Olson, S.T., I. Bjork, R. Sheffer, P.A. Craig, J.D. Shore, and J. Choay. 1992. Role of the antithrombin-binding pentasaccharide in heparin acceleration of antithrombin-proteinase reactions. Resolution of the antithrombin conformational change contribution to heparin rate enhancement. *J Biol Chem*. 267:12528-12538.

Ono, K., H. Hattori, S. Takeshita, A. Kurita, and M. Ishihara. 1999. Structural features in heparin that interact with VEGF165 and modulate its biological activity. *Glycobiology*. 9:705-711.

Ori, A., M.C. Wilkinson, and D.G. Fernig. 2011. A systems biology approach for the investigation of the heparin/heparan sulfate interactome. *J Biol Chem*. 286:19892-19904.

Ornitz, D.M., A. Yayon, J.G. Flanagan, C.M. Svahn, E. Levi, and P. Leder. 1992. Heparin is required for cell-free binding of basic fibroblast growth factor to a soluble receptor and for mitogenesis in whole cells. *Mol Cell Biol*. 12:240-247.

Paine-Saunders, S., B.L. Viviano, A.N. Economides, and S. Saunders. 2002. Heparan sulfate proteoglycans retain Noggin at the cell surface: a potential mechanism for shaping bone morphogenetic protein gradients. *J Biol Chem*. 277:2089-2096.

Papanas, N., C. Demetzos, N. Pippa, E. Maltezos, and N. Tentolouris. 2016. Efficacy of a New Heparan Sulfate Mimetic Dressing in the Healing of Foot and Lower Extremity Ulcerations in Type 2 Diabetes: A Case Series. *Int J Low Extrem Wounds*. 15:63-67.

Papoutsopoulou, S., M.D. Burkitt, F. Bergey, H. England, R. Hough, L. Schmidt, D.G. Spiller, M.H.R. White, P. Paszek, D.A. Jackson, V.A.P. Martins Dos Santos, G. Sellge, D.M. Pritchard, B.J. Campbell, W. Muller, and C.S. Probert. 2019. Macrophage-Specific NF-kappaB Activation Dynamics Can Segregate Inflammatory Bowel Disease Patients. *Front Immunol*. 10:2168.

Park, J.E., G.A. Keller, and N. Ferrara. 1993. The vascular endothelial growth factor (VEGF) isoforms: differential deposition into the subepithelial extracellular matrix and bioactivity of extracellular matrix-bound VEGF. *Mol Biol Cell*. 4:1317-1326.

Paschoa, A.F. 2016. Heparin: 100 years of pleiotropic effects. *J Thromb Thrombolysis*. 41:636-643.

Patel, V.N., K.M. Likar, S. Zisman-Rozen, S.N. Cowherd, K.S. Lassiter, I. Sher, E.A. Yates, J.E. Turnbull, D. Ron, and M.P. Hoffman. 2008. Specific heparan sulfate structures modulate FGF10-mediated submandibular gland epithelial morphogenesis and differentiation. *J Biol Chem*. 283:9308-9317.

Pearce, E.J., and A.S. MacDonald. 2002. The immunobiology of schistosomiasis. *Nat Rev Immunol*. 2:499-511.

Pellegrini, L., D.F. Burke, F. von Delft, B. Mulloy, and T.L. Blundell. 2000. Crystal structure of fibroblast growth factor receptor ectodomain bound to ligand and heparin. *Nature*. 407:1029-1034.

Piccinini, A.M., K. Knebl, A. Rek, G. Wildner, M. Diedrichs-Mohring, and A.J. Kungl. 2010. Rationally evolving MCP-1/CCL2 into a decoy protein with potent anti-inflammatory activity in vivo. *J Biol Chem*. 285:8782-8792.

Pichert, A., D. Schlorke, S. Franz, and J. Arnhold. 2012. Functional aspects of the interaction between interleukin-8 and sulfated glycosaminoglycans. *Biomatter*. 2:142-148.

Pillai-Kastoori, L., A.R. Schutz-Geschwender, and J.A. Harford. 2020. A systematic approach to quantitative Western blot analysis. *Anal Biochem*. 593:113608.

Pinhal, M.A., B. Smith, S. Olson, J. Aikawa, K. Kimata, and J.D. Esko. 2001. Enzyme interactions in heparan sulfate biosynthesis: uronosyl 5-epimerase and 2-O-sulfotransferase interact in vivo. *Proc Natl Acad Sci U S A*. 98:12984-12989.

Presto, J., M. Thuveson, P. Carlsson, M. Busse, M. Wilen, I. Eriksson, M. Kusche-Gullberg, and L. Kjellen. 2008. Heparan sulfate biosynthesis enzymes EXT1 and EXT2 affect NDST1 expression and heparan sulfate sulfation. *Proc Natl Acad Sci U S A*. 105:4751-4756.

Proudfoot, A.E., S. Fritchley, F. Borlat, J.P. Shaw, F. Vilbois, C. Zwahlen, A. Trkola, D. Marchant, P.R. Clapham, and T.N. Wells. 2001. The BBXB motif of RANTES is the principal site for heparin binding and controls receptor selectivity. *J Biol Chem*. 276:10620-10626.

Proudfoot, A.E., T.M. Handel, Z. Johnson, E.K. Lau, P. LiWang, I. Clark-Lewis, F. Borlat, T.N. Wells, and M.H. Kosco-Vilbois. 2003. Glycosaminoglycan binding and oligomerization are essential for the in vivo activity of certain chemokines. *Proc Natl Acad Sci U S A*. 100:1885-1890.

Pye, D.A., R.R. Vives, J.E. Turnbull, P. Hyde, and J.T. Gallagher. 1998. Heparan sulfate oligosaccharides require 6-O-sulfation for promotion of basic fibroblast growth factor mitogenic activity. *J Biol Chem*. 273:22936-22942.

Qian, B.Z., J. Li, H. Zhang, T. Kitamura, J. Zhang, L.R. Campion, E.A. Kaiser, L.A. Snyder, and J.W. Pollard. 2011. CCL2 recruits inflammatory monocytes to facilitate breast-tumour metastasis. *Nature*. 475:222-225.

Qin, L., I. Kufareva, L.G. Holden, C. Wang, Y. Zheng, C. Zhao, G. Fenalti, H. Wu, G.W. Han, V. Cherezov, R. Abagyan, R.C. Stevens, and T.M. Handel. 2015. Structural biology. Crystal structure of the chemokine receptor CXCR4 in complex with a viral chemokine. *Science*. 347:1117-1122.

Qiu, H., S. Shi, J. Yue, M. Xin, A.V. Nairn, L. Lin, X. Liu, G. Li, S.A. Archer-Hartmann, M. Dela Rosa, M. Galizzi, S. Wang, F. Zhang, P. Azadi, T.H. van Kuppevelt, W.V. Cardoso, K. Kimata, X. Ai, K.W. Moremen, J.D. Esko, R.J. Linhardt, and L. Wang. 2018. A mutant-cell library for systematic analysis of heparan sulfate structure-function relationships. *Nat Methods*. 15:889-899.

Qu, X., C. Carbe, C. Tao, A. Powers, R. Lawrence, T.H. van Kuppevelt, W.V. Cardoso, K. Grobe, J.D. Esko, and X. Zhang. 2011. Lacrimal gland development and Fgf10-Fgfr2b signaling are controlled by 2-O- and 6-O-sulfated heparan sulfate. *J Biol Chem*. 286:14435-14444.

Raman, K., and B. Kuberan. 2010. Chemical Tumor Biology of Heparan Sulfate Proteoglycans. *Curr Chem Biol*. 4:20-31.

Rapraeger, A.C., A. Krufka, and B.B. Olwin. 1991. Requirement of heparan sulfate for bFGF-mediated fibroblast growth and myoblast differentiation. *Science*. 252:1705-1708.

Rath, M., I. Muller, P. Kropf, E.I. Closs, and M. Munder. 2014. Metabolism via Arginase or Nitric Oxide Synthase: Two Competing Arginine Pathways in Macrophages. *Front Immunol*. 5:532.

Ratzka, A., S. Mundlos, and A. Vortkamp. 2010. Expression patterns of sulfatase genes in the developing mouse embryo. *Dev Dyn*. 239:1779-1788.

Rauch, J.N., J.J. Chen, A.W. Sorum, G.M. Miller, T. Sharf, S.K. See, L.C. Hsieh-Wilson, M. Kampmann, and K.S. Kosik. 2018. Tau Internalization is Regulated by 6-O Sulfation on Heparan Sulfate Proteoglycans (HSPGs). *Sci Rep*. 8:6382.

Reece, J.J., M.C. Siracusa, and A.L. Scott. 2006. Innate immune responses to lung-stage helminth infection induce alternatively activated alveolar macrophages. *Infect Immun*. 74:4970-4981.

Reijmers, R.M., R.W. Groen, A. Kuil, K. Weijer, F.C. Kimberley, J.P. Medema, T.H. van Kuppevelt, J.P. Li, M. Spaargaren, and S.T. Pals. 2011. Disruption of heparan sulfate proteoglycan conformation perturbs B-cell maturation and APRIL-mediated plasma cell survival. *Blood*. 117:6162-6171.

Rey-Giraud, F., M. Hafner, and C.H. Ries. 2012. In vitro generation of monocyte-derived macrophages under serum-free conditions improves their tumor promoting functions. *PLoS One*. 7:e42656.

Rider, C.C., and B. Mulloy. 2017. Heparin, Heparan Sulphate and the TGF-beta Cytokine Superfamily. *Molecules*. 22.

Ringvall, M., and L. Kjellen. 2010. Mice deficient in heparan sulfate N-deacetylase/N-sulfotransferase 1. *Prog Mol Biol Transl Sci*. 93:35-58.

Robben, P.M., M. LaRegina, W.A. Kuziel, and L.D. Sibley. 2005. Recruitment of Gr-1+ monocytes is essential for control of acute toxoplasmosis. *J Exp Med*. 201:1761-1769.

Rogers, K.J., B. Brunton, L. Mallinger, D. Bohan, K.M. Sevcik, J. Chen, N. Ruggio, and W. Maury. 2019. IL-4/IL-13 polarization of macrophages enhances Ebola virus glycoprotein-dependent infection. *PLoS Negl Trop Dis*. 13:e0007819.

Rops, A.L., C.W. Jacobs, P.C. Linssen, J.B. Boezeman, J.F. Lensen, T.J. Wijnhoven, L.P. van den Heuvel, T.H. van Kuppevelt, J. van der Vlag, and J.H. Berden. 2007. Heparan sulfate on activated glomerular endothelial cells and exogenous heparinoids influence the rolling and adhesion of leucocytes. *Nephrol Dial Transplant*. 22:1070-1077.

Rops, A.L., M.A. Loeven, J.J. van Gemst, I. Eversen, X.M. Van Wijk, H.B. Dijkman, T.H. van Kuppevelt, J.H. Berden, T.J. Rabelink, J.D. Esko, and J. van der Vlag. 2014. Modulation of heparan sulfate in the glomerular

endothelial glycocalyx decreases leukocyte influx during experimental glomerulonephritis. *Kidney Int*. 86:932-942.

Rot, A. 1992. Binding of neutrophil attractant/activation protein-1 (interleukin 8) to resident dermal cells. *Cytokine*. 4:347-352.

Rouet, V., Y. Hamma-Kourbali, E. Petit, P. Panagopoulou, P. Katsoris, D. Barritault, J.P. Caruelle, and J. Courty. 2005. A synthetic glycosaminoglycan mimetic binds vascular endothelial growth factor and modulates angiogenesis. *J Biol Chem*. 280:32792-32800.

Rueda, P., A. Richart, A. Recalde, P. Gasse, J. Vilar, C. Guerin, H. Lortat-Jacob, P. Vieira, F. Baleux, F. Chretien, F. Arenzana-Seisdedos, and J.S. Silvestre. 2012. Homeostatic and tissue reparation defaults in mice carrying selective genetic invalidation of CXCL12/proteoglycan interactions. *Circulation*. 126:1882-1895.

Ruppert, R., E. Hoffmann, and W. Sebald. 1996. Human bone morphogenetic protein 2 contains a heparin-binding site which modifies its biological activity. *Eur J Biochem*. 237:295-302.

Rusnati, M., D. Coltrini, P. Caccia, P. Dell'Era, G. Zoppetti, P. Oreste, B. Valsasina, and M. Presta. 1994. Distinct role of 2-O-, N-, and 6-O-sulfate groups of heparin in the formation of the ternary complex with basic fibroblast growth factor and soluble FGF receptor-1. *Biochem Biophys Res Commun*. 203:450-458.

Rydstrom, A., and M.J. Wick. 2007. Monocyte recruitment, activation, and function in the gut-associated lymphoid tissue during oral Salmonella infection. *J Immunol*. 178:5789-5801.

Sadir, R., E. Forest, and H. Lortat-Jacob. 1998. The heparan sulfate binding sequence of interferon-gamma increased the on rate of the interferon-gamma-interferon-gamma receptor complex formation. *J Biol Chem*. 273:10919-10925.

Saesen, E., S. Sarrazin, C. Laguri, R. Sadir, D. Maurin, A. Thomas, A. Imberty, and H. Lortat-Jacob. 2013. Insights into the mechanism by which interferon-gamma basic amino acid clusters mediate protein binding to heparan sulfate. *J Am Chem Soc*. 135:9384-9390.

Safaiyan, F., S.O. Kolset, K. Prydz, E. Gottfridsson, U. Lindahl, and M. Salmivirta. 1999. Selective effects of sodium chlorate treatment on the sulfation of heparan sulfate. *J Biol Chem*. 274:36267-36273.

Sakurai, D., H. Hase, Y. Kanno, H. Kojima, K. Okumura, and T. Kobata. 2007. TACI regulates IgA production by APRIL in collaboration with HSPG. *Blood*. 109:2961-2967.

Salanga, C.L., D.P. Dyer, J.G. Kiselar, S. Gupta, M.R. Chance, and T.M. Handel. 2014. Multiple glycosaminoglycan-binding epitopes of monocyte chemoattractant protein-3/CCL7 enable it to function as a non-oligomerizing chemokine. *J Biol Chem*. 289:14896-14912.

Salek-Ardakani, S., J.R. Arrand, D. Shaw, and M. Mackett. 2000. Heparin and heparan sulfate bind interleukin-10 and modulate its activity. *Blood*. 96:1879-1888.

Sarris, M., J.B. Masson, D. Maurin, L.M. Van der Aa, P. Boudinot, H. Lortat-Jacob, and P. Herbomel. 2012. Inflammatory chemokines direct and restrict leukocyte migration within live tissues as glycan-bound gradients. *Curr Biol*. 22:2375-2382.

Schebesta, M., P.L. Pfeffer, and M. Busslinger. 2002. Control of pre-BCR signaling by Pax5-dependent activation of the BLNK gene. *Immunity*. 17:473-485.

Schlessinger, J., A.N. Plotnikov, O.A. Ibrahimi, A.V. Eliseenkova, B.K. Yeh, A. Yayon, R.J. Linhardt, and M. Mohammadi. 2000. Crystal structure of a ternary FGF-FGFR-heparin complex reveals a dual role for heparin in FGFR binding and dimerization. *Mol Cell*. 6:743-750.

Schubert, K., L.E. Collins, P. Green, H. Nagase, and L. Troeberg. 2019. LRP1 Controls TNF Release via the TIMP-3/ADAM17 Axis in Endotoxin-Activated Macrophages. *J Immunol*. 202:1501-1509.

Schuksz, M., M.M. Fuster, J.R. Brown, B.E. Crawford, D.P. Ditto, R. Lawrence, C.A. Glass, L. Wang, Y. Tor, and J.D. Esko. 2008. Surfen, a small molecule antagonist of heparan sulfate. *Proc Natl Acad Sci U S A*. 105:13075-13080.

Schumann, K., T. Lammermann, M. Bruckner, D.F. Legler, J. Polleux, J.P. Spatz, G. Schuler, R. Forster, M.B. Lutz, L. Sorokin, and M. Sixt. 2010. Immobilized chemokine fields and soluble chemokine gradients cooperatively shape migration patterns of dendritic cells. *Immunity*. 32:703-713.

Seffouh, A., F. Milz, C. Przybylski, C. Laguri, A. Oosterhof, S. Bourcier, R. Sadir, E. Dutkowski, R. Daniel, T.H. van Kuppevelt, T. Dierks, H. Lortat-Jacob, and R.R. Vives. 2013. HSulf sulfatases catalyze processive and oriented 6-O-desulfation of heparan sulfate that differentially regulates fibroblast growth factor activity. *FASEB J*. 27:2431-2439.

Segarini, P.R., and S.M. Seyedin. 1988. The high molecular weight receptor to transforming growth factor-beta contains glycosaminoglycan chains. *J Biol Chem*. 263:8366-8370.

Shapouri-Moghaddam, A., S. Mohammadian, H. Vazini, M. Taghadosi, S.A. Esmaeili, F. Mardani, B. Seifi, A. Mohammadi, J.T. Afshari, and A. Sahebkar. 2018. Macrophage plasticity, polarization, and function in health and disease. *J Cell Physiol*. 233:6425-6440.

Sharma, B., and R.V. Iozzo. 1998. Transcriptional silencing of perlecan gene expression by interferon-gamma. *J Biol Chem*. 273:4642-4646.

Shi, C., and E.G. Pamer. 2011. Monocyte recruitment during infection and inflammation. *Nat Rev Immunol*. 11:762-774.

Shute, J.K., L. Calzetta, V. Cardaci, S. di Toro, C.P. Page, and M. Cazzola. 2018. Inhaled nebulised unfractionated heparin improves lung function in moderate to very severe COPD: A pilot study. *Pulm Pharmacol Ther*. 48:88-96.

Sikora, A.S., M. Delos, P. Martinez, M. Carpentier, F. Allain, and A. Denys. 2016. Regulation of the Expression of Heparan Sulfate 3-O-Sulfotransferase 3B (HS3ST3B) by Inflammatory Stimuli in Human Monocytes. *J Cell Biochem*. 117:1529-1542.

Sindrilaru, A., T. Peters, S. Wieschalka, C. Baican, A. Baican, H. Peter, A. Hainzl, S. Schatz, Y. Qi, A. Schlecht, J.M. Weiss, M. Wlaschek, C. Sunderkotter, and K. Scharffetter-Kochanek. 2011. An unrestrained proinflammatory M1 macrophage population induced by iron impairs wound healing in humans and mice. *J Clin Invest*. 121:985-997.

Smeds, E., H. Habuchi, A.T. Do, E. Hjertson, H. Grundberg, K. Kimata, U. Lindahl, and M. Kusche-Gullberg. 2003. Substrate specificities of mouse heparan sulphate glucosaminyl 6-O-sulphotransferases. *Biochem J*. 372:371-380.

Smith, C.W. 1993. Leukocyte-endothelial cell interactions. *Semin Hematol*. 30:45-53; discussion 54-45.

Spillmann, D., D. Witt, and U. Lindahl. 1998. Defining the interleukin-8-binding domain of heparan sulfate. *J Biol Chem*. 273:15487-15493.

Sponaas, A.M., A.P. Freitas do Rosario, C. Voisine, B. Mastelic, J. Thompson, S. Koernig, W. Jarra, L. Renia, M. Mauduit, A.J. Potocnik, and J. Langhorne. 2009. Migrating monocytes recruited to the spleen play an important role in control of blood stage malaria. *Blood*. 114:5522-5531.

Stoger, J.L., M.J. Gijbels, S. van der Velden, M. Manca, C.M. van der Loos, E.A. Biessen, M.J. Daemen, E. Lutgens, and M.P. de Winther. 2012. Distribution of macrophage polarization markers in human atherosclerosis. *Atherosclerosis*. 225:461-468.

Stoler-Barak, L., S. Barzilai, A. Zauberman, and R. Alon. 2014. Transendothelial migration of effector T cells across inflamed endothelial barriers does not require heparan sulfate proteoglycans. *Int Immunol*. 26:315-324.

Stuart, L.M., and R.A. Ezekowitz. 2005. Phagocytosis: elegant complexity. *Immunity*. 22:539-550.

Sugaya, N., H. Habuchi, N. Nagai, S. Ashikari-Hada, and K. Kimata. 2008. 6-O-sulfation of heparan sulfate differentially regulates various fibroblast growth factor-dependent signalings in culture. *J Biol Chem*. 283:10366-10376.

Swart, M., and L. Troeberg. 2019. Effect of Polarization and Chronic Inflammation on Macrophage Expression of Heparan Sulfate Proteoglycans and Biosynthesis Enzymes. *J Histochem Cytochem*. 67:9-27.

Sy, M.S., E. Schneeberger, R. McCluskey, M.I. Greene, R.D. Rosenberg, and B. Benacerraf. 1983. Inhibition of delayed-type hypersensitivity by heparin depleted of anticoagulant activity. *Cell Immunol*. 82:23-32.

Takeuchi, O., and S. Akira. 2010. Pattern recognition receptors and inflammation. *Cell*. 140:805-820.

Tandon, R., J.S. Sharp, F. Zhang, V.H. Pomin, N.M. Ashpole, D. Mitra, W. Jin, H. Liu, P. Sharma, and R.J. Linhardt. 2020. Effective Inhibition of SARS-CoV-2 Entry by Heparin and Enoxaparin Derivatives. *bioRxiv*.

Tanino, Y., M.Y. Chang, X. Wang, S.E. Gill, S. Skerrett, J.K. McGuire, S. Sato, T. Nikaido, T. Kojima, M. Munakata, S. Mongovin, W.C. Parks, T.R. Martin,

T.N. Wight, and C.W. Frevert. 2012. Syndecan-4 regulates early neutrophil migration and pulmonary inflammation in response to lipopolysaccharide. *Am J Respir Cell Mol Biol*. 47:196-202.

Thacker, B.E., D. Xu, R. Lawrence, and J.D. Esko. 2014. Heparan sulfate 3-O-sulfation: a rare modification in search of a function. *Matrix Biol*. 35:60-72.

Tong, M., B. Tuk, I.M. Hekking, M. Vermeij, D. Barritault, and J.W. van Neck. 2009. Stimulated neovascularization, inflammation resolution and collagen maturation in healing rat cutaneous wounds by a heparan sulfate glycosaminoglycan mimetic, OTR4120. *Wound Repair Regen*. 17:840-852.

Tong, M., B. Tuk, P. Shang, I.M. Hekking, E.M. Fijneman, M. Guijt, S.E. Hovius, and J.W. van Neck. 2012. Diabetes-impaired wound healing is improved by matrix therapy with heparan sulfate glycosaminoglycan mimetic OTR4120 in rats. *Diabetes*. 61:2633-2641.

Townley, R.A., and H.E. Bulow. 2011. Genetic analysis of the heparan modification network in Caenorhabditis elegans. *J Biol Chem*. 286:16824-16831.

Tran, T.H., X. Shi, J. Zaia, and X. Ai. 2012. Heparan sulfate 6-O-endosulfatases (Sulfs) coordinate the Wnt signaling pathways to regulate myoblast fusion during skeletal muscle regeneration. *J Biol Chem*. 287:32651-32664.

Trottein, F., L. Schaffer, S. Ivanov, C. Paget, C. Vendeville, A. Cazet, S. Groux-Degroote, S. Lee, M.A. Krzewinski-Recchi, C. Faveeuw, S.R. Head, P. Gosset, and P. Delannoy. 2009. Glycosyltransferase and sulfotransferase gene expression profiles in human monocytes, dendritic cells and macrophages. *Glycoconj J*. 26:1259-1274.

Tsou, C.L., W. Peters, Y. Si, S. Slaymaker, A.M. Aslanian, S.P. Weisberg, M. Mack, and I.F. Charo. 2007. Critical roles for CCR2 and MCP-3 in monocyte mobilization from bone marrow and recruitment to inflammatory sites. *J Clin Invest*. 117:902-909.

Turnbull, J.E., D.G. Fernig, Y. Ke, M.C. Wilkinson, and J.T. Gallagher. 1992. Identification of the basic fibroblast growth factor binding sequence in fibroblast heparan sulfate. *J Biol Chem*. 267:10337-10341.

Turnbull, J.E., and R.A. Field. 2007. Emerging glycomics technologies. *Nat Chem Biol*. 3:74-77.

Turpin, J., J.P. Hester, E.M. Hersh, and G. Lopez-Berestein. 1986. Centrifugal elutriation as a method for isolation of large numbers of functionally intact human peripheral blood monocytes. *J Clin Apher*. 3:111-118.

Uchimura, K., M. Morimoto-Tomita, A. Bistrup, J. Li, M. Lyon, J. Gallagher, Z. Werb, and S.D. Rosen. 2006. HSulf-2, an extracellular endoglucosamine-6-sulfatase, selectively mobilizes heparin-bound growth factors and chemokines: effects on VEGF, FGF-1, and SDF-1. *BMC Biochem*. 7:2.

Urban, J.F., Jr., N. Noben-Trauth, D.D. Donaldson, K.B. Madden, S.C. Morris, M. Collins, and F.D. Finkelman. 1998. IL-13, IL-4Ralpha, and Stat6 are required for the expulsion of the gastrointestinal nematode parasite Nippostrongylus brasiliensis. *Immunity*. 8:255-264.

van der Voort, R., R.M. Keehnen, E.A. Beuling, M. Spaargaren, and S.T. Pals. 2000. Regulation of cytokine signaling by B cell antigen receptor and CD40-controlled expression of heparan sulfate proteoglycans. *J Exp Med*. 192:1115-1124.

van der Voort, R., T.E. Taher, V.J. Wielenga, M. Spaargaren, R. Prevo, L. Smit, G. David, G. Hartmann, E. Gherardi, and S.T. Pals. 1999. Heparan sulfate-modified CD44 promotes hepatocyte growth factor/scatter factor-induced signal transduction through the receptor tyrosine kinase c-Met. *J Biol Chem*. 274:6499-6506.

Vanhaverbeke, C., J.P. Simorre, R. Sadir, P. Gans, and H. Lortat-Jacob. 2004. NMR characterization of the interaction between the C-terminal domain of interferon-gamma and heparin-derived oligosaccharides. *Biochem J*. 384:93-99.

Veldkamp, C.T., C. Seibert, F.C. Peterson, N.B. De la Cruz, J.C. Haugner, 3rd, H. Basnet, T.P. Sakmar, and B.F. Volkman. 2008. Structural basis of CXCR4 sulfotyrosine recognition by the chemokine SDF-1/CXCL12. *Sci Signal*. 1:ra4.

Vidal, B., A.L. Serrano, M. Tjwa, M. Suelves, E. Ardite, R. De Mori, B. Baeza-Raja, M. Martinez de Lagran, P. Lafuste, V. Ruiz-Bonilla, M. Jardi, R. Gherardi, C. Christov, M. Dierssen, P. Carmeliet, J.L. Degen, M. Dewerchin, and P. Munoz-Canoves. 2008. Fibrinogen drives dystrophic muscle fibrosis via a TGFbeta/alternative macrophage activation pathway. *Genes Dev*. 22:1747-1752.

Viviano, B.L., S. Paine-Saunders, N. Gasiunas, J. Gallagher, and S. Saunders. 2004. Domain-specific modification of heparan sulfate by Qsulf1 modulates the binding of the bone morphogenetic protein antagonist Noggin. *J Biol Chem*. 279:5604-5611.

Viviano, B.L., L. Silverstein, C. Pflederer, S. Paine-Saunders, K. Mills, and S. Saunders. 2005. Altered hematopoiesis in glypican-3-deficient mice results in decreased osteoclast differentiation and a delay in endochondral ossification. *Dev Biol*. 282:152-162.

Vlodavsky, I., A. Eldor, A. Haimovitz-Friedman, Y. Matzner, R. Ishai-Michaeli, O. Lider, Y. Naparstek, I.R. Cohen, and Z. Fuks. 1992. Expression of heparanase by platelets and circulating cells of the immune system: possible involvement in diapedesis and extravasation. *Invasion Metastasis*. 12:112-127.

Vlodavsky, I., M. Elkin, O. Pappo, H. Aingorn, R. Atzmon, R. Ishai-Michaeli, A. Aviv, I. Pecker, and Y. Friedmann. 2000. Mammalian heparanase as mediator of tumor metastasis and angiogenesis. *Isr Med Assoc J*. 2 Suppl:37-45.

Vreys, V., and G. David. 2007. Mammalian heparanase: what is the message? *J Cell Mol Med*. 11:427-452.

Vuong, T.T., T.M. Reine, A. Sudworth, T.G. Jenssen, and S.O. Kolset. 2015. Syndecan-4 is a major syndecan in primary human endothelial cells in vitro, modulated by inflammatory stimuli and involved in wound healing. *J Histochem Cytochem*. 63:280-292.

Walter, M.R., W.T. Windsor, T.L. Nagabhushan, D.J. Lundell, C.A. Lunn, P.J. Zauodny, and S.K. Narula. 1995. Crystal structure of a complex between interferon-gamma and its soluble high-affinity receptor. *Nature*. 376:230-235.

Wang, C., S. Poon, S. Murali, C.Y. Koo, T.J. Bell, S.F. Hinkley, H. Yeong, K. Bhakoo, V. Nurcombe, and S.M. Cool. 2014. Engineering a vascular endothelial growth factor 165-binding heparan sulfate for vascular therapy. *Biomaterials*. 35:6776-6786.

Wang, L., J.R. Brown, A. Varki, and J.D. Esko. 2002. Heparin's anti-inflammatory effects require glucosamine 6-O-sulfation and are mediated by blockade of L- and P-selectins. *J Clin Invest*. 110:127-136.

Wang, L., M. Fuster, P. Sriramarao, and J.D. Esko. 2005. Endothelial heparan sulfate deficiency impairs L-selectin- and chemokine-mediated neutrophil trafficking during inflammatory responses. *Nat Immunol*. 6:902-910.

Warwick, C.A., and Y.M. Usachev. 2017. Culture, Transfection, and Immunocytochemical Analysis of Primary Macrophages. *Methods Mol Biol*. 1554:161-173.

Weber, M., R. Hauschild, J. Schwarz, C. Moussion, I. de Vries, D.F. Legler, S.A. Luther, T. Bollenbach, and M. Sixt. 2013. Interstitial dendritic cell guidance by haptotactic chemokine gradients. *Science*. 339:328-332.

Wegrowski, Y., A.L. Milard, G. Kotlarz, E. Toulmonde, F.X. Maquart, and J. Bernard. 2006. Cell surface proteoglycan expression during maturation of human monocytes-derived dendritic cells and macrophages. *Clin Exp Immunol*. 144:485-493.

Wilkinson, T., R. Dixon, C. Page, M. Carroll, G. Griffiths, L.P. Ho, A. De Soyza, T. Felton, K.E. Lewis, K. Phekoo, J.D. Chalmers, A. Gordon, L. McGarvey, J. Doherty, R.C. Read, M. Shankar-Hari, N. Martinez-Alier, M. O'Kelly, G. Duncan, R. Walles, J. Sykes, C. Summers, D. Singh, and A. Collaborators. 2020. ACCORD: A Multicentre, Seamless, Phase 2 Adaptive Randomisation Platform Study to Assess the Efficacy and Safety of Multiple Candidate Agents for the Treatment of COVID-19 in Hospitalised Patients: A structured summary of a study protocol for a randomised controlled trial. *Trials*. 21:691.

Xian, X., S. Gopal, and J.R. Couchman. 2010. Syndecans as receptors and organizers of the extracellular matrix. *Cell Tissue Res*. 339:31-46.

Xu, D., and J.D. Esko. 2014. Demystifying heparan sulfate-protein interactions. *Annu Rev Biochem*. 83:129-157.

Xue, J., S.V. Schmidt, J. Sander, A. Draffehn, W. Krebs, I. Quester, D. De Nardo, T.D. Gohel, M. Emde, L. Schmidleithner, H. Ganesan, A. Nino-Castro, M.R. Mallmann, L. Labzin, H. Theis, M. Kraut, M. Beyer, E. Latz, T.C. Freeman, T. Ulas, and J.L. Schultze. 2014. Transcriptome-based network analysis reveals a spectrum model of human macrophage activation. *Immunity*. 40:274-288.

Yan, D., and X. Lin. 2009. Shaping morphogen gradients by proteoglycans. *Cold Spring Harb Perspect Biol*. 1:a002493.

Yang, C.Y., L. Troeberg, and S.D. Scilabra. 2020. Quantitative Mass Spectrometry-Based Secretome Analysis as a Tool to Investigate Metalloprotease and TIMP Activity. *Methods Mol Biol*. 2043:265-273.

Yayon, A., M. Klagsbrun, J.D. Esko, P. Leder, and D.M. Ornitz. 1991. Cell surface, heparin-like molecules are required for binding of basic fibroblast growth factor to its high affinity receptor. *Cell*. 64:841-848.

Yoon, P., K.T. Keylock, M.E. Hartman, G.G. Freund, and J.A. Woods. 2004. Macrophage hypo-responsiveness to interferon-gamma in aged mice is associated with impaired signaling through Jak-STAT. *Mech Ageing Dev*. 125:137-143.

Yu, M., T. Zhang, W. Zhang, Q. Sun, H. Li, and J.P. Li. 2020. Elucidating the Interactions Between Heparin/Heparan Sulfate and SARS-CoV-2-Related Proteins-An Important Strategy for Developing Novel Therapeutics for the COVID-19 Pandemic. *Front Mol Biosci*. 7:628551.

Yue, X., X. Li, H.T. Nguyen, D.R. Chin, D.E. Sullivan, and J.A. Lasky. 2008. Transforming growth factor-beta1 induces heparan sulfate 6-O-endosulfatase 1 expression in vitro and in vivo. *J Biol Chem*. 283:20397-20407.

Zak, B.M., B.E. Crawford, and J.D. Esko. 2002. Hereditary multiple exostoses and heparan sulfate polymerization. *Biochim Biophys Acta*. 1573:346-355.

Zhang, B., G. Yao, Y. Zhang, J. Gao, B. Yang, Z. Rao, and J. Gao. 2011. M2-polarized tumor-associated macrophages are associated with poor prognoses resulting from accelerated lymphangiogenesis in lung adenocarcinoma. *Clinics (Sao Paulo)*. 66:1879-1886.

Zhao, A., J.F. Urban, Jr., R.M. Anthony, R. Sun, J. Stiltz, N. van Rooijen, T.A. Wynn, W.C. Gause, and T. Shea-Donohue. 2008. Th2 cytokine-induced alterations in intestinal smooth muscle function depend on alternatively activated macrophages. *Gastroenterology*. 135:217-225 e211.

Zheng, X., X. Gai, S. Han, C.D. Moser, C. Hu, A.M. Shire, R.A. Floyd, and L.R. Roberts. 2013. The human sulfatase 2 inhibitor 2,4-disulfonylphenyl-tert-butylnitrone (OKN-007) has an antitumor effect in hepatocellular carcinoma mediated via suppression of TGFB1/SMAD2 and Hedgehog/GLI1 signaling. *Genes Chromosomes Cancer*. 52:225-236.

Zhou, D., C. Huang, Z. Lin, S. Zhan, L. Kong, C. Fang, and J. Li. 2014. Macrophage polarization and function with emphasis on the evolving roles of coordinated regulation of cellular signaling pathways. *Cell Signal*. 26:192-197.

Zhu, H., L. Duchesne, P.S. Rudland, and D.G. Fernig. 2010. The heparan sulfate co-receptor and the concentration of fibroblast growth factor-2 independently elicit different signalling patterns from the fibroblast growth factor receptor. *Cell Commun Signal*. 8:14.

Zhu, L., Q. Zhao, T. Yang, W. Ding, and Y. Zhao. 2015. Cellular metabolism and macrophage functional polarization. *Int Rev Immunol*. 34:82-100.

Zindel, J., and P. Kubes. 2020. DAMPs, PAMPs, and LAMPs in Immunity and Sterile Inflammation. *Annu Rev Pathol*. 15:493-518.

DOI: 10.1002/JLB.3RU0618-246R

JLB JOURNAL OF LEUKOCYTE BIOLOGY

REVIEW

Heparan sulfate as a regulator of inflammation and immunity

Laura E. Collins | **Linda Troeberg**

Nuffield Department of Orthopaedics, Rheumatology and Musculoskeletal Sciences, Kennedy Institute of Rheumatology, University of Oxford, Oxford, UK

Correspondence
Laura E. Collins, University of Oxford, Oxford, UK.
Email: laura.collins@lincoln.ox.ac.uk

Abstract

Heparan sulfate is found on the surface of most cell types, as well as in basement membranes and extracellular matrices. Its strong anionic properties and highly variable structure enable this glycosaminoglycan to provide binding sites for numerous protein ligands, including many soluble mediators of the immune system, and may promote or inhibit their activity. The formation of ligand binding sites on heparan sulfate (HS) occurs in a tissue- and context-specific fashion through the action of several families of enzymes, most of which have multiple isoforms with subtly different specificities. Changes in the expression levels of these biosynthetic enzymes occur in response to inflammatory stimuli, resulting in structurally different HS and acquisition or loss of binding sites for immune mediators. In this review, we discuss the multiple roles for HS in regulating immune responses, and the evidence for inflammation-associated changes to HS structure.

KEYWORDS
chemokines, cytokines, heparan sulfate, inflammation, leukocyte

1 | INTRODUCTION

Heparan sulfate (HS) is a ubiquitous but highly structurally variable polysaccharide found on cell surfaces and in extracellular matrices (ECMs), conjugated to one of several types of core protein. Due to its strong anionic properties and the numerous possible combinations of modifications, HS can bind to over 400 soluble protein mediators and cell-surface receptors,[1] with disparate effects on their activity.

HS plays well-established roles in the formation of chemokine gradients on the vascular endothelium and in regulating the activity of chemokines, cytokines, and growth factors through physical sequestration in the matrix and protection from enzymatic proteolysis (recently reviewed in Ref. 2). Here, we briefly outline our current knowledge of the role of HS in these processes, then discuss other currently less appreciated roles for HS in immune regulation, including direct signaling through TLR4, involvement in phagocytosis, and regulating the interaction of inflammatory mediators with their receptors. HS additionally functions in self versus non-self discrimination by the innate immune system through its role as a regulator of the alternative pathway of complement activation, which is reviewed in a number of excellent publications.[3–5] Here again, it is the structural variability of HS that enables it to perform various functions in a tissue- and context-specific manner, acting either as an inhibitor of the complement cascade through binding factor H on self surfaces and thus accelerating C3b inactivation, or as an activator through binding the stabilizing factor properdin on apoptotic cells.

HS is found covalently attached to one of several types of core protein, thus forming proteoglycans. The two most abundant types of cell-surface HS core protein are the trans-membrane syndecans and the GPI-anchored glypicans, but others such as the secreted proteins perlecan and agrin are also decorated with HS. In addition, some proteins, such as isoform 3 of the hylaruonan receptor (CD44), and betaglycan (TGFβR3) are "part-time HSPGs" in that they bear HS chains in certain tissues or under certain conditions. HS biosynthesis occurs in the Golgi network via the combined actions of more than 25 enzymes, which has been recently and comprehensively reviewed.[6] Briefly, biosynthesis begins with the assembly of a tetrasaccharide linkage region at glycosaminoglycan (GAG) attachment sites on the core protein, then the linear HS polysaccharide backbone is elongated by the sequential addition of alternating glucuronic acid and N-acetylglycosamine residues, catalyzed by enzymes of the exostosin (EXT) family. Concurrently, HS chains undergo extensive enzymatic modification beginning with N-de-acetylation/N-sulfation, and epimerization of some glucuronic acid residues to iduronic acid by the D-glycuronyl C5-epimerase (GLCE). Sequence complexity is further increased by sulfation at various

Abbreviations: A1AT, alpha-1 anti-trypsin; APC, antigen-presenting cell; DAMP, damage-associated molecular pattern; DC, dendritic cell; ECM, extracellular matrix; EXT, exostosin; EXTL, exostosin-like; FGF-2, fibroblast growth factor 2; GAG, glycosaminoglycan; HEV, high endothelial venule; HS, heparan sulfate; HS2S, heparan sulfate 2-O-sulfotransferase; HS3ST, heparan sulfate 3-O-sulfotransferase; HS6ST, heparan sulfate 6-O-sulfotransferase; HSPG, heparan sulfate proteoglycan; NDST, N-deacetylase/N-sulfotransferase; PMN, polymorphonuclear neutrophil; SLE, systemic lupus erythratomatus; TGFβR3, transforming growth factor beta receptor 3; WT, wild-type.

Received: 29 June 2018 | Revised: 30 September 2018 | Accepted: 1 October 2018

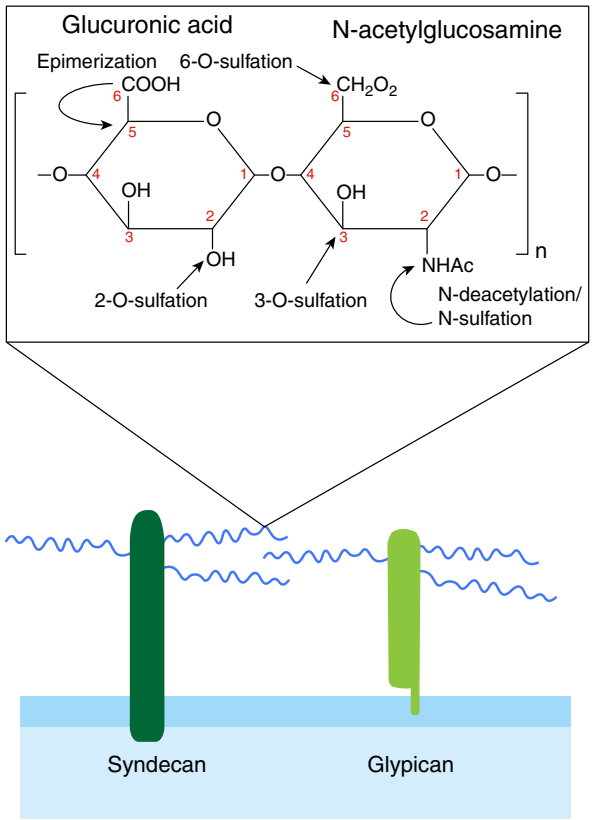

FIGURE 1 Heparan sulfate chains are extensively modified. Biosynthesis of heparan sulfate begins by attachment of a tetrasaccharide linkage region to the core protein (e.g., syndecan and glypican) and elongation of the polysaccharide backbone by alternate additions of glucuronic acid and N-acetylglucosamine residues by the EXT and EXTL enzymes. This is followed by N-deacetylation and N-sulfation of N-acetylglucosamine residues by the NDST enzymes, and epimerization of some glucuronic acid residues to iduronic acid by the D-glucuronyl C5-epimerase GLCE. Sulfotransferase enzymes (HS2ST, HS3STs, and HS6STs) then add sulfate groups at the 2-O-, 3-O-, and 6-O- positions of the sugar ring

positions by 2-O-, 3-O-, and 6-O-sulfotransferases that act in a template-independent manner, producing a varied and heterogeneous structure (Fig. 1). The requirement for previous modifications to form the substrate for subsequent reactions results in highly sulfated domains flanked by less sulfated transition zones, separated by regions of little or no modification.

How HS structure is regulated is poorly understood, but as most of the modifying enzymes have multiple isoforms with different substrate specificities,[7] it is thought that cells may regulate the structure of their HS by altering the relative expression levels of the modifying enzymes.[8]

2 | HS IN THE MICROENVIRONMENT REGULATES THE ACTIVITIES OF IMMUNE CELLS

HS is an important component of basement membranes and the ECM, where it immobilizes a variety of ligands. This can have a range of functional consequences including local retention, regulation of receptor interactions, and protection from the actions of proteases, as discussed below and illustrated in Fig. 2. In addition, HS can itself be a ligand for certain receptors involved in leukocyte recruitment to inflammatory sites.

2.1 | HS immobilizes chemokines on vascular and lymphatic endothelium

Circulating blood leukocytes such as monocytes and neutrophils are stimulated to crawl along the endothelium towards inflammatory sites by an immobilized gradient of chemokines, a process called haptotaxis or chemotaxis. More than 40 chemokines have been identified, all of which have been shown or are predicted to bind heparin or HS.[1] It is thought that a major role of endothelial HS is to form a concentration gradient that directs the migration of leukocytes by immobilizing chemokines and preventing them being washed away by the blood flow (Fig. 2). This hypothesis is supported by observations that mutant chemokines lacking the ability to bind HS fail to recruit leukocytes in vitro and in vivo.[9–11] Moreover, heparanase-overexpressing mice, which have very short HS chains, show impaired neutrophil crawling in response to wild-type (WT) chemokines,[12] further demonstrating the importance of the chemokine–GAG interaction.

It has also been observed that many chemokines oligomerize on HS and that the ability to form oligomers is required to achieve maximal local concentrations.[13] Oligomerization, as well as ability to bind HS, appears to be critical for the activity of certain chemokines, as monomeric mutants of RANTES, MIP-1β and MCP-1 have severely reduced chemotactic activity in vivo when injected IP into mice despite unchanged affinity for their receptors.[10]

The variation of HS structure in different tissues may be relevant to chemokine binding; for example, the HS from aortic and venous endothelial cells differs in degree of sulfation[14] which results in the formation of binding sites for chemokines only at post-capillary venules and small veins, where leukocyte emigration occurs, and not in capillaries and arteries.[15,16] Chemokine binding to HS also has some tissue specificity, as demonstrated by the retention of IL-8 in the lungs but not the skin.[13] These findings suggest that HS-mediated control of chemokine binding might determine to which sites leukocytes are recruited. Furthermore, it is possible that dynamic regulation of HS during inflammation modulates chemokine gradients and thus chemotaxis. In support of this, staining for HS in high endothelial venules (HEVs) of the lymph node revealed more HS on the basolateral side than the luminal side, and increased deposition of HS on only the basolateral side after stimulation with Total Freund's Adjuvant.[17] Thus HS may facilitate formation of a trans-epithelial chemokine gradient that becomes more pronounced during inflammation.

2.2 | Endothelial HS as a ligand for leukocyte selectins

In addition to their role in the presentation of chemokines, HS proteoglycans are more directly involved in leukocyte recruitment through their capacity to act as ligands for selectins (Fig. 2), thus

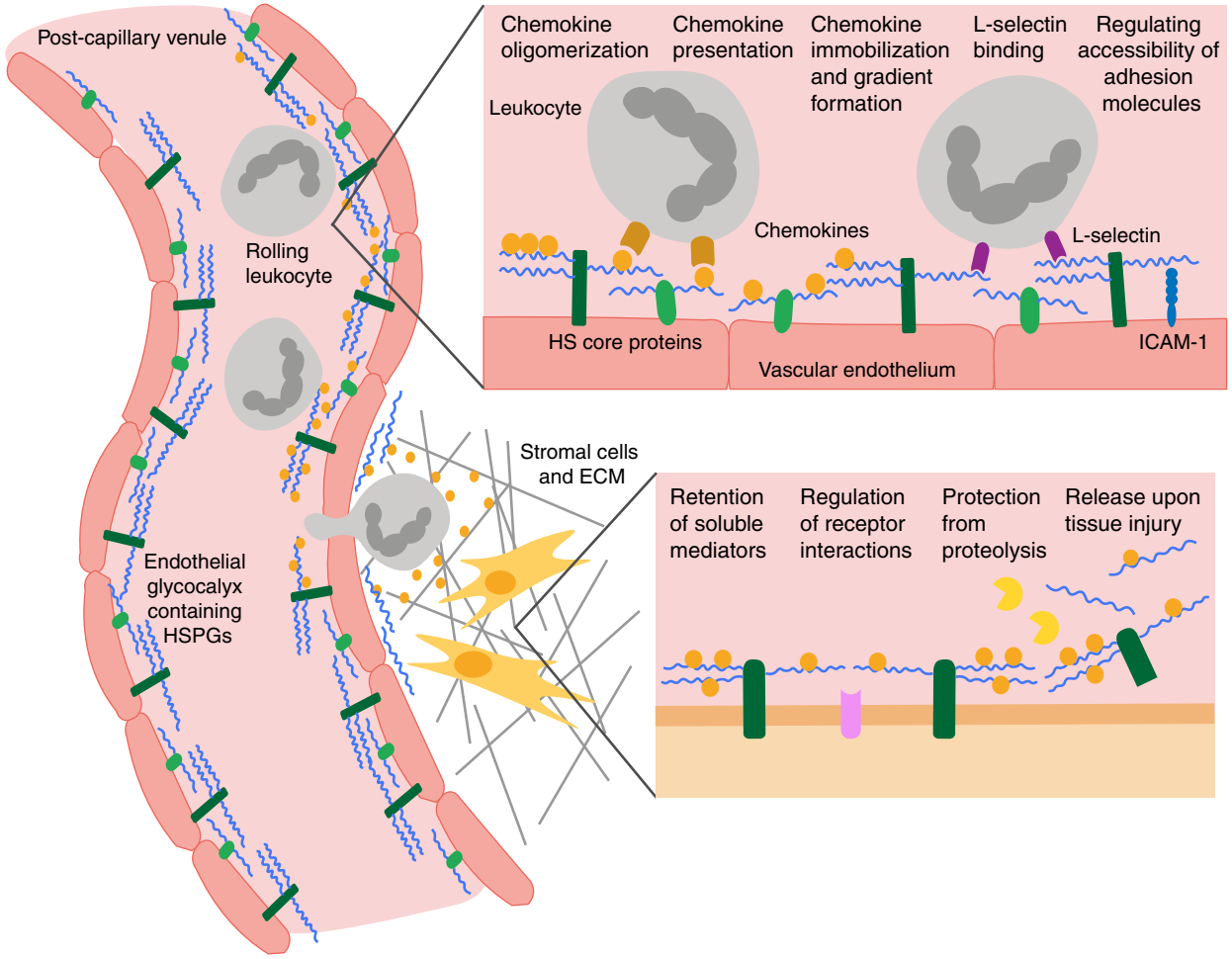

FIGURE 2 **Heparan sulfate plays several roles in local acute inflammation**. HS on the vascular endothelium binds chemokines and thus facilitates their oligomerization and presentation to circulating leukocytes, prevents them being washed away by the blood flow, and forms the chemokine gradient necessary for directional migration of leukocytes. Endothelial HS may also directly regulate the recruitment of leukocytes by acting as a ligand for leukocyte L-selectin, or by masking other adhesion molecules on the vascular endothelium to make them less accessible to leukocyte integrins. HS also functions in the extracellular matrix (ECM) to retain cytokines and growth factors. This interaction with HS can regulate local signaling by promoting or inhibiting receptor–ligand interactions, and can protect cytokines from inactivation by proteases. The core protein of the HSPG can be cleaved by the proteases released during an inflammatory response to release the ectodomain and its HS chains from the cell surface. Heparanase can digest the HS chains to release small active fragments that can act as danger-associated molecular patterns (DAMPs), or continue to regulate the activity of HS-bound cytokines through acting as a coreceptor (promotes signaling) or a decoy receptor (inhibits signaling)

facilitating leukocyte rolling and adhesion (reviewed in Ref. 18). The nature of this interaction has been difficult to unravel since HS is present on both endothelial cells and leukocytes, and selectins are also expressed by both cell types: leukocytes constitutively express L-selectin, whereas endothelial cells upregulate P-selectin upon activation.

In vitro studies using endothelial monolayers in flow chambers to mimic the physiological shear stress of blood vessels have provided evidence of a role for HS in leukocyte recruitment. For example, digesting HS from endothelial monolayers with heparinase III, or adding heparin or soluble HS to the medium, significantly reduces the number of rolling and firmly adhering granulocytes,[19] and the total HS deficiency resulting from knockdown of Ext1 in HUVECs prevents normal neutrophil arrest and transendothelial migration.[20] Similarly, genetic inactivation of Ndst1 in endothelial cells inhibits granulocyte adhesion to endothelial monolayers and is also associated with decreased binding of recombinant L-selectin[21] suggesting that HS is a physiological ligand for this adhesion molecule. Further supporting this hypothesis, pretreatment of monocytes with an L-selectin-blocking antibody inhibits their adhesion to endothelial monolayers,[22] while the binding of recombinant L-selectin to HEV in tissue sections from various organs is sensitive to heparinase digestion.[23]

In vivo studies also imply a major role for the HS-L-selectin interaction in leukocyte recruitment in various inflammatory models. Heparin infusion dramatically inhibited neutrophil infiltration into the peritoneal cavity following thioglycollate injection, and reduced ear thickness and inflammatory cell infiltrate in a contact dermatitis model.[24] Importantly, L- and P-selectin doubly deficient mice showed no further decrease in leukocyte recruitment following heparin treatment,

confirming that heparin inhibits inflammation primarily through these two selectins.[24] Similarly, the reduced HS sulfation achieved by conditional deletion of Ndst1 from only endothelial cells and leukocytes results in reduced leukocyte recruitment in models of peritonitis,[25] allergen-induced airway remodeling,[26,27] and diabetic[28] and experimental[21] glomerulonephritis. Of particular interest was the observation that chimeric WT mice with Ndst1-null bone marrow do not show any defect in thioglycollate-induced lymphocyte homing, whereas KO mice given WT bone marrow show the same reduction in cell infiltrate seen in the mice lacking both endothelial and leukocyte Ndst1.[25] Conversely, the compensatory increase in N- and 6-O-sulfation resulting from endothelial Hs2st deletion leads to increased leukocyte recruitment that is returned to control levels by an L-selectin-blocking antibody.[29] These results imply that the crucial interaction is that between the sulfated motifs of endothelial HS and leukocyte L-selectin, whereas leukocyte HS and P-selectin have little effect in this context.

However, while most data indicate that endothelial HS promotes leukocyte adhesion through L-selectin, some studies suggest that HS may have an inhibitory effect on leukocyte attachment. For example, heparinase digestion of microperfused murine venules results in more adherent leukocytes[30] and increased binding of fluorescently-labeled microspheres coated with anti-ICAM-1 antibody,[31] implying that the HS layer might inhibit leukocyte binding by masking endothelial adhesion molecules and making them less accessible to leukocyte integrins (Fig. 2). In support of this, intravital microscopy showed that the loss of endothelial glycocalyx following LPS infusion led to increased adhesion of GFP^+ neutrophils and of anti-ICAM-1 microspheres in WT but not heparanase-null mice.[32] These results suggest that heparanase-mediated shedding of endothelial HS in response to a potent inflammatory stimulus may expose more adhesion molecules such as ICAM-1. Thus HS may play two separate roles in leukocyte recruitment: directly by facilitating selectin-mediated leukocyte attachment and rolling, and indirectly through regulating accessibility of other adhesion ligands such as ICAM-1. Further studies are thus required to determine the relative contributions made by HS as a selectin ligand, and as a barrier to ICAM-1 accessibility, over time during the phases of initiation and resolution of an immune response.

Given the multi-faceted role for endothelial HS in leukocyte recruitment, one might expect the structure of HS to be altered in response to inflammatory stimuli or tissue damage in order to regulate immune cell infiltration, and there is evidence that this is indeed the case. For example, endothelial HS sulfation is increased by in vitro stimulation with TGF-β,[33] IFN-γ,[34] IL-1β,[35] or TNF[36] with associated upregulation of Ndst1, 2, Hs6st1 and 2,[36] and increased ability to bind L-selectin[22] and support the arrest and adherence of leukocytes.[19] In vivo, renal ischemia/reperfusion stimulates the formation of binding sites for L-selectin in the interstitial capillaries that are not present in the contralateral control kidney.[37] Experimentally induced nephritis is associated with increased expression of highly sulfated HS domains,[38] which are also seen in kidney sections from systemic lupus erythratomatus (SLE) patients and MRL/*lupr* mice[39] but not healthy controls. Thus, it seems likely that dynamically regulating the structure of endothelial HS may be a mechanism to fine-tune cell recruitment during an immune response.

2.3 | HS in the ECM regulates activity of cytokines

Cytokine activity is determined by a combination of factors including localization close to the target cell, susceptibility to inactivation by proteolytic cleavage, and ability to interact with high affinity receptors. Numerous cytokines have been demonstrated to bind heparin or HS in vitro[1] but the biological consequences of this interaction for cytokine activity have been explored for only a few cytokines. The available data indicate that HS exerts diverse effects on different cytokines, which is hardly surprising given the structural heterogeneity in this functional class of molecules.

Although often described as soluble mediators, cytokines exert their effects locally not systemically and binding to ECM HS has been proposed as a mechanism for retaining cytokines close to their site of production and action. For example, endogenous IL-2 is detectable in murine spleen, liver sinusoids, and kidney glomeruli, and staining is absent after treating the sections with heparitinase, but not with chondroitinase.[40] Similarly, IFN-γ injected into rats rapidly disappears from the circulation and accumulates in specific tissues including the liver, spleen, and kidney, which is inhibited by coinjection with heparin.[41] Thus, HS immobilizes certain cytokines in the extracellular space, forming localized reservoirs that may facilitate paracrine signaling (Fig. 2).

Whether HS-immobilized chemokines are able to interact with their receptor depends partly on whether the heparan- and receptor-binding sites overlap. Surface plasmon resonance experiments demonstrated that the binding of IFN-γ to its receptor or to HS are mutually exclusive,[42] which would imply that immobilized IFN-γ in the matrix cannot signal. However, endothelial monolayers pulsed with IFN-γ stimulate MHC-II upregulation by coincubated target cells which is abolished by heparinase II treatment,[43] suggesting that cell-surface HS might present IFN-γ in trans in a signaling-competent manner. Whether HS-bound IFN-γ must dissociate from the matrix to bind its high-affinity receptor, or can bind both simultaneously, remains unresolved. It was recently demonstrated for IL-2 that reservoirs on endothelial and smooth muscle cells of blood vessels are liberated by heparanase in a biologically active form that is competent to stimulate target cell proliferation.[44] Thus, changes to the matrix that occur during inflammation may release cytokines from ECM reservoirs and enable them to signal.

In addition to regulating availability of soluble cytokine, HS may also influence cytokine activity by controlling their accessibility to proteases (Fig. 2). For example, proteolytic cleavage of the C-terminal portion of IFN-γ increases receptor binding if fewer than ten terminal amino acids are removed,[42] but binding is decreased by larger deletions.[45] Heparin and highly sulfated HS bind IFN-γ at its C-terminus,[46] and coinjection of heparin protects IFN-γ from proteolytic degradation in vivo.[47] Heparin has also been shown to prevent degradation of other cytokines including IL-6[48] and IL-7[49] in vitro. Thus binding to matrix HS may serve to protect the active form of the cytokine, as well as forming local reservoirs.

Soluble HS fragments released in inflammation may also regulate signaling of some cytokines by promoting their interaction with receptors on target cells. It has been demonstrated that addition of soluble HS to cells that lack detectable levels of this GAG on their surface augments IL-5-induced proliferation[50] and IL-12-stimulated IFN-γ production.[51] The mechanism by which soluble HS promotes signaling of these cytokines has not been explored, and the relevance of these observations to inflammatory processes in vivo is not yet clear.

3 | SOLUBLE HS DIRECTLY STIMULATES IMMUNE CELLS, ACTING ON APCS TO CONTROL IMMUNE RESPONSES

HS fragments liberated from the ECM by enzymes released during inflammation can promote immune activation by signaling through TLR4 and activating APCs.

3.1 | HS is degraded in inflammation to become a potent TLR4 ligand

It has become evident that soluble fragments of HS can signal through TLR4, an innate pattern recognition receptor for which the prototypic ligand is bacterial LPS. Stimulation of dendritic cells (DCs) with HS fragments induces upregulation of costimulatory molecules including CD86 and CD40 and secretion of proinflammatory cytokines,[52] which is inhibited by TLR4 mutation or the TLR4 antagonist Rs-DPLA.[53] These findings suggest that HS is a non-classical ligand for TLR4 that is capable of signaling to trigger immune activation (Fig. 3). Similarly, cardiac fibroblasts stimulated with HS upregulate V-CAM1 and I-CAM1, leading to increased adhesion of polymorphonuclear neutrophils (PMNs) and smooth muscle cells, which is completely abolished by the TLR4 inhibitor TAK-242 or by blocking the downstream signaling molecules NFkB or PI3K/Akt.[54]

Proliferation of T cells after coincubation with allogeneic DCs is augmented by soluble HS, but not when the DCs come from mice deficient in TLR4 or its adaptor protein MyD88. However, knockout of these molecules in T cells had no effect,[55] and HS treatment of purified T cells stimulated with anti-CD3 in the absence of DCs did not augment proliferation,[56] demonstrating that HS indirectly controls lymphocyte activity through regulating APC maturation. Furthermore, murine peritoneal macrophages stimulated with HS upregulate IL-1, IL-6, TNF, and IL-12, and show increased cytotoxicity toward a leukemia cell line.[57] In vivo evidence for the role of the HS-TLR4 axis in inflammation comes from infusion of soluble HS into the pancreas of mice, which results in neutrophil infiltration and increased myeloperoxidase activity in WT but not TLR4-null mice.[58]

It is thought that the elevated activity of metalloproteases,[59] heparanase,[60] and other enzymes that occurs in inflammation liberates HS fragments from cell-surface and ECM HSPGs. These soluble HS fragments could then signal through TLR4 to alert the immune system to tissue damage, thus acting as a damage-associated molecular pattern (DAMP). In support of this hypothesis, endothelial cells with metabolically labeled sulfated GAGs show a decrease in cell-surface HS and an increase in smaller HS fragments in the conditioned medium upon LPS stimulation[61] or exposure to activated neutrophils, which can be reduced by inhibitors of serine proteases and elastase.[62] Furthermore, heparanase treatment of human PBMCs resulted in a reduction of cell-surface HS and an upregulation of proinflammatory cytokines similar to that seen by addition of HS fragments, which was abrogated by inhibitors of heparanase or by MyD88 or TLR4 deficiency.[63]

In vivo administration of the serum protease inhibitor alpha-1 antitrypsin (A1AT) to recipients of allogeneic bone marrow transplants increased survival and lowered serum HS and histological scores. Furthermore, while TLR4 gene deletion conferred some protection from graft-versus-host disease, no further benefit was seen with A1AT treatment,[55] indicating that the protective effects of A1AT are mediated through the HS-TLR4 axis. Similarly, injection of elastase into WT mice induced loss of HS from blood vessels, an increase in serum TNF and ultimately death of the mice, whereas TLR4-null mice showed improved survival.[64] Collectively, these results suggest a pathway in which fragments of HS produced enzymatically during inflammation signal through TLR4 to further activate the immune system, which may have beneficial or detrimental effects depending on the context.

There is evidence to suggest that the immune system is able to distinguish between endogenous stimuli indicative of tissue damage and exogenous stimuli present as a result of infection, enabling a context-appropriate response to be mounted. For example, macrophages stimulated with LPS or the matrix glycoprotein tenacin-C, which is produced upon tissue injury and also signals through TLR4, resulted in different transcriptional responses and two distinct macrophage phenotypes.[65] LPS-stimulated macrophages had greater collagen-degrading ability and inflammatory cytokine production, whereas tenacin-C treatment induced macrophages to synthesize collagens and other proteins associated with tissue repair. One might thus predict that HS, another endogenous DAMP that signals through TLR4, also stimulates an immune response different to that induced by LPS. In support of this, the kinetics of TLR4 signaling in response to LPS or HS are different, with LPS inducing much more rapid nuclear translocation of NFkB than HS[53] and HS triggering a slower and more sustained increase in intracellular calcium.[66] Further studies are required to define how TLR4 signaling induced by endogenous DAMPs such as HS is different to that induced by infection-associated stimuli such as LPS, and whether this results in context-appropriate responses from the immune cell.

4 | HS ON LEUKOCYTE SURFACE REGULATES THEIR IMMUNE AND INFLAMMATORY FUNCTIONS

Although frequently considered a matrix molecule, HS is expressed on the surface of most cells, including immune cells, in the form of proteoglycans. In addition to regulating receptor interactions both cell autonomously and through ligand presentation to other cells, leukocyte cell-surface HS appears to contribute to specific functions such

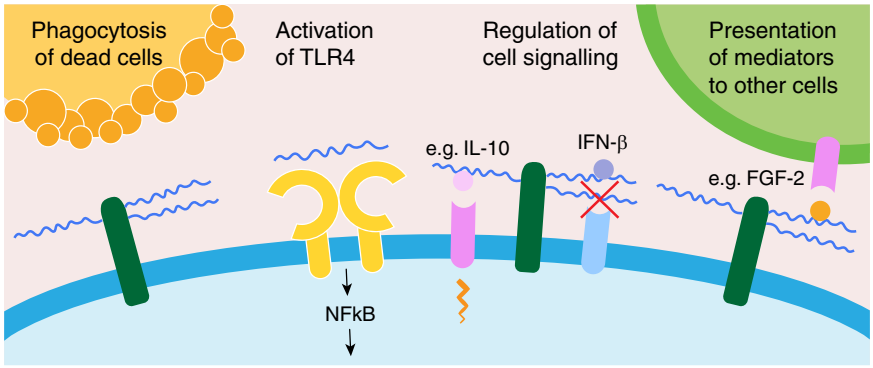

FIGURE 3 Leukocyte HS plays many roles in immune regulation. Heparan sulfate proteoglycans facilitate uptake of late apoptotic and necrotic cells, although the mechanism remains unclear. Soluble fragments of HS released during tissue inflammation activate cells through TLR4. HS chains on leukocyte membrane proteins can promote or inhibit receptor-ligand interactions for cytokines and growth factors. Cell-surface proteoglycans can also regulate signaling in trans by presenting growth factors such as FGF-2 to target cells

as phagocytosis. This may be a physiologically relevant mechanism of immune regulation, as the structure of leukocyte HS is altered in response to various inflammatory stimuli.

4.1 | Leukocyte HS promotes phagocytic activity

Cell-surface HS is thought to be involved in recognition and uptake of dead cells by phagocytes through exposure of HS binding sites on late apoptotic and necrotic cells that have lost membrane integrity (Fig. 3). For example, FITC-labeled heparin was found to bind to the surface of apoptotic and necrotic cells, but not live cells, and this interaction was inhibitable by heparin but not dermatan or chondroitin sulfates.[67] Beads coated with anti-HS antibodies were bound and internalized by epithelial cell lines, but not if the cells had been pretreated with heparinase III or in the presence of inhibitors of PKC or actin polymerization,[68] suggesting that ligation of cell-surface HS is sufficient to stimulate actin-mediated endocytosis in non-professional phagocytes. Similarly, CHO cells and human skin fibroblasts bind and internalize latex beads, and this is strongly reduced by the addition of heparin or soluble HS fragments or by pretreatment of the cells with heparinase III.[69] Additionally, CHO mutant cells lacking the ability to synthesize HS showed defective binding and internalization of the beads, adding further support to an HS-mediated mechanism of phagocytosis. These studies were performed in largely artificial systems with non-professional phagocytes, but there is some evidence that an HS-dependent mechanism of phagocytosis is conserved in a relevant immune setting: human PMNs more efficiently bind and internalize a strain of *Helicobacter pylori* that can bind HS than a strain without HS-binding ability, and preincubation of the bacteria with heparin inhibited uptake of the HS-binding strain but did not further reduce uptake of the non-HS-binding strain.[70] However, further studies are required to determine the relative contribution that HS makes as an endocytic receptor in the presence of canonical phagocytic receptors, antibodies and other opsonins that have an established role in phagocytosis in vivo.[71]

4.2 | Leukocyte HS regulates responses to inflammatory mediators

HS on the surface of leukocytes appears to play a role in regulating signaling of certain inflammatory mediators through their cell-surface receptors, either by promoting ligand interaction with its receptor, thus acting as a coreceptor, or by inhibiting receptor–ligand interactions, depending on the ligand (Fig. 3). For example, the B cell activating factor APRIL, which is essential for IgA class switching in response to mucosal antigens,[72] requires HS on the B cell surface for optimal receptor activation and downstream signaling. Heparinase III digestion of B cells strongly reduced APRIL-induced proliferation, IgA production, and NFkB translocation.[73] APRIL can be competed off the B cell surface by heparin, and mutant forms of APRIL without HS-binding ability fail to stimulate IgA production by B cells.[74] APRIL does not bind to the surface of $Glce^{-/-}$ B cells, which lack iduronic acid residues, and cannot promote their survival in vitro.[75] This may be due to altered downstream modifications by the 2-O- and 6-O-sulfotransferases, whose activity is affected by epimerase inactivation.[76]

Another B cell factor, IL-7, also binds heparin and HS, and IL-7-dependent proliferation is inhibited by the addition of heparin,[49] suggesting that binding to cell-surface HS promotes IL-7 interacting with its receptor. In support of this, heparitinase treatment of primary B cell precursors diminished surface binding of IL-7 and reduced IL-7-driven proliferation.[77]

IL-10 binds both heparin and HS, and the addition of soluble fragments of HS inhibits the ability of IL-10 to upregulate CD64 and CD16 on monocytes.[78] Similarly, IL-10 induced expression of these markers is inhibited by treatment of monocytes and macrophages with sodium chlorate, which prevents sulfation of GAGs,[78] indicating that cell-surface HS promotes the interaction of IL-10 with its receptor. The crystal structure for IL-10 bound to IL-10R1 shows no overlap with the GAG-binding site,[79] but there is currently no crystal structure of the ternary complex composed of IL-10 and both receptor subunits. Therefore, it remains unclear whether HS acts directly as a coreceptor in the formation of productive IL-10–IL-10R complexes, or simply facilitates IL-10 signaling by preventing diffusion of the cytokine away from the cell surface.

Cells transfected with the splice variant of the hyaluronan receptor (CD44) containing HS attachment sites retain hepatocyte growth factor (HGF) on their cell surface, whereas no binding is seen on cells expressing the isoform of CD44 lacking the HS attachment region.[80] The same study showed that ability to bind HGF on the surface resulted in phosphorylation of the HGF receptor tyrosine kinase c-Met, and of ERK-1 and ERK-2. Surface binding and signaling were abolished by heparitinase (but not chondroitinase ABC) treatment or by mutation of the HS-binding domain of HGF, suggesting that HS-mediated capture of HGF on the cell surface facilitates receptor

binding and activation. This appears to be a relevant mechanism in B cells since human tonsillar B cells activated by coincident ligation of CD40 and the BCR express a higher molecular weight form of CD44, with concurrent acquisition of HGF-binding ability. Downstream c-Met phosphorylation was abolished by heparitinase treatment of activated B cells,[81] indicating that CD44 is decorated with HS following proinflammatory stimulation.

However, leukocyte HS may not always promote ligand-receptor interactions, as for certain ligands it acts instead as a barrier and inhibits signaling. Macrophages deficient in HS sulfation through deletion of Ndst1 show increased responsiveness to IFN-β stimulation and elevated production of proinflammatory cytokines and chemokines,[82] suggesting that the role of HSPGs in IFN-β signaling is to sequester it away from its receptor and thus maintain macrophages in a quiescent state.

4.3 | Leukocyte HS regulates cell activation in trans

In addition to these cell-autonomous functions, leukocyte cell-surface HS can also be involved in presentation of growth factors or inflammatory mediators produced by leukocytes to their target cells, as has been demonstrated for fibroblast growth factor 2 (FGF-2) (Fig. 3). During monocyte-to-macrophage maturation, cells aquire the capacity to bind FGF-2, which is inhibitable by heparin and further augmented by stimulation with IL-1 or LPS.[83] The same study showed that activated macrophages augmented the proliferative response of HS-deficient BaF32 cells to low concentrations of FGF-2, which was abolished by heparinase III treatment, indicating that macrophage HS enables trans-presentation of FGF-2 to target cells in a signaling-competent manner. Similarly, activated macrophages increase expression of the CD44v3 isoform of the hyaluronan receptor that contains HS chain attachment sites, and cell lines transfected with this HS-sufficient form of CD44, but not those with the HS-deficient variant, augmented FGF-2-induced proliferation of BaF32 cells.[84] Interestingly, both studies found that T cells do not increase expression of CD44v3 or their total HS levels upon mitogenic stimulation, and T cells actually decrease HS expression and lose the ability to bind FGF-2 during consecutive rounds of proliferation.[85] These observations suggest that HS-mediated trans-presentation of growth factors may be a mechanism unique to those cells producing such growth factors upon activation. It remains to be determined whether modulation of HS expression regulates the activity of other HS-binding inflammatory mediators through surface presentation.

4.4 | Leukocyte HS structure is altered during inflammation

For leukocyte HS to be considered an active regulator of cell responses, it must itself be altered during the course of an immune response to facilitate changes in inflammatory processes, and there is increasing evidence that such dynamic regulation of HS does occur. B cells from virus-infected mice, or stimulated in vitro with the IFN-I-inducer Poly I:C or IFN-β, show increased surface expression of HS and augmented APRIL-induced production of IgA.[86] Similarly, stimulation with PMA or ligation of CD40 results in an increase in HS on the B cell surface and a switch to the higher molecular weight form of CD44 that has HS chains.[81] HS structure may also be regulated during B cell development, as ligation of the pre-BCR induces upregulation of numerous HS-associated genes including Hs3st1.[87] Furthermore, microarray analyses of different B cell subsets show greater expression of HS biosynthetic enzymes in plasma cells than memory B cells,[88] suggesting activation is associated with an increase in cell-surface HS.

Differential expression of HS is also a feature of macrophage subsets, as human monocyte-derived macrophages polarized to an anti-inflammatory reparative phenotype display greater upregulation of sulfotransferases than proinflammatory macrophages, resulting in more cell-surface HS with a higher degree of 2-O-sulfation.[89] Importantly, this differential expression of HS was shown to have functional consequences: reparative macrophages bound more FGF-2 and augmented the FGF-2-dependent proliferation of a target cell line, consistent with the requirement of 2-O-sulfation for FGF-2 binding.[90] This suggests that the expression of more highly sulfated HS in reparative macrophages may be important for their role in the resolution of inflammation. Various other stimuli have been reported to affect HS structure on macrophages, such as LPS and TNF which induce upregulation of HS3ST3B and consequently an increase in 3-O-sulfation,[91] and hypoxia which significantly reduces expression of biosynthetic enzymes and total HS content.[92]

Interestingly, macrophages from the synovial fluid of RA and SLE patients show greater FGF-2 binding than blood monocytes,[83] and CD44-HS splice variants were highly expressed in RA but not OA joints and colocalized with staining for macrophage markers and FGF-2.[84] These findings suggest that excessive growth factor activity seen during chronic inflammation may be partly due to aberrant regulation of leukocyte HS sulfation.

5 | CONCLUSIONS

It is becoming increasingly apparent that HS has multiple roles in immune regulation and signaling during inflammation, both in the microenvironment and on the cell-surface of leukocytes. Soluble HS fragments also have signaling properties and may serve as indicators of tissue damage. Further studies are required for a better understanding of the changes in HS expression that occur during inflammation and the structural requirements for binding and regulation of immune mediators. Understanding these structure–function relationships will be essential for the development of therapeutics that interfere these processes to combat immunopathology, which might take the form of synthetic HS oligosaccharides or HS-specific antibodies.

AUTHORSHIP

L.E.C. conceived the idea and wrote the manuscript. L.T. edited the paper.

ACKNOWLEDGMENTS

The authors are supported by the Kennedy Trust for Rheumatology Research. Linda Troeberg is funded in part by Arthritis Research UK (No. 20887).

DISCLOSURES

The authors declare no conflict of interest.

REFERENCES

1. Ori A, Wilkinson MC, Fernig DG. A systems biology approach for the investigation of the heparin/heparan sulfate interactome. *J Biol Chem*. 2011;286:19892–19904.
2. Proudfoot AEI, Johnson Z, Bonvin P, Handel TM. Glycosaminoglycan interactions with chemokines add complexity to a complex system. *Pharmaceuticals (Basel)*. 2017;10.
3. Borza DB. Glomerular basement membrane heparan sulfate in health and disease: a regulator of local complement activation. *Matrix Biol*. 2017;57–58:299–310.
4. Langford-Smith A, Day AJ, Bishop PN, Clark SJ. Complementing the sugar code: role of GAGs and sialic acid in complement regulation. *Front Immunol*. 2015;6:25.
5. Meri S. Self-nonself discrimination by the complement system. *FEBS Lett*. 2016;590:2418–2434.
6. Hull EE, Montgomery MR, Leyva KJ. Epigenetic regulation of the biosynthesis & enzymatic modification of heparan sulfate proteoglycans: implications for tumorigenesis and cancer biomarkers. *Int J Mol Sci*. 2017;18.
7. Liu J, Pedersen LC. Anticoagulant heparan sulfate: structural specificity and biosynthesis. *Appl Microbiol Biotechnol*. 2007;74:263–272.
8. Zhang X, Wang F, Sheng J. "Coding" and "Decoding": hypothesis for the regulatory mechanism involved in heparan sulfate biosynthesis. *Carbohydr Res*. 2016;428:1–7.
9. Weber M, Hauschild R, Schwarz J, et al. Interstitial dendritic cell guidance by haptotactic chemokine gradients. *Science*. 2013;339:328–332.
10. Proudfoot AE, Handel TM, Johnson Z, et al. Glycosaminoglycan binding and oligomerization are essential for the in vivo activity of certain chemokines. *Proc Natl Acad Sci USA*. 2003;100:1885–1890.
11. Severin IC, Gaudry JP, Johnson Z, et al. Characterization of the chemokine CXCL11-heparin interaction suggests two different affinities for glycosaminoglycans. *J Biol Chem*. 2010;285:17713–17724.
12. Massena S, Christoffersson G, Hjertstrom E, et al. A chemotactic gradient sequestered on endothelial heparan sulfate induces directional intraluminal crawling of neutrophils. *Blood*. 2010;116:1924–1931.
13. Frevert CW, Goodman RB, Kinsella MG, et al. Tissue-specific mechanisms control the retention of IL-8 in lungs and skin. *J Immunol*. 2002;168:3550–3556.
14. Lowe-Krentz LJ, Joyce JG. Venous and aortic porcine endothelial cells cultured under standardized conditions synthesize heparan sulfate chains which differ in charge. *Anal Biochem*. 1991;193:155–163.
15. Rot A. Binding of neutrophil attractant/activation protein-1 (interleukin 8) to resident dermal cells. *Cytokine*. 1992;4:347–352.
16. Hub E, Rot A. Binding of RANTES, MCP-1, MCP-3, and MIP-1alpha to cells in human skin. *Am J Pathol*. 1998;152:749–757.
17. Stoler-Barak L, Moussion C, Shezen E, Hatzav M, Sixt M, Alon R. Blood vessels pattern heparan sulfate gradients between their apical and basolateral aspects. *PLoS One*. 2014;9:e85699.
18. Parish CR. The role of heparan sulphate in inflammation. *Nat Rev Immunol*. 2006;6:633–643.
19. Rops AL, Jacobs CW, Linssen PC, et al. Heparan sulfate on activated glomerular endothelial cells and exogenous heparinoids influence the rolling and adhesion of leucocytes. *Nephrol Dial Transplant*. 2007;22:1070–1077.
20. Stoler-Barak L, Barzilai S, Zauberman A, Alon R. Transendothelial migration of effector T cells across inflamed endothelial barriers does not require heparan sulfate proteoglycans. *Int Immunol*. 2014;26:315–324.
21. Rops AL, Loeven MA, van Gemst JJ, et al. Modulation of heparan sulfate in the glomerular endothelial glycocalyx decreases leukocyte influx during experimental glomerulonephritis. *Kidney Int*. 2014;86:932–942.
22. Giuffre L, Cordey AS, Monai N, Tardy Y, Schapira M, Spertini O. Monocyte adhesion to activated aortic endothelium: role of L-selectin and heparan sulfate proteoglycans. *J Cell Biol*. 1997;136:945–956.
23. Celie JW, Keuning ED, Beelen RH, et al. Identification of L-selectin binding heparan sulfates attached to collagen type XVIII. *J Biol Chem*. 2005;280:26965–26973.
24. Wang L, Brown JR, Varki A, Esko JD. Heparin's anti-inflammatory effects require glucosamine 6-O-sulfation and are mediated by blockade of L- and P-selectins. *J Clin Invest*. 2002;110:127–136.
25. Wang L, Fuster M, Sriramarao P, Esko JD. Endothelial heparan sulfate deficiency impairs L-selectin- and chemokine-mediated neutrophil trafficking during inflammatory responses. *Nat Immunol*. 2005;6:902–910.
26. Ge XN, Ha SG, Rao A, et al. Endothelial and leukocyte heparan sulfates regulate the development of allergen-induced airway remodeling in a mouse model. *Glycobiology*. 2014;24:715–727.
27. Zuberi RI, Ge XN, Jiang S, et al. Deficiency of endothelial heparan sulfates attenuates allergic airway inflammation. *J Immunol*. 2009;183:3971–3979.
28. Talsma DT, Katta K, Ettema MAB, et al. Endothelial heparan sulfate deficiency reduces inflammation and fibrosis in murine diabetic nephropathy. *Lab Invest*. 2018.
29. Axelsson J, Xu D, Kang BN, et al. Inactivation of heparan sulfate 2-O-sulfotransferase accentuates neutrophil infiltration during acute inflammation in mice. *Blood*. 2012;120:1742–1751.
30. Constantinescu AA, Vink H, Spaan JA. Endothelial cell glycocalyx modulates immobilization of leukocytes at the endothelial surface. *Arterioscler Thromb Vasc Biol*. 2003;23:1541–1547.
31. Mulivor AW, Lipowsky HH. Role of glycocalyx in leukocyte-endothelial cell adhesion. *Am J Physiol Heart Circ Physiol*. 2002;283:H1282–1291.
32. Schmidt EP, Yang Y, Janssen WJ, et al. The pulmonary endothelial glycocalyx regulates neutrophil adhesion and lung injury during experimental sepsis. *Nat Med*. 2012;18:1217–1223.
33. Kasinath BS. Glomerular endothelial cell proteoglycans–regulation by TGF-beta 1. *Arch Biochem Biophys*. 1993;305:370–377.
34. Carter NM, Ali S, Kirby JA. Endothelial inflammation: the role of differential expression of N-deacetylase/N-sulphotransferase enzymes in alteration of the immunological properties of heparan sulphate. *J Cell Sci*. 2003;116:3591–3600.
35. Sorensson J, Bjornson A, Ohlson M, Ballermann BJ, Haraldsson B. Synthesis of sulfated proteoglycans by bovine glomerular endothelial cells in culture. *Am J Physiol Renal Physiol*. 2003;284:F373–380.
36. Rops AL, van den Hoven MJ, Baselmans MM, et al. Heparan sulfate domains on cultured activated glomerular endothelial cells mediate leukocyte trafficking. *Kidney Int*. 2008;73:52–62.
37. Celie JW, Rutjes NW, Keuning ED, et al. Subendothelial heparan sulfate proteoglycans become major L-selectin and monocyte chemoattractant protein-1 ligands upon renal ischemia/reperfusion. *Am J Pathol*. 2007;170:1865–1878.

38. Rops AL, Gotte M, Baselmans MH, et al. Syndecan-1 deficiency aggravates anti-glomerular basement membrane nephritis. *Kidney Int*. 2007;72:1204–1215.
39. Rops AL, van den Hoven MJ, Bakker MA, et al. Expression of glomerular heparan sulphate domains in murine and human lupus nephritis. *Nephrol Dial Transplant*. 2007;22:1891–1902.
40. Wrenshall LE, Platt JL. Regulation of T cell homeostasis by heparan sulfate-bound IL-2. *J Immunol*. 1999;163:3793–3800.
41. Lortat-Jacob H, Brisson C, Guerret S, Morel G. Non-receptor-mediated tissue localization of human interferon-gamma: role of heparan sulfate/heparin-like molecules. *Cytokine*. 1996;8:557–566.
42. Sadir R, Forest E, Lortat-Jacob H. The heparan sulfate binding sequence of interferon-gamma increased the on rate of the interferon-gamma-interferon-gamma receptor complex formation. *J Biol Chem*. 1998;273:10919–10925.
43. Fernandez-Botran R, Yan J, Justus DE. Binding of interferon gamma by glycosaminoglycans: a strategy for localization and/or inhibition of its activity. *Cytokine*. 1999;11:313–325.
44. Miller JD, Clabaugh SE, Smith DR, Stevens RB, Wrenshall LE. Interleukin-2 is present in human blood vessels and released in biologically active form by heparanase. *Immunol Cell Biol*. 2012;90:159–167.
45. Leinikki PO, Calderon J, Luquette MH, Schreiber RD. Reduced receptor binding by a human interferon-gamma fragment lacking 11 carboxyl-terminal amino acids. *J Immunol*. 1987;139:3360–3366.
46. Lortat-Jacob H, Grimaud JA. Interferon-gamma binds to heparan sulfate by a cluster of amino acids located in the C-terminal part of the molecule. *FEBS Lett*. 1991;280:152–154.
47. Lortat-Jacob H, Baltzer F, Grimaud JA. Heparin decreases the blood clearance of interferon-gamma and increases its activity by limiting the processing of its carboxyl-terminal sequence. *J Biol Chem*. 1996;271:16139–16143.
48. Mummery RS, Rider CC. Characterization of the heparin-binding properties of IL-6. *J Immunol*. 2000;165:5671–5679.
49. Clarke D, Katoh O, Gibbs RV, Griffiths SD, Gordon MY. Interaction of interleukin 7 (IL-7) with glycosaminoglycans and its biological relevance. *Cytokine*. 1995;7:325–330.
50. Lipscombe RJ, Nakhoul AM, Sanderson CJ, Coombe DR. Interleukin-5 binds to heparin/heparan sulfate. A model for an interaction with extracellular matrix. *J Leukoc Biol*. 1998;63:342–350.
51. Jayanthi S, Koppolu BP, Nguyen KG, et al. Modulation of Interleukin-12 activity in the presence of heparin. *Sci Rep*. 2017;7:5360.
52. Kodaira Y, Nair SK, Wrenshall LE, Gilboa E, Platt JL. Phenotypic and functional maturation of dendritic cells mediated by heparan sulfate. *J Immunol*. 2000;165:1599–1604.
53. Johnson GB, Brunn GJ, Kodaira Y, Platt JL. Receptor-mediated monitoring of tissue well-being via detection of soluble heparan sulfate by Toll-like receptor 4. *J Immunol*. 2002;168:5233–5239.
54. Olivares-Silva F, Landaeta R, Aranguiz P, et al. Heparan sulfate potentiates leukocyte adhesion on cardiac fibroblast by enhancing Vcam-1 and Icam-1 expression. *Biochim Biophys Acta*. 2018;1864:831–842.
55. Brennan TV, Lin L, Huang X, et al. Heparan sulfate, an endogenous TLR4 agonist, promotes acute GVHD after allogeneic stem cell transplantation. *Blood*. 2012;120:2899–2908.
56. Wrenshall LE, Cerra FB, Carlson A, Bach FH, Platt JL. Regulation of murine splenocyte responses by heparan sulfate. *J Immunol*. 1991;147:455–459.
57. Wrenshall LE, Stevens RB, Cerra FB, Platt JL. Modulation of macrophage and B cell function by glycosaminoglycans. *J Leukoc Biol*. 1999;66:391–400.
58. Akbarshahi H, Axelsson JB, Said K, Malmstrom A, Fischer H, Andersson R. TLR4 dependent heparan sulphate-induced pancreatic inflammatory response is IRF3-mediated. *J Transl Med*. 2011;9:219.
59. Nissinen L, Kahari VM. Matrix metalloproteinases in inflammation. *Biochim Biophys Acta*. 2014;1840:2571–2580.
60. Meirovitz A, Goldberg R, Binder A, Rubinstein AM, Hermano E, Elkin M. Heparanase in inflammation and inflammation-associated cancer. *FEBS J*. 2013;280:2307–2319.
61. Geller RL, Ihrcke NS, Maines J, Lindman BJ, Platt JL. Loss of heparan sulfate proteoglycan as a manifestation of cellular immunity in vivo and in vitro. *Transplant Proc*. 1993;25:144–145.
62. Key NS, Platt JL, Vercellotti GM. Vascular endothelial cell proteoglycans are susceptible to cleavage by neutrophils. *Arterioscler Thromb*. 1992;12:836–842.
63. Goodall KJ, Poon IK, Phipps S, Hulett MD. Soluble heparan sulfate fragments generated by heparanase trigger the release of pro-inflammatory cytokines through TLR-4. *PLoS One*. 2014;9:e109596.
64. Johnson GB, Brunn GJ, Platt JL. Cutting edge: an endogenous pathway to systemic inflammatory response syndrome (SIRS)-like reactions through Toll-like receptor 4. *J Immunol*. 2004;172:20–24.
65. Piccinini AM, Zuliani-Alvarez L, Lim JM, Midwood KS. Distinct microenvironmental cues stimulate divergent TLR4-mediated signaling pathways in macrophages. *Sci Signal*. 2016;9. ra86.
66. Wrenshall LE, Cerra FB, Singh RK, Platt JL. Heparan sulfate initiates signals in murine macrophages leading to divergent biologic outcomes. *J Immunol*. 1995;154:871–880.
67. Gebska MA, Titley I, Paterson HF, et al. High-affinity binding sites for heparin generated on leukocytes during apoptosis arise from nuclear structures segregated during cell death. *Blood*. 2002;99:2221–2227.
68. Dehio C, Freissler E, Lanz C, Gomez-Duarte OG, David G, Meyer TF. Ligation of cell surface heparan sulfate proteoglycans by antibody-coated beads stimulates phagocytic uptake into epithelial cells: a model for cellular invasion by Neisseria gonorrhoeae. *Exp Cell Res*. 1998;242:528–539.
69. Fukasawa M, Sekine F, Miura M, Nishijima M, Hanada K. Involvement of heparan sulfate proteoglycans in the binding step for phagocytosis of latex beads by Chinese hamster ovary cells. *Exp Cell Res*. 1997;230:154–162.
70. Chmiela M, Paziak-Domanska B, Wadstrom T. Attachment, ingestion and intracellular killing of *Helicobacter pylori* by human peripheral blood mononuclear leukocytes and mouse peritoneal inflammatory macrophages. *FEMS Immunol Med Microbiol*. 1995;10:307–316.
71. Stuart LM, Ezekowitz RA. Phagocytosis: elegant complexity. *Immunity*. 2005;22:539–550.
72. Castigli E, Scott S, Dedeoglu F, et al. Impaired IgA class switching in APRIL-deficient mice. *Proc Natl Acad Sci USA*. 2004;101:3903–3908.
73. Sakurai D, Hase H, Kanno Y, Kojima H, Okumura K, Kobata T. TACI regulates IgA production by APRIL in collaboration with HSPG. *Blood*. 2007;109:2961–2967.
74. Kimberley FC, van Bostelen L, Cameron K, et al. The proteoglycan (heparan sulfate proteoglycan) binding domain of APRIL serves as a platform for ligand multimerization and cross-linking. *FASEB J*. 2009;23:1584–1595.
75. Reijmers RM, Groen RW, Kuil A, et al. Disruption of heparan sulfate proteoglycan conformation perturbs B-cell maturation and APRIL-mediated plasma cell survival. *Blood*. 2011;117:6162–6171.
76. Townley RA, Bulow HE. Genetic analysis of the heparan modification network in *Caenorhabditis elegans*. *J Biol Chem*. 2011;286:16824–16831.

77. Borghesi LA, Yamashita Y, Kincade PW. Heparan sulfate proteoglycans mediate interleukin-7-dependent B lymphopoiesis. *Blood*. 1999;93:140–148.

78. Salek-Ardakani S, Arrand JR, Shaw D, Mackett M. Heparin and heparan sulfate bind interleukin-10 and modulate its activity. *Blood*. 2000;96:1879–1888.

79. Josephson K, Logsdon NJ, Walter MR. Crystal structure of the IL-10/IL-10R1 complex reveals a shared receptor binding site. *Immunity*. 2001;15:35–46.

80. van der Voort R, Taher TE, Wielenga VJ, et al. Heparan sulfate-modified CD44 promotes hepatocyte growth factor/scatter factor-induced signal transduction through the receptor tyrosine kinase c-Met. *J Biol Chem*. 1999;274:6499–6506.

81. van der Voort R, Keehnen RM, EA Beuling, Spaargaren M, Pals ST. Regulation of cytokine signaling by B cell antigen receptor and CD40-controlled expression of heparan sulfate proteoglycans. *J Exp Med*. 2000;192:1115–1124.

82. Gordts PL, Foley EM, Lawrence R, et al. Reducing macrophage proteoglycan sulfation increases atherosclerosis and obesity through enhanced type I interferon signaling. *Cell Metab*. 2014;20:813–826.

83. Clasper S, Vekemans S, Fiore M, et al. Inducible expression of the cell surface heparan sulfate proteoglycan syndecan-2 (fibroglycan) on human activated macrophages can regulate fibroblast growth factor action. *J Biol Chem*. 1999;274:24113–24123.

84. Jones M, Tussey L, Athanasou N, Jackson DG. Heparan sulfate proteoglycan isoforms of the CD44 hyaluronan receptor induced in human inflammatory macrophages can function as paracrine regulators of fibroblast growth factor action. *J Biol Chem*. 2000;275:7964–7974.

85. Garner OB, Yamaguchi Y, Esko JD, Videm V. Small changes in lymphocyte development and activation in mice through tissue-specific alteration of heparan sulphate. *Immunology*. 2008;125:420–429.

86. Jarousse N, Trujillo DL, Wilcox-Adelman S, Coscoy L. Virally-induced upregulation of heparan sulfate on B cells via the action of type I IFN. *J Immunol*. 2011;187:5540–5547.

87. Schebesta M, Pfeffer PL, Busslinger M. Control of pre-BCR signaling by Pax5-dependent activation of the BLNK gene. *Immunity*. 2002;17:473–485.

88. Bret C, Hose D, Reme T, et al. Expression of genes encoding for proteins involved in heparan sulphate and chondroitin sulphate chain synthesis and modification in normal and malignant plasma cells. *Br J Haematol*. 2009;145:350–368.

89. Martinez P, Denys A, Delos M, et al. Macrophage polarization alters the expression and sulfation pattern of glycosaminoglycans. *Glycobiology*. 2015;25:502–513.

90. Rahmoune H, Chen HL, Gallagher JT, Rudland PS, Fernig DG. Interaction of heparan sulfate from mammary cells with acidic fibroblast growth factor (FGF) and basic FGF. Regulation of the activity of basic FGF by high and low affinity binding sites in heparan sulfate. *J Biol Chem*. 1998;273:7303–7310.

91. Sikora AS, Delos M, Martinez P, Carpentier M, Allain F, Denys A. Regulation of the expression of heparan sulfate 3-O-sulfotransferase 3B (HS3ST3B) by inflammatory stimuli in human monocytes. *J Cell Biochem*. 2016;117:1529–1542.

92. Asplund A, Ostergren-Lunden G, Camejo G, Stillemark-Billton P, Bondjers G. Hypoxia increases macrophage motility, possibly by decreasing the heparan sulfate proteoglycan biosynthesis. *J Leukoc Biol*. 2009;86:381–388.

93. Ruppert R, Hoffmann E, Sebald W. Human bone morphogenetic protein 2 contains a heparin-binding site which modifies its biological activity. *Eur J Biochem*. 1996;237:295–302.

94. Sampath TK, Muthukumaran N, Reddi AH. Isolation of osteogenin, an extracellular matrix-associated, bone-inductive protein, by heparin affinity chromatography. *Proc Natl Acad Sci USA*. 1987;84:7109–7113.

95. Ohkawara B, Iemura S, ten Dijke P, Ueno N. Action range of BMP is defined by its N-terminal basic amino acid core. *Curr Biol*. 2002;12:205–209.

96. Irie A, Habuchi H, Kimata K, Sanai Y. Heparan sulfate is required for bone morphogenetic protein-7 signaling. *Biochem Biophys Res Commun*. 2003;308:858–865.

97. Brigstock DR, Steffen CL, Kim GY, Vegunta RK, Diehl JR, Harding PA. Purification and characterization of novel heparin-binding growth factors in uterine secretory fluids. Identification as heparin-regulated Mr 10,000 forms of connective tissue growth factor. *J Biol Chem*. 1997;272:20275–20282.

98. Kiefer P, Peters G, Dickson C. The Int-2/Fgf-3 oncogene product is secreted and associates with extracellular matrix: implications for cell transformation. *Mol Cell Biol*. 1991;11:5929–5936.

99. Bellosta P, Iwahori A, Plotnikov AN, Eliseenkova AV, Basilico C, Mohammadi M. Identification of receptor and heparin binding sites in fibroblast growth factor 4 by structure-based mutagenesis. *Mol Cell Biol*. 2001;21:5946–5957.

100. Clements DA, Wang JK, Dionne CA, Goldfarb M. Activation of fibroblast growth factor (FGF) receptors by recombinant human FGF-5. *Oncogene*. 1993;8:1311–1316.

101. Pizette S, Batoz M, Prats H, Birnbaum D, Coulier F. Production and functional characterization of human recombinant FGF-6 protein. *Cell Growth Differ*. 1991;2:561–566.

102. Loo BM, Salmivirta M. Heparin/Heparan sulfate domains in binding and signaling of fibroblast growth factor 8b. *J Biol Chem*. 2002;277:32616–32623.

103. Hecht HJ, Adar R, Hofmann B, Bogin O, Weich H, Yayon A. Structure of fibroblast growth factor 9 shows a symmetric dimer with unique receptor- and heparin-binding interfaces. *Acta Crystallogr D Biol Crystallogr*. 2001;57:378–384.

104. Igarashi M, Finch PW, Aaronson SA. Characterization of recombinant human fibroblast growth factor (FGF)-10 reveals functional similarities with keratinocyte growth factor (FGF-7). *J Biol Chem*. 1998;273:13230–13235.

105. Olsen SK, Garbi M, Zampieri N, et al. Fibroblast growth factor (FGF) homologous factors share structural but not functional homology with FGFs. *J Biol Chem*. 2003;278:34226–34236.

106. Asada M, Shinomiya M, Suzuki M, et al. Glycosaminoglycan affinity of the complete fibroblast growth factor family. *Biochim Biophys Acta*. 2009;1790:40–48.

107. Thompson LD, Pantoliano MW, Springer BA. Energetic characterization of the basic fibroblast growth factor-heparin interaction: identification of the heparin binding domain. *Biochemistry*. 1994;33:3831–3840.

108. Fan H, Vitharana SN, Chen T, O'Keefe D, Middaugh CR. Effects of pH and polyanions on the thermal stability of fibroblast growth factor 20. *Mol Pharm*. 2007;4:232–240.

109. Thompson SA, Higashiyama S, Wood K, et al. Characterization of sequences within heparin-binding EGF-like growth factor that mediate interaction with heparin. *J Biol Chem*. 1994;269:2541–2549.

110. Lustig F, Hoebeke J, Ostergren-Lunden G, et al. Alternative splicing determines the binding of platelet-derived growth factor (PDGF-AA) to glycosaminoglycans. *Biochemistry*. 1996;35:12077–12085.
111. Schilling D, Reid IJ, Hujer A, et al. Loop III region of platelet-derived growth factor (PDGF) B-chain mediates binding to PDGF receptors and heparin. *Biochem J*. 1998;333(Pt 3):637–644.
112. Krilleke D, DeErkenez A, Schubert W, et al. Molecular mapping and functional characterization of the VEGF164 heparin-binding domain. *J Biol Chem*. 2007;282:28045–28056.
113. Makinen T, Olofsson B, Karpanen T, et al. Differential binding of vascular endothelial growth factor B splice and proteolytic isoforms to neuropilin-1. *J Biol Chem*. 1999;274:21217–21222.
114. Lyon M, Rushton G, Gallagher JT. The interaction of the transforming growth factor-betas with heparin/heparan sulfate is isoform-specific. *J Biol Chem*. 1997;272:18000–18006.
115. Sue SC, Chen JY, Lee SC, Wu WG, Huang TH. Solution structure and heparin interaction of human hepatoma-derived growth factor. *J Mol Biol*. 2004;343:1365–1377.
116. Holmes O, Pillozzi S, Deakin JA, et al. Insights into the structure/function of hepatocyte growth factor/scatter factor from studies with individual domains. *J Mol Biol*. 2007;367:395–408.
117. Lau EK, Paavola CD, Johnson Z, et al. Identification of the glycosaminoglycan binding site of the CC chemokine, MCP-1: implications for structure and function in vivo. *J Biol Chem*. 2004;279:22294–22305.
118. Koopmann W, Krangel MS. Identification of a glycosaminoglycan-binding site in chemokine macrophage inflammatory protein-1alpha. *J Biol Chem*. 1997;272:10103–10109.
119. Koopmann W, Ediriwickrema C, Krangel MS. Structure and function of the glycosaminoglycan binding site of chemokine macrophage-inflammatory protein-1 beta. *J Immunol*. 1999;163:2120–2127.
120. Proudfoot AE, Fritchley S, Borlat F, et al. The BBXB motif of RANTES is the principal site for heparin binding and controls receptor selectivity. *J Biol Chem*. 2001;276:10620–10626.
121. Kuschert GS, Coulin F, Power CA, et al. Glycosaminoglycans interact selectively with chemokines and modulate receptor binding and cellular responses. *Biochemistry*. 1999;38:12959–12968.
122. Yu Y, Sweeney MD, Saad OM, et al. Chemokine-glycosaminoglycan binding: specificity for CCR2 ligand binding to highly sulfated oligosaccharides using FTICR mass spectrometry. *J Biol Chem*. 2005;280:32200–32208.
123. Ellyard JI, Simson L, Bezos A, Johnston K, Freeman C, Parish CR. Eotaxin selectively binds heparin. An interaction that protects eotaxin from proteolysis and potentiates chemotactic activity in vivo. *J Biol Chem*. 2007;282:15238–15247.
124. Hoover DM, Mizoue LS, Handel TM, Lubkowski J. The crystal structure of the chemokine domain of fractalkine shows a novel quaternary arrangement. *J Biol Chem*. 2000;275:23187–23193.
125. Escher SE, Forssmann U, Frimpong-Boateng A, et al. Functional analysis of chemically synthesized derivatives of the human CC chemokine CCL15/HCC-2, a high affinity CCR1 ligand. *J Pept Res*. 2004;63:36–47.
126. Patel DD, Koopmann W, Imai T, Whichard LP, Yoshie O, Krangel MS. Chemokines have diverse abilities to form solid phase gradients. *Clin Immunol*. 2001;99:43–52.
127. de Paz JL, Moseman EA, Noti C, Polito L, von Andrian UH, Seeberger PH. Profiling heparin-chemokine interactions using synthetic tools. *ACS Chem Biol*. 2007;2:735–744.
128. Godiska R, Chantry D, Raport CJ, et al. Human macrophage-derived chemokine (MDC), a novel chemoattractant for monocytes, monocyte-derived dendritic cells, and natural killer cells. *J Exp Med*. 1997;185:1595–1604.
129. Rajarathnam K, Li Y, Rohrer T, Gentz R. Solution structure and dynamics of myeloid progenitor inhibitory factor-1 (MPIF-1), a novel monomeric CC chemokine. *J Biol Chem*. 2001;276:4909–4916.
130. Culley FJ, Fadlon EJ, Kirchem A, Williams TJ, Jose PJ, Pease JE. Proteoglycans are potent modulators of the biological responses of eosinophils to chemokines. *Eur J Immunol*. 2003;33:1302–1310.
131. Witt DP, Lander AD. Differential binding of chemokines to glycosaminoglycan subpopulations. *Curr Biol*. 1994;4:394–400.
132. Wolpe SD, Sherry B, Juers D, Davatelis G, Yurt RW, Cerami A. Identification and characterization of macrophage inflammatory protein 2. *Proc Natl Acad Sci USA*. 1989;86:612–616.
133. Ori A, Free P, Courty J, Wilkinson MC, Fernig DG. Identification of heparin-binding sites in proteins by selective labeling. *Mol Cell Proteomics*. 2009;8:2256–2265.
134. Teixeira MG, Austin KJ, Perry DJ, et al. Bovine granulocyte chemotactic protein-2 is secreted by the endometrium in response to interferon-tau (IFN-tau). *Endocrine*. 1997;6:31–37.
135. Campanella GS, Lee EM, Sun J, Luster AD. CXCR3 and heparin binding sites of the chemokine IP-10 (CXCL10). *J Biol Chem*. 2003;278:17066–17074.
136. Cox JH, Dean RA, Roberts CR, Overall CM. Matrix metalloproteinase processing of CXCL11/I-TAC results in loss of chemoattractant activity and altered glycosaminoglycan binding. *J Biol Chem*. 2008;283:19389–19399.
137. Najjam S, Mulloy B, Theze J, Gordon M, Gibbs R, Rider CC. Further characterization of the binding of human recombinant interleukin 2 to heparin and identification of putative binding sites. *Glycobiology*. 1998;8:509–516.
138. Gupta P, Oegema TR, Jr., Brazil JJ, Dudek AZ, Slungaard A, Verfaillie CM. Human LTC-IC can be maintained for at least 5 weeks in vitro when interleukin-3 and a single chemokine are combined with O-sulfated heparan sulfates: requirement for optimal binding interactions of heparan sulfate with early-acting cytokines and matrix proteins. *Blood*. 2000;95:147–155.
139. Lortat-Jacob H, Garrone P, Banchereau J, Grimaud JA. Human interleukin 4 is a glycosaminoglycan-binding protein. *Cytokine*. 1997;9:101–105.
140. Hasan M, Najjam S, Gordon MY, Gibbs RV, Rider CC. IL-12 is a heparin-binding cytokine. *J Immunol*. 1999;162:1064–1070.
141. Kenig M, Gaberc-Porekar V, Fonda I, Menart V. Identification of the heparin-binding domain of TNF-alpha and its use for efficient TNF-alpha purification by heparin-Sepharose affinity chromatography. *J Chromatogr B Analyt Technol Biomed Life Sci*. 2008;867:119–125.
142. Spencer JL, Stone PJ, Nugent MA. New insights into the inhibition of human neutrophil elastase by heparin. *Biochemistry*. 2006;45:9104–9120.
143. Kan M, Wang F, Xu J, Crabb JW, Hou J, McKeehan WL. An essential heparin-binding domain in the fibroblast growth factor receptor kinase. *Science*. 1993;259:1918–1921.
144. Powell AK, Fernig DG, Turnbull JE. Fibroblast growth factor receptors 1 and 2 interact differently with heparin/heparan sulfate. Implications for dynamic assembly of a ternary signaling complex. *J Biol Chem*. 2002;277:28554–28563.
145. Olsen SK, Ibrahimi OA, Raucci A, et al. Insights into the molecular basis for fibroblast growth factor receptor autoinhibition

and ligand-binding promiscuity. *Proc Natl Acad Sci USA*. 2004;101:935–940.

146. Loo BM, Kreuger J, Jalkanen M, Lindahl U, Salmivirta M. Binding of heparin/heparan sulfate to fibroblast growth factor receptor 4. *J Biol Chem*. 2001;276:16868–16876.
147. Jones AL, Poon IK, Hulett MD, Parish CR. Histidine-rich glycoprotein specifically binds to necrotic cells via its amino-terminal domain and facilitates necrotic cell phagocytosis. *J Biol Chem*. 2005;280:35733–35741.
148. Weisgraber KH, Rall SC, Jr., Mahley RW, Milne RW, Marcel YL, Sparrow JT. Human apolipoprotein E. Determination of the heparin binding sites of apolipoprotein E3. *J Biol Chem*. 1986;261:2068–2076.
149. Ma Y, Henderson HE, Liu MS, et al. Mutagenesis in four candidate heparin binding regions (residues 279–282, 291–304, 390–393, and 439–448) and identification of residues affecting heparin binding of human lipoprotein lipase. *J Lipid Res*. 1994;35:2049–2059.
150. Norgard-Sumnicht KE, Varki NM, Varki A. Calcium-dependent heparin-like ligands for L-selectin in nonlymphoid endothelial cells. *Science*. 1993;261:480–483.
151. Koenig A, Norgard-Sumnicht K, Linhardt R, Varki A. Differential interactions of heparin and heparan sulfate glycosaminoglycans with the selectins. Implications for the use of unfractionated and low molecular weight heparins as therapeutic agents. *J Clin Invest*. 1998;101:877–889.
152. Jang JH, Hwang JH, Chung CP, Choung PH. Identification and kinetics analysis of a novel heparin-binding site (KEDK) in human tenascin-C. *J Biol Chem*. 2004;279:25562–25566.
153. Yu H, Munoz EM, Edens RE, Linhardt RJ. Kinetic studies on the interactions of heparin and complement proteins using surface plasmon resonance. *Biochim Biophys Acta*. 2005;1726:168–176.
154. Sahu A, Pangburn MK. Identification of multiple sites of interaction between heparin and the complement system. *Mol Immunol*. 1993;30:679–684.

SUPPORTING INFORMATION

Additional information may be found online in the Supporting Information section at the end of the article.

How to cite this article: Collins LE, Troeberg L. Heparan sulfate as a regulator of inflammation and immunity. *J Leukoc Biol*. 2019;105:81–92. https://doi.org/10.1002/JLB.3RU0618-246R